TURKISH SOCIETY OF CARDIOLOGY

September 2026
Volume 54, Number 6

ARCHIVES OF THE TURKISH SOCIETY OF CARDIOLOGY

ORIGINAL ARTICLES

KARE MEDYA

ISSN - 1016 - 5169 eISSN 1308 - 4488
www.archivestsc.com

ARCHIVES OF THE TURKISH SOCIETY OF CARDIOLOGY

Sahibi/Owner

Türk Kardiyoloji Derneği adına
On behalf of the Turkish Society of Cardiology
Dr. Ertuğrul Okuyan

Yazı İşleri Müdürü / Publishing Manager

Dr. Dilek Ural

Yayın Sekreteri / Publication Secretary

Ebru Boz Sandıkçı

Yayın Koordinatörü / Publication Coordinator

Zeynep Sena Pekşen

Yönetim Yeri Adresi / Corresponding Address

Turkish Society of Cardiology
Nish İstanbul A Blok Kat: 8
No: 47-48, Çobançeşme
Sanayi Cad. 11, Yenibosna,
Bahçelievler, İstanbul
Phone: +90 212 221 1730 - 221 17 38
Fax: +90 212 221 17 54
E-Mail: tkd@tkd.org.tr
URL: http://www.tkd.org.tr

Yayıncı / Publisher

Kare Yayıncılık
www.karepb.com
Circulation: 12

Indexed in PubMed, Europe PMC, Index Medicus, Web of Science, Emerging Sources Citation Index (ESCI), SCOPUS, EMBASE (the Excerpta Medica database), EBSCO, DOAJ, CNKI (China National Knowledge Infrastructure), GENAMICS, Research4Life, Hinari, SCILIT, OUCI, Turkish Medical Index and Turkiye Citation Index./PubMed, Europe PMC, Index Medicus, Web of Science, Emerging Sources Citation Index (ESCI), SCOPUS, EMBASE (Excerpta Medica), EBSCO, DOAJ, CNKI (China National Knowledge Infrastructure), GENAMICS, Research4Life, Hinari, SCILIT, OUCI, TÜBİTAK ULAKBİM Türk Tıp Dizini ve Türkiye Atıf Dizini'nde yer almaktadır.

Issued by the Turkish Society of Cardiology. / Türk Kardiyoloji Derneği'nin yayın organıdır.

Commercial activites are carried out by Turkish Society of Cardiology Economic Enterprise. / Ticari faaliyeti TKD İktisadi İşletmesi'nce yürütülmektedir.

Published eight issues a year. / Yılda sekiz sayı yayınlanır.

Publication Type: Periodical Publication / Yayın Türü: Yaygın Süreli.

ARCHIVES OF THE TURKISH SOCIETY OF CARDIOLOGY

CONTENTS/İÇİNDEKİLER

Volume: 54 / Issue: 6 / Year: 2026

REVIEW/DERLEME

ORIGINAL ARTICLES/ARAŞTIRMA MAKALELERİ

CASE REPORTS/OLGU SUNUMLARI

CASE IMAGES/OLGU GÖRÜNTÜLERİ

LETTERS TO THE EDITOR/EDİTÖRE MEKTUPLAR

ARCHIVES OF THE TURKISH SOCIETY OF CARDIOLOGY

CONTENTS/İÇİNDEKİLER

Volume: 54 / Issue: 6 / Year: 2026

ARCHIVES OF THE TURKISH SOCIETY OF CARDIOLOGY

Official journal of the TURKISH SOCIETY OF CARDIOLOGY

Transient Receptor Potential Channel Signaling in Hypertension: Mechanisms, Translation, and Therapeutic Targeting

Hipertansiyonda Geçici Reseptör Potansiyel Kanal Sinyal İletimi: Mekanizmalar, Translasyon ve Terapötik Hedefler

ABSTRACT

Arterial hypertension (HT) is a major risk factor in the pathogenesis of cardiovascular diseases and has a high prevalence. The pathogenesis of primary HT, which accounts for the majority of HT cases, has not been fully elucidated; therefore, effective treatment targets remain an important area of research. Transient receptor potential (TRP) channels represent a distinct class of cation channels that play a pivotal role in signal transduction by altering membrane potential or intracellular Ca^{2+} concentration. Based on sequence similarity, TRP channels are classified into six subfamilies: TRP canonical (TRPC), TRP melastatin (TRPM), TRP vanilloid (TRPV), TRP mucolipin (TRPML), TRP ankyrin (TRPA), and TRP polycystin (TRPP). These channels exhibit broad expression across diverse tissues and cell types and play critical roles in numerous pathophysiological processes through the regulation of ion concentrations (Ca^{2+}, Mg^{2+}, Na^{+}, and K^{+}) and the modulation of intracellular signal transduction pathways. Research involving human subjects, as well as experimental models, highlights the essential role of TRP channels in maintaining vascular homeostasis and regulating blood pressure. TRP channels, particularly TRPCs, have gained increasing attention for their role in resistant HT, a condition in which blood pressure remains uncontrolled despite the use of multiple antihypertensive drugs. Additionally, these channels have been identified as central mediators of inflammation and oxidative stress, processes that are pivotal in the pathogenesis of cardiovascular disorders, including HT. This review summarizes current evidence on TRPC, TRPV, and TRPM channels in HT, highlighting emerging translational findings and potential therapeutic implications.

Keywords: Blood pressure, hypertension, nitric oxide, transient receptor potential channels, vascular smooth muscle

ÖZET

Arteriyel hipertansiyon (HT), kardiyovasküler hastalıkların patogenezinde önemli bir risk faktörüdür ve yüksek prevalansa sahiptir. Hipertansiyon vakalarının çoğunu oluşturan primer HT'nin patogenezi tam olarak aydınlatılamamıştır; bu nedenle, etkili tedavi hedefleri hala önemli bir araştırma alanıdır. Geçici reseptör potansiyel (TRP) kanalları, membran potansiyelini veya hücre içi Ca^{2+} konsantrasyonunu değiştirerek sinyal iletiminde kritik bir rol oynayan belirgin bir katyon kanal sınıfını temsil eder. Dizi benzerliğine dayalı olarak, TRP kanalları altı alt aileye ayrılır: TRP kanonik (TRPC), TRP melastatin (TRPM), TRP vanilloid (TRPV), TRP mukolipin (TRPML), TRP ankirin (TRPA) ve TRP polikistitin (TRPP). Bu kanallar, çeşitli dokularda ve hücre tiplerinde yaygın bir şekilde ifade edilir ve iyon konsantrasyonlarını (Ca^{2+}, Mg^{2+}, Na^{+} ve K^{+}) düzenleyerek ve hücre içi sinyal iletim yollarını modüle ederek birçok patofizyolojik süreçte kritik roller oynar. İnsan denekleri ile yapılan araştırmalar ve deneysel modeller, TRP kanallarının vasküler homeostazın korunmasında ve kan basıncının düzenlenmesinde önemli bir rol oynadığını vurgulamaktadır. TRP kanalları, özellikle TRPC'ler, kan basıncının birden fazla antihipertansif ilaç kullanılmasına rağmen kontrol altına alınamadığı dirençli HT'deki rolleri nedeniyle giderek daha fazla ilgi görmektedir. Ayrıca, bu kanallar, HT dahil kardiyovasküler bozuklukların patogenezinde önemli bir rol oynayan inflamasyon ve oksidatif stresin merkezi aracısı olarak tanımlanmıştır. Bu derleme, HT'deki TRPC, TRPV ve TRPM kanalları ile ilgili mevcut kanıtları özetlemekte, ortaya çıkan çeviri bulguları ve potansiyel terapötik çıkarımları vurgulamaktadır.

Anahtar Kelimeler: Kan basıncı, hipertansiyon, nitrik oksit, geçici reseptör potansiyel kanalları, vasküler düz kas

REVIEW
DERLEME

Algül Dilara Dokumacı[1]

Belgin Alaşehirli[2]

Akif Serhat Balcıoğlu[3]

[1]*Department of Medical Pharmacology, Faculty of Medicine, Kahramanmaraş Sütçü İmam University, Kahramanmaraş, Türkiye*
[2]*Department of Medical Pharmacology, Faculty of Medicine, Gaziantep University, Gaziantep, Türkiye*
[3]*Department of Cardiology, Faculty of Medicine, Kahramanmaraş Sütçü İmam University, Kahramanmaraş, Türkiye*

Corresponding author:
Algül Dilara Dokumacı
✉ dilaradokumaci@gmail.com

Received: December 11, 2025
Accepted: April 06, 2026

Cite this article as: Dokumacı AD, Alaşehirli B, Balcıoğlu AS. Transient Receptor Potential Channel Signaling in Hypertension: Mechanisms, Translation, and Therapeutic Targeting. *Turk Kardiyol Dern Ars.* 2026;54(6):463–470.

DOI: 10.5543/tkda.2026.34864

Hypertension (HT) is a clinical condition characterized by chronically elevated blood pressure in the systemic arteries and is considered a critical risk factor for cardiovascular and cerebrovascular diseases.[1] Approximately 1.4 billion adults worldwide (aged 30–79 years) have arterial HT, and more than 73% of these patients do not have controlled blood pressure.[2] Chronic high blood pressure increases morbidity and mortality because it leads to serious complications, such as left ventricular hypertrophy, congestive heart failure, stroke, myocardial infarction, and chronic kidney disease; furthermore, it imposes a significant burden on healthcare systems and the global economy.[3]

The development of HT can be influenced by anatomic, genetic, endocrine, humoral, hemodynamic, environmental, and neural factors.[1] Although primary HT accounts for the majority of cases, treatment failure is a significant challenge because its pathogenesis has not yet been fully elucidated. Understanding the pathogenesis of primary HT is essential for identifying novel therapeutic targets. Numerous studies have underscored the role of ion channels in the pathogenesis of vascular disorders.[4] Ion channels frequently studied in HT include voltage-dependent Ca^{2+} channels, Ca^{2+}-activated K^+ (KCa) channels, voltage-sensitive K^+ channels, and transient receptor potential (TRP) channels.[4,5]

Transient receptor potential channels are cation channels that contribute significantly to signal transduction by modulating membrane potential or intracellular Ca^{2+} concentration. In humans, a total of 28 TRP channels have been characterized and classified into six distinct families according to sequence similarity: TRP canonical (TRPC), TRP melastatin (TRPM), TRP vanilloid (TRPV), TRP ankyrin (TRPA), TRP mucolipin (TRPML), and TRP polycystin (TRPP).[5] These channels are broadly distributed across human tissues, including the brain, kidneys, heart, and lungs.[6]

Transient receptor potential channels are integral to a wide array of physiological and pathological processes, including cell biology, migration, proliferation, carcinogenesis, immunological responses, tissue homeostasis, sensory transduction, and electrolyte homeostasis. These processes occur in response to a variety of extracellular and intracellular stimuli, including alterations in temperature, changes in pH or osmolarity, depletion of intracellular Ca^{2+} stores, and exposure to volatile chemicals and cytokines.[5-7]

Transient receptor potential channels are expressed in various tissues, such as the brain, kidney, heart, lung, and vascular tissue.[6] In vascular tissue, TRP channels are expressed in endothelial cells, vascular smooth muscle (VSM) cells, perivascular sensory neurons, and perivascular adipose tissue, where they play important roles in regulating cell proliferation, angiogenesis, permeability, and vascular tone.[5] Studies investigating the involvement of TRP channels in blood pressure regulation have indicated that alterations in their expression and function may contribute to vascular dysfunction and HT.[5,7] This review examines the roles of TRPC, TRPV, and TRPM channels in HT.

Hypertension and Transient Receptor Potential Channels

Hypertension is defined by a sustained elevation in vascular tone. The predominant pathological manifestation of this condition is vascular remodeling, characterized by increased medial thickness resulting from hyperplastic and/or hypertrophic changes in VSM cells.[5] Hypertensive vasculopathy can be explained by alterations in cytosolic Ca^{2+} handling and increased intracellular Ca^{2+} concentration, impaired nitric oxide (NO) bioavailability in endothelial cells, and the release of vasoactive agonists that influence Ca^{2+} signaling in VSM cells.[8] Some isoforms, such as TRPC3 and TRPC5, play a role in HT pathogenesis by contributing to vascular remodeling and vasoconstriction through their effects on intracellular Ca^{2+} concentration and VSM cell proliferation.[5] These isoforms are associated with abnormal Ca^{2+} utilization and vascular dysfunction related to HT and other cardiovascular diseases.[9,10] In contrast, some TRP isoforms, such as TRPV1 and TRPV4, exert protective effects against HT by contributing to endothelium-mediated vasodilation (Figure 1). Decreased expression and dysfunction of these channels have been observed in HT.[11,12]

Transient Receptor Potential Canonical Channels

In vascular tissue, TRPC1, TRPC3, TRPC4, TRPC5, TRPC6, and TRPC7 are expressed in VSM and endothelial cells. These channels play important roles in receptor-operated Ca^{2+} entry, store-operated Ca^{2+} entry, angiogenesis, regulation of vascular permeability, and vascular tone.[5,6]

TRPC1, a member of the TRP channel family, is primarily localized in VSM and endothelial cells and is involved in VSM contraction, proliferation, migration, and endothelium-mediated vasodilation.[6] Recent studies have demonstrated that VSM-specific TRPC1 deletion significantly mitigates angiotensin II–induced HT and cardiovascular remodeling.[13] Furthermore, endothelial TRPC1 deficiency has been shown to promote aortic hypercontractility and exacerbate hypertensive responses.[14]

The TRPC3 channel is expressed in VSM cells in various vascular beds (such as the coronary, pulmonary, renal, and cerebral arteries) as well as in the aorta. It contributes to the regulation of vascular tone though activation of G-protein-coupled receptors, including angiotensin II (Ang II) and endothelin-1 receptors.[6] The expression of TRPC3 is elevated in monocytes from spontaneously hypertensive rats (SHRs) and in patients with primary HT, and this increase correlates with elevated levels of proinflammatory cytokines, such as tumor necrosis factor-α and interleukin-1 (IL-1).[10-15] This finding suggests that TRPC3-mediated calcium influx in monocytes may activate specific intracellular signaling cascades (e.g., nuclear factor of activated T cells [NFAT] and mitogen-activated protein

ABBREVIATIONS

Ang II	Angiotensin II
EnaCs	Epithelial sodium channels
HT	Hypertension
IL	Interleukin
KCa	Calcium-activated potassium channel
NO	Nitric oxide
SHR	Spontaneously hypertensive rat
TRP	Transient receptor potential
TRPA	Transient receptor ankyrin
TRPC	Transient receptor canonical
TRPM	Transient receptor melastatin
TRPML	Transient receptor mucolipin
TRPP	Transient receptor polycystin
TRPV	Transient receptor vanilloid
VSM	Vascular smooth muscle

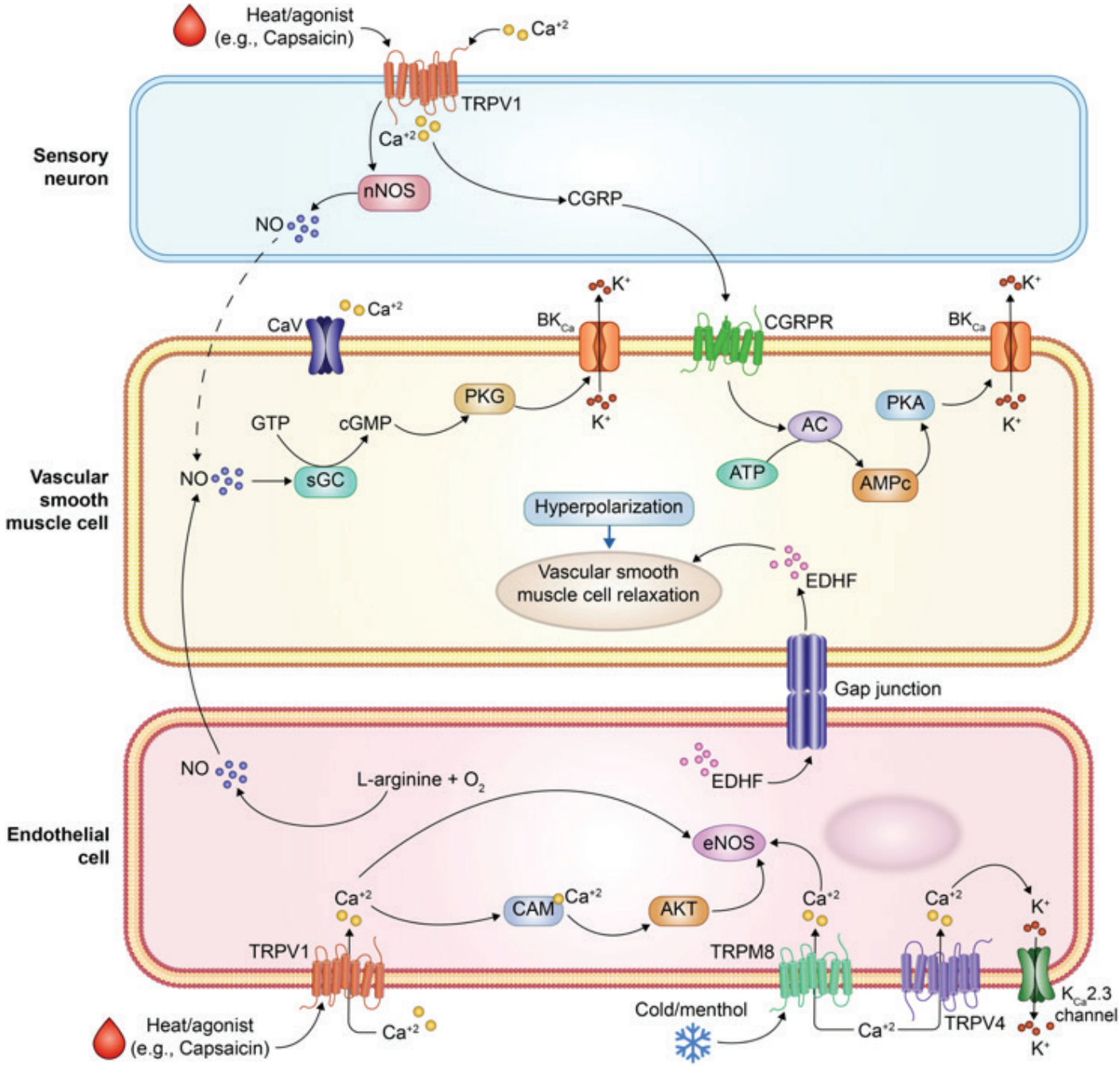

Figure 1. Signal transduction mechanisms of transient receptor potential vanilloid 1 (TRPV1), transient receptor potential vanilloid 4 (TRPV4), and transient receptor potential melastatin 8 (TRPM8) channels in vascular tissue.

AC, Adenylate cyclase; AKT, Protein kinase B; ATP, Adenosine triphosphate; BKCa, Large-conductance Ca^{2+}-activated K^+ channel; CaM, Calmodulin; cAMP, Cyclic adenosine monophosphate; Cav, Voltage-activated Ca^{2+} channel; CGRP, Calcitonin gene-related peptide; CGRPR, Calcitonin gene-related peptide receptor; cGMP, Cyclic guanosine monophosphate; EDHF, Endothelium-derived hyperpolarization factor; eNOS, Endothelial nitric oxide synthase; GTP, Guanosine triphosphate; KCa2.3, Small-conductance Ca^{2+}-activated K^+ channel 2.3; nNOS, Neuronal nitric oxide synthase; PKA, Protein kinase A; PKG, Protein kinase G; sGC, Soluble guanylate cyclase (Adapted from reference 7).

kinase [MAPK] pathways) that drive the transcription and release of these cytokines, thereby contributing to vascular inflammation and the pathogenesis of HT. In monocytes from patients with primary HT, the expression of TRPC3 and TRPC5 is increased, while store-operated Ca^{2+} entry facilitated by these channels, as well as cation influx triggered by 1-oleoyl-2-acetyl-sn-glycerol, are also enhanced. Consequently, enhanced activation of monocytes via TRPC channels may contribute to the pathogenesis of HT.[9] In a separate study, increased monocyte migration in patients with HT was correlated with elevated TRPC3 expression.[16] Additionally, a positive correlation between high salt intake, systolic blood pressure, and TRPC3 expression has been identified in patients with HT.[17]

The TRPC6 channel is permeable to cations, including Ca^{2+}, Na^{+}, and Mg^{2+}, and plays a significant role in both physiological and pathophysiological processes in vascular tissue.[6] Research using animal and cell culture models has demonstrated that TRPC6 channel plays a significant role in essential vascular processes, such as VSM responses to changes in arterial blood pressure, known as the Bayliss effect, and endothelium-mediated vasodilation.[18] TRPC1 and TRPC6 channels together contribute to increases in medial thickness, medial area, lumen diameter, collagen accumulation, and medial VSM hyperplasia, which are indicators of arterial remodeling associated with aging and elevated systolic blood pressure.[19] Additionally, heteromultimeric structures of TRPC3 and TRPC6 are altered in HT, thereby enhancing depolarization of VSM cells.[20] Elucidating the specific roles of TRPC3 and TRPC6 in the pathogenesis of HT presents significant challenges, as these channels are integral components of complex and compensatory networks involving multiple TRP subtypes and ion channels.[6]

Transient Receptor Potential Vanilloid Channels

TRPV1, TRPV2, TRPV3, and TRPV4 channels are expressed in vascular tissue and mediate functions such as mechanosensitive Ca^{2+} entry, vasoconstriction, vasodilation, angiogenesis, and permeability.[5,6]

Research examining the association between the TRPV1 channel, which is integral to the regulation of vascular tone and arterial blood pressure, and HT has demonstrated that deletion of the TRPV1 gene in rats results in increased blood pressure, enhanced salt sensitivity, exacerbation of salt-induced HT, and elevated renal inflammatory responses and kidney damage.[21,22] In salt-induced HT models, TRPV1 gene expression is reduced in the mesenteric arteries of rats.[22] Reduced TRPV1 mRNA expression has also been detected in aortic tissue from patients with HT.[12]

Studies examining the relationship between TRPV1 gene polymorphisms and HT have shown that these polymorphisms correlate with elevated systolic and diastolic blood pressure in a Mexican population. Similarly, in a population in Iran, these polymorphisms have been associated with increased salt consumption and a higher risk of HT.[23,24] Moreover, TRPV1 gene polymorphisms have been linked to salt sensitivity, salt intake, and the risk of HT.[25]

Furthermore, the TRPV1 channel plays a crucial role in regulating salt-induced HT in mice, functioning in conjunction with epithelial sodium channels (ENaCs), which are essential for renal sodium reabsorption and systemic blood pressure regulation.[26] Prolonged activation of TRPV1 by capsaicin may inhibit ENaC activity and exert a protective effect against salt-induced HT by reducing ENaC-mediated Na^{+} reabsorption.[7] In Dahl salt-sensitive rats fed a high-salt diet, increased susceptibility to HT has been attributed, in part, to reduced involvement of the TRPV1 pathway.[7]

The TRPV4 channel is involved in processes such as vasodilation and vasoconstriction, vascular permeability, vascular remodeling, and vascular injury.[6] Studies examining the relationship between TRPV4 expression alterations and dysfunction in the pathogenesis of HT has shown that both the expression and function of TRPV4 are reduced in the mesenteric artery tissue of SHRs and in the cerebral parenchymal arterioles of mice with Ang II-induced HT.[27,28] Additionally, TRPV4 mRNA expression is decreased in the aortic tissue of patients with HT.[12] Conversely, some studies have reported increased TRPV4 expression and function in the mesenteric arteries of rats with salt-induced HT. However, in the aortic tissue of mice with salt-induced HT, TRPV4 expression remains unchanged, whereas TRPV4-mediated vasoconstriction is enhanced.[29]

Studies investigating the role of TRPV4 channel in obesity-related HT have reported increased TRPV4 expression in VSM cells of the mesenteric arteries in obese mice. These findings suggest that TRPV4 channels in VSM cells may contribute to the development of vasoconstriction and HT, whereas endothelial TRPV4 dysfunction may also play a role in obesity-induced HT.[30,31]

The TRPV4 channel physically and functionally interacts with KCa2.3 (Figure 1).[32] This interaction is crucial for the response mediated by the endothelium-derived hyperpolarizing factor, which significantly contributes to vasodilation, blood flow, and the regulation of blood pressure in resistance arteries. Decreased expression of the TRPV4 channel and reduced TRPV4–KCa2.3 interaction in endothelial cells may lead to endothelial dysfunction and HT.[32,33] Additionally, when the endothelial TRPV4 channel is activated, Ca^{2+} influx induces Ca^{2+}-mediated activation of endothelial NO synthase and subsequent NO production.[33] Consequently, the TRPV4 channel may serve as a potential therapeutic target in the management of HT.[7]

Transient Receptor Potential Melastatins

TRPM2, TRPM4, TRPM6, TRPM7, and TRPM8 channels are expressed in vascular tissue and play integral roles in the regulation of vascular tone, endothelial permeability, and angiogenesis.[6]

TRPM channels, especially TRPM6, TRPM7, and TRPM8, have significant roles in HT, and alterations in TRPM channel activity have been associated with multiple forms of HT.[34] In the VSM cells of the mesenteric arteries of SHRs, TRPM7 expression and intracellular Mg^{2+} concentration are reduced.[35] Disrupted Mg^{2+} regulation, linked to altered TRPM7 activity, may contribute to inflammatory responses, cellular proliferation, and vascular remodeling associated with HT.[36]

TRPM8 is a polymodal, Ca^{2+}-permeable, nonselective cation channel primarily recognized as the physiological sensor for environmental cold. Furthermore, activation of TRPM8 influences vascular function and blood pressure regulation.[7] A genome-wide association study conducted in China identified a significant correlation between TRPM8 polymorphisms and susceptibility to HT development.[37] In a study using a renovascular HT model, the TRPM8 expression level in the aortic tissues of hypertensive rats was lower than that in the aortic tissues of rats in the control group, and exogenous Ang II administration reduced TRPM8 gene expression levels in cultured rat VSM cells.[38] In another study, TRPM8 gene expression in the hypothalamic tissue of rats with hereditary stress-induced arterial HT was lower than that in the hypothalamic tissue of normotensive rats.[39] Additionally, the TRPM8 gene expression level in the aortic tissue of patients with HT was lower than that in the ascending aortic tissue of individuals in the normotensive control group.[12]

Activation of the TRPM8 channel through the topical application of menthol has been shown to elevate proinflammatory cytokines, such as IL-6 and IL-1β, in the bloodstream of normotensive rats. However, this elevation was not detected in rats with hereditary stress-induced arterial HT, indicating a potential reduction in TRPM8 channel activity in HT.[40] Additionally, topical application of menthol has been demonstrated to induce cutaneous vasorelaxation through mechanisms involving sensory neurons, endothelium-derived relaxing factors, and NO.[41] Intravenous administration of menthol resulted in a reduction in systemic blood pressure in cats and rabbits. Furthermore, dietary intake of menthol has been associated with decreased blood pressure in mice, SHRs, and individuals with pre-HT.[42] The context-dependent outcomes of TRPM8 activation underscore the complexity of its role in HT. These variations likely stem from differences in specific vascular beds, the nature of stimuli (e.g., menthol vs. cold), the overall physiological state of the organism, and interactions with autonomic nervous system activity. Future research is needed to delineate these contextual factors and clarify whether TRPM8 activation primarily exerts protective or detrimental effects in specific hypertensive conditions.[7]

Clinical and Translational Evidence for Dietary/ Environmental TRP Channel Activation

In recent years, the cardiovascular effects mediated by TRPV1 following dietary capsaicin intake have garnered significant attention in clinical research. Several population-based studies have identified an inverse correlation between the consumption of spicy foods and the risk of HT, supporting the hypothesis that chronic dietary exposure to TRPV1 agonists may contribute to blood pressure regulation.[43,44] Nevertheless, meta-analyses of randomized controlled trials investigating capsaicin or red pepper supplementation have generally not demonstrated a significant impact on either systolic or diastolic blood pressure.[45] Consequently, although current clinical data suggest a potential role of TRPV1 activation, they do not conclusively establish that capsaicin consistently exerts an antihypertensive effect on HT. This discrepancy may arise from several factors, including differences in patient populations, the specific formulation and dosage of capsaicin, the duration of the intervention, and the potential for compensatory mechanisms within the more complex human physiological system compared to controlled animal models.

Translational human data concerning TRPM8 activation are notably supported by findings derived from menthol studies. In research involving prehypertensive individuals, administration of menthol capsules over an eight-week period resulted in a moderate reduction in blood pressure and an improvement in flow-mediated dilation.[42] Furthermore, menthol-induced cutaneous vasodilation has been directly investigated in both male and female subjects with essential HT. Although menthol has been shown to induce dose-dependent vasodilation, with the magnitude of the response comparable to that observed in normotensive individuals, the underlying mechanisms differ. Specifically, nitric oxide synthase inhibition and sensory nerve blockade were found to attenuate the menthol response in patients with HT, suggesting that TRPM8-related vasoreactivity is context dependent and influenced by associated signaling pathways.[46] A systematic review assessing interventions involving Mentha species underscores the inconsistency of their effects on blood pressure and highlights the necessity for higher-quality randomized studies.[47] Collectively, these findings suggest that, while the TRPM8/menthol axis holds translational promise for HT research, further elucidation of its clinical efficacy and underlying mechanisms is required.

Integrating Omics and Translational Evidence in TRP Channel Dysregulation in Hypertension

Recent advancements in translational and omics-based research have provided novel insights into the involvement of TRP channels in the pathophysiology of HT. Evidence indicates that the expression levels of TRPC6, TRPV1/2/4, and TRPM8 transcripts in human aortic tissues are altered in patients with HT, underscoring the potential clinical relevance of vascular TRP channels.[12] Furthermore, multi-omics analyses of human aortic arch tissue have identified Piezo-type mechanosensitive ion channel component 1 (PIEZO1), TRPV2, and TRPM4 channels as potential ion channels associated with baroreceptor function.[48] These findings suggest the need to re-evaluate TRP channels in HT research using cell-type specific and translational methodologies. Integrating omics-based data with functional vascular studies could significantly enhance the understanding of TRP channel-mediated mechanisms and facilitate the identification of patient subgroups that may benefit from targeted therapeutic interventions.

Strength of Evidence and Translational Limitations

Although evidence supporting the role of TRP channels in HT has increased significantly, findings remain heterogeneous across TRP subfamilies, vascular beds, and experimental designs. The strongest inferences regarding causality are derived from genetic and mechanistic animal studies; however, these models have limitations, including developmental adaptation, compensatory channel rearrangement, and interspecies physiological differences. For example, phenotypes observed after germline gene deletion may reflect network-level compensatory mechanisms rather than a simple "loss-of-function" effect. Indeed, in mice deficient in TRPC6, increased blood pressure and vascular contractility have been observed; this has been partly attributed to increased basal cation influx and could be reduced by suppression of TRPC3. These findings indicate functional overlap within the TRPC3/6 axis.[49] Additionally, many pharmacological studies rely on research compounds with limited selectivity or tissue penetration, making it difficult to attribute observed blood pressure phenotypes to a specific TRP isoform. These limitations underscore the need for greater caution when directly translating mechanistic findings into claims of druggability and highlight the importance of considering cell type-specific roles (e.g., endothelial cells, vascular smooth muscle cells, or sensory neurons) as well as contextual factors such as salt load, obesity, or activation of the renin–angiotensin–aldosterone system (RAAS). Future research endeavors integrating human vascular tissue data, omics technologies, and clinical phenotyping—including resistant HT—will be crucial in determining whether TRP channels can transition from mechanistic interests to viable therapeutic targets.

Therapeutic Targeting of TRP Channels in Hypertension

Research findings suggest that alterations in the expression of TRP channels may represent promising therapeutic targets in the pathogenesis and management of HT. Notably, TRPC1 and TRPC6 channels have been shown to be susceptible to pharmacological modulation, and certain existing cardiovascular medications—such as losartan and nifedipine—may influence the expression of these channels.[50,51] However, the formation of heteromultimeric structures by TRP channels and their mutual interactions complicate the targeting of a single subtype. For instance, inhibition of TRPC1 may inadvertently enhance TRPC6 activity, potentially resulting in adverse effects. Furthermore, the role of TRPC1 in vasodilation through its interaction with TRPV4 in endothelial cells suggests that nonselective inhibition strategies could negatively affect endothelial function.

TRPC3 and TRPC6 channels have been identified as critical contributors to the pathogenesis of resistant HT and myocardial fibrosis.[52] In this context, therapeutic targeting of TRPC3/6 channels may represent a dual strategy, potentially lowering blood pressure while mitigating fibrotic progression. Nevertheless, the structural similarities among TRPC channels and the scarcity of selective modulators pose significant challenges to translational advancement in this field. Therefore, the development of highly selective TRPC3/6 inhibitors, characterized by optimized bioavailability and minimized off-target effects, is essential for validating the therapeutic potential of these channels in preclinical models.

While activation of TRPV1 has demonstrated notable cardiovascular protective effects in experimental models, clinical data remain inconsistent.[43–45] Consequently, the precise role and therapeutic potential of TRPV1 in HT remain uncertain. TRPV2 and TRPV3 channels have emerged as promising targets, particularly in the context of cardiovascular complications such as cardiac hypertrophy, myocardial infarction, and heart failure; however, their roles in HT are not yet fully elucidated. Although TRPV4-mediated vasodilation can be enhanced by various pharmacological agents, the potential for this channel to exert vasoconstrictive effects under certain conditions and to produce divergent outcomes in different tissues necessitates caution when considering it as a therapeutic target.

Activation of TRPM8 is supported by translational evidence derived from menthol studies and has been associated with vasodilation and reductions in blood pressure.[42] Nevertheless, further large-scale studies are required to assess the long-term effects and clinical applicability of TRPM8 activation.

In summary, TRP channels represent promising yet complex targets for the treatment of HT. Given their cell type-specific effects, mutual interactions, and context-dependent functions, future research should prioritize more selective, tissue-specific, and mechanism-based strategies.

Conclusion

Recent advances have deepened our understanding of how TRP channels contribute to vascular function and myogenic tone and have clarified that their altered expression and activity are key factors in conditions such as HT, atherosclerosis, and cardiovascular injuries. Despite their distinct effects, the precise intracellular signaling mechanisms of TRP channels remain largely unclear because of their complex structures, isoform interactions, dual roles as ion channels and signaling regulators, and diverse cell-type specific expression patterns. Additionally, the limited specificity of pharmacological compounds and antibodies targeting TRP channels poses significant challenges in this field of research. Clarifying the precise mechanisms through which TRP channels regulate vascular function in both physiological and pathological states is essential for the development of targeted cardiovascular therapies, particularly as these channels are increasingly recognized as promising therapeutic targets. Future studies integrating clinical research, omics-based approaches, and selective pharmacological modulators will be crucial in determining whether TRP channels can serve as viable therapeutic targets in HT.

Conflict of Interest: The authors have no conflicts of interest to declare.

Funding: The authors declared that this study received no financial support.

Use of AI for Writing Assistance: No use of AI-assisted technologies was declared by the authors.

Author Contributions: Concept – A.D.D., B.A., A.S.B.; Design – A.D.D., B.A.; Supervision – B.A., A.S.B.; Literature Review – A.D.D., A.S.B.; Writing – A.D.D., B.A., A.S.B.; Critical Review – B.A., A.S.B.

Peer-review: Externally peer-reviewed.

References

1. Güneş Y, Gürdoğan M, Altay S, Ekici B, et al. Hypertension and Occupational Health: A General Overview and Expert Consensus Suggestions. Turk Kardiyol Dern Ars. 2024;52(2):125-137. [CrossRef]
2. World Health Organization. *Hypertension*. 2025. Accessed Janıuary 8, 2026. https://www.who.int/news-room/fact-sheets/detail/hypertension
3. Masenga SK, Kirabo A. Hypertensive heart disease: risk factors, complications and mechanisms. *Front Cardiovasc Med*. 2023;10:1205475. [CrossRef]
4. Cheng J, Wen J, Wang N, Wang C, Xu Q, Yang Y. Ion Channels and Vascular Diseases. *Arterioscler Thromb Vasc Biol*. 2019;39(5):e146-e156. [CrossRef]
5. Martín-Bórnez M, Galeano-Otero I, Del Toro R, Smani T. TRPC and TRPV Channels' Role in Vascular Remodeling and Disease. *Int J Mol Sci*. 2020;21(17):6125. [CrossRef]
6. Earley S, Brayden JE. Transient receptor potential channels in the vasculature. *Physiol Rev*. 2015;95(2):645-690. [CrossRef]
7. Jesus RLC, Araujo FA, Alves QL, Dourado KC, Silva DF. Targeting temperature-sensitive transient receptor potential channels in hypertension: far beyond the perception of hot and cold. *J Hypertens*. 2023;41(9):1351-1370. [CrossRef]
8. Zeng X, Yang Y. Molecular Mechanisms Underlying Vascular Remodeling in Hypertension. *Rev Cardiovasc Med*. 2024;25(2):72. [CrossRef]
9. Liu DY, Thilo F, Scholze A, et al. Increased store-operated and 1-oleoyl-2-acetyl-sn-glycerol-induced calcium influx in monocytes is mediated by transient receptor potential canonical channels in human essential hypertension. *J Hypertens*. 2007;25(4):799-808. [CrossRef]
10. Thilo F, Scholze A, Liu DY, Zidek W, Tepel M. Association of transient receptor potential canonical type 3 (TRPC3) channel transcripts with proinflammatory cytokines. *Arch Biochem Biophys*. 2008;471(1):57-62. [CrossRef]

11. Wang Y, Wang DH. A novel mechanism contributing to development of Dahl salt-sensitive hypertension: role of the transient receptor potential vanilloid type 1. *Hypertension*. 2006;47(3):609-614. [CrossRef]
12. Dokumacı AD, Alaşehirli B, Balcıoğlu AS, et al. Decreased transient receptor potential channel mRNA expression in the aortas of patients with hypertension. *Anatol J Cardiol*. 2025;29(9):472-479. [CrossRef]
13. Wen X, Peng Y, Yang W, et al. VSMC-specific TRPC1 deletion attenuates angiotensin II-induced hypertension and cardiovascular remodeling. *J Mol Med (Berl)*. 2025;103(2):205-218. [CrossRef]
14. Zhu Y, Chu Y, Lan Y, et al. Loss of Endothelial TRPC1 Induces Aortic Hypercontractility and Hypertension. *Circ Res*. 2025;136(5):508-523. [CrossRef]
15. Liu D, Scholze A, Zhu Z, et al. Increased transient receptor potential channel TRPC3 expression in spontaneously hypertensive rats. *Am J Hypertens*. 2005;18(11):1503-1507. [CrossRef]
16. Zhao Z, Ni Y, Chen J, et al. Increased migration of monocytes in essential hypertension is associated with increased transient receptor potential channel canonical type 3 channels. *PLoS One*. 2012;7(3):e32628. [CrossRef]
17. Hu Y, Xia W, Li Y, et al. High-salt intake increases TRPC3 expression and enhances TRPC3-mediated calcium influx and systolic blood pressure in hypertensive patients. *Hypertens Res*. 2020;43(7):679-687. [CrossRef]
18. Abdinghoff J, Servello D, Jacobs T, Beckmann A, Tschernig T. Evaluation of the presence of TRPC6 channels in human vessels: A pilot study using immunohistochemistry. *Biomed Rep*. 2022;16(5):42. [CrossRef]
19. Lin XH, Hong HS, Zou GR, Chen LL. Upregulation of TRPC1/6 may be involved in arterial remodeling in rat. *J Surg Res*. 2015;195(1):334-343. [CrossRef]
20. Álvarez-Miguel I, Cidad P, Pérez-García MT, López-López JR. Differences in TRPC3 and TRPC6 channels assembly in mesenteric vascular smooth muscle cells in essential hypertension. *J Physiol*. 2017;595(5):1497-1513. [CrossRef]
21. Yu SQ, Ma S, Wang DH. Activation of TRPV1-Expressing Renal Sensory Nerves of Rats with N-Oleoyldopamine Attenuates High-Fat-Diet-Induced Impairment of Renal Function. *Int J Mol Sci*. 2023;24(7):6207. [CrossRef]
22. Wang Y, Babánková D, Huang J, Swain GM, Wang DH. Deletion of transient receptor potential vanilloid type 1 receptors exaggerates renal damage in deoxycorticosterone acetate-salt hypertension. *Hypertension*. 2008;52(2):264-270. [CrossRef]
23. González-Mercado A, Magaña-Torres MT, Sánchez-López JY, et al. The Relationship of Single Nucleotide Polymorphisms in the TRPV1 Gene with Lipid Profile, Glucose, and Blood Pressure in Mexican Population. *Genet Test Mol Biomarkers*. 2020;24(7):420-424. [CrossRef]
24. Mohammadifard N, Moazeni F, Azizian-Farsani F, et al. Genetic variation in salt taste receptors impact salt intake and blood pressure. *Sci Rep*. 2023;13(1):4037. [CrossRef]
25. Tapanee P, Tidwell DK, Schilling MW, Peterson DG, Tolar-Peterson T. Genetic Variation in Taste Receptor Genes (SCNN1B, TRPV1) and Its Correlation with the Perception of Saltiness in Normotensive and Hypertensive Adults. *Int J Hypertens*. 2021;2021:5559831. [CrossRef]
26. Li L, Wang F, Wei X, et al. Transient receptor potential vanilloid 1 activation by dietary capsaicin promotes urinary sodium excretion by inhibiting epithelial sodium channel α subunit-mediated sodium reabsorption. *Hypertension*. 2014;64(2):397-404. [CrossRef]
27. Seki T, Goto K, Kiyohara K, et al. Downregulation of Endothelial Transient Receptor Potential Vanilloid Type 4 Channel and Small-Conductance of Ca^{2+}-Activated K^+ Channels Underpins Impaired Endothelium-Dependent Hyperpolarization in Hypertension. *Hypertension*. 2017;69(1):143-153. [CrossRef]
28. Diaz-Otero JM, Yen TC, Ahmad A, et al. Transient receptor potential vanilloid 4 channels are important regulators of parenchymal arteriole dilation and cognitive function. *Microcirculation*. 2019;26(6):e12535. [CrossRef]
29. Hu XQ, Zhang L. Role of transient receptor potential channels in the regulation of vascular tone. *Drug Discov Today*. 2024;29(7):104051. Erratum in: *Drug Discov Today*. 2025;30(5):104358. [CrossRef]
30. Zhu Y, Chu Y, Wang S, et al. Vascular Smooth Muscle TRPV4 (Transient Receptor Potential Vanilloid Family Member 4) Channels Regulate Vasoconstriction and Blood Pressure in Obesity. *Hypertension*. 2023;80(4):757-770. [CrossRef]
31. Ottolini M, Hong K, Cope EL, et al. Local Peroxynitrite Impairs Endothelial Transient Receptor Potential Vanilloid 4 Channels and Elevates Blood Pressure in Obesity. *Circulation*. 2020;141(16):1318-1333. [CrossRef]
32. He D, Pan Q, Chen Z, et al. Treatment of hypertension by increasing impaired endothelial TRPV4-KCa2.3 interaction. *EMBO Mol Med*. 2017;9(11):1491-1503. [CrossRef]
33. Touyz RM. TRPV4 Channel-Regulated Microdomains Define a New Paradigm in Hypertension. *Circulation*. 2022;146(7):565-568. [CrossRef]
34. Rios FJ, Sarafian RD, Camargo LL, Montezano AC, Touyz RM. Recent Advances in Understanding the Mechanistic Role of Transient Receptor Potential Ion Channels in Patients with Hypertension. *Can J Cardiol*. 2023;39(12):1859-1873. [CrossRef]
35. Touyz RM, He Y, Montezano AC, et al. Differential regulation of transient receptor potential melastatin 6 and 7 cation channels by ANG II in vascular smooth muscle cells from spontaneously hypertensive rats. *Am J Physiol Regul Integr Comp Physiol*. 2006;290(1):R73-R78. [CrossRef]
36. Touyz RM. Transient receptor potential melastatin 6 and 7 channels, magnesium transport, and vascular biology: implications in hypertension. *Am J Physiol Heart Circ Physiol*. 2008;294(3):H1103-H1118. [CrossRef]
37. He J, Kelly TN, Zhao Q, et al. Genome-wide association study identifies 8 novel loci associated with blood pressure responses to interventions in Han Chinese. *Circ Cardiovasc Genet*. 2013;6(6):598-607. [CrossRef]
38. Huang F, Ni M, Zhang JM, Li DJ, Shen FM. TRPM8 downregulation by angiotensin II in vascular smooth muscle cells is involved in hypertension. *Mol Med Rep*. 2017;15(4):1900-1908. [CrossRef]
39. Voronova IP, Khramova GM, Evtushenko AA, Kozyreva TV. Effect of Skin Ion Channel TRPM8 Activation by Cold and Menthol on Thermoregulation and the Expression of Genes of Thermosensitive TRP Ion Channels in the Hypothalamus of Hypertensive Rats. *Int J Mol Sci*. 2022;23(11):6088. [CrossRef]
40. Kozyreva TV, Khramova GM, Voronova IP, Evtushenko AA. The influence of cooling and TRPM8 ion channel activation on the level of pro-inflammatory cytokines in normotensive and hypertensive rats. *J Therm Biol*. 2016;61:119-124. [CrossRef]
41. Craighead DH, Alexander LM. Topical menthol increases cutaneous blood flow. *Microvasc Res*. 2016;107:39-45. [CrossRef]
42. Sun J, Yang T, Wang P, et al. Activation of cold-sensing transient receptor potential melastatin subtype 8 antagonizes vasoconstriction and hypertension through attenuating RhoA/Rho kinase pathway. *Hypertension*. 2014;63(6):1354-1363. [CrossRef]
43. Wang H, Chen L, Shen D, et al. Association between frequency of spicy food consumption and hypertension: a cross-sectional study in Zhejiang Province, China. *Nutr Metab (Lond)*. 2021;18(1):70. [CrossRef]
44. You D, Sun D, Zhao Z, et al.; China Kadoorie Biobank Collaborative Group. Spicy food consumption and risk of vascular disease: Evidence from a large-scale Chinese prospective cohort of 0.5 million people. *Chin Med J (Engl)*. 2025;138(14):1696-1704. [CrossRef]
45. Shirani F, Foshati S, Tavassoly M, Clark CCT, Rouhani MH. The effect of red pepper/capsaicin on blood pressure and heart rate: A systematic review and meta-analysis of clinical trials. *Phytother Res*. 2021;35(11):6080-6088. [CrossRef]
46. Craighead DH, Alexander LM. Menthol-Induced Cutaneous Vasodilation Is Preserved in Essential Hypertensive Men and Women. *Am J Hypertens*. 2017;30(12):1156-1162. [CrossRef]

47. Nematolahi F, Mohtashamian A, Kaveh G, Sharifi N, Milajerdi A. Effects of Mentha on blood pressure: a GRADE-assessed systematic review and meta-analysis of randomized controlled trials. *BMC Complement Med Ther*. 2024;24(1):406. [CrossRef]
48. Yundung Y, Pelisek J, Maccio U, et al. Identification of putative baroreceptors in human aortic arch by histological and omics analyses. *Hypertens Res*. 2025;48(7):2083-2094. [CrossRef]
49. Dietrich A, Mederos Y Schnitzler M, et al. Increased vascular smooth muscle contractility in TRPC6-/- mice. *Mol Cell Biol*. 2005;25(16):6980-6989. Erratum in: *Mol Cell Biol*. 2005;25(24):11191. [CrossRef]
50. Zhou Y, Yan H, Li T, Xie M, Li X, Zhao C. New use of old medicine: Nifedipine acts on the TRP family and inflammatory proteins in the treatment of chilblain. *Burns*. 2022;48(2):372-380. [CrossRef]
51. Chi-Xianggeng, Hu-Bo, Yu SY, et al. Losartan treating podocyte injury induced by Ang II via downregulation of TRPC6 in podocytes. *J Renin Angiotensin Aldosterone Syst*. 2015;16(4):1118-1124. [CrossRef]
52. Kumar S, Govindaraju K, Syed Abdul Kadir S, Abdul Majeed A, Hajirah Abd Jamil A, Abdul Rahim N. TRPC3 and TRPC6 as molecular mediators of resistant hypertension and cardiac fibrosis: a new therapeutic frontier. *Arterial Hypertension*. 2025;29:123-132. [CrossRef]

ARCHIVES OF THE TURKISH SOCIETY OF CARDIOLOGY

Official journal of the TURKISH SOCIETY OF CARDIOLOGY

Structural and Functional Cardiac Reverse Remodeling After Bariatric Surgery: A Prospective Comparison of Sleeve Gastrectomy and Roux-en-Y Gastric Bypass

Bariatrik Cerrahi Sonrası Yapısal ve Fonksiyonel Kardiyak Ters Yeniden Şekillenme: Sleeve Gastrektomi ve Roux-en-Y Gastrik Bypass'ın Prospektif Karşılaştırması

ABSTRACT

Objective: Obesity is associated with characteristic cardiac remodeling, including left ventricular (LV) hypertrophy, concentric geometry, and subclinical myocardial dysfunction. Bariatric surgery induces reverse cardiac remodeling; however, it remains unclear whether structural and functional recovery differ between sleeve gastrectomy (SG) and Roux-en-Y gastric bypass (RYGB), and to what extent these changes are driven by weight loss versus metabolic and inflammatory mechanisms.

Method: In this prospective observational cohort study, 100 adults with severe obesity (body mass index [BMI] > 35 kg/m^2) undergoing primary bariatric surgery (SG, n = 50; RYGB, n = 50) were evaluated at baseline and six months postoperatively. Clinical, metabolic, inflammatory, and echocardiographic parameters—including left ventricular mass index (LVMI), epicardial adipose tissue (EAT) thickness, diastolic function, and global longitudinal strain (GLS)—were assessed using standardized transthoracic echocardiography with speckle-tracking analysis. Multivariable regression identified independent predictors of structural (ΔLVMI) and functional (ΔGLS) improvement.

Results: Baseline characteristics were comparable between groups (mean age 35.9 years; 67% female; BMI 47.1 kg/m^2). Both procedures resulted in significant improvements in anthropometric, metabolic, inflammatory, and cardiac parameters. RYGB was associated with greater reductions in BMI (−10.74 ± 2.42 vs. −9.32 ± 2.42 kg/m^2; P = 0.004), glycated hemoglobin (HbA1c) (median −1.40% vs. −0.90%; P = 0.007), and C-reactive protein (CRP) (P = 0.029). Structural reverse remodeling was more pronounced following RYGB, with greater reductions in LVMI (median −12.0 vs. −6.5 g/m$^{2.7}$; P < 0.001) and EAT thickness (−1.20 vs. −0.70 mm; P = 0.014). GLS improved in both groups (−2.33% vs. −1.40%; P = 0.031). However, multivariable analysis demonstrated that improvement in GLS was independently associated with baseline GLS, reduction in LV mass, and improvements in HbA1c and CRP, rather than the type of surgical procedure.

Conclusion: Bariatric surgery leads to significant reverse cardiac remodeling in patients with severe obesity. RYGB is associated with greater structural regression, whereas improvement in myocardial deformation appears to be primarily driven by metabolic improvement and inflammatory changes rather than surgical technique. These findings suggest that cardiac recovery reflects an integrated process involving structural, metabolic, and inflammatory restoration beyond weight loss alone.

Keywords: Bariatric surgery, epicardial adipose tissue, global longitudinal strain, left ventricular remodeling, obesity

ÖZET

Amaç: Obezitenin karakteristik bir kardiyak yeniden şekillenme süreciyle yakın ilişkisi vardır. Bu süreç, sıklıkla sol ventrikül (LV) hipertrofisini, konsantrik geometri değişimlerini ve alt düzeyde seyreden subklinik miyokardiyal disfonksiyonu kapsar. Bariatrik cerrahi girişimlerinin kardiyak yapıda tersine iyileşme sağladığı bilinmektedir. Ancak sleeve gastrektomi (SG) ile Roux-en-Y gastrik bypass (RYGB) uygulamaları arasında yapısal ya da fonksiyonel düzelme açısından belirgin bir fark olup olmadığı henüz tam olarak aydınlatılamamıştır. Ayrıca gözlenen bu olumlu değişimlerin doğrudan kilo kaybına mı, yoksa altta yatan metabolik ve inflamatuar mekanizmalara mı dayandığı sorusu literatürde güncelliğini korumaktadır.

ORIGINAL ARTICLE
ARAŞTIRMA MAKALESİ

Kareem Ali Maher[1]
Reda Nabil Dawoud[1]
Osama Abouelfetouh Elshaer[1]
Ramy Magdy Elgamal[1]
Mohamed Shokry Fahmy[1]
Ezz Eldin Ebrahim Gaber[1]
Dina Ahmed Muhammad Abdelmoneim[2]
Mohamed Elsayed Abdelfattah[1]
Reda Biomy[1]
Wael Anwar Hasib[1]

[1]*Department of Cardiovascular Medicine, Kafrelsheikh University Hospital, Kafrelsheikh, Egypt*
[2]*Mansoura Specialized Hospital, Mansoura, Egypt*

Corresponding author:
Osama Abouelfetouh Elshaer
✉ osamaelshaer568@gmail.com

Received: March 10, 2026
Accepted: April 08, 2026

Cite this article as: Maher KA, Dawoud RN, Elshaer OA, et al. Structural and Functional Cardiac Reverse Remodeling After Bariatric Surgery: A Prospective Comparison of Sleeve Gastrectomy and Roux-en-Y Gastric Bypass. *Turk Kardiyol Dern Ars.* 2026;54(6):471–479.

DOI: 10.5543/tkda.2026.23796

Yöntem: Prospektif ve gözlemsel olarak tasarlanan bu kohort araştırmasına, primer bariatrik cerrahi geçirecek ve şiddetli obezite tanısı almış (VKİ>35 kg/m²) 100 yetişkin hasta dâhil edildi. Cerrahi yöntem olarak katılımcıların yarısına SG (n=50), diğer yarısına ise RYGB (n=50) uygulandı. Tüm olgular, ameliyat öncesi başlangıç döneminde ve postoperatif altıncı ayda ayrıntılı olarak incelendi. Hastaların klinik, metabolik ve inflamatuar bulguları ile birlikte çok sayıda ekokardiyografik parametresi ölçüldü. Bu kapsamda, standardize transtorasik ekokardiyografi ve speckle-tracking analizi kullanılarak sol ventrikül kitle indeksi (LVMİ), epikardiyal yağ dokusu (EAT) kalınlığı, diyastolik işlevler ve global longitudinal strain (GLS) değerleri kaydedildi. Yapısal (ΔLVMİ) ve fonksiyonel (ΔGLS) düzelmelerin bağımsız yordayıcılarını belirlemek amacıyla çok değişkenli regresyon analizleri yapıldı.

Bulgular: Grupların başlangıçtaki klinik özellikleri birbiriyle oldukça benzerdi (ortalama yaş 35,9; katılımcıların %67'si kadın; ortalama VKİ 47,1 kg/m²). Uygulanan her iki cerrahi yöntem de hastaların antropometrik, metabolik, inflamatuar ve kardiyak profillerinde kayda değer düzelmeler sağladı. Ancak bazı parametrelerde RYGB uygulamasının daha üstün sonuçlar verdiği gözlendi. Özellikle VKİ'de (−10.74±2.42'ye karşı −9.32±2.42 kg/m²; P = 0.004), HbA1c'de (ortanca −%1.40'a karşı −%0.90; P = 0.007) ve CRP düzeylerinde (P = 0.029) görülen düşüş RYGB grubunda daha belirgindi. Yapısal ters yeniden şekillenme açısından da RYGB sonrası tablo daha dikkat çekiciydi; nitekim LVMİ gerilemesi (ortanca −12.0'a karşı −6.5 g/m²,⁷; P<0.001) ve EAT azalması (−1.20'ye karşı −0.70 mm; P = 0.014) daha fazlaydı. Beklenildiği üzere GLS değerleri her iki grupta da iyileşme eğilimi gösterdi (−%2.33'e karşı −%1.40; P = 0.031). Buna rağmen çok değişkenli analizler, miyokardiyal fonksiyondaki bu toparlanmanın cerrahi prosedürden ziyade hastanın başlangıç GLS değeri, sol ventrikül kitlesindeki azalma, HbA1c regülasyonu ve CRP düşüşü ile bağımsız olarak ilişkili olduğunu gösterdi.

Sonuç: Şiddetli obezite olgularında bariatrik cerrahinin, kardiyak yapıda güçlü bir tersine iyileşme sağladığı açıktır. RYGB, daha yüksek düzeyde yapısal gerilemeyle ilişkilidir. Öte yandan miyokardiyal deformasyondaki toparlanma süreci, seçilen anatomik cerrahiden çok metabolik iyileşme ve inflamasyonun baskılanmasıyla tetiklenmektedir. Tüm bu bulgular, kardiyak işlevlerin geri kazanılmasının yalnızca basit bir kilo kaybının sonucu olmadığını; aksine yapısal, metabolik ve inflamatuar mekanizmaların karmaşık ve eş güdümlü restorasyonu sayesinde gerçekleştiğini düşündürmektedir.

Anahtar Kelimeler: Bariatrik cerrahi, epikardiyal yağ dokusu, global longitudinal strain, sol ventrikül yeniden şekillenmesi, obezite

Obesity affects more than 650 million adults worldwide and has redefined the traditional spectrum of cardiovascular disease.[1,2] It is associated with a distinct pattern of cardiac disease characterized by left ventricular (LV) hypertrophy and concentric remodeling. Although standard assessments often demonstrate preserved ejection fraction, affected individuals frequently exhibit underlying diastolic dysfunction and subclinical systolic impairment. Because conventional echocardiography may fail to detect these early abnormalities, two-dimensional speckle-tracking-derived global longitudinal strain (GLS) has emerged as an optimal diagnostic tool.[3] This remodeling is driven by multiple interrelated mechanisms, including chronic hemodynamic stress resulting from increased blood volume and elevated cardiac output, compounded by metabolic disturbances such as lipotoxicity and insulin resistance.[4] Additionally, visceral and epicardial fat depots contribute to ongoing tissue injury through systemic and paracrine inflammatory mechanisms.[5]

Bariatric surgery is the most effective long-term treatment for severe obesity (body mass index [BMI] ≥ 35 kg/m²), offering substantial benefits for both body composition and metabolic function. Sleeve gastrectomy (SG) and Roux-en-Y gastric bypass (RYGB) both result in significant weight loss; however, their distinct surgical approaches produce different physiological effects. RYGB alters gut hormone pathways—most notably increasing glucagon-like peptide-1 (GLP-1) and peptide YY (PYY)—leading to rapid improvements in blood sugar control, often preceding meaningful weight reduction. In contrast, SG primarily restricts stomach size and modulates ghrelin levels.[6] Following either procedure, the heart undergoes significant reverse remodeling, including reductions in LV mass, improved diastolic function, and enhanced GLS.[7] Systemic inflammation

ABBREVIATIONS

ASE	American Society of Echocardiography
CRP	C-reactive protein
EACVI	European Association of Cardiovascular Imaging
EAT	Epicardial adipose tissue
GLP-1	Glucagon-like peptide-1
GLS	Global longitudinal strain
HbA1c	Glycated hemoglobin
LDL-C	Low-density lipoprotein cholesterol
LV	Left ventricular
LVEF	Left ventricular ejection fraction
LVMI	Left ventricular mass index
LVMI	Left ventricular mass index
PYY	Peptide YY
RYGB	Roux-en-Y gastric bypass
SG	Sleeve gastrectomy
TNF-α	Tumor necrosis factor-alpha

also declines markedly after surgery, as evidenced by decreased levels of C-reactive protein (CRP), interleukin-6 (IL-6), and tumor necrosis factor-alpha (TNF-α).[8] However, most studies combine multiple procedures or rely on uncontrolled observational data, limiting the availability of true direct comparisons.[6] Any procedure-specific advantage may have important clinical implications.

A critical question emerges from these findings: does cardiac recovery simply reflect mechanical unloading from weight loss, or do the distinct metabolic effects of specific procedures drive differential remodeling? The emerging concept of an "enterocardiac" pathway supports the latter. Indeed, reductions in visceral fat and resolution of systemic inflammation may influence cardiac outcomes more profoundly than absolute reductions in BMI.[9] This potential procedure-specific advantage carries substantial clinical significance. If RYGB confers superior, weight-independent cardiac benefits, this could fundamentally reshape surgical decision-making for patients with obesity and underlying heart failure.

To address this gap in the literature, we prospectively compared SG and RYGB in patients with severe obesity. Our primary objective was to quantify six-month changes in LV mass index and GLS, enabling us to disentangle the contributions of mechanical unloading, metabolic adaptation, and inflammatory attenuation to cardiac reverse remodeling. Our hypothesis was specific. We expected RYGB to induce greater structural regression of LV mass. In contrast, we anticipated that improvements in GLS would be largely independent of anatomy, reflecting instead profound systemic metabolic and inflammatory changes.

Materials and Methods

This prospective observational cohort study was conducted at the Departments of Cardiology and General Surgery of a large university hospital between May 2024 and June 2025. Participants were evaluated at baseline (preoperative) and at six months following surgery. The study protocol received The Scientific Research Ethics Committee of Kafrelsheikh University (Approval Number: KFSIRB200-225, Date: 29.04.2024), and was conducted in accordance with the Declaration of Helsinki. Written informed consent was obtained from all participants prior to enrollment. The study was reported in accordance with the Strengthening the Reporting of Observational Studies in Epidemiology (STROBE) guidelines for observational studies.

Eligible participants were adults (≥ 18 years) with obesity and a BMI > 35 kg/m^2 who had an indication for primary bariatric surgery, as determined by the treating surgical team. Patients were enrolled consecutively. To isolate obesity-related subclinical cardiac remodeling, individuals with established cardiac disease were excluded, including prior myocardial infarction or ischemic heart disease, greater-than-mild valvular disease, previous cardiac surgery, persistent atrial fibrillation, left bundle branch block, or prior bariatric procedures. Patients with inadequate acoustic windows for speckle-tracking analysis (defined as > 2 non-traceable myocardial segments on baseline echocardiography) were also excluded.[10]

During recruitment, 27 patients were excluded to achieve the target of 50 evaluable patients per group: five due to prior myocardial infarction, one due to previous cardiac surgery, two due to persistent atrial fibrillation, seven due to prior bariatric surgery, and 12 due to poor acoustic windows.

Sample size was calculated a priori based on the primary endpoint, defined as the absolute change in global longitudinal strain (ΔGLS). To detect a between-group difference of 1.5 percentage points (assuming a standard deviation of 2.2) with 90% statistical power and a two-sided α level of 0.05, at least 46 patients per group was required. To account for potential attrition during follow-up, 100 patients were initially enrolled.[4]

Participants were recruited consecutively according to their scheduled surgical procedure. Enrollment continued until 50 evaluable patients were obtained in each surgical group: sleeve gastrectomy and Roux-en-Y gastric bypass. The choice of surgical procedure was determined by the treating surgical team in accordance with routine clinical practice.

At both study visits, standardized clinical evaluation included medical history, medication use, smoking status, and physical measurements (resting blood pressure and heart rate). Fasting blood samples were analyzed in the hospital laboratory using validated assays to measure plasma glucose, glycated hemoglobin (HbA1c), total cholesterol, triglycerides, low-density lipoprotein cholesterol (LDL-C), C-reactive protein, and interleukin-6.

Transthoracic echocardiography was performed using a Philips EPIQ 7C system with electrocardiographic (ECG) gating, in accordance with recommendations from the European Association of Cardiovascular Imaging and the American Society of Echocardiography.[11] Three cardiac cycles per view were stored in DICOM (Digital Imaging and Communications in Medicine) format, and identical acquisition and analysis settings were applied at baseline and follow-up to minimize measurement variability.

Left ventricular dimensions and wall thickness were measured from parasternal long-axis views using 2D-guided M-mode recordings to ensure optimal alignment with the LV long axis, in accordance with current recommendations from the American Society of Echocardiography (ASE) and the European Association of Cardiovascular Imaging (EACVI). Left ventricular mass was calculated using the Devereux-modified ASE formula and indexed to height$^{2.7}$ to derive the left ventricular mass index (LVMI), while left ventricular ejection fraction (LVEF) was calculated using the biplane Simpson method. Epicardial adipose tissue (EAT) thickness was measured at the end-systole over the right ventricular free wall in parasternal long- and short-axis views at the point of maximal thickness. The mean of three measurements was recorded.

Two-dimensional speckle-tracking echocardiography was acquired from apical two-, three-, and four-chamber views, with frame rates optimized between 50 and 80 frames/s. Offline analysis was performed using Philips QLAB software, with semi-automated endocardial border tracking and manual adjustment when required. Global longitudinal strain was calculated as the mean peak systolic strain across a 17-segment model.

All analyses were performed by a single primary reader blinded to patient identifiers, surgical procedure, and time point. Baseline and follow-up studies were analyzed in randomized order to

Table 1. Baseline characteristics of patients undergoing sleeve gastrectomy and RYGB

Variables	Sleeve gastrectomy (n = 50)	RYGB (n = 50)	*P*	Effect size
Demographic characteristics				
Age (years), mean ± SD	36.52 ± 8.52	35.28 ± 7.84	0.451	d = 0.15
Female sex, n (%)	32 (64%)	35 (70%)	0.523	Φ = 0.064
Comorbidities				
Hypertension, n (%)	28 (56%)	26 (52%)	0.688	Φ = 0.040
Diabetes mellitus, n (%)	15 (30%)	20 (40%)	0.295	Φ = 0.105
Hyperlipidemia, n (%)	27 (54%)	29 (58%)	0.687	Φ = 0.040
Smoking, n (%)	9 (18%)	7 (14%)	0.585	Φ = 0.055
Medications				
Antihypertensive therapy, n (%)	18 (36%)	18 (36%)	1.000	Φ = 0.000
Antidiabetic therapy, n (%)	13 (26%)	17 (34%)	0.383	Φ = 0.087
Statin therapy, n (%)	19 (38%)	21 (42%)	0.683	Φ = 0.041
Clinical parameters				
SBP (mmHg)	139.26 ± 17.60	135.96 ± 18.77	0.367	d = 0.18
DBP (mmHg)	92.10 ± 9.83	90.64 ± 7.29	0.401	d = 0.17
BMI (kg/m²)	46.49 ± 5.43	47.80 ± 6.87	0.291	d = −0.21
Waist circumference (cm)	127.08 ± 17.70	130.20 ± 18.48	0.391	d = −0.17
CRP (mg/L)	12.27 ± 8.80	12.34 ± 7.63	0.966	d = −0.01
Echocardiographic parameters				
LVMI (g/m$^{2.7}$)	51.39 ± 11.95	50.13 ± 10.60	0.579	d = 0.11
Ejection fraction (%)	57.46 ± 4.91	57.09 ± 5.63	0.730	d = 0.07
E/A ratio	1.16 ± 0.33	1.20 ± 0.30	0.579	d = −0.14
E/e′ ratio	9.28 ± 2.42	9.94 ± 2.34	0.166	d = -0.28
LAVI (mL/m²)	15.90 ± 2.84	15.75 ± 2.52	0.774	d = 0.06
GLS (%)	−17.97 ± 1.56	−17.61 ± 1.89	0.291	d = −0.21
Epicardial adipose tissue thickness (mm)	5.10 ± 0.78	5.24 ± 0.90	0.391	d = −0.17

BMI, Body mass index; CRP, C-reactive protein; DBP, Diastolic blood pressure; E/A, Ratio of peak early to late diastolic filling velocity; EAT, Epicardial adipose tissue; GLS, Global longitudinal strain; LAVI, Left atrial volume index; LVMI, Left ventricular mass index; RYGB, Roux-en-Y gastric bypass; SBP, Systolic blood pressure; SD, Standard deviation; SG, Sleeve gastrectomy. Continuous variables are presented as mean ± standard deviation and compared using the independent samples t-test. Categorical variables are presented as number (percentage) and compared using Pearson's chi-square test. Effect sizes are reported as Cohen's d for continuous variables and the Phi coefficient for categorical variables. A P value < 0.05 was considered statistically significant.

minimize chronological bias. Interobserver reproducibility for GLS was assessed in 20 randomly selected studies, demonstrating excellent agreement (intraclass correlation coefficient 0.946, 95% confidence interval [CI]: 0.872–0.978; P < 0.001).

Statistical Analysis

Continuous variables are reported as mean ± standard deviation or median (interquartile range), as appropriate, and categorical variables as counts and percentages. Normality was assessed using the Shapiro–Wilk test and visual inspection of histograms. Between-group comparisons were performed using the independent samples t-test or the Mann–Whitney U test for continuous variables, and Pearson's chi-square test for categorical variables. Between-group differences are presented as mean differences with 95% confidence intervals for parametric variables and as Hodges–Lehmann median differences with 95% CI for nonparametric variables. Associations between continuous variables were evaluated using Spearman rank correlation. Effect sizes (Cohen's d, rank-biserial r, or Phi φ) were also calculated.

Multivariable linear regression (enter method) was used to identify independent predictors of cardiac improvement. Standardized (β) and unstandardized (B) coefficients with 95% CI are reported. The ΔLVMI model included baseline LV mass index, procedure type, ΔHbA1c, and excess weight loss (EWL%). The ΔGLS model included baseline GLS, ΔLV mass, ΔHbA1c, ΔCRP, ΔEAT, EWL%, and procedure type. Baseline values of the dependent variables were included to account for regression to the mean. Collinearity diagnostics confirmed no significant multicollinearity. Change in BMI was not entered separately into the multivariable models to preserve model parsimony and avoid conceptual redundancy. Instead, excess weight loss was retained as the primary anthropometric predictor, as it represents the standardized metric in bariatric literature and accounts for baseline variations in excess weight. Statistical analyses were performed using SPSS version 28.0 (IBM Corp., Armonk, NY, USA). All tests were two-sided, with P < 0.05 considered statistically significant.

Table 2. Six-month changes following sleeve gastrectomy and RYGB

Variables	Sleeve gastrectomy (n = 50)	RYGB (n = 50)	*p*	Effect size	Difference (95% CI)
Anthropometric and hemodynamic changes					
ΔBMI (kg/m²)	−9.32 ± 2.42	−10.74 ± 2.42	0.004	d = 0.59	1.42 (0.46 to 2.38)
EWL (%)	45.55 ± 14.73	50.22 ± 14.30	0.112	d = 0.32	4.66 (−1.10 to 10.43)
ΔSBP (mmHg)	−13.96 ± 6.66	−13.12 ± 6.22	0.516	d = -0.13	−0.84 (−3.40 to 1.72)
Metabolic improvements					
ΔHbA1c (%)	−0.90 (−1.40 to −0.30)	−1.40 (−2.10 to −0.70)	0.007	r = 0.27	0.30 (0.10 to 0.50)
ΔTC (mg/dL)	−29.38 ± 25.10	−42.42 ± 21.00	0.006	d = 0.56	13.04 (3.88 to 22.20)
ΔTG (mg/dL)	−48 (−90 to −15)	−65 (−120 to −30)	0.200	r = 0.13	11 (−6 to 29)
Inflammatory markers					
ΔCRP (mg/L)	−3.10 (−6.00 to −1.00)	−4.80 (−8.20 to −2.30)	0.029	r = 0.22	2.10 (0.20 to 3.90)
ΔIL-6 (pg/mL)	−1.20 (−2.10 to −0.40)	−2.10 (−3.50 to −1.10)	0.028	r = 0.22	0.73 (0.08 to 1.32)
Cardiac structural remodeling and functional improvement					
ΔLVMI (g/m²)	−6.50 (−11.00 to −2.00)	−12.00 (−18.00 to −6.00)	<0.001	r = 0.43	1.76 (1.04 to 2.39)
ΔRWT	−0.035 (−0.050 to −0.030)	−0.050 (−0.060 to −0.040)	<0.001	r = 0.36	0.01 (0.01 to 0.02)
ΔEAT (mm)	−0.70 (−1.20 to −0.30)	−1.20 (−1.80 to −0.60)	0.014	r = 0.26	0.50 (0.10 to 0.90)
ΔGLS (%)	−1.40 ± 2.22	−2.33 ± 2.01	0.031	d = 0.44	0.93 (0.10 to 1.76)
ΔE/A ratio	0.10 (−0.05 to 0.30)	0.18 (0.02 to 0.40)	<0.001	r = 0.41	−0.08 (−0.04 to −0.12)
ΔE/e′ ratio	−0.74 ± 1.04	−1.00 ± 1.68	0.353	d = 0.19	0.26 (−0.29 to 0.82)
ΔLAVI (mL/m²)	1.27 ± 1.37	1.15 ± 1.45	0.684	d = 0.08	0.12 (−0.45 to 0.68)
ΔEF (%)	2.10 ± 2.13	2.48 ± 2.48	0.411	d = 0.17	−0.38 (−1.29 to 0.53)

Δ, Absolute change from baseline; BMI, Body mass index; CI, Confidence interval; CRP, C-reactive protein; E/A, Ratio of peak early to late diastolic filling velocity; E/e′, Ratio of early diastolic mitral inflow velocity to early diastolic annular velocity; EAT, Epicardial adipose tissue; EF, Ejection fraction; EWL, Excess weight loss; GLS, Global longitudinal strain; HbA1c, Glycated hemoglobin; IL-6, Interleukin-6; LAVI, Left atrial volume index; LVMI, Left ventricular mass index; RWT, Relative wall thickness; RYGB, Roux-en-Y gastric bypass; SBP, Systolic blood pressure; SG, Sleeve gastrectomy; TC, Total cholesterol; TG, Triglycerides. Data are presented as mean ± standard deviation for normally distributed variables and as median (interquartile range) for non-normally distributed variables. Between-group comparisons were performed using the independent samples t-test for normally distributed variables and the Mann–Whitney U test for non-normally distributed variables. Effect sizes are reported as Cohen's d for parametric variables and rank-biserial correlation (r) for nonparametric variables. Between-group differences are presented as mean differences with 95% confidence intervals (CI) for parametric variables and as Hodges–Lehmann median differences with 95% CI for nonparametric variables. All tests were two-tailed, and a P value < 0.05 was considered statistically significant.

Results

A total of 100 patients with severe obesity were prospectively enrolled, including 50 undergoing sleeve gastrectomy and 50 undergoing Roux-en-Y gastric bypass. Baseline demographic, clinical, metabolic, and echocardiographic characteristics were broadly comparable between the groups, with no statistically significant differences observed (Table 1). The cohort had a mean age of 35.9 years (SG: 36.52 ± 8.52 years; RYGB: 35.28 ± 7.84 years), and two-thirds of participants were female. The mean BMI was 47.1 kg/m². Comorbidities, including hypertension, diabetes mellitus, and hyperlipidemia, were similarly distributed between groups. Baseline echocardiographic parameters, including left ventricular mass index, global longitudinal strain, ejection fraction, E/A ratio, and epicardial adipose tissue thickness, were also comparable across groups.

At the six-month follow-up, both procedures produced substantial improvements in anthropometric, hemodynamic, metabolic, and inflammatory parameters (Table 2). RYGB was associated with a significantly greater reduction in BMI compared with SG (P = 0.004; Cohen's d = 0.59). However, excess weight loss and reductions in systolic blood pressure did not differ significantly between groups. Metabolic improvements were more pronounced following RYGB, including greater reductions in HbA1c (P = 0.007; rank-biserial r = 0.27) and total cholesterol (P = 0.006; Cohen's d = 0.56), while triglyceride reductions were comparable (P = 0.200). Inflammatory markers decreased significantly in both groups, with RYGB yielding larger reductions in C-reactive protein (P = 0.029; r = 0.22) and interleukin-6 (P = 0.028; r = 0.22).

Significant cardiac reverse remodeling was observed postoperatively in both groups, with greater reductions in LVMI (P < 0.001; r = 0.43), relative wall thickness (RWT; P < 0.001; r = 0.36), and EAT thickness (P = 0.014; r = 0.26) following RYGB. Myocardial function improved more markedly after RYGB, as evidenced by improvements in GLS (P = 0.031; Cohen's d = 0.44) and the E/A ratio (P < 0.001; r ≈ 0.41). Changes in left ventricular ejection fraction were modest and similar between groups (P = 0.411).

A moderate positive correlation was observed between ΔLVMI and ΔGLS (Spearman ρ = 0.465, P < 0.001), indicating that greater structural regression was associated with greater functional recovery (Figure 1). Multivariable linear regression analyses (Table 3) identified independent predictors of cardiac remodeling. For

Table 3. Multivariable linear regression analysis of predictors of left ventricular mass regression and global longitudinal strain improvement

Predictor	ΔLVMI (Structural remodeling)			ΔGLS (Functional Improvement)		
	B (95% CI)	β	*P*	B (95% CI)	β	*P*
Procedure type	−1.521 (−2.05 to −0.99)	−0.372	< 0.001	0.232 (−0.49 to 0.95)	0.055	0.529
Baseline LVMI	−0.122 (−0.15 to −0.09)	−0.670	< 0.001	—	—	—
Baseline GLS	—	—	—	−0.321 (−0.54 to −0.10)	−0.260	0.004
ΔHbA1c	0.463 (0.01 to 0.91)	0.133	0.045	0.674 (0.02 to 1.33)	0.185	0.043
EWL (%)	−0.004 (−0.02 to 0.01)	−0.030	0.627	−0.015 (−0.04 to 0.01)	−0.105	0.239
ΔLV Mass	—	—	—	0.261 (0.08 to 0.44)	0.250	0.006
ΔCRP	—	—	—	0.046 (0.00 to 0.09)	0.181	0.032
ΔEAT	—	—	—	0.360 (−0.01 to 0.73)	0.168	0.052

B, Unstandardized coefficient; β, Standardized beta coefficient; CI, Confidence interval; CRP, C-reactive protein; EAT, Epicardial adipose tissue; EWL, Excess weight loss; GLS, Global longitudinal strain; HbA1c, Glycated hemoglobin; LV, Left ventricular; LVMI, Left ventricular mass index.Multivariable linear regression analyses were performed using the enter method. Results are presented as standardized beta coefficients (β) and unstandardized coefficients (B) with 95% confidence intervals (CI). The ΔLVMI model included baseline left ventricular mass index (LVMI), procedure type (sleeve gastrectomy vs. Roux-en-Y gastric bypass), change in glycated hemoglobin (ΔHbA1c), and excess weight loss (EWL%). The ΔGLS model included baseline global longitudinal strain (GLS), change in LV mass index (ΔLVMI), ΔHbA1c, change in C-reactive protein (ΔCRP), change in epicardial adipose tissue thickness (ΔEAT), EWL%, and procedure type. Baseline values of the dependent variables were included to account for regression to the mean and interindividual variability. Collinearity diagnostics were assessed using variance inflation factors (VIF), with no evidence of significant multicollinearity. All tests were two-tailed, and a P value < 0.05 was considered statistically significant.

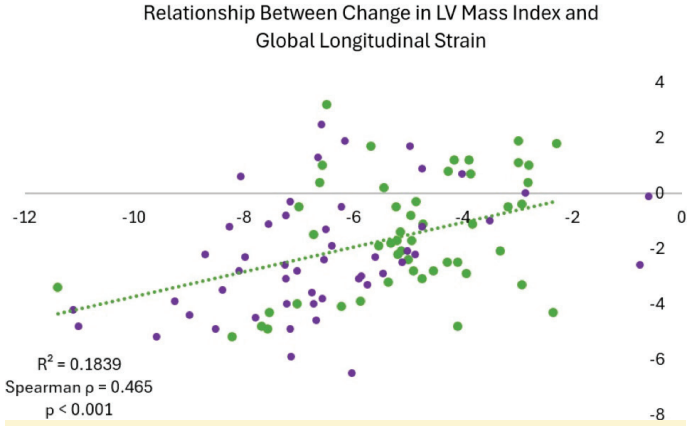

Figure 1. Association between changes in left ventricular mass index and global longitudinal strain following bariatric surgery. Scatter plot illustrating the relationship between change in left ventricular mass index (ΔLVMI) and change in global longitudinal strain (ΔGLS) at six months after bariatric surgery. Each point represents an individual patient. A moderate positive correlation was observed between LVMI regression and improvement in myocardial deformation (Spearman ρ = 0.465; P < 0.001), indicating that greater structural reverse remodeling was associated with greater functional recovery.

ΔLVMI, significant predictors included procedure type (RYGB vs. SG; β = -0.372; P < 0.001), baseline LVMI (β = -0.670; P < 0.001), and ΔHbA1c (β = 0.133; P = 0.045), whereas EWL% was not significant. This model explained 64% of the variance (adjusted R^2 = 0.643). For ΔGLS, independent predictors were baseline GLS (β = -0.260; P = 0.004), ΔLVMI (β = 0.250; P = 0.006), ΔHbA1c (β = 0.185; P = 0.043), and ΔCRP (β = 0.181; P = 0.032), with ΔEAT showing borderline significance (β = 0.168; P = 0.052). Procedure type and EWL% were not independently associated. No multicollinearity was detected (variance inflation factors < 2.5), and the model explained 44% of the variance (adjusted R^2 = 0.441).

Discussion

In this prospective cohort of patients with severe obesity undergoing bariatric surgery, we observed a coordinated pattern of cardiac recovery characterized by partially distinct structural and functional responses. Structural reverse remodeling of the left ventricle was strongly influenced by surgical procedure, with Roux-en-Y gastric bypass producing greater regression of LV mass. In contrast, improvement in myocardial deformation appeared largely independent of surgical anatomy and was instead associated with metabolic improvement, attenuation of systemic inflammation, and the magnitude of LV mass regression. Collectively, these findings suggest that structural and functional myocardial recovery after bariatric surgery are driven by overlapping but distinct mechanisms: surgical anatomy primarily influences LV mass regression, whereas metabolic and inflammatory improvements predominantly drive recovery of myocardial deformation.

Both procedures resulted in significant regression of LVMI; however, the magnitude of change was substantially greater after Roux-en-Y gastric bypass, with nearly double the median reduction compared with sleeve gastrectomy (P < 0.001). Importantly, procedure type remained an independent predictor of LVMI regression after multivariable adjustment (β = −0.372, P < 0.001), supporting a procedure-specific effect beyond baseline metabolic differences.

The degree of LV mass regression observed in our cohort is consistent with prior pooled analyses. Aggarwal et al.[4] reported a 12.2% reduction in LV mass, a finding supported by the large meta-analysis of Sargsyan et al.[12] Similarly, Cuspidi et al.,[13] in a meta-analysis of 1,022 patients, demonstrated significant reductions in both LV mass and relative wall thickness following bariatric surgery. Our findings extend this evidence by directly comparing surgical modalities within a single prospective cohort.

Interestingly, excess weight loss did not independently predict LVMI regression in our cohort. This finding is consistent with the long-term study by Sorimachi et al.,[14] which demonstrated

that reductions in visceral adipose tissue, rather than overall BMI change, were more strongly associated with improvements in LV mass. This concept is further supported by prior work indicating that obesity-related cardiac remodeling is influenced not only by total body weight but also by visceral adiposity, inflammatory activation, and neurohormonal pathways that directly affect myocardial structure. Direct comparisons of cardiac outcomes between SG and RYGB are limited. Kokkinos et al.[15] reported broadly comparable effects on weight loss and cardiovascular parameters, with RYGB conferring modestly greater benefits on selected indices. More recently, Henry et al.[16] demonstrated that both RYGB and sleeve gastrectomy produced greater reverse remodeling (particularly in LV mass and concentric geometry) than adjustable gastric banding. These findings support our observation of procedure-related differences in structural regression, while also highlighting that both restrictive–malabsorptive and purely restrictive approaches outperform gastric banding.

The more pronounced reverse remodeling observed after Roux-en-Y gastric bypass may therefore reflect not only greater metabolic improvement but also procedure-specific physiological effects. The BRAVE mechanisms (Bile flow alteration, Reduction of gastric size, Anatomical gut rearrangement and altered nutrient flow, Vagal manipulation, and Enteric hormone modulation) described by Ashrafian et al.,[17] including alterations in gut hormone signaling such as GLP-1 and ghrelin, provide a plausible biological framework. These hormonal adaptations may exert direct myocardial effects via an enterocardiac axis, potentially contributing to the enhanced structural response observed in our cohort.

Both surgical groups demonstrated significant improvement in global longitudinal strain, with a greater mean change observed after Roux-en-Y gastric bypass (P = 0.031). The magnitude of GLS improvement is consistent with prior pooled evidence, including the large meta-analysis by Sargsyan et al.[12] and earlier observations by Ikonomidis et al.[18] However, after multivariable adjustment, procedure type was no longer independently associated with ΔGLS. Instead, functional recovery was independently associated with baseline GLS, reduction in LV mass, improvement in HbA1c, and reduction in CRP. The independent association between ΔCRP and ΔGLS provides imaging-based support for the concept that low-grade inflammation contributes meaningfully to obesity-related myocardial dysfunction, as proposed by Ashrafian et al.[17,19]

These findings align with growing evidence that adipose tissue distribution, rather than total body weight alone, plays a central role in obesity-related cardiac dysfunction. Sorimachi et al.[14] demonstrated stronger associations between reductions in visceral adipose tissue and improvements in myocardial strain parameters than with BMI reduction. Consistent with this observation, excess weight loss was not independently associated with ΔGLS in our cohort. Epicardial adipose tissue thickness declined significantly after surgery—more prominently following RYGB—with a borderline association between ΔEAT and ΔGLS after multivariable adjustment (P = 0.052). Although this did not reach conventional statistical significance, the direction and magnitude of the association suggest that epicardial adiposity may contribute to myocardial functional recovery.

Experimental and imaging studies provide further mechanistic context. Epicardial fat is increasingly recognized as a metabolically active compartment capable of modulating myocardial function through local inflammatory signaling and mechanical ventricular interaction. Cardiac magnetic resonance imaging offers additional insight into this relationship. Gaborit et al.[20] reported a 27% reduction in epicardial fat volume six months after bariatric surgery—proportionally smaller than the 40% decrease in visceral abdominal fat—yet independent of BMI or visceral fat changes, with no alteration in myocardial triglyceride content. These observations suggest that epicardial adipose tissue represents a metabolically distinct compartment, with effects on myocardial function mediated primarily through paracrine inflammatory signaling and ventricular mechanical interaction rather than direct lipid infiltration.

The independent association between improvement in HbA1c and recovery of myocardial deformation in our cohort likely reflects restoration of myocardial metabolic efficiency following bariatric surgery. Using combined positron emission tomography (PET) and cardiac magnetic resonance imaging, Hannukainen et al.[21] demonstrated that morbid obesity is characterized by impaired myocardial substrate metabolism, including increased reliance on free fatty acid utilization and reduced glucose uptake—abnormalities that normalize after bariatric surgery in parallel with improvements in cardiac structure and function. Consistent with this concept, Iqbal et al.[22] reported that bariatric surgery leads to rapid improvements in insulin sensitivity and glycemic control, often preceding substantial weight loss, thereby highlighting a weight-independent metabolic contribution to cardiovascular recovery. Together, these findings provide a mechanistic framework linking glycemic improvement to recovery of myocardial deformation after bariatric surgery.

Beyond systolic deformation, our study also demonstrated improvement in diastolic function alongside regression of concentric geometry, reflected by a significant increase in the E/A ratio and a reduction in relative wall thickness. Additional indices of filling pressure and atrial remodeling improved following surgery in both groups. The E/e′ ratio declined after intervention; however, the magnitude of change did not differ significantly between procedures (ΔE/e′ −0.74 vs. −1.00; P = 0.353). Similarly, the left atrial volume index (LAVI), indexed to body surface area, showed modest changes without a significant between-group difference (ΔLAVI 1.27 vs. 1.15 mL/m²; P = 0.684). These findings suggest that early postoperative improvement in diastolic function occurs after both procedures and may primarily reflect enhanced ventricular relaxation and more favorable loading conditions, whereas structural atrial remodeling may require longer follow-up to become evident.[23]

This overall pattern of reverse remodeling is consistent with pooled imaging evidence across diverse bariatric cohorts. In the largest contemporary meta-analysis including over 1,000 patients, Cuspidi et al.,[13] reported significant reductions in LV mass and RWT, accompanied by improvements in diastolic indices without meaningful change in ejection fraction. Similarly, Aggarwal et al.,[4] in a systematic review of 40 imaging studies (n = 1,486), demonstrated a weighted mean increase in E/A ratio of 0.189, along with an 11.2% reduction in LV mass index and an

approximately 2-mm decrease in left atrial diameter. Sargsyan et al.[12] further confirmed a pooled increase in E/A ratio of 0.155 (95% confidence interval [CI]: 0.106–0.205), accompanied by reductions in left atrial diameter and LV diastolic dimension, reinforcing the consistency of diastolic improvement following bariatric surgery.

Taken together, these findings suggest that the determinants of cardiac recovery after bariatric surgery may differ between structural and functional domains. In our cohort, Roux-en-Y gastric bypass was associated with more pronounced structural unloading and greater reductions in inflammation, whereas improvement in myocardial deformation was more closely related to metabolic and inflammatory changes than to surgical anatomy itself. This distinction shifts the focus from identifying a universally superior surgical procedure toward understanding the mechanisms most relevant for individual patients, potentially supporting a more tailored approach to cardiovascular risk reduction in severe obesity.

This study has several strengths. It was prospectively designed, with well-balanced baseline characteristics and rigorous exclusion criteria aimed at isolating obesity-related cardiac remodeling. Speckle-tracking analysis was standardized using a single imaging platform, demonstrating excellent reproducibility (intraclass correlation coefficient [ICC] = 0.946), and multivariable modeling accounted for baseline values and potential regression to the mean.

Certain limitations warrant consideration. First, the single-center, nonrandomized design introduces a risk of residual confounding despite robust statistical adjustment. Although the multivariable models accounted for excess weight loss, RYGB was associated with a significantly greater absolute reduction in BMI (P = 0.004); therefore, we cannot fully exclude the possibility that differences in the magnitude of weight loss contributed, at least in part, to the observed procedure-specific differences in LV mass regression. Second, although the six-month follow-up captures the most dynamic phase of reverse remodeling, it limits extrapolation to longer-term cardiac adaptation. Third, pharmacotherapy represents a potential confounder. While medication use was documented, we did not systematically quantify dose reduction or discontinuation of antihypertensive and antidiabetic agents. As these changes were more frequent following RYGB, withdrawal of hemodynamically active medications may have contributed to the observed myocardial recovery independently of surgical anatomy. Future studies should incorporate detailed tracking of medication dose adjustments to better isolate true procedure-specific effects. Finally, the absence of routine measurement of cardiac biomarkers, such as N-terminal pro–B-type natriuretic peptide (NT-proBNP), limits our ability to firmly bridge echocardiographic observations with the corresponding serological data and objective biochemical markers of ventricular wall stress.

Conclusion

In this prospective observational cohort of patients with severe obesity undergoing bariatric surgery, significant reverse cardiac remodeling was observed at six months, including reductions in left ventricular mass index and epicardial adipose tissue thickness, along with improvements in myocardial deformation and diastolic function. Roux-en-Y gastric bypass was associated with greater structural regression, whereas recovery of myocardial deformation was primarily related to metabolic improvement and reduction in systemic inflammation rather than surgical anatomy itself. These findings suggest that cardiac recovery after bariatric surgery reflects coordinated structural, metabolic, and inflammatory restoration that extends beyond weight loss alone.

Ethics Committee Approval: Ethics committee approval was obtained from The Scientific Research Ethics Committee of Kafrelsheikh University (Approval Number: KFSIRB200-225, Date: 29.04.2024).

Informed Consent: Written informed consent was obtained from the patients.

Conflict of Interest: The authors have no conflicts of interest to declare.

Funding: The authors declared that this study received no financial support.

Use of AI for Writing Assistance: Artificial intelligence-based tools were used to assist with language refinement and paraphrasing of the manuscript.

Author Contributions: Concept – K.A.M., O.A.E., M.E.A.; Design – K.A.M., R.N.D., O.A.E., M.S.F.; Supervision – R.M.E., M.S.F., E.E.E.G.; Resource – R.M.E., M.S.F., D.A.M.A.; Materials – K.A.M., R.N.D., O.A.E.; Data Collection and/or Processing – M.E.A., R.B., W.A.H.; Analysis and/or Interpretation – R.N.D., R.M.E., W.A.H.; Literature Review – E.E.E.G., D.A.M.A., R.B.; Writing – R.M.E., E.E.E.G., M.E.A., R.B.; Critical Review – M.S.F., D.A.M.A., W.A.H.

Peer-review: Externally peer-reviewed.

References

1. NCD Risk Factor Collaboration (NCD-RisC). Worldwide trends in underweight and obesity from 1990 to 2022: a pooled analysis of 3663 population-representative studies with 222 million children, adolescents, and adults. *Lancet*. 2024;403(10431):1027-1050.
2. Haththotuwa RN, Wijeyaratne CN, Senarath U. Chapter 1 - Worldwide epidemic of obesity. In: Mahmood TA, Arulkumaran S, Chervenak FA, eds. Obesity and Obstetrics. *Elsevier*;2020:3-8. [CrossRef]
3. Gherbesi E, Gianstefani S, Angeli F, et al. Myocardial strain of the left ventricle by speckle tracking echocardiography: From physics to clinical practice. *Echocardiography*. 2024;41(1):e15753. [CrossRef]
4. Aggarwal R, Harling L, Efthimiou E, Darzi A, Athanasiou T, Ashrafian H. The Effects of Bariatric Surgery on Cardiac Structure and Function: a Systematic Review of Cardiac Imaging Outcomes. *Obes Surg*. 2016;26(5):1030-1040. [CrossRef]
5. Henry JA, Abdesselam I, Deal O, et al. Changes in epicardial and visceral adipose tissue depots following bariatric surgery and their effect on cardiac geometry. *Front Endocrinol (Lausanne)*. 2023;14:1092777. [CrossRef]
6. Nauck MA, Quast DR, Wefers J, Pfeiffer AFH. The evolving story of incretins (GIP and GLP-1) in metabolic and cardiovascular disease: A pathophysiological update. *Diabetes Obes Metab*. 2021;23(S3):5-29. [CrossRef]
7. Lascaris B, Pouwels S, Houthuizen P, et al. Cardiac structure and function before and after bariatric surgery: a clinical overview. *Clin Obes*. 2018;8(6):434-443. [CrossRef]
8. Askarpour M, Khani D, Sheikhi A, Ghaedi E, Alizadeh S. Effect of Bariatric Surgery on Serum Inflammatory Factors of Obese Patients: a Systematic Review and Meta-Analysis. *Obes Surg*. 2019;29(8):2631-2647. [CrossRef]
9. Vicardi M, Farzaneh-Far A, Fava C, Dalle Carbonare L, Romano S. Epicardial and Visceral Adipose Tissue and Global Longitudinal Strain: A Review of Cardiac Imaging Insights in Subclinical Myocardial Dysfunction. *Nutrients*. 2026;18(6):1009. [CrossRef]

10. Voigt JU, Pedrizzetti G, Lysyansky P, et al. Definitions for a common standard for 2D speckle tracking echocardiography: consensus document of the EACVI/ASE/Industry Task Force to standardize deformation imaging. *Eur Heart J Cardiovasc Imaging*. 2015;16(1):1-11. [CrossRef]
11. Lang RM, Badano LP, Mor-Avi V, et al. Recommendations for cardiac chamber quantification by echocardiography in adults: an update from the American Society of Echocardiography and the European Association of Cardiovascular Imaging. *J Am Soc Echocardiogr*. 2015;28(1):1-39.e14. [CrossRef]
12. Sargsyan N, Chen JY, Aggarwal R, Fadel MG, Fehervari M, Ashrafian H. The effects of bariatric surgery on cardiac function: a systematic review and meta-analysis. *Int J Obes (Lond)*. 2024;48(2):166-176. [CrossRef]
13. Cuspidi C, Rescaldani M, Tadic M, Sala C, Grassi G. Effects of bariatric surgery on cardiac structure and function: a systematic review and meta-analysis. *Am J Hypertens*. 2014;27(2):146-156. [CrossRef]
14. Sorimachi H, Obokata M, Omote K, et al. Long-Term Changes in Cardiac Structure and Function Following Bariatric Surgery. *J Am Coll Cardiol*. 2022;80(16):1501-1512. [CrossRef]
15. Kokkinos A, Alexiadou K, Liaskos C, et al. Improvement in cardiovascular indices after Roux-en-Y gastric bypass or sleeve gastrectomy for morbid obesity. *Obes Surg*. 2013;23(1):31-38. [CrossRef]
16. Henry JA, Abdesselam I, Deal O, et al. The effect of bariatric surgery type on cardiac reverse remodelling. *Int J Obes (Lond)*. 2024;48(6):808-814. [CrossRef]
17. Ashrafian H, le Roux CW, Darzi A, Athanasiou T. Effects of Bariatric Surgery on Cardiovascular Function. *Circulation*. 2008;118(20):2091-2102. [CrossRef]
18. Ikonomidis I, Mazarakis A, Papadopoulos C, et al. Weight loss after bariatric surgery improves aortic elastic properties and left ventricular function in individuals with morbid obesity: a 3-year follow-up study. *J Hypertens*. 2007;25(2):439-447. [CrossRef]
19. Erbay İ, Aladağ P. The Hemoglobin, Albumin, Lymphocyte, and Platelet Score as a Simple Blood-Based Predictor of Residual Coronary Disease Burden in Diabetic Patients with Non-ST-Elevation Myocardial Infarction. *Turk Kardiyol Dern Ars*. 2025;53(7):483-491. [CrossRef]
20. Gaborit B, Jacquier A, Kober F, et al. Effects of bariatric surgery on cardiac ectopic fat: lesser decrease in epicardial fat compared to visceral fat loss and no change in myocardial triglyceride content. *J Am Coll Cardiol*. 2012;60(15):1381-1389. [CrossRef]
21. Hannukainen JC, Lautamäki R, Pärkkä J, et al. Reversibility of myocardial metabolism and remodelling in morbidly obese patients 6 months after bariatric surgery. *Diabetes Obes Metab*. 2018;20(4):963-973. [CrossRef]
22. Iqbal Z, Adam S, Ho JH, et al. Metabolic and cardiovascular outcomes of bariatric surgery. *Curr Opin Lipidol*. 2020;31(4):246-256. [CrossRef]
23. Karagöz U, Kahya Eren N, Özdemir E, Emren SV, Gürsoy MO, Tokaç M. Left Ventricular Hypertrophy Findings on Electrocardiogram Predict Impaired Left Atrial Functions. *Turk Kardiyol Dern Ars*. 2024;52(5):322-329. [CrossRef]

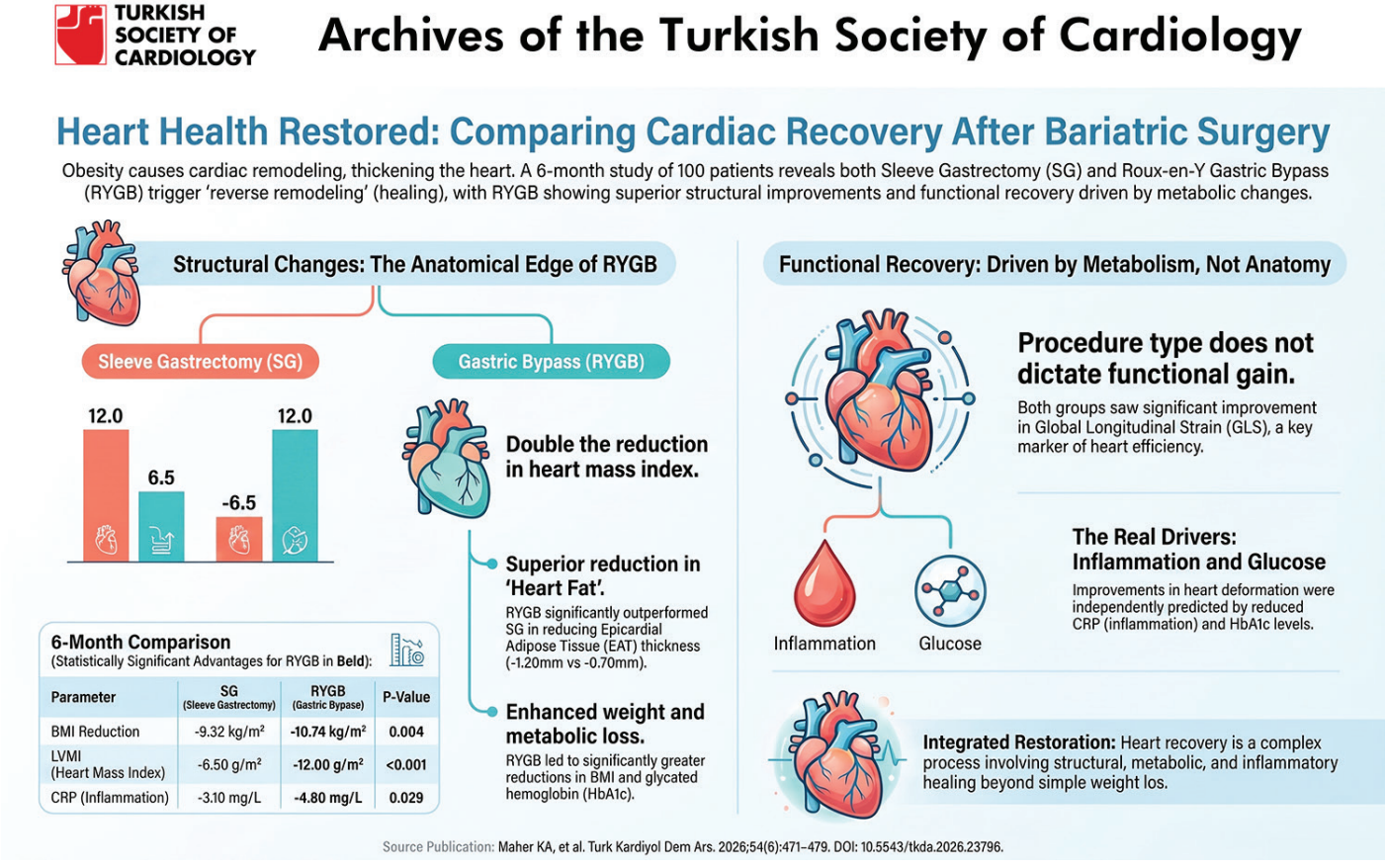

ARCHIVES OF THE TURKISH SOCIETY OF CARDIOLOGY

Official journal of the TURKISH SOCIETY OF CARDIOLOGY

Subclinical Cardiac Dysfunction in Children with Iron Deficiency Anemia Assessed by Tissue Doppler and Speckle-Tracking Echocardiography

Demir Eksikliği Anemisi Olan Çocuklarda Subklinik Kardiyak Disfonksiyonun Doku Doppler ve Benek İzleme Ekokardiyografi ile Değerlendirilmesi

ABSTRACT

Objective: Iron deficiency is the leading cause of anemia in childhood and may induce cardiovascular adaptations, including increased heart rate, elevated cardiac output, plasma volume expansion, and myocardial remodeling. Beyond hematologic consequences, reduced iron availability may also affect myocardial structure and function. This study aimed to assess biventricular function in children with iron deficiency anemia using two-dimensional speckle-tracking echocardiography.

Method: This prospective case–control study included pre- and post-treatment evaluations. Forty children with iron deficiency anemia and 29 healthy controls were enrolled. Of the 40 patients, 24 were re-evaluated after treatment. Tissue Doppler imaging was used to measure myocardial velocities, isovolumic contraction time, isovolumic relaxation time, and ejection time at the interventricular septum and the basal segments of both ventricles. Speckle-tracking echocardiography was used to assess left ventricular longitudinal strain (LS) and strain rate, left ventricular circumferential strain and strain rate, as well as right ventricular global longitudinal strain and strain rate.

Results: Left and right ventricular LS values improved following treatment, indicating recovery of myocardial function. Tissue Doppler parameters also demonstrated improvement in both systolic and diastolic function.

Conclusion: Although significant improvement was observed after treatment, some echocardiographic parameters did not fully normalize, suggesting that subtle myocardial alterations may persist. These findings should be interpreted with caution due to the relatively small sample size and the predominance of mild-to-moderate anemia in the study population. Children with iron deficiency anemia may benefit from longer-term follow-up and post-treatment evaluation.

Keywords: Anemia, doppler tissue imaging, echocardiography, iron deficiency, speckle tracking, two-dimensional

ÖZET

Amaç: Çocukluk çağındaki aneminin en sık nedeni olan demir eksikliği; kardiyak hipertrofiye, kalp hızında artışa, kardiyak debide ve plazma volümünde artışa yol açabilir. Demir eksikliği miyokartta yapısal ve fonksiyonel değişikliklere neden olabilir. Bu çalışmanın amacı, anemisi olan ve anemisi olmayan hastalarda sol ve sağ ventrikül fonksiyonlarını iki boyutlu "benek izleme" ekokardiyografi (2D STE) ile değerlendirmektir.

Yöntem: Bu çalışma, tedavi öncesi ve sonrası değerlendirmeyi içeren prospektif bir olgu-kontrol çalışmasıdır. Çalışmaya demir eksikliği anemisi tanısı alan 40 çocuk ve kontrol grubu olarak 29 sağlıklı çocuk dâhil edilmiştir. Anemili 40 çocuğun 24'ü tedavi sonrasında yeniden değerlendirilmiştir. Doku Doppler görüntüleme ile interventriküler septum ile sol ve sağ ventrikül bazal segmentlerinde miyokardiyal hızlar, izovolümik kontraksiyon süresi, izovolümik relaksasyon süresi ve ejeksiyon zamanı ölçülmüştür. Benek izleme ekokardiyografi ile sol ventrikül global longitudinal strain (GLS) ve strain hızı, sol ventrikül global sirkumferansiyel strain ve strain hızı ile sağ ventrikül GLS ve strain hızı değerlendirilmiştir.

Bulgular: Sol ve sağ ventrikül GLS değerlerindeki artış miyokardiyal iyileşmeyi yansıtmakta olup Doku Doppler incelemesinde sistolik ve diyastolik fonksiyonlarda iyileşme gözlenmiştir.

Sonuç: Doku Doppler görüntüleme ve benek izleme ekokardiyografi; hafif ve orta dereceli anemisi olan hastalarda demir eksikliğinin sistolik ve diyastolik fonksiyonları anlamlı şekilde etkileyebildiğini, hatta tedavi tamamlandıktan sonra dahi bu etkinin devam edebileceğini göstermede etkili yöntemlerdir. Demir eksikliği anemisi olan çocuklar daha uzun süre izlenmeli ve tedavi sonrasında da kardiyak fonksiyonlar açısından değerlendirilmelidir.

Anahtar Kelimeler: Anemi, doku Doppler görüntüleme, ekokardiyografi, demir eksikliği, benek izleme, iki boyutlu

ORIGINAL ARTICLE
ARAŞTIRMA MAKALESİ

Betül Pehlivan Zorlu[1]
İbrahim İlker Çetin[2]
Emine Azak[2]
Hazım Alper Gürsü[2]
Utku Pamuk[2]
Namık Yaşar Özbek[3]

[1]*Department of Pediatric Nephrology, Ankara Bilkent City Hospital, Ankara, Türkiye*
[2]*Department of Pediatric Cardiology, Ankara Bilkent City Hospital, Ankara, Türkiye*
[3]*Department of Pediatric Hematology, Ankara Bilkent City Hospital, Ankara, Türkiye*

Corresponding author:
Betül Pehlivan Zorlu
✉ betulpehlivantr@gmail.com

Received: February 18, 2026
Accepted: April 27, 2026

Cite this article as: Pehlivan Zorlu B, Çetin İİ, Azak E, Gürsü HA, Pamuk U, Özbek NY. Subclinical Cardiac Dysfunction in Children with Iron Deficiency Anemia Assessed by Tissue Doppler and Speckle-Tracking Echocardiography. *Turk Kardiyol Dern Ars.* 2026;54(6):480–486.

DOI: 10.5543/tkda.2026.21477

Iron deficiency anemia (IDA) in pediatric patients is associated with significant clinical manifestations related to tissue hypoxia.[1] Iron plays a critical role in systemic oxygen transport, cellular metabolism, mitochondrial energy production, and the function of iron-dependent enzymes.[2] Impairment of these processes may lead to tachycardia, fatigue, exercise intolerance, pallor, and irritability, as well as cardiovascular adaptations such as increased cardiac stroke volume, chamber dilatation or hypertrophy, expanded plasma volume, and, in severe cases, heart failure.[3–5]

Tissue Doppler imaging (TDI) is a noninvasive echocardiographic technique that enables the assessment of myocardial velocities and is widely used to evaluate global systolic and diastolic cardiac function.[6,7] Speckle-tracking echocardiography is a more recently developed modality that allows for the evaluation of myocardial contraction and relaxation in multiple planes by assessing myocardial deformation under physiological loading conditions, thereby providing detailed insights into cardiac function.[8–12]

The objective of the present study was to investigate subclinical systolic dysfunction in pediatric patients with reduced ferritin levels and to determine whether cardiac alterations improve following treatment, using speckle-tracking echocardiography to assess myocardial deformation.

ABBREVIATIONS

EF	Ejection fraction
ET	Ejection time
FS	Fractional shortening
GAS	Global area strain
GCS	Global circumferential strain
GRS	Global radial strain
ICT	Isovolumic contraction time
IDA	Iron deficiency anemia
IRT	Isovolumic relaxation time
IVSTd	Interventricular septal thickness in diastole
LS	Longitudinal strain
LVDd	Left ventricular end-diastolic diameter
LVDs	Left ventricular end-systolic diameter
LVLS	Left ventricular longitudinal strain
MPI	Myocardial performance index
PWTd	Posterior wall thickness in diastole
STAT3	Signal transducer and activator of transcription 3
TDI	Tissue Doppler imaging
WHO	World Health Organization

Materials and Methods

Study Design and Population

Between January 2016 and June 2017, 40 children diagnosed with iron deficiency anemia and 29 age- and sex-matched healthy controls were prospectively enrolled. Ethical approval was obtained from Ankara Children's Health and Diseases Hematology Oncology Training and Research Hospital Clinical Research Ethics Committee (Approval Number: 2015-080, Date: 21.12.2015). Participants with structural heart disease, hypertension, chronic respiratory disease, arrhythmias, dyslipidemia, chronic inflammatory conditions, diabetes mellitus, renal dysfunction, or gastrointestinal disorders were excluded.

Complete blood count analyses (Beckman Coulter LH 780, 2010) and serum ferritin measurements (Beckman Coulter Unicel DxI 8800, 2010) were performed for all participants. Iron deficiency anemia was defined according to age-specific World Health Organization (WHO) hemoglobin thresholds, supported by low ferritin levels and reduced transferrin saturation.[13]

The diagnosis of iron deficiency anemia was established in accordance with World Health Organization recommendations. Age-specific hemoglobin thresholds were applied (< 11 g/dL for children younger than 5 years and < 11.5 g/dL for those aged 5 years or older), with further classification into mild, moderate, and severe categories based on hemoglobin ranges. For additional analysis, patients were also stratified according to anemia severity: hemoglobin levels ≥ 10 g/dL were classified as mild anemia, whereas values < 10 g/dL were considered moderate anemia. Biochemical evidence of iron deficiency was required, defined as serum ferritin levels < 12 µg/L and transferrin saturation < 16–20%.

C-reactive protein levels were measured to exclude falsely elevated ferritin levels due to acute inflammation.[14] All children in the study group received oral iron sulfate therapy for at least three months.[15] Normal hemoglobin and ferritin levels were confirmed in all treated patients within six months. Physical examination findings, including cardiovascular system assessments, were normal in all participants.

Conventional Echocardiographic Imaging and Analysis

All participants underwent echocardiographic evaluation in the left lateral decubitus position with continuous electrocardiographic monitoring. Imaging was performed using a Philips iE33 system equipped with a 5-MHz transducer (Philips, The Netherlands). For each parameter, measurements were averaged over three consecutive cardiac cycles. Conventional transthoracic echocardiography included two-dimensional, M-mode, and Doppler assessments in accordance with current pediatric imaging standards. Left ventricular systolic function was evaluated using fractional shortening (FS) and ejection fraction (EF) derived from M-mode measurements.

Two-dimensional images were obtained from the apical four-chamber and long-axis views. The following parameters were measured: left ventricular end-diastolic diameter (LVDd), left ventricular end-systolic diameter (LVDs), interventricular septal thickness in diastole (IVSTd), posterior wall thickness in diastole (PWTd), and the ratio of early-to-late transmitral flow velocities (E/A). Left ventricular systolic function was assessed using FS and EF, with EF > 55% and FS > 28% considered normal.

Tissue Doppler imaging measurements were acquired from the apical four-chamber view. Peak myocardial velocities of the systolic (S), early diastolic (E), and late diastolic (A) waves were recorded. Isovolumic relaxation time (IRT), isovolumic contraction time (ICT), and ejection time (ET) were measured for the left ventricle, right ventricle, and interventricular septum. The myocardial performance index (MPI) was calculated as (IRT + ICT) / ET.

For myocardial deformation analysis, two-dimensional images were obtained from the apical four-chamber view and the mid-

Table 1. Demographic and clinical characteristics of the study population

Group	n	Mean age (years)	Male/ Female
Iron deficiency anemia	40	2.5 ± 2.0	21/19
Healthy controls	29	3.0 ± 1.4	14/15
IDA after 3 months (normalized hemoglobin)	24	2.4 ± 1.6	10/14

IDA, Iron deficiency anemia.

ventricular short-axis plane of the left ventricle. Left ventricular longitudinal strain was derived from the apical four-chamber view, whereas circumferential strain was obtained from the mid-ventricular short-axis view.

Right ventricular longitudinal strain was assessed from the apical four-chamber view, including both the free wall and the interventricular septum, and reported as global right ventricular strain. Image sequences were stored as cine loops over three consecutive cardiac cycles. Offline strain analysis was performed using QLAB Advanced Quantification software (version 6.0; Philips, The Netherlands).

All echocardiographic recordings were obtained in the left lateral position with simultaneous electrocardiographic guidance. Analyses were performed by a single experienced investigator. Measurements were obtained at two time points, before treatment and after completion of iron therapy, to assess longitudinal changes. Myocardial deformation indices are presented as absolute values, reflecting systolic shortening.

Statistical Analysis

All statistical analyses were performed using IBM SPSS Statistics software (version 25.0; IBM Corp., Chicago, IL, USA). The distribution of continuous variables was assessed using the Kolmogorov–Smirnov test to determine the appropriate analytical methods. Data are presented as mean ± standard deviation. Comparisons between groups were conducted using the Student's t-test for normally distributed variables and the Mann–Whitney U test for non-normally distributed variables. Categorical variables were analyzed using the chi-square test. Correlations between variables were assessed using Pearson or Spearman correlation coefficients, depending on data distribution. A two-tailed p value < 0.05 was considered statistically significant.

Results

Demographic Data

The study group comprised 40 children with iron deficiency anemia (mean age: 2.5 years; male/female: 21/19), while the control group included 29 healthy children (mean age: 3.0 years; male/female: 14/15). Of the 40 patients who received three months of treatment, 24 achieved normalization of hematological parameters (mean age: 2.4 years; male/female: 10/14). No significant differences were observed between groups with respect to demographic characteristics. Baseline demographic and clinical characteristics are summarized in Table 1.

Evaluation of Hematological Parameters

Comparisons of hematological parameters among the pre-treatment, post-treatment, and control groups are presented in Table 2. Mean hemoglobin levels increased significantly to normal ranges after approximately three months of treatment ($P < 0.001$). Similarly, mean ferritin levels and mean corpuscular volume increased significantly, while red cell distribution width decreased to normal values. All hematological parameters were within normal limits in the control group (Table 2). Ferritin levels increased significantly following treatment (mean difference: 17.6 µg/L, $P < 0.001$), and all patients achieved ferritin values ≥ 12 µg/L, indicating restoration of iron stores. Among patients with iron deficiency anemia, 35% were classified as having mild anemia and 65% as having moderate anemia based on hemoglobin levels.

Comparison of Conventional Echocardiographic and Tissue Doppler Imaging Findings

Tissue Doppler imaging parameters were compared across pre-treatment, post-treatment, and control groups to evaluate the impact of iron deficiency anemia and the effects of treatment (Table 3). In the study group, pre-treatment fractional shortening, left ventricular isovolumic relaxation time, right ventricular ejection time, interventricular septal myocardial performance index, and both left and right ventricular MPI values differed significantly from post-treatment measurements. Following treatment, FS and right ventricular ejection time increased significantly, whereas left ventricular IRT and MPI values of the interventricular septum, left ventricle, and right ventricle decreased significantly compared with pre-treatment values.

Significant differences observed between the pre-treatment and control groups in FS, left ventricular IRT, interventricular septal MPI, and left and right ventricular MPI were no longer present after treatment, except for right ventricular ejection time.

Table 2. Biochemical and hematologic parameters in study and control groups

Laboratory parameters	Study group		Control group	P1	P2	P3
	Pre-treatment	Post-treatment				
Hemoglobin (g/dL)	8.7 ± 1.3	12.2 ± 0.7	12.6 ± 0.8	**0.001**	**0.001**	0.134
MCV (fL)	59.9 ± 7.8	72.3 ± 3.4	76.9 ± 4.7	**0.001**	**0.001**	**0.001**
RDW (%)	19.2 ± 4.4	16.5 ± 3	14 ± 1.2	**0.002**	**0.001**	**0.002**
Ferritin (ng/mL)	4.9 ± 2.8	22.6 ± 11.7	24.5 ± 10.2	**0.001**	**0.001**	0.905

MCV, Mean corpuscular volume; RDW, Red cell distribution width. Data are presented as mean ± standard deviation (SD) P1 indicates comparison between pre- and post-treatment values; P2, Comparison between pre-treatment and control groups; P3, Comparison between post-treatment and control groups.

Table 3. Conventional echocardiographic and tissue Doppler imaging parameters

Echocardiography and tissue Doppler imaging parameters	Study group		Control group	P1	P2	P3
	Pre-treatment	Post-treatment				
LVDd (mm)	27.5 ± 4.4	29 ± 4.3	30.5 ± 3.9	0.073	**0.009**	0.463
EF (%)	70.3 ± 4.1	72.2 ± 3	70.7 ± 3.9	0.051	0.970	0.282
FS (%)	37.9 ± 3.5	39.9 ± 2.8	38.9 ± 3.2	**0.016**	0.563	0.504
IVSS (cm/s)	6 ± 0.8	6 ± 0.8	6.7 ± 0.7	0.733	**0.001**	**0.004**
IVSE (cm/s)	11.1 ± 1.5	11.1 ± 1.9	12.3 ± 1.8	0.808	**0.024**	**0.024**
IVSA (cm/s)	5.8 ± 1.5	5.3 ± 0.9	5.6 ± 1	0.136	0.894	0.477
IVSICT (ms)	59.6 ± 11.9	57.6 ± 7.9	61 ± 9	0.568	0.930	0.391
IVSIRT (ms)	57.3 ± 9.9	54.5 ± 6.4	57.4 ± 7.1	0.265	1.000	0.335
IVSET (ms)	200.2 ± 33.9	215.3 ± 18.7	231.9 ± 20.3	0.117	**0.001**	**0.01**
IVSMPI	0.58 ± 0.1	0.51 ± 0.1	0.5 ± 0.1	**0.001**	**0.001**	0.949
LVS (cm/s)	5.6 ± 1	6.1 ± 1.2	7.2 ± 0.9	0.115	**0.001**	**0.002**
LVE (cm/s)	13.9 ± 2.3	13.8 ± 2.1	15.4 ± 2.2	0.967	**0.021**	**0.028**
LVA (cm/s)	6.2 ± 1.5	5.8 ± 1.1	5.9 ± 1	0.462	0.664	0.975
LVICT (ms)	60.5 ± 14.1	58 ± 8.3	60.7 ± 8.3	0.601	1.000	0.586
LVIRT (ms)	63.9 ± 11.1	58.2 ± 8.5	56.8 ± 6.2	**0.021**	**0.004**	0.885
LVET (ms)	198.3 ± 29.7	213.2 ± 22.7	230.5 ± 21.5	0.082	**0.001**	**0.019**
LVMPI	0.62 ± 0.1	0.54 ± 0.1	0.5 ± 0.1	**0.002**	**0.001**	0.084
RVS (cm/s)	9.2 ± 1.9	9.9 ± 1.4	9.6 ± 1.6	0.092	0.795	0.766
RVE (cm/s)	14.8 ± 3.1	15.5 ± 3.1	15.3 ± 2.5	0.264	0.836	0.991
RVA (cm/s)	8.6 ± 2.6	8.7 ± 2.5	7.3 ± 1.7	0.917	**0.035**	0.084
RVICT (ms)	61 ± 12.6	54.7 ± 9.8	57.3 ± 7.5	0.053	0.357	0.645
RVIRT (ms)	59.3 ± 10.3	55.3 ± 7	55.9 ± 5.7	0.084	0.225	0.984
RVET (ms)	195.9 ± 30.6	217.5 ± 19.8	234.4 ± 22.3	**0.008**	**0.001**	**0.015**
RVMPI	0.61 ± 0.1	0.5 ± 0.1	0.48 ± 0.1	**0.001**	**0.001**	0.578

EF, Ejection fraction; ET, Ejection time; FS, Fractional shortening; ICT, Isovolumic contraction time; IRT, Isovolumic relaxation time; IVS S/E/A, Interventricular septal systolic/early diastolic/late diastolic velocities; LVDd, Left ventricular end-diastolic diameter; LV S/E/A, Left ventricular systolic/early diastolic/late diastolic velocities; MPI, Myocardial performance index; RV S/E/A, Right ventricular systolic/early diastolic/late diastolic velocities. Data are presented as mean ± standard deviation (SD). P1 indicates comparison between pre- and post-treatment; P2, Pre-treatment vs. control; P3, Post-treatment vs. control.

However, differences in interventricular septal and left ventricular S and E wave velocities, as well as ejection time values, remained significant even after treatment (Table 3).

A moderate linear correlation was identified between pre-treatment hemoglobin levels and interventricular septal isovolumic contraction time and ejection time, right ventricular isovolumic contraction time and ejection time, and left ventricular isovolumic contraction time on TDI examination ($r > 0.4$; $P < 0.005$). Hemoglobin levels also demonstrated a weak but significant linear correlation with left ventricular ejection time ($r = 0.322$; $P = 0.042$). Additionally, a moderate linear correlation was observed between post-treatment hemoglobin levels and interventricular septum ejection time ($r = 0.418$; $P = 0.042$). No significant correlations were found between hemoglobin levels and other TDI parameters in either the pre- or post-treatment groups ($P > 0.05$).

Evaluation of Speckle-Tracking Echocardiography Findings

Pre-treatment left ventricular longitudinal strain (LS) and strain rate values were significantly lower than those in the post-treatment and control groups. Although all speckle-tracking echocardiography parameters improved after treatment, statistically significant changes were observed only in left ventricular LS and strain rate and right ventricular global longitudinal strain (RVGLS) ($P < 0.05$) (Table 4). No significant correlations were identified between hemoglobin levels and speckle-tracking echocardiography (STE) parameters in either the pre- or post-treatment groups ($P > 0.05$). Similarly, no significant correlation was found between ferritin levels and left ventricular longitudinal strain in either the pre-treatment ($r = 0.185$; $P = 0.254$) or post-treatment groups ($r = 0.100$; $P = 0.643$). Furthermore, left ventricular longitudinal strain did not differ significantly between patients with mild and moderate anemia ($P = 0.214$).

Discussion

In the present study, we demonstrated that children with iron deficiency anemia exhibit subclinical myocardial dysfunction detectable by advanced echocardiographic techniques, despite preserved conventional systolic function. Left ventricular longitudinal strain and strain rate were particularly sensitive in identifying these abnormalities. Following iron therapy, significant improvements were observed in both tissue Doppler and speckle-tracking parameters; however, some parameters

Table 4. Speckle-tracking echocardiography parameters

Speckle-tracking echocardiography parameters	Study group		Control group	P1	P2	P3
	Pre-treatment	Post-treatment				
LVLS (%)	22.2 ± 4.1	25.3 ± 3.4	24.9 ± 4.4	**0.003**	**0.031**	0.975
LVLSR (s-1)	0.4 ± 0.4	0.7 ± 0.4	0.8 ± 0.5	**0.001**	**0.008**	0.994
RVGLS (%)	30.7 ± 5.2	34.5 ± 8.4	28.8 ± 5.1	**0.042**	0.343	**0.016**
RVGLSR (s-1)	0.7 ± 0.5	0.8 ± 0.5	0.8 ± 0.4	0.491	0.992	0.997
LVCS (%)	27.5 ± 5.6	30.7 ± 7.3	30.1 ± 5.6	0.072	0.232	0.982
LVCSR (s-1)	0.8 ± 0.4	1 ± 0.5	0.9 ± 0.4	0.051	0.342	0.747

LVCS, Left ventricular circumferential strain; LVCSR, Left ventricular circumferential strain rate; LVLS, Left ventricular longitudinal strain; LVLSR, Left ventricular longitudinal strain rate; RVGLS, Right ventricular global longitudinal strain; RVGLSR, Right ventricular global longitudinal strain rate. Data are presented as mean ± standard deviation (SD). P1 indicates comparison between pre- and post-treatment; P2, Pre-treatment vs. control; P3, Post-treatment vs. control.

did not fully normalize. These findings suggest that myocardial involvement in iron deficiency anemia may be subtle and partially reversible.

Iron deficiency anemia is associated with several cardiovascular adaptations, including increased heart rate and stroke volume, cardiac dilatation or hypertrophy, expanded plasma volume, and, in advanced stages, heart failure during both exercise and rest.[16] Recent studies, primarily in adults, have shown that IDA may lead to left ventricular hypertrophy.[17] This process has been linked to erythropoietin receptor activity in various tissues, including the myocardium. Chronic iron deficiency anemia may result in increased erythropoietin production and activation of intracellular signaling pathways, such as phosphorylation of signal transducer and activator of transcription 3 (STAT3), suggesting ongoing structural cardiac adaptation.[3]

In our study, cardiac structure and systolic function were evaluated in children with IDA using tissue Doppler imaging and speckle-tracking echocardiography. Previous studies have demonstrated alterations in strain parameters, including LS, global radial strain (GRS), global circumferential strain (GCS), and global area strain (GAS), in patients with hemoglobin levels between 6 and 9 g/dL, even in the absence of left ventricular hypertrophy or chamber enlargement and with preserved conventional systolic function. Among these parameters, GAS and LS appear to be the most sensitive indicators of left ventricular systolic dysfunction.[12] In our study, no significant association was observed between ferritin levels and myocardial deformation parameters. This finding suggests that the observed cardiac alterations may not be solely attributable to iron deficiency per se, but rather reflect a combination of iron-related metabolic effects and hemodynamic adaptations associated with anemia. Strain values were expressed as absolute values to facilitate interpretation and comparison.

Improvement in systolic function following treatment was primarily reflected by significant increases in fractional shortening and right ventricular ejection time on tissue Doppler imaging. Although ejection fraction did not change significantly, the increase in fractional shortening suggests recovery of systolic performance. Additionally, the significant reduction in left ventricular isovolumic relaxation time indicates improved diastolic function, likely related to enhanced myocardial relaxation. Ferritin levels normalized in all patients following treatment, supporting adequate restoration of iron stores.

Consistent with previous observations, the most important hematological complication of IDA is its impact on the cardiovascular system, largely due to impaired oxygen transport capacity. In the present study, ejection time values increased after treatment; however, these changes did not reach statistical significance and did not fully normalize compared with controls. Before treatment, ejection time values were significantly lower in the interventricular septum and both ventricles. Furthermore, myocardial performance index values of the left ventricle, right ventricle, and interventricular septum were significantly higher in the pre-treatment group, indicating global ventricular dysfunction. These findings suggest that although IDA predominantly affects systolic function, its impact on the heart is global. Evaluation using myocardial performance index and ejection time may therefore provide additional insight beyond conventional parameters. Although transferrin saturation was not available, normalization of ferritin levels together with improvement in hemoglobin suggests substantial recovery of iron status.

Myocardial strain analysis has been shown to detect early systolic dysfunction even when left ventricular ejection fraction is preserved. Accordingly, speckle-tracking echocardiography has emerged as a sensitive tool for evaluating myocardial systolic function.[18] It has also been demonstrated to detect early subclinical myocardial dysfunction in various pediatric conditions, even when conventional echocardiographic parameters are normal.[19] In our study, although ejection fraction remained normal and unchanged after treatment, strain and strain rate values improved following therapy, with the most pronounced changes observed in left ventricular longitudinal strain and strain rate. These findings suggest that STE may more accurately reflect myocardial functional recovery than conventional echocardiographic measures.

Consistent with previous reports, Shen et al.[20] demonstrated that longitudinal strain is a sensitive marker for detecting subclinical left ventricular dysfunction in patients with mild-to-moderate iron deficiency. Similarly, in our study, left ventricular LS and strain rate showed the most pronounced improvement following treatment. The absence of significant differences between post-treatment and control values further supports the effectiveness of appropriate iron replacement therapy. In line with the findings of Şahin et al.,[21] left ventricular longitudinal strain (LVLS) has been identified as a strong and independent predictor of adverse cardiovascular

outcomes, underscoring its importance in risk stratification and longitudinal follow-up. The relatively young age of our study population should be considered when interpreting these results. Because myocardial deformation parameters may vary with age, the generalizability of these findings to older pediatric populations is limited. Therefore, these results should be interpreted with caution when extrapolated beyond early childhood.

A significant positive correlation was observed between hemoglobin levels and ejection time values of the interventricular septum, left ventricle, and right ventricle, reflecting systolic activity. No significant correlations were found between hemoglobin levels and other tissue Doppler imaging parameters. Notably, the correlation between hemoglobin level and interventricular septal ejection time persisted after treatment.

Previous studies have suggested hemoglobin thresholds of 6 g/dL and 9 g/dL as potential cut-off values for the development of cardiac dysfunction.[20,22] In the present study, the lack of a significant correlation between hemoglobin levels and speckle-tracking echocardiography parameters may be explained by the predominance of mild-to-moderate anemia. The absence of a clear gradient of myocardial dysfunction according to anemia severity suggests that even mild anemia may be associated with subclinical myocardial changes.

In summary, IDA was associated with impairments in both systolic and diastolic cardiac function prior to treatment, affecting both ventricles. Although hemoglobin and ferritin levels improved following iron therapy, TDI and STE findings indicated only partial recovery of cardiac function, with some parameters remaining abnormal.

Our findings suggest that fractional shortening and myocardial performance index may provide more sensitive information than ejection fraction alone in assessing systolic function in anemic children. The absence of significant differences between post-treatment and control values further highlights the importance of timely and adequate iron replacement therapy in preventing persistent cardiac dysfunction.

Limitations of the Study

This study has several limitations. The relatively small sample size and single-center design may limit generalizability. The follow-up period was relatively short and may not fully capture long-term cardiac recovery. Transferrin saturation was not assessed, and iron status parameters were not systematically evaluated in the control group. Some patients were excluded from TDI and STE analyses due to poor cooperation, which may have introduced selection bias. Interobserver variability was not assessed, potentially limiting reproducibility. Finally, STE measurements are operator-dependent and may be influenced by image quality.

Conclusion

Iron deficiency anemia should be treated promptly to restore cardiac function. Long-term follow-up is necessary to assess the sustained effects of IDA, which may significantly impair both systolic and diastolic function, even in mild-to-moderate cases. In addition, anemia severity should be considered when evaluating children from a cardiovascular perspective.

Ethics Committee Approval: Ethics committee approval was obtained from Ankara Children's Health and Diseases Hematology Oncology Training and Research Hospital Clinical Research Ethics Committee (Approval Number: 2015-080, Date: 21.12.2015).

Informed Consent: Written informed consent was obtained from the patients and/or their legal guardians.

Conflict of Interest: The authors have no conflicts of interest to declare.

Funding: The authors declared that this study received no financial support.

Use of AI for Writing Assistance: No use of AI-assisted technologies was declared by the authors.

Author Contributions: Concept – B.P.Z., N.Y.Ö.; Design – B.P.Z., İ.İ.Ç.; Supervision – B.P.Z., N.Y.Ö.; Data Collection and/or Processing – H.A.G., U.P.; Analysis and/or Interpretation – İ.İ.Ç., E.A.; Literature Review – B.P.Z.; Writing – B.P.Z., E.A.; Critical Review – İ.İ.Ç., N.Y.Ö.

Peer-review: Externally peer-reviewed.

References

1. Lanzkowsky P, Lipton J, Fish JD. Lanzkowsky's manual of pediatric hematology and oncology. *Elsevier*; 2016.
2. Sawicki KT, De Jesus A, Ardehali H. Iron Metabolism in Cardiovascular Disease: Physiology, Mechanisms, and Therapeutic Targets. *Circ Res*. 2023;132(3):379-396. [CrossRef]
3. Naito Y, Sawada H, Oboshi M, et al. Cardiac remodeling in response to chronic iron deficiency: role of the erythropoietin receptor. *J Hypertens*. 2015;33(6):1267-1275. [CrossRef]
4. Fang X, Cai Z, Wang H, et al. Loss of Cardiac Ferritin H Facilitates Cardiomyopathy via Slc7a11-Mediated Ferroptosis. *Circ Res*. 2020;127(4):486-501. [CrossRef]
5. Beavers CJ, Ambrosy AP, Butler J, et al. Iron Deficiency in Heart Failure: A Scientific Statement from the Heart Failure Society of America. *J Card Fail*. 2023;29(7):1059-1077. [CrossRef]
6. Greenberg NL, Firstenberg MS, Castro PL, et al. Doppler-derived myocardial systolic strain rate is a strong index of left ventricular contractility. *Circulation*. 2002;105(1):99-105. [CrossRef]
7. Abraham TP, Dimaano VL, Liang HY. Role of tissue Doppler and strain echocardiography in current clinical practice. *Circulation*. 2007;116(22):2597-2609. [CrossRef]
8. Cantinotti M, Kutty S, Giordano R, et al. Review and status report of pediatric left ventricular systolic strain and strain rate nomograms. *Heart Fail Rev*. 2015;20(5):601-612. [CrossRef]
9. Hensel KO, Grimmer F, Jenke AC, Wirth S, Heusch A. The influence of real-time blood glucose levels on left ventricular myocardial strain and strain rate in pediatric patients with type 1 diabetes mellitus - a speckle tracking echocardiography study. *BMC Cardiovasc Disord*. 2015;15:175. [CrossRef]
10. Pellikka PA, Nagueh SF, Elhendy AA, Kuehl CA, Sawada SG; American Society of Echocardiography. American Society of Echocardiography recommendations for performance, interpretation, and application of stress echocardiography. *J Am Soc Echocardiogr*. 2007;20(9):1021-1041. [CrossRef]
11. Zhou Q, Shen J, Liu Y, Luo R, Tan B, Li G. Assessment of left ventricular systolic function in patients with iron deficiency anemia by three-dimensional speckle-tracking echocardiography. *Anatol J Cardiol*. 2017;18(3):194-199. [CrossRef]
12. Elçioğlu BC, Baydar O, Kılıç A, et al. Effects of iron deficiency on left ventricular functions in young women regardless of anemia: A speckle tracking echocardiography study. *Turk J Med Sci*. 2022;52(3):754-761. [CrossRef]
13. Iron Deficiency Anaemia. *Assessment, Prevention, and Control: A guide for programme managers*. World Health Organization; 2001:47-62.
14. Baker RD, Greer FR; Committee on Nutrition American Academy of Pediatrics. Diagnosis and prevention of iron deficiency and iron-deficiency anemia in infants and young children (0-3 years of age). *Pediatrics*. 2010;126(5):1040-1050. [CrossRef]

15. Zlotkin S, Arthur P, Antwi KY, Yeung G. Randomized, controlled trial of single versus 3-times-daily ferrous sulfate drops for treatment of anemia. *Pediatrics*. 2001;108(3):613-616. [CrossRef]
16. Alioglu B, Cetin II, Emeksiz ZS, Dindar N, Tapci E, Dallar Y. Iron deficiency anemia in infants: does it really affect the myocardial functions? *Pediatr Hematol Oncol*. 2013;30(3):239-245. [CrossRef]
17. Hegde N, Rich MW, Gayomali C. The cardiomyopathy of iron deficiency. *Tex Heart Inst J*. 2006;33(3):340-344.
18. Reant P, Barbot L, Touche C, et al. Evaluation of global left ventricular systolic function using three-dimensional echocardiography speckle-tracking strain parameters. *J Am Soc Echocardiogr*. 2012;25(1):68-79. [CrossRef]
19. El Amrousy D, Elshehaby W, Elsharaby R, Badr S, Hamza M, Elbarky A. Myocardial function using two dimension speckle-tracking echocardiography in children with celiac disease. *Eur J Pediatr*. 2024;183(2):947-954. [CrossRef]
20. Shen J, Zhou Q, Liu Y, Luo R, Tan B, Li G. Evaluation of left atrial function in patients with iron-deficiency anemia by two-dimensional speckle tracking echocardiography. *Cardiovasc Ultrasound*. 2016;14(1):34. [CrossRef]
21. Şahin T, Çiçek M, Atmaca S, Şahin AA, Çelik Ö. Implications of Procedure of Thoracic Endovascular Aortic Repair on Left Ventricular Global Longitudinal Strain. *Turk Kardiyol Dern Ars*. 2025;53(6):406-414. [CrossRef]
22. Hayashi R, Ogawa S, Watanabe Z, Yamamoto M. Cardiovascular function before and after iron therapy by echocardiography in patients with iron deficiency anemia. *Pediatr Int*. 1999;41(1):13-17. [CrossRef]

ARCHIVES OF THE TURKISH SOCIETY OF CARDIOLOGY

Official journal of the TURKISH SOCIETY OF CARDIOLOGY

The Effect of Predilatation on Procedural Outcomes in Patients Undergoing Saphenous Vein Graft Percutaneous Coronary Intervention for Acute Coronary Syndrome

Akut Koroner Sendromla Başvuran ve Safen Ven Greftine Perkütan Koroner Girişim Yapılan Hastalarda Predilatasyonun İşlem Sonucuna Etkisi

ABSTRACT

Objective: Percutaneous coronary interventions (PCI) of saphenous vein grafts (SVG) are technically challenging due to friable plaques, high thrombus burden, and the risk of distal embolization. The impact of balloon predilatation on outcomes in patients presenting with acute coronary syndrome (ACS) remains unclear. This study aimed to evaluate the effect of predilatation in patients undergoing SVG PCI.

Method: In this single-center retrospective study, 202 patients with ACS and prior coronary artery bypass graft (CABG) surgery who underwent PCI to an SVG between 2007 and 2024 were analyzed. Patients were categorized according to whether predilatation was performed before stent implantation (predilatation group, n = 112; no predilatation group, n = 90). Coronary flow was assessed using the Thrombolysis in Myocardial Infarction (TIMI) classification. Logistic regression analysis was performed to identify independent predictors of inadequate post-procedural flow (TIMI < 3).

Results: Baseline demographic and clinical characteristics were comparable between the groups. Post-procedural TIMI 3 flow was achieved in 69.6% of the predilatation group and 55.6% of the non-predilatation group (P = 0.039). Predilatation (odds ratio [OR] = 0.51, P = 0.030) and the use of glycoprotein IIb/IIIa inhibitors (OR = 0.39, P = 0.003) were independently associated with a lower risk of inadequate flow. ST-segment elevation myocardial infarction (STEMI) was associated with a higher risk of inadequate TIMI flow (OR = 2.37, P = 0.039). Lipid parameters and statin use were not associated with TIMI flow outcomes.

Conclusion: In patients with ACS undergoing SVG PCI, predilatation before stent implantation was associated with improved reperfusion, as reflected by higher rates of post-procedural TIMI 3 flow. The use of glycoprotein IIb/IIIa (GP IIb/IIIa) inhibitors was associated with additional protection. Larger prospective studies are warranted.

Keywords: Acute coronary syndrome, percutaneous coronary intervention, predilatation, saphenous vein graft, Thrombolysis in Myocardial Infarction flow

ÖZET

Amaç: Safen ven greftlerine (SVG) uygulanan perkütan koroner girişimler (PCI), kırılgan plak yapısı, yüksek trombüs yükü ve distal embolizasyon riski nedeniyle teknik olarak zorludur. Akut koroner sendrom (ACS) ile başvuran hastalarda balon predilatasyonunun sonuçlar üzerindeki etkisi net değildir. Bu çalışmada, SVG PCI uygulanan hastalarda predilatasyonun etkisini değerlendirmeyi amaçladık.

Yöntem: Bu tek merkezli retrospektif çalışmada, 2007–2024 yılları arasında safen ven greftine PCI uygulanan, akut koroner sendromlu ve daha önce koroner arter baypas greft (CABG) cerrahisi geçirmiş 202 hasta analiz edildi. Hastalar, stent implantasyonundan önce predilatasyon uygulanıp uygulanmamasına göre iki gruba ayrıldı (predilatasyon yapılan, n = 112; predilatasyon yapılmayan, n = 90). Koroner akım, Thrombolysis in Myocardial Infarction (TIMI) sınıflamasına göre değerlendirildi. İşlem sonrası yetersiz akımın (TIMI < 3) bağımsız belirleyicilerini belirlemek için lojistik regresyon analizi yapıldı.

ORIGINAL ARTICLE
ARAŞTIRMA MAKALESİ

Mustafa Berat Dumlu[1]
Mehmet Şahinbaş[1]
Gülaçan Tekin[2]
Anıl Şahin[3]
Yücel Kanal[2]
Nurcansu Oğrak Dumlu[4]

[1]*Department of Cardiology, Sivas Numune Hospital, Sivas, Türkiye*
[2]*Department of Cardiology, Sivas Cumhuriyet University, Faculty of Medicine, Sivas, Türkiye*
[3]*Department of Cardiology, Çanakkale Onsekiz Mart University, Faculty of Medicine, Çanakkale, Türkiye*
[4]*Department of Psychiatry, Sivas State Hospital, Sivas, Türkiye*

Corresponding author:
Mustafa Berat Dumlu
✉ mberatdumlu@hotmail.com

Received: March 04, 2026
Accepted: April 06, 2026

Cite this article as: Dumlu MB, Şahinbaş M, Tekin G, Şahin A, Kanal Y, Oğrak Dumlu N. The Effect of Predilatation on Procedural Outcomes in Patients Undergoing Saphenous Vein Graft Percutaneous Coronary Intervention for Acute Coronary Syndrome. *Turk Kardiyol Dern Ars.* 2026;54(6):487–495.

DOI: 10.5543/tkda.2026.99740

Bulgular: Başlangıç demografik ve klinik özellikler gruplar arasında benzerdi. İşlem sonrası TIMI 3 akım, predilatasyon grubunda %69.6 ve predilatasyon yapılmayan grupta %55.6 oranında elde edildi (P = 0.039). Predilatasyon (OR = 0.51, P = 0.030) ve glikoprotein IIb/IIIa inhibitörü kullanımı (OR = 0.39, P = 0.003) yetersiz akım riskinin azalmasıyla bağımsız olarak ilişkili bulundu. ST-segment elevasyonlu miyokard enfarktüsü (STEMI), yetersiz TIMI akım riski ile ilişkili bulundu (OR = 2.37, P = 0.039). Lipid parametreleri ve statin kullanımı, TIMI akım sonuçlarıyla ilişkili değildi.

Sonuç: Akut koroner sendromlu ve SVG PCI uygulanan hastalarda, stentleme öncesi predilatasyon yapılması, işlem sonrası TIMI 3 akım oranlarını artırarak reperfüzyon başarısını iyileştirmiştir. GP IIb/IIIa inhibitörü kullanımı ek koruyucu etki sağlamıştır. Daha büyük, prospektif çalışmalara ihtiyaç vardır.

Anahtar Kelimeler: Akut koroner sendrom, perkütan koroner girişim, predilatasyon, safen ven grefti, Thrombolysis in Myocardial Infarction akımı

Cardiovascular diseases (CVDs) are among the leading causes of mortality and morbidity worldwide and frequently manifest clinically as acute coronary syndrome (ACS). Deaths due to ischemic heart disease (IHD) account for 38% of all CVD-related deaths in women and 44% in men.[1] Technological advances in revascularization techniques, including percutaneous coronary intervention (PCI) and coronary artery bypass grafting (CABG) have improved long-term survival rates and reduced the incidence of restenosis.[2]

Saphenous vein grafts (SVGs) have become one of the most commonly used graft types in coronary bypass surgery due to their technical ease of use and wide availability. However, both early and late SVG failure rates remain considerably high. Approximately 30% of SVGs occlude within the first year after CABG, and the rate of graft failure continues to increase over 5–10 years following surgery.[3] The treatment of SVG lesions poses significant challenges due to technical difficulties, increased mortality risk, and the potential for graft re-injury. In this setting, repeat surgical revascularization is often not a suitable option for many patients. Additionally, PCI targeting native coronary arteries often have limited success due to anatomical complexities such as chronic total occlusions (CTO), tortuosity, and severe calcification.[4]

Several studies have demonstrated that stent implantation in SVG lesions provides superior clinical and angiographic outcomes compared with balloon angioplasty in both the short and mid-to-long term.[5,6] However, PCI performed on SVGs using a stenting strategy following balloon lesion preparation has been reported to increase the incidence of periprocedural myocardial infarction (MI) and stent thrombosis compared with a direct stenting approach.[7] Conversely, other studies with long-term follow-up have reported no significant difference in clinical outcomes between these two treatment strategies.[8] Thus, the current literature provides conflicting evidence, and no studies have specifically evaluated patients presenting with ACS. Therefore, the present study aimed to investigate the impact of a predilatation strategy on procedural outcomes in patients with ACS undergoing PCI to an SVG.

ABBREVIATIONS

ACS	Acute coronary syndrome
AF	Atrial fibrillation
ASA	Acetylsalicylic acid
CABG	Coronary artery bypass graft
CK-MB	Creatine kinase–myocardial band
CTO	Chronic total occlusions
CVD	Cardiovascular disease
ECG	Electrocardiography
HDL	High-density lipoprotein
HIMS	Hospital Information Management System
ICA	Invasive coronary angiography
IHD	Ischemic heart disease
IV	Intravenous
LDL	Low-density lipoprotein
LVEF	Left ventricular ejection fraction
MACE	Major adverse cardiac events
NSTEMI	Non–ST-elevation myocardial infarction
PCI	Percutaneous coronary interventions
STEMI	ST-segment elevation myocardial infarction
SVG	Saphenous vein grafts
TIMI	Thrombolysis in Myocardial Infarction
TVF	Target vessel failure
USAP	Unstable angina pectoris
WBC	White blood cell

Materials and Methods

Study Population

In this retrospective, single-center study, patients with a history of CABG who were admitted with ACS between 2007 and 2024 were screened through the Hospital Information Management System (HIMS). Patients who underwent percutaneous coronary intervention to a saphenous vein graft during the procedure were included in the study.

According to the predefined exclusion criteria, individuals younger than 18 years of age, patients with chronic liver failure, those with chronic kidney failure, patients who underwent intervention

only to native coronary arteries, and cases in which more than one coronary vessel was treated simultaneously were excluded. Additionally, patients who underwent post-dilatation or sequential predilatation, those in whom distal embolic protection devices were used during the procedure, cases in which graft dissection occurred during the intervention, and patients with multiple sequential lesions in the same SVG were also excluded. Furthermore, patients using oral anticoagulants for any indication were excluded from the analysis. Patients whose invasive coronary angiography (ICA) procedural images were not accessible and those without available laboratory data recorded in the HIMS within ±7 days of the ICA date were also excluded. Ultimately, 202 patients were included in the final analysis. Regardless of procedural outcome, patients were classified into two subgroups according to whether predilatation was performed.

All patients underwent selective left and right coronary angiography, as well as CABG angiography, using the Judkins technique. A transfemoral or transradial approach was used for ICA. When necessary, aortic root angiography was performed to assess graft patency. The degree of stenosis was determined using angiographic images with vessel calibration techniques. Stenosis > 70% in the SVG was considered severe, and PCI was performed in these patients. Before PCI, patients received a loading dose of clopidogrel, ticagrelor, or prasugrel. For patients not already taking acetylsalicylic acid (ASA), a 300 mg chewable loading dose was administered prior to the procedure. During the intervention, intravenous (IV) unfractionated heparin (70–100 U/kg) was administered. In cases of high thrombus burden or the development of no-reflow, a glycoprotein IIb/IIIa inhibitor was administered as an IV bolus at the operator's discretion. The type of stent used was also determined by the operator.

Coronary angiographic images were obtained in at least two orthogonal projections using the Philips Allura Xper FD10 cardiovascular X-ray system (Philips Healthcare, Philips Medical Systems). Coronary flow status was assessed independently by two cardiologists using the Thrombolysis in Myocardial Infarction (TIMI) flow grading system. Cases with TIMI flow grades of 0, 1, or 2 were classified as having impaired coronary flow, whereas those with a TIMI grade of 3 were categorized as having normal coronary flow.

In addition, patient files and hospital archive records were reviewed, and the following data were collected: demographic characteristics (age, sex, smoking status, date of CABG, statin use, medical history, antiplatelet therapy, etc.), electrocardiographic (ECG) findings, laboratory parameters (lipid profile, complete blood count indices, liver function tests, etc.), and echocardiographic measurements.

Written informed consent was obtained from all patients prior to the procedure. The study protocol was approved by the Sivas Cumhuriyet University Non-Interventional Clinical Research Ethics Committee (Approval Number: 2024-02/32, Date: 22.02.2024) and conducted in accordance with the Declaration of Helsinki.

Statistical Analysis

Descriptive statistics were expressed as mean ± standard deviation or median (minimum–maximum) for numerical variables and as frequency and percentage [n (%)] for categorical variables. The normality of data distribution was assessed using the Kolmogorov–Smirnov test and histogram plots. The Mann–Whitney U test was used to compare non-normally distributed (nonparametric) continuous variables between two groups, while differences between categorical variables were analyzed using the chi-square test. The degree of correlation between variables was evaluated using Pearson or Spearman correlation analyses, depending on data distribution. Logistic regression analysis was performed to identify independent predictors of TIMI flow. Results were reported as odds ratios (ORs) with 95% confidence intervals (CIs). Covariates included in the multivariable model were selected a priori based on clinical relevance, previous literature, and potential confounding effects. To avoid overfitting and unstable estimates, not all recorded variables were entered simultaneously into the final model. Statistical analyses were performed using IBM SPSS Statistics for Windows, version 25.0 (IBM Corp., Armonk, NY, USA), and a P-value < 0.05 was considered statistically significant. Graphs were generated using GraphPad Prism version 10.6.0.

Results

Among patients who underwent ICA between 2007 and 2024 and had a prior history of CABG, a total of 202 individuals diagnosed with ACS met the inclusion criteria for the study. These patients were divided into two groups according to whether predilatation was performed during the procedure (predilatation group, n = 112; no predilatation group, n = 90). Demographic data, laboratory findings, ECG records, echocardiographic results, and ICA images of all patients were reviewed. The baseline demographic and clinical characteristics of the study population are presented in Table 1.

The two groups were generally comparable with respect to demographic and clinical characteristics. However, when the target SVGs were evaluated, 43.1% of the interventions were performed on saphenous vein grafts to the right coronary artery (RCA–SVGs), 37.1% on saphenous vein grafts to the circumflex/obtuse marginal arteries (Cx/OM–SVGs), and 19.8% on saphenous vein grafts to the left anterior descending/diagonal arteries (LAD/D–SVGs). Interventions targeting RCA grafts were significantly more frequent than those targeting other grafts (P = 0.011).

The rate of statin use prior to ACS presentation was 78.6% in the predilatation group and 62.2% in the no predilatation group, with this difference reaching statistical significance (P = 0.011). In contrast, no significant differences were observed between the two groups in terms of anticoagulant or antiplatelet therapy use (P = 0.116 and P = 0.269, respectively).

One of the main outcomes of the study, post-procedural TIMI 3 flow, was observed in 63.4% of the overall patient population. The rate of TIMI 3 flow was 69.6% in the predilatation group and 55.6% in the no predilatation group, indicating a significantly higher proportion among patients who underwent predilatation (P = 0.039).

Laboratory parameters were generally comparable between the two groups. However, white blood cell (WBC) levels, although within normal clinical limits, were significantly higher in the predilatation group (P = 0.037). In the lipid profile analysis, both

Table 1. Baseline demographic and clinical characteristics

Variables	Without predilatation (n = 90)	With predilatation (n = 112)	All patients (n = 202)	*P*
Female, n (%)	21 (23.3)	24 (21.4)	45 (22.3)	0.746
Mean age, years	66.8 ± 8.0	67.9 ± 8.3	67.4 ± 8.2	0.339
STEMI, n (%)	12 (13.3)	20 (17.9)	32 (15.8)	0.573
SVG location				0.011*
RCA, n (%)	49 (54.4)	38 (33.9)	87 (43.1)	
Cx/OM, n (%)	25 (27.8)	50 (44.6)	75 (37.1)	
LAD/D, n (%)	16 (17.8)	24 (21.4)	40 (19.8)	
Number of grafts	1.9 ± 0.7	1.7 ± 0.7	1.8 ± 0.7	0.105
SGV age, years	9.3 ± 5.0	10.2 ± 4.6	9.8 ± 4.8	0.193
Diabetes mellitus, n (%)	48 (53.3)	65 (58.0)	113 (55.9)	0.503
Hypertension, n (%)	85 (94.4)	104 (92.9)	189 (93.6)	0.866
COPD, n (%)	23 (25.6)	22 (19.6)	45 (22.3)	0.315
Smoking, n (%)	7 (7.8)	10 (8.9)	17 (8.4)	0.970
Malignancy, n (%)	4 (4.4)	6 (5.4)	10 (5.0)	1.000
Atrial fibrillation, n (%)	8 (8.9)	14 (12.5)	22 (10.9)	0.554
LVEF (%)	46 ± 9	46 ± 9	46 ± 9	0.678
GP IIb/IIIa inhibitor use, n (%)	30 (33.3)	36 (32.1)	66 (32.7)	0.858
Adenosine use, n (%)	0 (0.0)	2 (1.8)	2 (1.0)	0.503
Nitrate use, n (%)	0 (0.0)	5 (4.5)	5 (4.5)	0.067
Adrenaline use, n (%)	0 (0.0)	1 (0.9)	1 (0.5)	1.000
Statin use, n (%)	56 (62.2)	88 (78.6)	144 (71.3)	0.011*
Antiplatelet use, n (%)	87 (96.7)	103 (92.0)	190 (94.1)	0.269
Insulin use, n (%)	32 (35.6)	43 (38.4)	75 (37.1)	0.678
TIMI 3 flow, n (%)	50 (55.6)	78 (69.6)	128 (63.4)	0.039*
Hemoglobin, g/dL	13.7 ± 2.2	13.5 ± 1.7	13.6 ± 1.9	0.601
Hematocrit, %	39.3 ± 6.3	40.8 ± 5.0	40.7 ± 5.6	0.822
WBC (×10³/L)	8.5 ± 3.1	9.5 ± 3.6	9.0 ± 3.4	0.037*
Platelet count (×10³/L)	212 ± 56	228 ± 71	221 ± 65	0.086
Creatinine, mg/dL	1.15 ± 0.48	1.15 ± 0.49	1.15 ± 0.49	0.910
TSH (mIU/L)	0.94 (0.47–1.68)	1.09 (0.69–1.79)	1.04 (0.56–1.76)	0.113
T3 (pg/mL)	2.68 ± 0.55	2.61 ± 0.47	2.64 ± 0.51	0.334
T4 (pg/mL)	1.19 ± 0.26	1.23 ± 0.28	1.22 ± 0.27	0.269
CRP (mg/L)	4.94 (2.32–10.75)	7.44 (3.30–14.62)	6.74 (2.93–13.99)	0.241
Troponin T (ng/L)	168 (16–649)	262 (36–882)	223 (28–827)	0.131
Triglycerides (mg/dL)	139 (96–221)	132 (94–196)	134 (96–204)	0.409
Total cholesterol (mg/dL)	181 ± 49	167 ± 44	173 ± 47	0.043*
HDL (mg/dL)	36 ± 8	36 ± 10	36 ± 9	0.941
LDL (mg/dL)	117 ± 40	105 ± 38	110 ± 39	0.028*
Albumin, g/L	38.1 ± 5.2	38.1 ± 4.7	38.1 ± 4.9	0.988
Uric acid, mg/dL	6.0 ± 1.8	6.3 ± 1.9	6.2 ± 1.8	0.311
ALT (U/L)	21 (15–31)	19 (13–25)	20 (14–27)	0.171
AST (U/L)	26 (20–43)	24 (19–34)	25 (19–37)	0.721
Potassium (mEq/L)	4.3 ± 0.5	4.4 ± 0.5	4.4 ± 0.5	0.245
Sodium (mEq/L)	137 ± 4	137 ± 4	137 ± 4	0.934
Calcium (mEq/L)	8.98 ± 0.59	8.97 ± 0.52	8.97 ± 0.55	0.894

*P < 0.05; ALT, Alanine aminotransferase; AST, Aspartate aminotransferase; COPD, Chronic obstructive pulmonary disease; CRP, C-reactive protein; Cx, Circumflex artery; D, Diagonal; GP IIb/IIIa, Glycoprotein IIb/IIIa; HDL, High-density lipoprotein; LAD, Left anterior descending artery; LDL, Low-density lipoprotein; LVEF, Left ventricular ejection fraction; OM, Obtuse marginal artery; RCA, Right coronary artery; STEMI, ST-elevation myocardial infarction; SVG, Saphenous vein graft; TIMI, Thrombolysis in Myocardial Infarction; TSH, Thyroid-stimulating hormone.

Table 2. Distribution of patients by diagnosis, troponin levels, and percentages of coronary artery lesions causing acute coronary syndrome

Diagnosis	Number of patients (n = 202)	Percentage (%)	Vessel stenosis (%)			Troponin		
			25th percentile	Median	75th percentile	25th percentile	Median	75th percentile
USAP	70	34.7	80	95	99	3.00	12.50	33.00
NSTEMI	100	49.5	90	95	99	239.00	388.50	975.50
STEMI	32	15.8	95	99	100	230.50	1027.00	3458.50

NSTEMI, Non–ST-elevation myocardial infarction; STEMI, ST-elevation myocardial infarction; USAP, Unstable angina pectoris. High-sensitivity cardiac troponin T (hs-cTnT) laboratory reference values: 0–13 ng/L, normal; 14–50 ng/L, intermediate risk (repeat testing recommended); > 50 ng/L, high risk.

total cholesterol and low-density lipoprotein (LDL) levels were above target ranges in both groups but were significantly lower in the predilatation group (P = 0.043 and P = 0.028, respectively). High-density lipoprotein (HDL) levels were below target ranges in both groups, with no significant differences observed between the groups in terms of HDL or triglyceride levels (P = 0.941 and P = 0.409, respectively).

The distribution of patients according to diagnosis, troponin levels, and the percentages of culprit vessel stenoses leading to ACS are presented in Table 2. Approximately half of the patients who underwent intervention (49.5%) were diagnosed with non–ST-elevation myocardial infarction (NSTEMI), representing the largest subgroup within the study population. When patients with unstable angina pectoris (USAP) and NSTEMI were considered together, they accounted for 84.2% of the entire cohort. When the stenosis rates detected by ICA were evaluated, the median degree of stenosis was 95% in both the USAP and NSTEMI groups. In contrast, patients diagnosed with ST-elevation myocardial infarction (STEMI) had a significantly higher median stenosis rate of 99%. Evaluation of high-sensitivity cardiac troponin T (hs-cTnT) levels showed that the median troponin concentration in the USAP group was 12.50 ng/L, which was within the normal reference range. In the NSTEMI and STEMI groups, troponin levels were markedly elevated, with the highest median value observed in the STEMI group at 1027.00 ng/L (230.50–3458.50). The laboratory reference ranges for hs-cTnT were as follows: 0–13 ng/L, normal; 14–50 ng/L, intermediate risk (repeat testing recommended); and > 50 ng/L, high risk.

Table 3 presents a comparative analysis of the diameters and lengths of balloons and/or stents used in patients with and without predilatation. The mean stent diameter was 3.0 ± 0.5 mm in the predilatation group and 3.2 ± 0.5 mm in the no predilatation group, with no statistically significant difference between the groups (P = 0.187). In contrast, the mean stent length was significantly greater in patients who underwent predilatation (20.2 ± 6.0 mm) than in those who did not (18.0 ± 4.6 mm), demonstrating a statistically significant difference (P = 0.010).

According to the correlation analysis presented in Table 4, a statistically significant positive correlation was observed between patient age and SVG age (P < 0.01). Similarly, creatinine levels were found to increase significantly with age (P < 0.01).

Predilatation was associated with significantly improved post-procedural TIMI flow (P < 0.05). A statistically significant positive correlation was also observed between troponin levels and patient age (P < 0.05). Additionally, troponin levels showed a strong positive association with the diagnosis of STEMI (P < 0.01). In contrast, the relationship between STEMI diagnosis and TIMI flow was negative, as patients diagnosed with STEMI exhibited significantly lower TIMI flow levels (P < 0.01). Although not statistically significant, a weak negative correlation was observed between SVG age and balloon diameter. Similarly, a nonsignificant positive correlation was found between LDL levels and balloon length, while a negative correlation was observed between creatinine levels and balloon length.

Table 3. Balloon and/or stent sizes

Variables	Without predilatation (n = 90)	With predilatation (n = 112)	All patients (n = 202)
Stent diameter (mm)	3.2 ± 0.5	3.0 ± 0.5	0.187
Stent length (mm)	18.0 ± 4.6	20.2 ± 6.0	0.010*
Balloon diameter (mm)	-	2.6 ± 0.5	-
Balloon length (mm)	-	17.2 ± 4.8	-

*P < 0.05.

According to logistic regression analysis, insufficient TIMI flow was not significantly associated with SVG age, smoking status, atrial fibrillation (AF), statin use, or uric acid levels (P = 0.784, P = 0.132, P = 0.253, P = 0.239, and P = 0.228, respectively). Likewise, sex, hypertension, antiplatelet use, nitrate therapy, and the presence of chronic obstructive pulmonary disease (COPD) were not significantly associated with insufficient TIMI flow (P = 0.304, P = 0.367, P = 0.800, P = 0.423, and P = 0.209, respectively). Similarly, patient age, diabetes mellitus, left ventricular ejection fraction (LVEF), LDL levels, and creatinine concentration were not significantly associated with the development of insufficient TIMI flow (P = 0.337, P = 0.840, P = 0.788, P = 0.199, and P = 0.562, respectively).

In contrast, the use of glycoprotein IIb/IIIa (GP IIb/IIIa) inhibitors and the performance of predilatation during the procedure were identified as significant factors associated with a reduced risk of insufficient TIMI flow (P = 0.003 and P = 0.030, respectively). Conversely, patients who underwent the procedure for STEMI had a significantly higher likelihood of developing insufficient TIMI flow (P = 0.039). These findings are illustrated in Figure 1.

Among patients who underwent predilatation, TIMI 3 flow was achieved in 78 cases, which were classified as having no flow limitation. In the same group, 34 patients exhibited TIMI flow grades of 0, 1, or 2, indicating impaired flow. In the no

Table 4. Correlation analysis of variables

Variables	TIMI flow	Age	SGV age	Balloon diameter	Balloon length	Creatinine	LDL	Troponin	Predilatation	STEMI
TIMI flow	1									
Age	0.004	1								
SGV age	0.057	0.244**	1							
Balloon diameter	0.004	-0.177	-0.059	1						
Balloon length	-0.047	-0.102	0.017	0.065	1					
Creatinine	-0.051	0.305**	0.105	0.004	0.052	1				
LDL	0.001	-0.094	-0.089	0.166	0.031	-0.043	1			
Troponin	-0.116	0.212*	0.098	-0.177	0.050	0.119	0.124	1		
Predilatation	0.153*	0.058	0.107	-	-	0.039	-0.146*	0.096	1	
STEMI	-0.184**	0.019	0.054	0.073	0.041	-0.004	0.014	0.363**	0.062	1

*P < 0.05, **P < 0.01; LDL, Low-density lipoprotein cholesterol; STEMI, ST-elevation myocardial infarction; SVG, Saphenous vein graft; TIMI, Thrombolysis in myocardial infarction.

predilatation group, TIMI 3 flow was observed in 50 patients, whereas 40 patients demonstrated TIMI flow grades of 0, 1, or 2. Comparison between the groups showed that the rate of TIMI 3 flow was significantly higher in the predilatation group (P = 0.039). These findings, along with the distribution of SVGs according to their corresponding native vessels, are illustrated in Figure 2.

Discussion

In this study, we evaluated the effect of predilatation on coronary flow during PCI of SVGs in patients presenting with ACS and a prior history of CABG. Our results demonstrated that patients who underwent predilatation before stent implantation had significantly higher rates of TIMI 3 flow. This finding suggests that predilatation may help preserve distal flow and improve procedural success, particularly in graft interventions. Moreover, the more frequent occurrence of impaired TIMI flow among patients with STEMI may be attributed to a higher thrombus burden and the graft characteristics. Additionally, the observed improvement in TIMI flow with the use of GP IIb/IIIa inhibitors supports the role of antiplatelet therapy in achieving successful reperfusion.

Despite increasing recognition of their limited long-term patency, saphenous vein grafts remain widely used in the surgical treatment of obstructive coronary artery disease. Reported patency rates for SVGs vary considerably in the literature, with graft failure rates reaching up to 61% in follow-up periods exceeding 10 years.[9] In patients with prior CABG, current guidelines recommend PCI of the native coronary artery as the preferred revascularization strategy whenever feasible, whereas PCI of SVGs is considered a secondary option because of its higher risk of adverse events.[10] Furthermore, as the time elapsed after CABG increases, the incidence of diffuse atherosclerosis, calcified lesions, and CTOs in native coronary arteries also rises. The development of de novo CTOs even in initially patent vessels has been documented, further contributing to the need for graft interventions.[11] Consequently, PCI of SVG may become unavoidable in certain clinical scenarios. However, it should be recognized that graft PCI carries an increased risk of complications, including friable plaque, high thrombus burden, distal embolization, and the no-reflow phenomenon. Therefore, interventional strategies should be planned with particular caution.[9] Considering these technical challenges and the potential to improve long-term outcomes in interventions targeting SVG lesions, our study evaluated factors influencing coronary flow during the procedure, with particular emphasis on the role of predilatation.

In interventions involving SVGs, whether stent implantation should be performed directly or after predilatation remains a matter of debate in the literature. Direct stenting may reduce the risk of distal embolization by minimizing plaque manipulation, whereas predilatation facilitates lesion preparation and may promote optimal stent expansion and full apposition to the vessel wall.[12] However, studies evaluating the effects of these two strategies on clinical outcomes have yielded heterogeneous results.

Among studies comparing different strategies in SVG-PCI, a subgroup analysis of the DIVA trial (Drug-Eluting Stents vs Bare-Metal Stents in Saphenous Vein Graft Angioplasty) conducted by Latif et al.[7] evaluated stenting with and without predilatation and found no significant difference in 12-month target vessel failure (TVF).[13] Moreover, during long-term follow-up, the direct stenting group demonstrated lower incidences of stent thrombosis and target vessel myocardial infarction. Similarly, Leborgne et al.[14] compared a direct stenting strategy with predilatation followed by stenting in patients with SVG stenosis, evaluating outcomes including creatine kinase–myocardial band (CK-MB) release, major adverse cardiac events (MACE), and long-term clinical outcomes. The authors reported that direct stenting may reduce the risk of distal embolization and limit long-term MACE rates compared with predilatation. However, both of these studies primarily focused on long-term clinical outcomes. In contrast, our study evaluated a more selective population consisting exclusively of patients presenting with ACS, and coronary flow was directly assessed using the TIMI flow system. Our findings demonstrated significantly higher rates of TIMI 3 flow in the predilatation group, highlighting the role of predilatation in improving acute procedural success during SVG-PCI.

Parameter	Odds Ratio (OR)	95% Confidence Interval (CI)	P Value
Age	1.00	0.96–1.04	0.337
Sex (Females)	0.64	0.27–1.50	0.304
SVG Age	1.01	0.94–1.08	0.748
Hypertension	0.50	0.11–2.26	0.367
Diabetes Mellitus	1.07	0.54–2.13	0.840
Atrial Fibrillation	2.30	0.55–9.59	0.253
COPD	1.64	0.76–3.54	0.209
Smoking	2.75	0.74–10.25	0.132
STEMI	2.37	1.04–5.39	0.039*
LVEF	1.00	0.96–1.03	0.788
Antiplatet Use	0.82	0.18–3.80	0.800
Statin Use	0.64	0.30–1.35	0.239
GP IIb/IIIa Inh. Use	0.39	0.21–0.73	0.003*
Nitrate Use	0.42	0.05–3.51	0.423
Predilatation	0.51	0.28–0.94	0.030*
LDL	1.01	1.00–1.02	0.199
Creatinine	0.81	0.40–1.66	0.562
Uric Acid	1.13	0.93–1.37	0.228

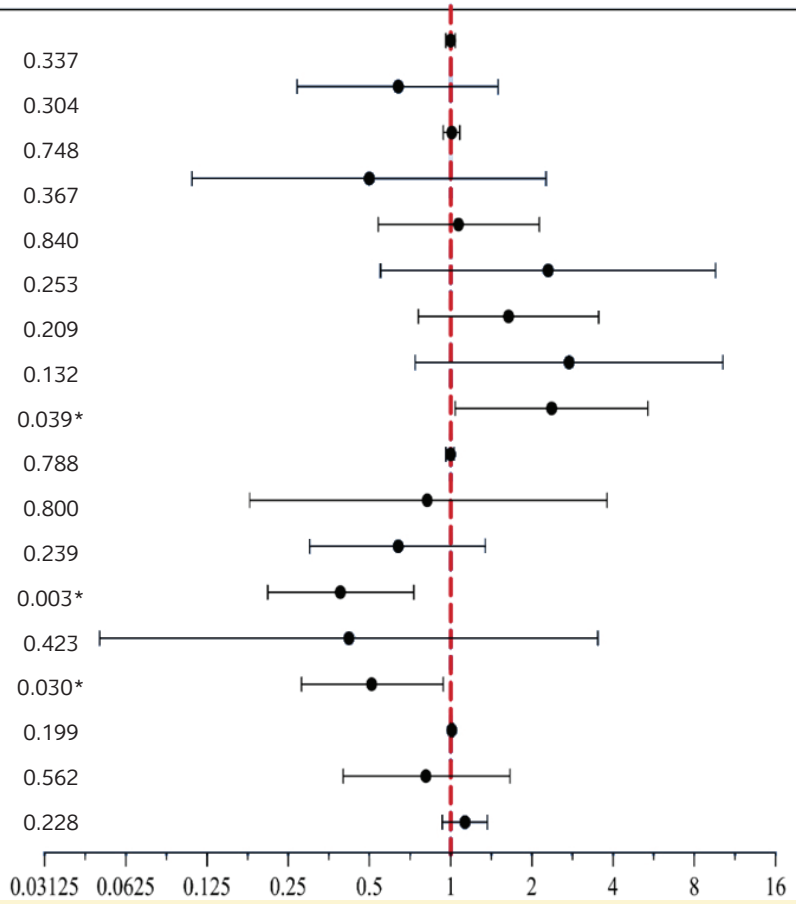

Figure 1. Logistic regression analysis of factors associated with inadequate Thrombolysis in Myocardial Infarction (TIMI) flow after saphenous vein graft percutaneous coronary intervention (SVG-PCI). The forest plot demonstrates odds ratios (ORs) with 95% confidence intervals (Cis) for each parameter.

***P < 0.05; COPD, Chronic obstructive pulmonary disease; GP Iib/IIIa inh., Glycoprotein Iib/IIIa inhibitor; LDL, Low-density lipoprotein cholesterol; LVEF, Left ventricular ejection fraction; STEMI, ST-elevation myocardial infarction; SVG, Saphenous vein graft; TIMI, Thrombolysis in Myocardial Infarction.**

Lee et al.[15] suggested that, in SVG lesions, direct stenting may represent a more advantageous strategy than predilatation because it may reduce vascular wall injury and the risk of distal embolization associated with repeated balloon dilatations. However, in our study, patients who underwent postdilatation or multiple sequential predilatations were excluded. Therefore, the favorable outcomes observed were likely associated with an effective and controlled predilatation approach. This finding highlights the crucial role of appropriate patient selection and meticulous lesion preparation in procedural success and, when interpreted alongside the results of comparative studies,[7,14] provides a clinically meaningful perspective.

In our cohort of patients presenting with ACS, the most frequently involved graft was the RCA–SVG, whereas the least commonly affected was the LAD/D–SVG. The mean interval between CABG and the ACS event was approximately 10 years, which corresponds to the period when graft degeneration typically becomes clinically evident. Vessel-based analysis demonstrated that the best procedural TIMI flow was observed in Cx/OM–SVG. These findings suggest that the hemodynamic performance of grafts may vary depending on the target coronary artery segment, flow demand, and the quality of the surgical anastomosis. Consistent with our findings, previous studies have reported lower long-term patency rates for RCA grafts and variable TIMI flow outcomes depending on distal vessel bed characteristics and flow requirements.[16,17]

In our study, factors associated with impaired TIMI flow were evaluated. Predilatation (OR = 0.51, P = 0.030) and the use of GP IIb/IIIa inhibitors (OR = 0.39, P = 0.003) were identified as protective factors, whereas the presence of STEMI was significantly associated with impaired flow (OR = 2.37, P = 0.039). This finding is consistent with previous studies reporting that periprocedural complications and inadequate distal flow during SVG-PCI are particularly common in STEMI cases and are closely related to a high thrombus burden.[13,18] Similarly, Keeley et al.[19] demonstrated that impaired flow in SVG lesions is frequently

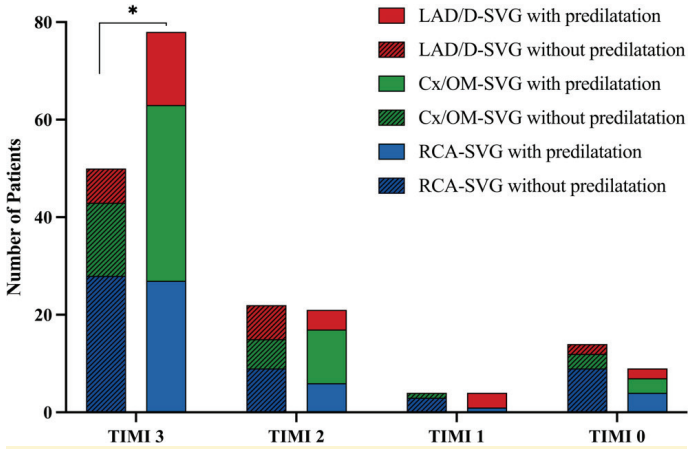

Figure 2. Distribution of Thrombolysis in Myocardial Infarction (TIMI) flow grades in patients with and without predilatation.

*** P < 0.05, Cx, Circumflex artery; D, Diagonal; LAD, Left anterior descending artery; OM, Obtuse marginal artery; RCA, Right coronary artery; SVG, Saphenous vein graft.**

associated with thrombotic occlusion and the no-reflow phenomenon. The identification of STEMI as an independent predictor of impaired TIMI flow in our study is therefore consistent with these observations. Conversely, the protective effect of GP IIb/IIIa inhibitors is well supported by the literature, as these agents have been shown to significantly increase the rate of TIMI 3 flow by reducing microvascular thrombus formation.[20] De Luca et al.[21] demonstrated that early administration of GP IIb/IIIa inhibitors significantly improves reperfusion success, particularly in STEMI patients with a high thrombus burden. These findings further support the protective role of GP IIb/IIIa inhibitors against impaired TIMI flow observed in our study.

Although LDL cholesterol levels were significantly lower in the predilatation group in our study, LDL values in both groups remained above guideline-recommended targets. The low rate of statin use observed in both groups is also noteworthy. However, in the logistic regression analysis, neither LDL levels nor statin use were significantly associated with impaired TIMI flow. Several explanations may account for this finding. First, lipid parameters in the setting of ACS are often influenced by the acute-phase response, which may prevent LDL levels from accurately reflecting the true chronic burden of dyslipidemia.[22-24] Moreover, in the acute phase, the primary determinants of TIMI flow, such as thrombus burden, distal embolization, and microvascular reperfusion impairment, are more closely related to procedural hemodynamic and thrombotic factors than to lipid levels. The well-established anti-inflammatory, endothelial-protective, and plaque-stabilizing effects of statins are known to become more evident over the long term, particularly in reducing restenosis, lowering the need for repeat revascularization, and maintaining graft patency, rather than influencing acute outcomes.[25,26] This observation is consistent with the lack of a significant association between LDL levels or statin use and impaired TIMI flow in our study, which focused on the acute phase.

In summary, among patients presenting with ACS who underwent SVG-PCI, our findings demonstrate that predilatation not only facilitates mechanical lesion preparation but may also contribute to preserving post-procedural coronary flow. Considering the dynamic thrombus burden and microvascular reperfusion impairment characteristic of ACS, these results indicate that a careful and selective predilatation strategy may be critical for optimizing procedural success. Furthermore, the observed protective effect of GP IIb/IIIa inhibitors against impaired TIMI flow underscores the importance of optimizing antiplatelet therapy in ACS patients. By focusing specifically on ACS cases treated with SVG-PCI, our study provides a modest yet meaningful contribution to the limited data on this challenging clinical subset.

Study Limitations

This study was conducted at a single center and had a retrospective design. The relatively limited number of patients may have increased the potential for bias in patient selection and data recording processes. Furthermore, information regarding statin use, as well as antiplatelet and anticoagulant therapies, was obtained from electronic medical records; therefore, regular medication adherence could not be verified. The lack of access to detailed surgical data related to CABG and technical factors that might have affected graft patency constitutes another limitation. Additionally, data regarding the patency status of native coronary arteries at the time of index ICA were not available. Cases with graft dissection during the procedure were excluded, which may have introduced selection bias and limited the generalizability of the findings. Coronary flow was evaluated solely using the TIMI flow classification, which represents a methodological limitation for the assessment of microvascular reperfusion with more sensitive parameters. Nevertheless, TIMI flow is one of the fundamental indicators of reperfusion success in ACS, and its clinical significance should not be overlooked.

Conclusion

In this study, the impact of predilatation on post-procedural coronary flow was evaluated in patients presenting with ACS who underwent PCI to SVGs. The findings indicate that predilatation may improve reperfusion success in the acute phase by increasing the rate of post-procedural TIMI 3 flow. Moreover, the protective effect observed with the use of GP IIb/IIIa inhibitors highlights the importance of optimized antiplatelet strategies. Conversely, the presence of STEMI was associated with impaired distal flow. Although our study provides valuable insights, the generalizability of these findings is limited. Larger randomized controlled trials are warranted to confirm these results.

Ethics Committee Approval: Ethics committee approval was obtained from Sivas Cumhuriyet University Non-Interventional Clinical Research Ethics Committee (Approval Number: 2024-02/32, Date: 22.02.2024).

Informed Consent: Written informed consent was obtained from all patients prior to the procedure.

Conflict of Interest: The authors have no conflicts of interest to declare.

Funding: The authors declared that this study received no financial support.

Use of AI for Writing Assistance: Artificial intelligence (ChatGPT) was used for language editing and translation during manuscript preparation. The authors reviewed and approved the final manuscript.

Author Contributions: Concept – M.B.D., M.Ş., G.T., A.Ş., Y.K., N.O.D.; Design – M.B.D., M.Ş., G.T., A.Ş., Y.K., N.O.D.; Supervision – M.B.D., G.T., A.Ş., Y.K.; Resource – G.T., A.Ş., Y.K.; Materials – M.B.D., M.Ş., A.Ş., N.O.D.; Data Collection and/or Processing – M.B.D., M.Ş., G.T., A.Ş., Y.K.; Analysis and/or Interpretation – M.B.D., A.Ş., Y.K., N.O.D.; Literature Review – M.B.D., A.Ş., Y.K.; Writing – M.B.D., M.Ş., A.Ş., Y.K.; Critical Review – M.B.D., M.Ş., G.T., A.Ş., Y.K., N.O.D.

Peer-review: Externally peer-reviewed.

References

1. Timmis A, Vardas P, Townsend N, et al.; Atlas Writing Group, European Society of Cardiology. European Society of Cardiology: cardiovascular disease statistics 2021. *Eur Heart J*. 2022;43(8):716-799. Erratum in: *Eur Heart J*. 2022;43(8):799. [CrossRef]
2. Bansal A, Hiwale K. Updates in the Management of Coronary Artery Disease: A Review Article. *Cureus*. 2023;15(12):e50644. [CrossRef]
3. Goldman S, Zadina K, Moritz T, et al.; VA Cooperative Study Group #207/297/364. Long-term patency of saphenous vein and left internal mammary artery grafts after coronary artery bypass surgery: results from a Department of Veterans Affairs Cooperative Study. *J Am Coll Cardiol*. 2004;44(11):2149-2156. [CrossRef]
4. Brilakis ES, Banerjee S, Burke MN. A New Treatment Strategy for Saphenous Vein Graft Lesions?: Letting it Go. *J Am Coll Cardiol*. 2018;71(18):1983-1985. [CrossRef]
5. Hanekamp CE, Koolen JJ, Den Heijer P, et al.; Venestent Study Group. Randomized study to compare balloon angioplasty and elective stent implantation in venous bypass grafts: the Venestent study. *Catheter Cardiovasc Interv*. 2003;60(4):452-457. [CrossRef]
6. Savage MP, Douglas JS Jr, Fischman DL, et al. Stent placement compared with balloon angioplasty for obstructed coronary bypass grafts. Saphenous Vein De Novo Trial Investigators. *N Engl J Med*. 1997;337(11):740-747. [CrossRef]
7. Latif F, Uyeda L, Edson R, et al. Stent-Only Versus Adjunctive Balloon Angioplasty Approach for Saphenous Vein Graft Percutaneous Coronary Intervention: Insights from DIVA Trial. *Circ Cardiovasc Interv*. 2020;13(2):e008494. [CrossRef]
8. Lozano I, López-Palop R, Pinar E, et al. Direct stenting in saphenous vein grafts. Immediate and long-term results. *Rev Esp Cardiol*. 2005;58(3):270-277. Spanish. [CrossRef]
9. Back L, Ladwiniec A. Saphenous Vein Graft Failure: Current Challenges and a Review of the Contemporary Percutaneous Options for Management. *J Clin Med*. 2023;12(22):7118. [CrossRef]
10. Xenogiannis I, Zenati M, Bhatt DL, et al. Saphenous Vein Graft Failure: From Pathophysiology to Prevention and Treatment Strategies. *Circulation*. 2021;144(9):728-745. [CrossRef]
11. Çoner A, Akıncı S, Akbay E, Budak AB, Saba T, Müderrisoğlu H. Development of De Novo Chronic Total Occlusion in Native Coronary Arteries of Coronary Artery Bypass Grafting Surgery Patients. *Acta Medica Alanya*. 2020;4(3):230-235. [CrossRef]
12. Lee M, Kong J. Current State of the Art in Approaches to Saphenous Vein Graft Interventions. *Interv Cardiol*. 2017;12(2):85-91. [CrossRef]
13. Ergelen M, Uyarel H, Gül M, et al. Efficacy and outcome of primary percutaneous coronary intervention in patients with ST-elevation myocardial infarction due to saphenous vein graft occlusion. *Turk Kardiyol Dern Ars*. 2010;38(8):531-536. Turkish.
14. Leborgne L, Cheneau E, Pichard A, et al. Effect of direct stenting on clinical outcome in patients treated with percutaneous coronary intervention on saphenous vein graft. *Am Heart J*. 2003;146(3):501-506. [CrossRef]
15. Lee MS, Park SJ, Kandzari DE, et al. Saphenous vein graft intervention. *JACC Cardiovasc Interv*. 2011;4(8):831-843. [CrossRef]
16. Nakajima H, Iguchi A, Tabata M, et al. Predictors and prevention of flow insufficiency due to limited flow demand. *J Cardiothorac Surg*. 2014;9:188. [CrossRef]
17. Porto I, Belloni F, Niccoli G, et al. Filter no-reflow during percutaneous coronary intervention of saphenous vein grafts: incidence, predictors and effect of the type of protection device. *EuroIntervention*. 2011;7(8):955-961. [CrossRef]
18. Januszek RA, Dziewierz A, Siudak Z, Rakowski T, Dudek D, Bartuś S. Predictors of periprocedural complications in patients undergoing percutaneous coronary interventions within coronary artery bypass grafts. *Cardiol J*. 2019;26(6):633-644. [CrossRef]
19. Keeley EC, Velez CA, O'Neill WW, Safian RD. Long-term clinical outcome and predictors of major adverse cardiac events after percutaneous interventions on saphenous vein grafts. *J Am Coll Cardiol*. 2001;38(3):659-665. [CrossRef]
20. de Lemos JA, Antman EM, Gibson CM, et al. Abciximab improves both epicardial flow and myocardial reperfusion in ST-elevation myocardial infarction. Observations from the TIMI 14 trial. *Circulation*. 2000;101(3):239-243. [CrossRef]
21. De Luca G, Gibson CM, Bellandi F, et al. Early glycoprotein IIb-IIIa inhibitors in primary angioplasty (EGYPT) cooperation: an individual patient data meta-analysis. *Heart*. 2008;94(12):1548-1558. [CrossRef]
22. Balci B. The modification of serum lipids after acute coronary syndrome and importance in clinical practice. *Curr Cardiol Rev*. 2011;7(4):272-276. [CrossRef]
23. Rosenson RS, Brewer HB, Rader DJ. Lipoproteins as biomarkers and therapeutic targets in the setting of acute coronary syndrome. *Circ Res*. 2014;114(12):1880-1889. [CrossRef]
24. Yılmaz C, Üngan İ, Arslan E, et al. The HALP Score's Prognostic Value for the Elderly (≥75 years) Patients Following Percutaneous Coronary Intervention for Acute Myocardial Infarction. *Turk Kardiyol Dern Ars*. 2025;53(6):388-397. [CrossRef]
25. Olsson AG, Schwartz GG, Szarek M, et al. High-density lipoprotein, but not low-density lipoprotein cholesterol levels influence short-term prognosis after acute coronary syndrome: results from the MIRACL trial. *Eur Heart J*. 2005;26(9):890-896. [CrossRef]
26. Ridker PM, Danielson E, Fonseca FA, et al.; JUPITER Study Group. Rosuvastatin to prevent vascular events in men and women with elevated C-reactive protein. *N Engl J Med*. 2008;359(21):2195-2207. [CrossRef]

ARCHIVES OF THE TURKISH SOCIETY OF CARDIOLOGY

Official journal of the TURKISH SOCIETY OF CARDIOLOGY

An Independent Predictor of Technical Success in Patients with Chronic Total Occlusions: The Atherogenic Index of Plasma

Kronik Total Oklüzyonu Olan Hastalarda Teknik Başarının Bağımsız Bir Öngördürücüsü: Plazmanın Aterojenik İndeksi

ABSTRACT

Objective: The atherogenic index of plasma (AIP) has been increasingly associated with coronary artery disease and adverse cardiovascular outcomes. This study aimed to evaluate the clinical relevance of AIP in predicting technical success in percutaneous coronary intervention (PCI) for chronic total occlusion (CTO).

Method: This retrospective study included 197 patients who met the eligibility criteria. AIP was calculated as the base-10 logarithm of the triglyceride (TG)-to-high-density lipoprotein cholesterol (HDL-C) ratio (log10[TG/HDL-C]). Technical success was defined as successful recanalization of the CTO with residual stenosis < 30% and restoration of antegrade flow.

Results: Based on the receiver operating characteristic (ROC)–derived AIP cutoff value (0.802), patients were classified into low-AIP (n = 125, 64%) and high-AIP (n = 72, 36%) groups. Higher AIP levels were associated with lower technical success rates. To assess the incremental predictive value of AIP, two nested models (Model 1 and Model 2) were constructed. Model discrimination improved with the inclusion of AIP (area under the curve [AUC]: 0.73 vs. 0.83), and likelihood ratio testing confirmed a significant enhancement in model performance (P < 0.001). In both models, estimated glomerular filtration rate and the Japanese Chronic Total Occlusion (J-CTO) score remained independent predictors of CTO PCI technical success. In Model 2, AIP was also independently associated with technical success (odds ratio: 0.03, 95% confidence interval: 0.01–0.12, P < 0.001). Although AIP demonstrated a numerically higher AUC than the J-CTO score in ROC analysis for predicting CTO PCI success, the difference was not statistically significant (P = 0.097).

Conclusion: AIP may serve as a useful predictor of technical success in chronic total occlusion percutaneous coronary intervention and may provide incremental value during procedural planning.

Keywords: Atherogenic index of plasma, chronic total occlusion, technical success

ÖZET

Amaç: Plazmanın aterojenik indeksi (AİP), önceki çalışmalarda koroner arter hastalığı ve olumsuz kardiyovasküler prognoz ile giderek daha fazla ilişkilendirilmiştir. Bu çalışma, kronik total oklüzyonun (KTO) perkütan koroner girişiminde (PKG) teknik başarı açısından AİP'in klinik önemini değerlendirmeyi amaçlamıştır.

Yöntem: Bu retrospektif çalışmaya, uygunluk kriterlerini karşılayan toplam 197 hasta dahil edilmiştir. AİP, trigliserid (TG) ile yüksek yoğunluklu lipoprotein kolesterol (HDL-K) oranının logaritmik dönüşümü kullanılarak hesaplanmıştır (log10 [TG/HDL-K]). Teknik başarı; KTO'nun başarılı şekilde rekanalizasyonu, rezidüel darlığın <%30 olması ve antegrad TIMI akım derecesinin 3 olarak sağlanması şeklinde tanımlanmıştır.

Bulgular: ROC eğrisinden elde edilen AİP eşik değerine (0.802) göre hastalar düşük AİP (n = 125, %64) ve yüksek AİP (n = 72, %36) gruplarına ayrılmıştır. Daha yüksek AİP seviyeleri, daha düşük teknik başarı oranlarıyla ilişkilendirilmiştir. AİP'in artımlı tahmin değerini değerlendirmek için iki iç içe geçmiş model (Model 1 ve Model 2) oluşturulmuştur. AİP'in dahil edilmesinden sonra model ayrımcılığı iyileşmiştir (AUC: 0.73'e karşı 0.83) ve olasılık oranı testi, model performansında önemli bir iyileşmeyi doğrulamıştır (P <0.001). Her iki modelde de tahmini glomerüler filtrasyon oranı ve J-CTO skoru, KTO PKG'de teknik başarının bağımsız tahmincileri olarak kalmıştır; Model 2'de ise AİP, teknik başarıyla bağımsız olarak ilişkilendirilmiştir (OR: 0.03, %95 CI: 0.01–0.12, P <0.001). KTO PKG teknik başarısını öngörmek için yapılan ROC analizinde, AİP'in J-CTO skorundan sayısal olarak daha yüksek bir AUC değeri göstermesine rağmen, bu fark istatistiksel olarak anlamlı değildir (P = 0.097).

Sonuç: AİP, KTO PKG'de teknik başarının yararlı bir göstergesi olabilir ve işlem planlaması sırasında ek değer sağlayabilir.

Anahtar Kelimeler: Plazmanın aterojenik indeksi, kronik total oklüzyon, teknik başarı

ORIGINAL ARTICLE
ARAŞTIRMA MAKALESİ

Büşra Güvendi Şengör[1]

Cemalettin Yılmaz[2]

[1]*Department of Cardiology, Kartal Koşuyolu Training and Research Hospital, İstanbul, Türkiye*
[2]*Department of Cardiology, Yalova University Faculty of Medicine, Yalova, Türkiye*

Corresponding author:
Büşra Güvendi Şengör
✉ guvendi2861@hotmail.com

Received: January 23, 2026
Accepted: April 26, 2026

Cite this article as: Güvendi Şengör B, Yılmaz C. An Independent Predictor of Technical Success in Patients with Chronic Total Occlusions: The Atherogenic Index of Plasma. *Turk Kardiyol Dern Ars.* 2026;54(6):496–502.

DOI: 10.5543/tkda.2026.94745

Chronic total occlusion (CTO) is defined as a complete (100%) occlusion of a coronary artery with thrombolysis in myocardial infarction (TIMI) 0 flow persisting for at least three months. It is observed in approximately 15%–20% of patients with coronary artery disease (CAD).[1,2] Although the benefits of CTO recanalization remain debated, prior studies have demonstrated symptomatic improvement following successful percutaneous coronary intervention (PCI) for CTO.[3,4] Outcomes of CTO PCI have progressively improved with advances in equipment, techniques, and operator experience, making PCI a preferred treatment option for eligible patients.

Dyslipidemia is a well-recognized and significant risk factor for CAD. Elevated levels of low-density lipoprotein cholesterol (LDL-C) and triglycerides (TG), along with reduced levels of high-density lipoprotein cholesterol (HDL-C), have been associated with adverse cardiovascular outcomes.[5,6] Beyond traditional lipid parameters, the atherogenic index of plasma (AIP), calculated as the logarithm of the TG-to-HDL-C ratio, has emerged as a novel marker reflecting lipid profiles and predicting plasma atherogenicity.[7,8] AIP has been identified as an independent risk factor for CAD and cardiovascular events and may also be associated with CTO progression.[9-11] However, data regarding its impact on the outcomes of CTO PCI are limited. Therefore, this study aimed to investigate the relationship between AIP and the technical success of CTO PCI procedures.

ABBREVIATIONS

AIP	Atherogenic index of plasma
CAD	Coronary artery disease
CCC	Coronary collateral circulation
CTO	Chronic total occlusion
eGFR	Estimated glomerular filtration rate
HDL-C	High-density lipoprotein cholesterol
HT	Hypertension
J-CTO	Japanese Chronic Total Occlusion
LDL-C	Low-density lipoprotein cholesterol
LVEF	Left ventricular ejection fraction
MPS	Myocardial perfusion scintigraphy
PCI	Percutaneous coronary intervention
ROC	Receiver operating characteristic
TG	Triglyceride
TIMI	Thrombolysis in myocardial infarction

Materials and Methods

The retrospective study enrolled 197 patients who underwent CTO PCI at our tertiary center between January 2018 and December 2022. All patients had documented myocardial ischemia in the territory of the occluded artery on myocardial perfusion scintigraphy (MPS) or had a clinical indication for CTO PCI. Patients with severe heart failure, advanced renal or hepatic failure, active malignancy, a history of systemic inflammatory disease, lipid-lowering drug use within two weeks prior to the procedure, or missing data were excluded (Figure 1 and Supplementary Figure 1). Baseline demographic, clinical, laboratory, imaging, and angiographic data were obtained from the hospital database.

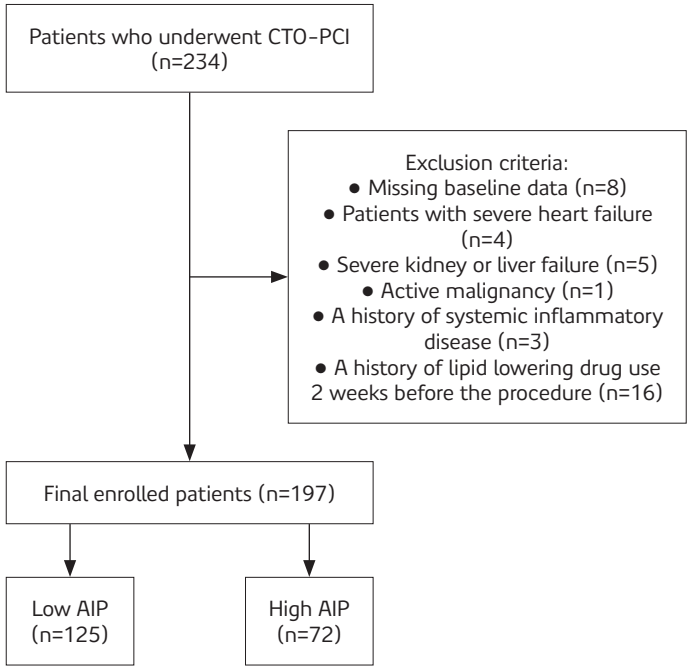

Figure 1. CONSORT diagram of the study population.

AIP, Atherogenic index of plasma; CTO, Chronic total occlusion; PCI, Percutaneous coronary intervention.

Peripheral blood samples were collected 24 hours prior to the procedure, and fasting lipid levels were analyzed using standard laboratory methods. AIP was calculated as the logarithm of the TG-to-HDL-C ratio (log10[TG/HDL-C]).

All patients underwent coronary angiography via the femoral approach, including at least two projections of the right coronary artery and four projections of the left coronary artery. Angiographic images were independently evaluated by two experienced interventional cardiologists. Patients with involvement of two or more vessels were classified as having multivessel disease. CTO was defined as TIMI 0 antegrade flow within the occluded segment for a duration of at least three months. Coronary collateral circulation (CCC) was assessed according to the Rentrop classification, and lesion complexity was evaluated using the Japanese Chronic Total Occlusion (J-CTO) score.[12,13] Rentrop grades 2 and 3 were considered indicative of well-developed CCC. The J-CTO score was calculated based on the presence of calcification, bending > 45° within the CTO segment, a blunt proximal cap, occlusion length, and prior failed attempts. The choice of CTO PCI technique (antegrade or retrograde) and antiplatelet therapy was left to the operator's discretion. Drug-eluting stents were implanted in all patients. Technical success was defined as successful recanalization of the CTO with residual stenosis < 30% and restoration of antegrade TIMI flow grade 3. Unlike procedural success, major adverse cardiac events were not included in this definition.

The study was approved by Kartal Koşuyolu High Specialization Training and Research Hospital (Approval Number: 2024/03/773, Date: 06.02.2024), and the requirement for written informed consent was waived due to the retrospective study design.

Table 1. Baseline demographic, clinical, and laboratory characteristics of the study groups

Variables	Low AIP (n = 125, 64%)	High AIP (n = 72, 36%)	*P*
Age (years)	65 (57–70)	64 (56–70)	0.429
Male sex, n (%)	103 (82)	59 (83)	0.891
BMI (kg/m^2)	26.5 (25.2–28.1)	27.3 (24.4–28.1)	0.901
DM, n (%)	81 (65)	48 (68)	0.691
HT, n (%)	95 (76)	53 (75)	0.832
HLD, n (%)	112 (90)	60 (85)	0.296
Smoking, n (%)	33 (26)	19 (26)	0.719
Prior PCI, n (%)	78 (62)	35 (49)	0.074
Prior CABG, n (%)	34 (27)	13 (18)	0.161
LVEF (%)	55 (45–65)	55 (45–65)	0.994
Ischemia on MPS, n (%)	118 (94)	70 (99)	0.154
Myocardial scar on MPS, n (%)	39 (31)	24 (34)	0.708
WBC (×10^3/μL)	7.5 (6.5–8.8)	7.8 (6.9–8.8)	0.392
Hemoglobin (g/dL)	13 (12–14)	14 (12.85–15)	**0.009**
Platelet (×10^3/μL)	218 (187–267)	238 (198–294)	0.114
Glucose (mg/dL)	116 (100–170)	139 (103–193)	0.076
Urea (mg/dL)	35 (29–45)	36 (30–46)	0.954
Creatinine (mg/dL)	0.9 (0.79–1)	0.92 (0.8–1.1)	0.487
eGFR (mL/min/1.73 m^2)	85 (69–95)	81.5 (65.5–98)	0.664
AST (U/L)	18 (14–21)	18 (14–22)	0.661
ALT (U/L)	16 (13–24)	18 (13–25.5)	0.464
Total cholesterol (mg/dL)	167 (137–201)	181 (161.5–213)	**0.013**
Triglycerides (mg/dL)	141 (105–180)	345 (297.5–432)	**< 0.001**
LDL-C (mg/dL)	93 (69–131)	92 (61.5–120.5)	0.593
HDL-C (mg/dL)	41 (35–48)	36 (32–42)	**< 0.001**
CRP (mg/L)	2.9 (1.29–8.15)	3.7 (1.55–8.3)	0.725
AIP	0.52 (0.39–0.67)	0.95 (0.89–1.03)	**< 0.001**

*Continuous variables are presented as mean ± standard deviation or median (interquartile range), as appropriate. Categorical variables are expressed as n (%). Statistically significant values are shown in bold. AIP, Atherogenic index of plasma; ALT, Alanine aminotransferase; AST, Aspartate aminotransferase; BMI, Body mass index; CABG, Coronary artery bypass grafting; CAD, Coronary artery disease; CRP, C-reactive protein; DM, Diabetes mellitus; eGFR, Estimated glomerular filtration rate; HDL-C, High-density lipoprotein cholesterol; HLD, Hyperlipidemia; HT, Hypertension; LDL-C, Low-density lipoprotein cholesterol; LVEF, Left ventricular ejection fraction; MPS, Myocardial perfusion scintigraphy; PCI, Percutaneous coronary intervention; WBC, White blood cell count.

Statistical Analysis

Continuous variables were expressed as mean ± standard deviation or median and interquartile range (IQR), depending on data distribution, while categorical variables were presented as counts and percentages. Normality of distribution was assessed using the Shapiro–Wilk test. Receiver operating characteristic (ROC) curve analysis was performed to determine the cut-off value of AIP. The study population was subsequently divided into two groups based on this threshold (0.801; area under the curve [AUC]: 0.753 (0.677–0.828), P < 0.001). Comparisons between groups were conducted using Fisher's exact test or Pearson's chi-squared test for categorical variables, and the Student's t-test or Mann–Whitney U test for continuous variables. Univariate logistic regression analysis was initially performed to identify factors associated with technical success of CTO PCI. Variables included in the multivariable models were selected based on univariate results, clinical relevance, and prior literature. To evaluate the incremental predictive value of AIP, two nested multivariable logistic regression models were constructed and compared using the likelihood ratio test. Associations were reported as odds ratios (OR) with 95% confidence intervals (CI). The discriminatory performance of the J-CTO score and AIP for predicting technical success was assessed using ROC curve analysis, and DeLong's test was used to compare correlated ROC curves. A two-sided p value < 0.05 was considered statistically significant. Statistical analyses were performed using Jamovi software (The Jamovi Project, Sydney, Australia) and R version 4.01 (R Foundation for Statistical Computing, Vienna, Austria), with the "rms" package.

Results

The study included 197 patients. Based on the optimal cut-off value determined by ROC analysis, patients were stratified into two groups (cut-off: 0.801; AUC: 0.753 [0.677–0.828], P < 0.001). Of the total cohort, 125 patients (64%) were assigned

Table 2. Angiographic and clinical characteristics according to atherogenic index of plasma (AIP) levels

Variables	Low AIP (n = 125, 64%)	High AIP (n = 72, 36%)	*P*
LAD CTO, n (%)	34 (27)	20 (28)	0.884
CX CTO, n (%)	22 (18)	15 (21)	0.544
RCA CTO, n (%)	81 (65)	42 (59)	0.432
One-vessel disease, n (%)	25 (20)	13 (18)	0.774
Multivessel disease, n (%)	98 (78)	58 (82)	0.680
Right coronary dominance, n (%)	111 (89)	65 (92)	0.541
Proximal cap ambiguity, n (%)	55 (44)	34 (48)	0.599
Calcification, n (%)	67 (54)	34 (48)	0.442
Bending > 45°, n (%)	36 (29)	20 (28)	0.925
Occlusion length > 20 mm, n (%)	73 (58)	46 (65)	0.379
Previous failed attempt, n (%)	14 (11)	11 (15)	0.387
Well-developed collateral, n (%)	97 (78)	52 (73)	0.492
J-CTO score	2 (1–3)	2 (1–3)	0.508
J-CTO score ≥ 3, n (%)	41 (33)	24 (34)	0.886
Antegrade approach, n (%)	122 (98)	69 (97)	0.859
Retrograde approach, n (%)	7 (6)	7 (10)	0.266
Technical success, n (%)	110 (88)	31 (44)	**< 0.001**
Periprocedural CVE, n (%)	0	2 (3)	0.059
Periprocedural pericardial effusion, n (%)	3 (2)	3 (4)	0.476
Periprocedural tamponade, n (%)	0 (0)	2 (3)	0.059
In-hospital mortality, n (%)	1 (1)	0 (0)	0.45

*Continuous variables are presented as mean ± standard deviation or median (interquartile range), as appropriate. Categorical variables are expressed as n (%). Statistically significant values are shown in bold. CTO, Chronic total occlusion; CVE, Cerebrovascular event; CX, Circumflex artery; LAD, Left anterior descending artery; RCA, Right coronary artery.

to the low AIP group and 72 patients (36%) to the high AIP group. Male patients comprised 82% of the cohort. The median age was 65 years (57–70) in the low AIP group and 64 years (56–70) in the high AIP group. There were no significant differences between the groups in terms of hypertension (HT), diabetes, hyperlipidemia, smoking status, prior PCI, or coronary artery bypass grafting (CABG) (all P > 0.05). Similarly, no significant differences were observed in left ventricular ejection fraction (LVEF), or the presence of ischemia or scar on MPS (all P > 0.05). Patients in the high AIP group had significantly higher levels of hemoglobin, total cholesterol, and TG, along with significantly lower HDL-C levels (P = 0.009, P = 0.013, P < 0.001, and P < 0.001, respectively). Baseline demographic, clinical, and laboratory characteristics are summarized in Table 1.

Most patients had multivessel disease (79%) and right coronary dominance (89%). The J-CTO score was similar between the groups. The overall technical success rate of CTO PCI was significantly lower in the high AIP group compared with the low AIP group (31 [44%] vs. 110 [88%]; P < 0.001). Figure 2 presents a box plot comparing AIP values between patients with and without technical success. In-hospital procedural complications were infrequent and comparable between the groups. Rates of pericardial effusion were similar; however, cardiac tamponade occurred only in the high AIP group (all P > 0.05). Two cerebrovascular events occurred in the high AIP group, and

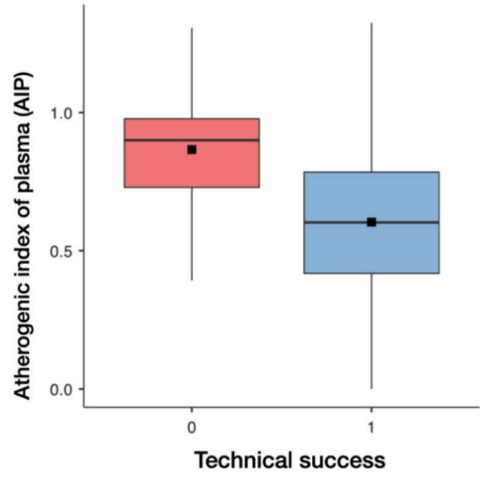

Figure 2. Comparison of the atherogenic index of plasma levels between patients with and without technical success.

one patient in the low AIP group died following the procedure. Angiographic and clinical outcomes are summarized in Table 2.

To evaluate the incremental predictive value of AIP, two nested multivariable logistic regression models were constructed. The baseline model (Model 1) included age, sex, estimated glomerular filtration rate (eGFR), LVEF, presence of well-developed CCC, and the J-CTO score. The extended model (Model 2) additionally

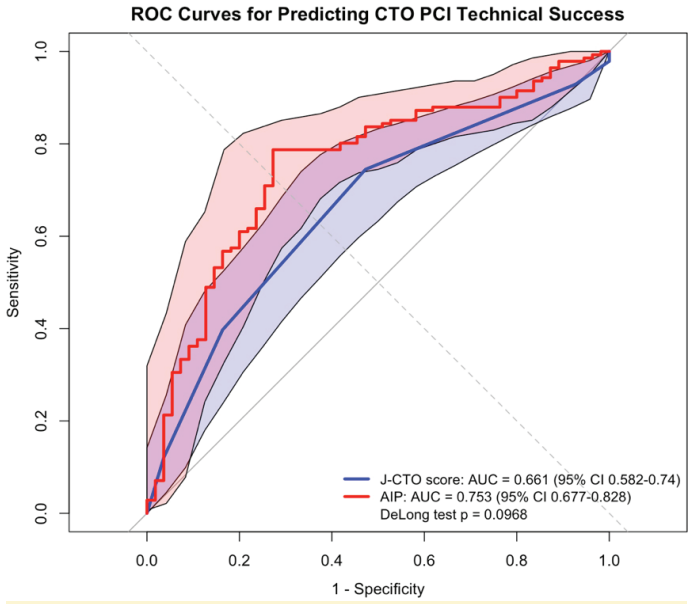

Figure 3. Receiver operating characteristic curves of the atherogenic index of plasma (AIP) and the Japanese Chronic Total Occlusion (J-CTO) score for predicting coronary total occlusion (CTO) percutaneous coronary intervention (PCI) technical success. Shaded areas indicate 95% confidence intervals.

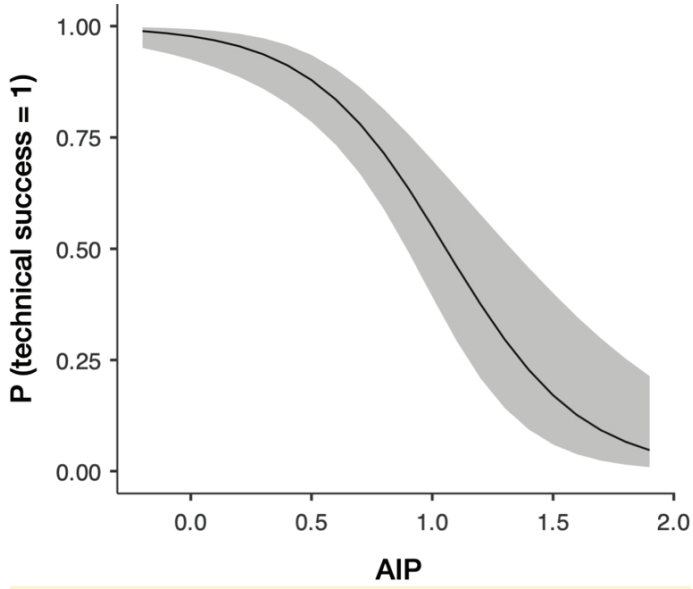

Figure 4. Estimated marginal means showing the adjusted probability of chronic total occlusion (CTO) percutaneous coronary intervention (PCI) technical success according to atherogenic index of plasma (AIP) levels. The model was adjusted for age, sex, estimated glomerular filtration rate (eGFR), left ventricular ejection fraction (LVEF), well-developed coronary collateral circulation (CCC), and the Japanese Chronic Total Occlusion (J-CTO) score.

included AIP. Model 1 demonstrated moderate discriminative ability (AUC: 0.73), which improved to 0.83 after inclusion of AIP. Comparison of the two models using the likelihood ratio test confirmed that the inclusion of AIP significantly improved model performance (χ^2 = 32.17, df = 1, P < 0.001).

As shown in Table 3, eGFR and the J-CTO score remained consistent independent predictors of CTO PCI technical success across both models. In Model 2, eGFR was positively associated with technical success (OR: 1.02, 95% CI: 1.00–1.04, P = 0.023), whereas the J-CTO score was inversely associated with technical success (OR: 0.62, 95% CI: 0.44–0.89, P = 0.008). Furthermore, AIP emerged as a strong independent predictor (OR: 0.03, 95% CI: 0.01–0.12, P < 0.001).

Model calibration was assessed using the Hosmer–Lemeshow goodness-of-fit test, which indicated good calibration (χ^2 = 5.39, df = 8, P = 0.715). Calibration was further evaluated using a bootstrap calibration plot, demonstrating good agreement between predicted and observed probabilities (Supplementary Figure 2).

ROC curve analysis identified optimal cut-off values of 0.802 for AIP and 2 for the J-CTO score in predicting CTO PCI technical success (Figure 3). The AIP threshold was determined using the Youden index, yielding a sensitivity of 78.7%, specificity of 72.7%, positive predictive value of 88.1%, and negative predictive value of 57.1%. Although AIP demonstrated a numerically higher AUC

Table 3. Multivariable logistic regression models for predictors of coronary total occlusion (CTO) percutaneous coronary intervention (PCI) technical success

Variables	Model 1 (Baseline model)		Model 2 (Baseline model + AIP)	
	OR (95% CI)	*P*	OR (95% CI)	*P*
Age (years)	1.00 (0.96–1.04)	0.886	0.98 (0.94–1.03)	0.476
Male sex	0.43 (0.16–1.17)	0.097	0.41 (0.14–1.24)	0.115
eGFR (mL/min/1.73 m²)	1.02 (1–1.04)	**0.023**	1.02 (1–1.04)	**0.023**
LVEF (%)	1.00 (0.98–1.03)	0.725	1.01 (0.98–1.04)	0.578
Well-developed collateral	2.02 (0.95–4.30)	0.067	1.95 (0.84–4.49)	0.119
J-CTO score	0.65 (0.48–0.89)	**0.007**	0.62 (0.44–0.89)	**0.008**
AIP	–	–	0.03 (0.01–0.12)	**<0.001**

The baseline model demonstrated an area under the curve (AUC) of 0.73. Inclusion of atherogenic index of plasma (AIP) improved the model's discriminative performance to an AUC of 0.83. Comparison of the models using the likelihood ratio test showed that adding AIP significantly improved model performance (χ^2 = 32.17, df = 1, P < 0.001). AIP, Atherogenic index of plasma; CI, Confidence interval; eGFR, Estimated glomerular filtration rate; LVEF, Left ventricular ejection fraction; OR, Odds ratio.

compared with the J-CTO score (AUC: 0.753 [0.677–0.828], P < 0.001 vs. AUC: 0.661 [0.582–0.74], P = 0.003), the difference between the two correlated ROC curves was not statistically significant according to DeLong's test (z = 1.66, P = 0.097).

The adjusted probability of CTO PCI technical success across AIP levels was further evaluated using estimated marginal means. As shown in Figure 4, higher AIP levels were associated with a lower probability of technical success after adjustment for covariates.

Discussion

In this study, we investigated the relationship between AIP and the technical success of CTO PCI and found that AIP is a significant predictor of procedural success. Higher AIP values were associated with a markedly lower success rate of CTO PCI. In addition, both the J-CTO score and eGFR were identified as independent predictors of technical success.

Lipid metabolism plays a pivotal role in the development and progression of coronary atherosclerosis. Triglycerides are well-established risk factors for atherosclerotic cardiovascular disease and play a fundamental role in the processes of atherogenesis and thrombogenesis.[14] HDL-C exerts antioxidant effects and contributes to improved endothelial function, whereas reduced HDL-C levels are associated with increased cardiovascular risk.[15] Previous studies have demonstrated that composite indices derived from routine laboratory parameters may provide valuable insight into the presence and severity of coronary artery disease.[16–18] Dobiásová and Frohlich were the first to describe the AIP, a simple yet informative lipid parameter proposed to predict the development, progression, and prognosis of CAD.[7] Cai et al.[19] reported that AIP levels were significantly higher in patients with CAD and independently predicted its presence. Elevated AIP has also been associated with greater disease severity.[20] Furthermore, a study involving 1,124 patients undergoing coronary artery calcium scoring demonstrated a significant correlation between AIP and the development of coronary artery calcification.[21] In the present study, no significant difference in calcification burden was observed between the groups. Dong et al.[22] reported an association between AIP and CCC in CTO patients, with higher AIP levels indicating a greater risk of poorly developed collaterals. Although well-developed collateral circulation was more frequent in the low AIP group in our cohort, this difference did not reach statistical significance.

Several studies have suggested that AIP is associated with both the presence and complexity of CTO.[10,11,23] Guelker et al.[10] evaluated 317 patients undergoing CTO PCI and reported that AIP may provide useful information for procedural planning by helping predict recanalization success. Elevated AIP reflects a more atherogenic lipid profile and has been linked to endothelial dysfunction and vascular inflammation. These processes may accelerate atherosclerotic plaque progression and contribute to more complex lesion morphology. In CTO lesions, such adverse plaque characteristics may lead to increased calcification and longer lesion length.[7,13] Consistent with these observations, we found a significantly lower technical success rate in patients with higher AIP levels, and multivariable analysis demonstrated a strong association between AIP and CTO PCI technical success. These findings support the concept of a metabolic phenotype influencing procedural outcomes in CTO PCI, suggesting that systemic metabolic conditions may affect lesion characteristics and procedural complexity. However, the magnitude of the observed effect size for AIP should be interpreted with caution, as it reflects the logarithmic transformation and scaling of the variable. Accordingly, even modest variations in AIP may translate into substantial changes in the estimated odds ratio, which should be considered when interpreting its clinical relevance.

Technical success of CTO PCI is strongly influenced by operator experience; however, several clinical and angiographic features, particularly components of the J-CTO score, including calcification, lesion length, tortuosity, and prior failed attempts, have also been associated with procedural success.[13,24,25] In our study, the J-CTO score was independently associated with technical success. While the J-CTO score primarily reflects anatomical lesion complexity, AIP may capture systemic metabolic and inflammatory processes. Thus, beyond anatomical characteristics, systemic metabolic factors may also contribute to procedural outcomes. Although AIP demonstrated a numerically higher AUC compared with the J-CTO score in our analysis, no significant difference was observed between the ROC curves according to DeLong's test. Therefore, AIP may provide incremental predictive value beyond traditional anatomical predictors and could serve as an adjunct marker in clinical risk stratification for CTO PCI. It should be emphasized that operator-related factors, such as procedural experience and strategy, play a critical role in CTO PCI outcomes. Accordingly, the predictive model presented in this study primarily reflects patient- and lesion-related characteristics rather than operator-dependent factors. In addition to metabolic factors, renal dysfunction may contribute to endothelial dysfunction, calcification, and systemic inflammation, thereby increasing lesion complexity and procedural difficulty. Malik et al.[26] reported that success rates of the CTO PCI were associated with the severity of renal dysfunction, although differences were less pronounced in patients without advanced chronic kidney disease. Although patients with severe renal impairment (eGFR < 15 mL/min/1.73 m²) were excluded from our study, eGFR was independently associated with technical success in multivariable analysis. These findings suggest that systemic metabolic and clinical factors, such as renal function, may contribute to procedural complexity and outcomes in CTO PCI.

Limitations

Several limitations should be acknowledged. First, this was a retrospective, single-center study. The relatively modest sample size may have limited statistical power. Although the events-per-variable ratio was within an acceptable range, the possibility of model overfitting cannot be entirely excluded. Second, AIP was measured only once, within 24 hours prior to the procedure. Additionally, selection bias and operator-related bias could not be completely avoided, particularly given the subjective nature of angiographic assessment. Operator experience, a well-known determinant of CTO PCI success, could not be included in the analysis due to the retrospective design. Furthermore, the choice between antegrade and retrograde techniques was left to operator discretion, representing a potential confounder. Therefore, the results of this study should be interpreted with caution, and further studies are required to validate these findings. Although the Hosmer–Lemeshow test indicated good model calibration, this method has recognized limitations and should be interpreted cautiously. However, the calibration plot demonstrated good agreement between predicted and observed probabilities.

Conclusion

The AIP, an easily obtainable and comprehensive lipid parameter, may be associated with technical success in CTO PCI. Incorporation of AIP into clinical practice may provide additional value for procedural planning.

Ethics Committee Approval: Ethics committee approval was obtained from Kartal Koşuyolu High Specialization Training and Research Hospital (Approval Number: 2024/03/773, Date: 06.02.2024).

Informed Consent: The requirement for written informed consent was waived due to the retrospective study design.

Conflict of Interest: The authors have no conflicts of interest to declare.

Funding: The authors declared that this study received no financial support.

Use of AI for Writing Assistance: No use of AI-assisted technologies was declared by the authors.

Author Contributions: Concept – B.G.Ş., C.Y.; Design – B.G.Ş., C.Y.; Supervision – B.G.Ş., C.Y.; Resource – B.G.Ş., C.Y.; Materials – B.G.Ş., C.Y.; Data Collection and/or Processing – B.G.Ş., C.Y.; Analysis and/or Interpretation – B.G.Ş., C.Y.; Literature Review – B.G.Ş., C.Y.; Writing – B.G.Ş., C.Y.; Critical Review – B.G.Ş., C.Y.

Peer-review: Externally peer-reviewed.

References

1. Brilakis ES, Mashayekhi K, Tsuchikane E, et al. Guiding Principles for Chronic Total Occlusion Percutaneous Coronary Intervention. *Circulation*. 2019;140(5):420-433. [CrossRef]
2. Fefer P, Knudtson ML, Cheema AN, et al. Current perspectives on coronary chronic total occlusions: the Canadian Multicenter Chronic Total Occlusions Registry. *J Am Coll Cardiol*. 2012;59(11):991-997. [CrossRef]
3. Werner GS, Martin-Yuste V, Hildick-Smith D, et al.; EUROCTO trial investigators. A randomized multicentre trial to compare revascularization with optimal medical therapy for the treatment of chronic total coronary occlusions. *Eur Heart J*. 2018;39(26):2484-2493. [CrossRef]
4. Lee SW, Lee PH, Ahn JM, et al. Randomized Trial Evaluating Percutaneous Coronary Intervention for the Treatment of Chronic Total Occlusion. *Circulation*. 2019;139(14):1674-1683. [CrossRef]
5. Mach F, Baigent C, Catapano AL, et al.; ESC Scientific Document Group. 2019 ESC/EAS Guidelines for the management of dyslipidaemias: lipid modification to reduce cardiovascular risk. *Eur Heart J*. 2020;41(1):111-188. Erratum in: *Eur Heart J*. 2020;41(44):4255. [CrossRef]
6. Sniderman AD, Williams K, Contois JH, et al. A meta-analysis of low-density lipoprotein cholesterol, non-high-density lipoprotein cholesterol, and apolipoprotein B as markers of cardiovascular risk. *Circ Cardiovasc Qual Outcomes*. 2011;4(3):337-345. [CrossRef]
7. Dobiásová M, Frohlich J. The plasma parameter log (TG/HDL-C) as an atherogenic index: correlation with lipoprotein particle size and esterification rate in apoB-lipoprotein-depleted plasma (FER(HDL)). *Clin Biochem*. 2001;34(7):583-588. [CrossRef]
8. Quispe R, Manalac RJ, Faridi KF, et al. Relationship of the triglyceride to high-density lipoprotein cholesterol (TG/HDL-C) ratio to the remainder of the lipid profile: The Very Large Database of Lipids-4 (VLDL-4) study. *Atherosclerosis*. 2015;242(1):243-250. [CrossRef]
9. Kim SH, Cho YK, Kim YJ, et al. Association of the atherogenic index of plasma with cardiovascular risk beyond the traditional risk factors: a nationwide population-based cohort study. *Cardiovasc Diabetol*. 2022;21(1):81. [CrossRef]
10. Guelker JE, Bufe A, Blockhaus C, et al. The atherogenic index of plasma and its impact on recanalization of chronic total occlusion. *Cardiol J*. 2020;27(6):756-761. [CrossRef]
11. Liu T, Liu J, Wu Z, Lv Y, Li W. Predictive value of the atherogenic index of plasma for chronic total occlusion before coronary angiography. *Clin Cardiol*. 2021;44(4):518-525. [CrossRef]
12. Rentrop KP, Cohen M, Blanke H, Phillips RA. Changes in collateral channel filling immediately after controlled coronary artery occlusion by an angioplasty balloon in human subjects. *J Am Coll Cardiol*. 1985;5(3):587-592. [CrossRef]
13. Morino Y, Abe M, Morimoto T, et al.; J-CTO Registry Investigators. Predicting successful guidewire crossing through chronic total occlusion of native coronary lesions within 30 minutes: the J-CTO (Multicenter CTO Registry in Japan) score as a difficulty grading and time assessment tool. *JACC Cardiovasc Interv.* 2011;4(2):213-221. [CrossRef]
14. Budoff M. Triglycerides and Triglyceride-Rich Lipoproteins in the Causal Pathway of Cardiovascular Disease. *Am J Cardiol*. 2016;118(1):138-145. [CrossRef]
15. Potì F, Simoni M, Nofer JR. Atheroprotective role of high-density lipoprotein (HDL)-associated sphingosine-1-phosphate (S1P). *Cardiovasc Res*. 2014;103(3):395-404. [CrossRef]
16. Candemir M, Kiziltunç E, Nurkoç S, Şahinarslan A. Relationship Between Systemic Immune-Inflammation Index (SII) and the Severity of Stable Coronary Artery Disease. *Angiology*. 2021;72(6):575-581. [CrossRef]
17. Topal S, Kızıltunç E, Sezenöz B, et al. Gamma-glutamyl transferase to albumin ratio can predict severity of coronary artery disease detected by coronary computed tomography angiography. *Anatol J Cardiol*. 2021;25(9):653-660. [CrossRef]
18. Tudurachi BS, Anghel L, Tudurachi A, Sascău RA, Stătescu C. Assessment of Inflammatory Hematological Ratios (NLR, PLR, MLR, LMR and Monocyte/HDL-Cholesterol Ratio) in Acute Myocardial Infarction and Particularities in Young Patients. *Int J Mol Sci*. 2023;24(18):14378. [CrossRef]
19. Cai G, Shi G, Xue S, Lu W. The atherogenic index of plasma is a strong and independent predictor for coronary artery disease in the Chinese Han population. *Medicine (Baltimore)*. 2017;96(37):e8058. [CrossRef]
20. da Luz PL, Favarato D, Faria-Neto JR Jr, Lemos P, Chagas AC. High ratio of triglycerides to HDL-cholesterol predicts extensive coronary disease. *Clinics (Sao Paulo)*. 2008;63(4):427-432. [CrossRef]
21. Nam JS, Kim MK, Nam JY, et al. Association between atherogenic index of plasma and coronary artery calcification progression in Korean adults. *Lipids Health Dis*. 2020;19(1):157. [CrossRef]
22. Dong S, Qiao J, Gao A, et al. Association between the atherogenic index of plasma and coronary collateral circulation in patients with chronic total occlusion. *BMC Cardiovasc Disord*. 2024;24(1):360. [CrossRef]
23. Han H, Liu X, Zhao Q, et al. The synergistic effect of the atherogenic index of plasma and hyperuricemia on the prediction of coronary chronic total occlusion lesion: an observational cross-sectional study. *Front Cardiovasc Med*. 2024;11:1437096. [CrossRef]
24. Noguchi T, Miyazaki MD S, Morii I, Daikoku S, Goto Y, Nonogi H. Percutaneous transluminal coronary angioplasty of chronic total occlusions. Determinants of primary success and long-term clinical outcome. *Catheter Cardiovasc Interv*. 2000;49(3):258-264. [CrossRef]
25. Michael TT, Karmpaliotis D, Brilakis ES, et al. Temporal trends of fluoroscopy time and contrast utilization in coronary chronic total occlusion revascularization: insights from a multicenter United States registry. *Catheter Cardiovasc Interv*. 2015;85(3):393-399. [CrossRef]
26. Malik AO, Spertus JA, Grantham JA, et al. Outcomes of Chronic Total Occlusion Percutaneous Coronary Intervention in Patients With Renal Dysfunction. *Am J Cardiol*. 2020;125(7):1046-1053. [CrossRef]

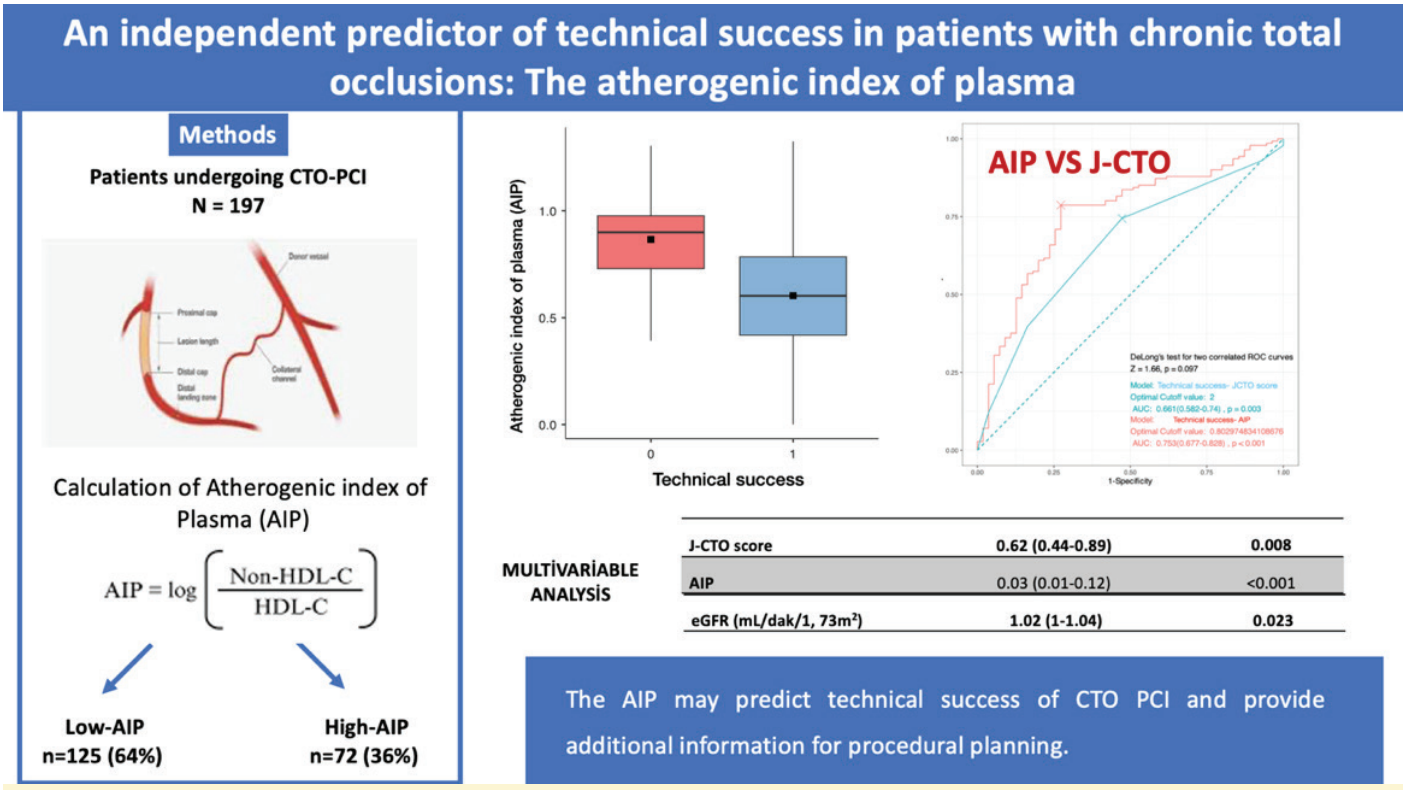

Supplementary Figure 1. Graphical abstract.

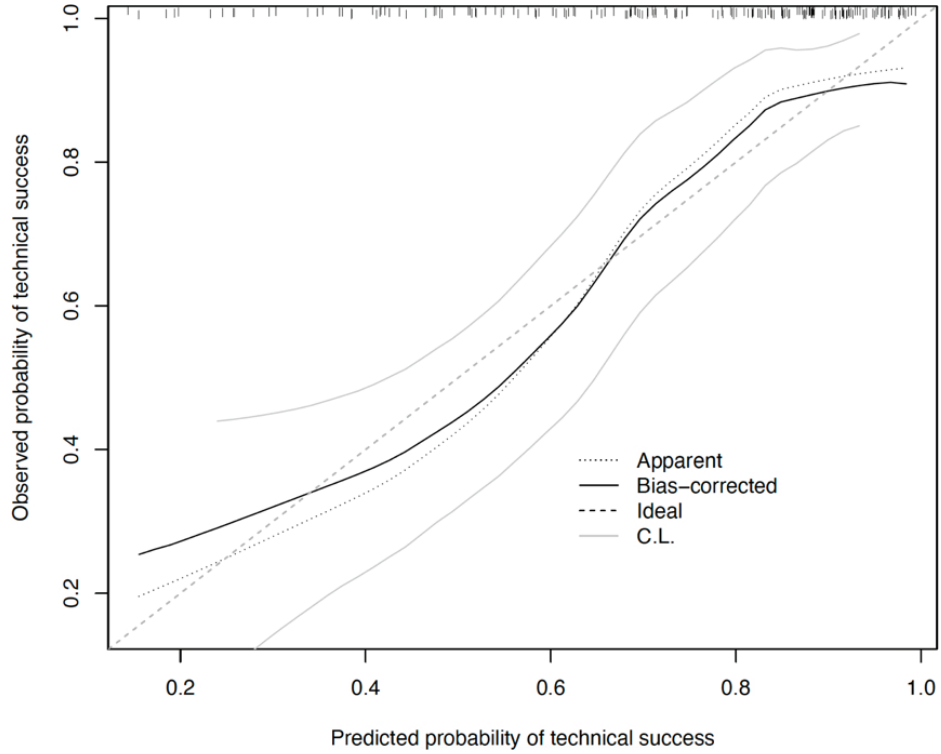

Supplementary Figure 2. Calibration plot of the multivariable model predicting coronary total occlusion (CTO) percutaneous coronary intervention (PCI) technical success. The bias-corrected curve demonstrates good agreement between predicted and observed probabilities.

ARCHIVES OF THE TURKISH SOCIETY OF CARDIOLOGY

Official journal of the TURKISH SOCIETY OF CARDIOLOGY

Quality of Life Outcomes in Patients with Pulmonary Hypertension Receiving Prostacyclin Therapy: Impact of Anxiety, Depression, Sociodemographic Characteristics, and Treatment-Related Factors

Prostasiklin Tedavisi Alan Pulmoner Hipertansiyon Hastalarında Yaşam Kalitesi Sonuçları: Anksiyete, Depresyon, Sosyodemografik Özellikler ve Tedaviye İlişkin Faktörlerin Etkisi

ABSTRACT

Objective: Despite advances in prostacyclin therapy, pulmonary hypertension (PH) continues to impair patients' quality of life (QoL). This study aimed to identify the clinical and psychological factors associated with QoL in patients receiving prostacyclin therapy.

Method: This cross-sectional study was conducted between July 2023 and September 2024 and included 58 patients with PH receiving prostacyclin therapy. Data were collected using a structured questionnaire assessing sociodemographic and disease-related characteristics. Symptom severity, anxiety, depression, and QoL were evaluated using the Pulmonary Arterial Hypertension Symptom Scale (PAHSS), the Hospital Anxiety and Depression Scale (HADS), and the EmPHasis-10 Questionnaire.

Results: The mean age of the patients was 48.89 ± 16.17 years, and 69% were female. Overall, 69% had at least one chronic comorbidity, 19% required continuous oxygen therapy, and the mean disease duration was 7.45 ± 6.84 years. The average duration of prostacyclin therapy was 28.03 ± 34.21 months. Mean scores were 71.52 ± 36.40 for PAHSS, 8.70 ± 5.23 for HADS-Anxiety, 7.82 ± 5.32 for HADS-Depression, and 30.05 ± 14.92 for EmPHasis-10. EmPHasis-10 scores showed moderate correlations with PAHSS, HADS-Anxiety, HADS-Depression, and 6-minute walk test (6MWT) scores. In multivariate analysis, age, PAHSS score, anxiety, depression, and vomiting explained 80% of the variance in EmPHasis-10 scores.

Conclusion: QoL was substantially impaired in patients with PH receiving prostacyclin therapy and was influenced by age, symptom severity, anxiety, depression, and vomiting.

Keywords: Depressive symptoms, prostacyclin therapy, pulmonary hypertension, quality of life, symptom burden

ÖZET

Amaç: Prostasiklin tedavisindeki ilerlemelere rağmen, pulmoner hipertansiyon (PH) hastaların yaşam kalitesini (QoL) olumsuz etkilemeye devam etmektedir. Bu çalışma, QoL ile ilişkili klinik ve psikolojik faktörleri belirlemeyi amaçlamaktadır.

Yöntem: Çalışma, Temmuz 2023 ile Eylül 2024 tarihleri arasında kesitsel olarak yürütüldü ve prostasiklin tedavisi alan 58 PH hastası çalışmaya dahil edildi. Veriler, sosyodemografik ve hastalığa ilişkin özellikleri değerlendiren yapılandırılmış bir anket kullanılarak toplandı. Semptom şiddeti, anksiyete, depresyon ve yaşam kalitesi; Pulmoner Arteriyel Hipertansiyon Semptom Ölçeği (PAHSS), Hastane Anksiyete ve Depresyon Ölçeği (HADS) ve EmPHasis-10 Anketi kullanılarak değerlendirildi.

Bulgular: Hastaların ortalama yaşı 48,89 ± 16,17 idi ve %69'u kadındı. Toplamda, hastaların %69'unda en az bir kronik komorbidite mevcuttu, %19'u sürekli oksijen tedavisine ihtiyaç duyuyordu ve ortalama hastalık süresi 7,45 ± 6,84 yıldı. Prostasiklin tedavisinin ortalama süresi 28,03 ± 34,21 aydı. Ortalama puanlar PAHSS için 71,52 ± 36,40, HADS-Anksiyete için 8,70 ± 5,23, HADS-Depresyon için 7,82 ± 5,32 ve EmPHasis-10 için 30,05 ± 14,92 idi. EmPHasis-10 skorları; PAHSS, HADS-Anksiyete, HADS-Depresyon ve 6 dakikalık yürüme testi (6DYT) skorları ile orta düzeyde ilişkiliydi. Çok değişkenli analizde yaş, PAHSS, anksiyete, depresyon ve kusma, EmPHasis-10 skorlarındaki varyansın %80'ini açıklıyordu.

ORIGINAL ARTICLE
ARAŞTIRMA MAKALESİ

Fatma Yıldırım[1]
Elif Ok[2]
Vesile Ünver[3]
Dilek Sezgin[4]
Halil Ataş[5]
Betül Şentürk Saraç[6]

[1]*Acıbadem Mehmet Ali Aydınlar University, Institute of Health Sciences, Nursing Doctorate Program, İstanbul, Türkiye*
[2]*Department of Nursing, Health Science Faculty, İzmir Democracy University, İzmir, Türkiye*
[3]*Department of Nursing, Institute of Health Sciences, Acıbadem Mehmet Ali Aydınlar University, İstanbul, Türkiye*
[4]*Department of Internal Medical Nursing, Nursing Faculty, Dokuz Eylül University, İzmir, Türkiye*
[5]*Department of Cardiology, Faculty of Medicine, Marmara University, İstanbul, Türkiye*
[6]*Marmara University Pendik Training and Research Hospital, İstanbul, Türkiye*

Corresponding author:
Fatma Yıldırım
✉ fkahve6@gmail.com

Received: January 14, 2026
Accepted: May 04, 2026

Cite this article as: Yıldırım F, Ok E, Ünver V, Sezgin D, Ataş H, Şentürk Saraç B. Quality of Life Outcomes in Patients with Pulmonary Hypertension Receiving Prostacyclin Therapy: Impact of Anxiety, Depression, Sociodemographic Characteristics, and Treatment-Related Factors. *Turk Kardiyol Dern Ars.* 2026;54(6):503–512.

DOI: 10.5543/tkda.2026.01628

Sonuç: Prostasiklin tedavisi gören pulmoner hipertansiyon hastalarının yaşam kalitesinin düşük olduğu ve bunun yaş, semptom şiddeti, anksiyete, depresyon ve kusma gibi faktörlerden etkilendiği saptanmıştır.

Anahtar Kelimeler: Depresif semptomlar, prostasiklin tedavisi, pulmoner hipertansiyon, yaşam kalitesi, semptom yükü

Pulmonary hypertension (PH) is a progressive and complex chronic disease characterized by a mean pulmonary artery pressure > 20 mmHg at rest and may result from a variety of cardiac, pulmonary, or rheumatologic conditions.[1] PH is classified into five groups: pulmonary arterial hypertension (PAH, Group 1), PH due to left heart disease (Group 2), PH associated with lung disease or hypoxia (Group 3), PH due to pulmonary artery obstruction (Group 4), and PH with unclear or multifactorial mechanisms (Group 5).[2-4] PH is also categorized according to World Health Organization (WHO) functional class, which reflects the degree of limitation in physical activity.[5]

Patients with PH commonly experience symptoms such as dyspnea, fatigue, abdominal distension, and peripheral edema, all of which negatively affect quality of life.[6] As the disease progresses, particularly in patients with PAH, complications such as palpitations, chest discomfort, syncope, and severe dyspnea may develop.[7] Additional symptoms related to the structural and hemodynamic abnormalities of PH include hemoptysis, hoarseness, and wheezing.[4,8,9]

Treatment strategies guided by WHO functional class II–IV recommendations aim to reduce symptoms, improve functional capacity, and slow disease progression. Therapies targeting the prostacyclin pathway are used primarily in PAH to improve hemodynamic parameters, exercise tolerance, and overall symptom burden, making them essential components of PAH management.[10-13]

To maximize the benefits of prostacyclin therapy in PAH, treatment-related adverse effects must be carefully monitored and managed. Common side effects include headache and gastrointestinal symptoms, particularly nausea and vomiting, which may trigger vagal responses and negatively affect treatment tolerability and adherence.[13] Importantly, these adverse effects, together with the overall symptom burden, may impair not only physical health but also the psychological and social well-being of patients with PAH.[14]

Pulmonary hypertension is a complex cardiovascular disorder associated with diagnostic and therapeutic challenges, substantial medical and psychological burden, reduced quality of life, and a high prevalence of symptoms such as anxiety, depression, fatigue, and pain.[8,15,16] Collectively, these factors may adversely affect psychological health and contribute to the development of anxiety and depressive disorders, particularly among patients with PAH.[17]

A patient-centered, multidisciplinary approach is recommended for PH, and the European Society of Cardiology (ESC) and the European Respiratory Society (ERS) guidelines emphasize the importance of coordinated treatment and psychological support.[5] Individualized care strategies have also been highlighted as essential for patients with PAH.[18] Healthcare professionals therefore play a central role in PH management through comprehensive multidisciplinary care.[19] Their responsibilities include monitoring cardiopulmonary function, optimizing treatment, assessing treatment response and adherence, educating patients, and promoting physical activity and healthy lifestyle behaviors.[20] Multidisciplinary, nurse-led, guideline-based care has been shown to improve long-term survival and clinical outcomes in patients with PH, including those with chronic thromboembolic pulmonary hypertension (CTEPH).[19,20] Although these components are essential in PH management, the effects of symptom burden and prostacyclin-related adverse effects on patients' quality of life are unclear. Therefore, this study aimed to identify factors associated with quality of life in patients receiving prostacyclin therapy.

ABBREVIATIONS

BPA	Balloon pulmonary angioplasty
ERA	Endothelin receptor antagonist
ERS	European Respiratory Society
ESC	European Society of Cardiology
HADS	Hospital Anxiety Depression Scale
PAH	Pulmonary arterial hypertension
PAHSS	Pulmonary Arterial Hypertension Symptom Scale
PDE-5İ	Phosphodiesterase type 5 inhibitor
PEA	Pulmonary endarterectomy
PH	Pulmonary hypertension
QoL	Quality of life
SD	Standard deviations
WHO	World Health Organization

This study contributes to the literature by evaluating quality of life (QoL) in a prostacyclin-treated cohort receiving various treatment modalities, including oral, inhaled, intravenous, and subcutaneous therapies. In addition, validated Turkish versions of PAH-specific instruments were used to assess symptom burden and psychological status. This cross-sectional study aimed to identify factors affecting the QoL of patients with PH receiving prostacyclin therapy.

Materials and Methods

Patients and Study Protocol

The study population consisted of patients followed at the PH center of a training and research hospital in Istanbul. Data were collected between July 2023 and September 2024.

Sample size calculation was not performed, and all patients receiving prostacyclin therapy during the study period were included. In 2022, a total of 478 patients with PH were followed at the center, of whom 63 were receiving prostacyclin therapy. During the data collection period, five patients died. All patients meeting the inclusion criteria were enrolled, resulting in a final sample of 58 patients. Data were collected through face-to-face interviews conducted during routine follow-up visits, each lasting approximately 20–25 minutes.

According to the 2022 ESC/ERS guidelines, prostacyclin therapy is initiated following multidisciplinary evaluation by the PH team. In patients with Group 1 PH, oral or inhaled prostanoid agonists are added when low-risk status according to ESC risk stratification cannot be achieved despite combination therapy with an endothelin receptor antagonist (ERA) and a phosphodiesterase type 5 inhibitor (PDE-5i). Patients classified as intermediate-high or high risk receive parenteral prostanoid therapy. In Group 4 PH patients with residual or recurrent PH following pulmonary endarterectomy (PEA) and/or balloon pulmonary angioplasty (BPA), parenteral prostanoid therapy is initiated. For patients in whom definitive classification between Group 1 and Group 3 PH is not possible, inhaled prostanoid therapy with a lower systemic adverse-effect profile may be administered when hemodynamic impairment is severe.

Patients aged ≥ 18 years who were receiving prostacyclin therapy (oral, subcutaneous, inhaled, or intravenous) according to these indications were included in the study. Patients who had been receiving treatment for less than three months were excluded.

The adequacy of the sample size for multivariate linear regression was evaluated according to the number of predictor variables included in the model. With a total of 58 participants and five independent variables, the study met the criterion of at least 10 observations per predictor, indicating acceptable model stability. In addition, the model demonstrated high explanatory power (R^2 = 0.805), corresponding to a very large effect size.

To further support sample size adequacy, a post hoc power analysis was conducted using G*Power version 3.1.9.7. The statistical power of the linear regression model including five independent variables was calculated as 0.961 (f^2 = 0.40, α = 0.05, n = 58). These findings indicate that the study has sufficient statistical power to detect the observed effect size.

Data Collection Tools

Sociodemographic and Disease-Related Characteristics Form

This form was developed by the researchers based on a review of the relevant literature.[16,17,21] It consists of 17 items assessing patients' sociodemographic characteristics and disease-related clinical features.

Pulmonary Arterial Hypertension Symptom Scale (PAHSS)

Developed to identify core health problems reported by individuals with PAH, this scale provides a structured method for summarizing symptom patterns. Studies have demonstrated that both the original and Turkish versions provide reliable assessment of symptom severity.[22,23] Responses to 17 items are summed to generate a total score reflecting symptom severity. In the present study, the scale also demonstrated good reliability.

Hospital Anxiety and Depression Scale (HADS)

The HADS is a brief instrument used to assess anxiety and depressive symptoms in adults.[24] The Turkish version has been validated and shown to have good reliability. The questionnaire contains 14 items equally divided into anxiety and depression subscales. Each subscale is scored from 0 to 21, with cutoff values of 7/8 for anxiety and 10/11 for depression. Scores above these thresholds indicate clinically significant symptoms. In the Turkish validation study, Cronbach's alpha coefficients were 0.85 for anxiety and 0.77 for depression. In our study, Cronbach's alpha coefficients were 0.88 for both subscales, indicating strong internal consistency.[25]

EmPHasis-10

The EmPHasis-10 questionnaire was developed to assess QoL in patients with PH.[26] The Turkish version has been validated and shown to be reliable. The questionnaire consists of 10 items rated on a 6-point Likert scale. Scores range from 0 to 50, with higher scores indicating poorer QoL. In the Turkish validation study, the Cronbach's alpha coefficient was 0.98, whereas in the present study it was 0.95, indicating excellent interval consistency.[27]

Ethics Committee Approval

Ethical approval was obtained from the Acıbadem Mehmet Ali Aydınlar University Medical Research Evaluation Ethics Committee (Approval Number: 2023/10, Date: 16.06.2023). Institutional permission was also obtained. All participants provided written and verbal informed consent after receiving information about the study. The study was conducted in accordance with the principles of the Declaration of Helsinki.

Statistical Analysis

Data were analyzed using IBM SPSS Statistics for Windows, version 23.0 (IBM Corp., Armonk, NY, USA). Demographic and descriptive variables are presented as numbers (n) and percentages (%). Skewness and kurtosis values for HADS, PAHSS, and EmPHasis-10 scores ranged between -1.5 and + 1.5, indicating approximate normal distribution.[28] Accordingly, parametric tests were used, and variables are presented as mean ± standard deviation (SD). Differences between groups were analyzed using Student's t-test and one-way analysis of variance. Correlations between variables were analyzed using Pearson correlation analysis. A backward linear regression analysis was conducted to identify factors affecting QoL. Statistical significance was set at $P < 0.05$, with all analyses evaluated at a 95% confidence interval.

Results

Table 1 presents the sociodemographic and disease-related characteristics of the participants (n = 58). The mean age was 48.89 ± 16.17 years, and 69% of the participants were female. Most participants were married (72.4%), and 46.6% had completed high school education or higher. The majority were unemployed (69%), and 84.5% reported that their income was equal to their expenses. Regarding clinical characteristics, the mean duration since diagnosis was 7.45 ± 6.84 years, and the mean duration of prostacyclin therapy was 28.03 ± 34.21 months. Mean oxygen saturation was 93.19 ± 6.69%, mean pro–B-type natriuretic peptide (pro-BNP) level was 800.26 ± 1124.80 pg/mL, mean ejection fraction was 58.59 ± 7.14%, and the mean

Table 1. Sociodemographic and disease-related characteristics of the participants (n = 58)

Characteristics	Mean ± SD / n	Range / %
Age (years)	48.89 ± 16.17	20–84
Duration of diagnosis (years)	7.45 ± 6.84	1–31
Duration of prostacyclin therapy (months)	28.03 ± 34.21	6–204
Saturation (%)	93.19 ± 6.69	70–99
Pro-BNP (pg/mL)	800.26 ± 1124.80	10–4370
Left ventricular ejection fraction (%)	58.59 ± 7.14	35–65
6-minute walk test (m)	310.37 ± 166.64	0–515
	n	**%**
Sex		
Female	40	69
Male	18	31
Marital status		
Married	42	72.4
Single	16	27.6
Educational status		
Illiterate	8	13.8
Primary education	23	39.6
High school and above	27	46.6
Economic status		
Income less than expenditure	9	15.5
Income equal to expenditure	49	84.5
Employment status		
Employed	18	31
Unemployed	40	69
Comorbid chronic disease		
Yes	36	62.1
No	22	37.9
Therapy type		
Selexipag (oral)	40	69
Epoprestenol (IV)	2	3.4
Iloprost (inhaled)	14	24.2
Treprostinil (subcutaneous)	2	3.4
Continuous oxygen therapy		
Yes	11	19
No	47	81
PH group		
Group 1	44	75.9
Group 3	7	12.1
Group 4	7	12.1
WHO functional classification		
Stage II	20	34.5
Stage III	28	48.3
Stage IV	10	17.2

WHO, World Health Organization; PH, Pulmonary hypertension; Pro-BNP, Pro-B-type natriuretic peptide; 6MWT, 6-minute walk test; EF, Ejection fraction.

Table 2. Distribution of mean scores for the PAHSS, HADS, and EmPHasis-10 (n = 58

Scales	Mean ± SD	Range
Pulmonary Arterial Hypertension Symptom Scale (PAHSS)	71.52 ± 36.40	3–145
Shortness of breath with exertion	7.64 ± 2.68	0–10
Fatigue	7.00 ± 2.59	0–10
Rapid heartbeat / palpitations	5.81 ± 3.49	0–10
Shortness of breath while lying down	5.55 ± 3.37	0–10
Sleep disturbance	5.21 ± 3.81	0–10
Awakening with shortness of breath	4.88 ± 3.76	0–10
Shortness of breath at rest	4.76 ± 3.53	0–10
Chest pain / discomfort	4.29 ± 3.41	0–10
Loss of appetite	4.07 ± 3.35	0–10
Abdominal bloating	3.93 ± 3.41	0–10
Nausea	3.86 ± 3.53	0–10
Dizziness / lightheadedness	3.66 ± 2.81	0–10
Foot / ankle swelling	3.59 ± 3.23	0–10
Cough	2.53 ± 2.96	0–10
Cold, numb, painful hands or feet (Raynaud's phenomenon)	1.98 ± 3.40	0–10
Hoarseness	1.62 ± 2.62	0–10
Fainting / syncope	1.16 ± 2.15	0–9
EmPHasis-10	30.05 ± 14.92	2–50
HADS-anxiety	8.70 ± 5.23	0–21
HADS-depression	7.82 ± 5.32	0–21
	n	**%**
HADS-anxiety (presence of anxiety)		
≥ 8 points (yes)	34	58.6
<8 points (no)	24	41.4
HADS-depression (presence of depression)		
≥ 11 points (yes)	17	29.3
< 11 points (no)	41	70.7

HADS, Hospital Anxiety & Depression Scale.

6-minute walk test (6MWT) distance was 310.37 ± 166.64 meters. Comorbid chronic diseases were present in 62.1% of participants. Most patients were receiving oral selexipag therapy (69%), and 19% required continuous oxygen therapy. Group 1 PH accounted for 75.9% of the study population, and nearly half of the participants were classified as WHO functional class III (48.3%).

Table 2 presents the mean PAHSS, HADS-Anxiety (HADS-A), HADS-Depression (HADS-D), and EmPHasis-10 scores of the participants. Mean scores were 71.52 ± 36.40 for PAHSS, 8.70 ± 5.23 for HADS-Anxiety, 7.82 ± 5.32 for HADS-Depression, and 30.05 ± 14.92 for EmPHasis-10. According to the PAHSS, the most severe symptoms were shortness of breath on exertion, fatigue, palpitations, and shortness of breath while lying down. Based on HADS cutoff values, 58.6% of participants had anxiety symptoms, and 29.3% had depression.

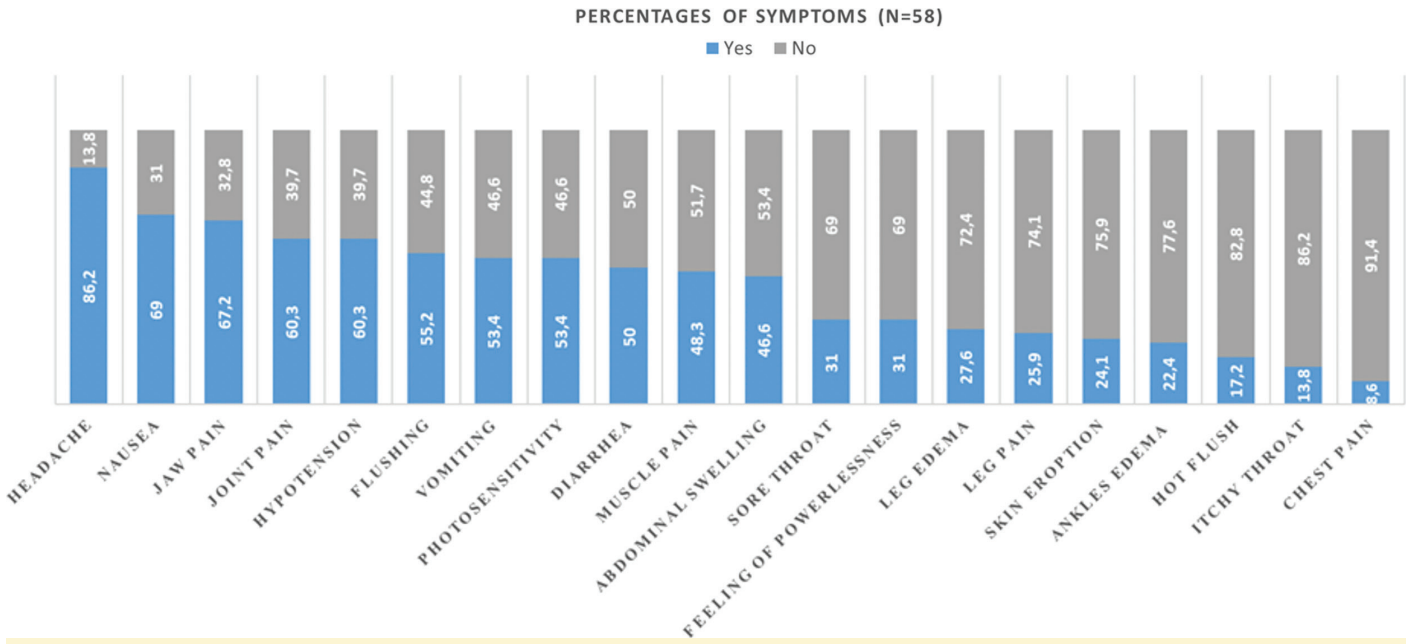

Figure 1. Distribution of symptoms experienced by patients receiving prostacyclin therapy.

Figure 1 illustrates the distribution of symptoms experienced by participants in relation to prostacyclin therapy. Symptoms reported by more than 50% of patients related to prostacyclin therapy included headache, nausea, jaw pain, hypotension, flushing, vomiting, and photosensitivity.

Table 3 presents PAHSS, EmPHasis-10, and HADS scores according to participants' sociodemographic and clinical characteristics. Single participants had significantly lower HADS-D (P = 0.03) and EmPHasis-10 (P = 0.006) scores than married participants. Illiterate participants had higher PAHSS (P = 0.006) and EmPHasis-10 (P = 0.001) scores than participants with a high school education or higher. Employment status was significantly associated with all scale scores, with employed participants reporting lower scores (PAHSS, P = 0.04; HADS-A, P = 0.01; HADS-D, P < 0.001; EmPHasis-10, P = 0.002). Participants without comorbid chronic diseases had lower PAHSS (P < 0.001), HADS-A (P = 0.02), HADS-D (P = 0.003), and EmPHasis-10 (P < 0.001) scores compared with those with comorbidities. Functional class significantly affected all scale scores (PAHSS, P = 0.002; HADS-A, P = 0.01; HADS-D, P = 0.01; EmPHasis-10, P < 0.001), with patients in functional classes III and IV demonstrating higher scores than those in class II. Continuous oxygen therapy was also associated with higher scores across all measures (PAHSS, P = 0.004; HADS-A, P < 0.001; HADS-D, P = 0.01; EmPHasis-10, P < 0.001), indicating greater symptom burden among patients receiving oxygen therapy.

Table 4 presents the correlation analysis between participant characteristics and PAHSS, HADS, and EmPHasis-10 scores. EmPHasis-10 scores were significantly correlated with PAHSS (r = 0.72; P < 0.001), HADS-Anxiety (r = 0.61; P < 0.001), and HADS-Depression (r = 0.57; P < 0.001). PAHSS scores were positively correlated with both HADS-Anxiety (r = 0.39; P = 0.03) and HADS-Depression (r = 0.28; P = 0.03). Age was positively correlated with all scores (PAHSS: r = 0.32, P = 0.01; EmPHasis-10: r = 0.60, P < 0.001; HADS-Anxiety: r = 0.43, P = 0.001; HADS-Depression: r = 0.45, P < 0.001). Oxygen saturation was negatively correlated with PAHSS (r = -0.30; P = 0.02) and EmPHasis-10 (r = -0.28; P = 0.03). The 6MWT distance was negatively correlated with PAHSS (r = -0.50; P < 0.001), EmPHasis-10 (r = -0.60; P < 0.001), HADS-Anxiety (r = -0.61; P < 0.001), and HADS-Depression (r = -0.49; P < 0.001). No significant associations were found between pro-BNP or ejection fraction and EmPHasis-10 scores.

Table 5 presents the linear regression analysis of factors associated with EmPHasis-10 scores. The backward regression model identified age, PAHSS score, HADS-A score, HADS-D score, and prostacyclin-related vomiting as significant predictors. The model was statistically significant (F = 42.892; P < 0.001) and explained 80.5% of the variance in EmPHasis-10 scores (R^2 = 0.805). Older age, higher PAHSS scores, anxiety, depression, and prostacyclin-related vomiting were all independently associated with higher EmPHasis-10 scores.

Discussion

In this study, patients with PH receiving prostacyclin therapy had impaired QoL and moderate levels of PAH symptom severity. Anxiety and depression were present in 58.6% and 29.3% of patients, respectively. Factors associated with QoL included marital status, educational level, employment status, chronic comorbidities, PH functional class, and continuous oxygen therapy use. Higher levels of anxiety and depression, older age, greater symptom severity, lower oxygen saturation, and shorter 6MWT distance were associated with poorer QoL. Furthermore, age, symptom severity, anxiety, depression, and prostacyclin-related vomiting explained 80% of the variance in QoL scores, with QoL worsening as age and symptom severity increased and among patients experiencing anxiety, depression, or vomiting.

Table 3. Comparison of EmPHasis-10, PAHSS, and HADS scores according to sociodemographic and disease-related characteristics of the participants (n = 58)

Characteristics	PAHSS	HADS-anxiety	HADS-depression	EmPHasis-10
Sex				
Female (n = 40)	72.50 ± 37.29	8.82 ± 5.28	7.45 ± 5.21	28.55 ± 14.53
Male (n = 18)	69.33 ± 35.40	8.44 ± 5.24	8.66 ± 5.60	33.39 ± 15.63
Statistical analysis				
t	0.304	0.254	−0.803	−1.146
P	0.76	0.80	0.42	0.26
Marital status				
Married (n = 42)	75.38 ± 36.88	9.26 ± 5.56	8.73 ± 5.54	32.98 ± 15.24
Single (n = 16)	61.38 ± 34.15	7.25 ± 4.02	5.43 ± 3.88	22.38 ± 11.12
Statistical analysis				
t	1.318	1.317	2.179	2.910
P	0.19	0.19	**0.03**	**0.006**
Educational status				
Illiterate[a] (n = 8)	97.63 ± 19.73	9.50 ± 4.56	8.00 ± 6.48	44.50 ± 8.73
Primary education[b] (n = 23)	79.87 ± 35.44	10.26 ± 6.00	9.52 ± 6.30	32.48 ± 14.71
High school and above[c] (n = 27)	56.67 ± 35.16	7.14 ± 4.35	6.33 ± 3.50	23.70 ± 13.15
Statistical analysis				
F	5.723	2.420	2.339	8.123
P	**0.006 (a > c)**	0.98	0.10	**0.001 (a > c)**
Economic status				
Income less than expenditure (n = 9)	92.44 ± 31.86	10.88 ± 3.85	8.11 ± 6.71	37.22 ± 15.72
Income equal to expenditure (n = 49)	67.67 ± 36.15	8.30 ± 5.38	7.77 ± 5.10	28.73 ± 14.55
Statistical analysis				
t	1.920	1.372	0.172	1.589
P	0.06	0.17	0.86	0.11
Employment status				
Employed (n = 18)	57.33 ± 41.88	6.11 ± 4.43	4.22 ± 3.17	21.33 ± 14.34
Unemployed (n = 40)	77.90 ± 32.21	9.87 ± 5.18	9.45 ± 5.32	33.98 ± 13.59
Statistical analysis				
t	-2.045	-2.667	-4.645	-3.221
P	**0.04**	**0.01**	**<0.001**	**0.002**
Comorbid chronic disease				
Yes (n = 36)	86.44 ± 32.71	9.94 ± 5.41	9.25 ± 5.78	36.69 ± 13.21
No (n = 22)	47.09 ± 28.39	6.68 ± 4.29	5.50 ± 3.44	19.18 ± 10.65
Statistical analysis				
t	4.666	2.399	3.092	5.252
P	**<0.001**	**0.02**	**0.003**	**<0.001**
Functional classification				
Class II[a] (n = 20)	50.05 ± 31.58	6.25 ± 3.73	5.20 ± 3.17	18.15 ± 9.82
Class III[b] (n = 28)	80.31 ± 31.66	9.48 ± 5.26	8.65 ± 5.47	36.10 ± 13.35
Class IV[c] (n = 10)	90.89 ± 41.35	11.66 ± 6.14	11.00 ± 6.46	37.00 ± 13.83
Statistical analysis				
F	6.721	4.444	5.004	14.243
P	**0.002 (b > a; c > a)**	**0.01 (c > a)**	**0.01 (c > a)**	**<0.001 (b > a; c > a)**
Continuous oxygen therapy				
Yes (n = 11)	99.55 ± 28.89	14.54 ± 5.20	12.63 ± 6.28	44.09 ± 9.92
No (n = 47)	64.96 ± 35.05	7.34 ± 4.23	6.70 ± 4.37	26.77 ± 14.01
Statistical analysis				
t	3.034	4.860	2.965	3.868
P	**0.004**	**<0.001**	**0.01**	**<0.001**

Educational status: a = Illiterate, b = Primary education, c = High school and above. Functional classification: a = Class II, b = Class III, c = Class IV; t: Student's t-test; F: One-way analysis of variance (ANOVA); PAHSS, Pulmonary Arterial Hypertension Symptom Scale; HADS, Hospital Anxiety & Depression Scale.

Table 4. Correlations between participant characteristics and EmPHasis-10, PAHSS, and HADS scores (n = 58)

Scales and characteristics	PAHSS	EmPHasis-10	HADS-anxiety	HADS-depression
EmPHasis-10				
r	0.72	–	0.61	0.57
P	**< 0.001**	–	**< 0.001**	**< 0.001**
HADS-anxiety				
r	0.39	0.61	–	0.73
P	**0.03**	**< 0.001**	–	**< 0.001**
HADS-depression				
r	0.28	0.57	0.73	–
P	**0.03**	**< 0.001**	**< 0.001**	–
Age				
r	0.32	0.60	0.43	0.45
P	**0.01**	**< 0.001**	**0.001**	**< 0.001**
Saturation				
r	-0.30	-0.28	-0.08	-0.06
P	**0.02**	**0.03**	0.51	0.63
Pro-BNP				
r	0.20	0.20	-0.08	0.08
P	0.13	0.13	0.55	0.54
Ejection fraction				
r	-0.01	0.002	0.27	0.22
P	0.91	0.98	**0.04**	0.09
6-minute walk test				
r	-0.50	-0.60	-0.61	-0.49
P	**< 0.001**	**< 0.001**	**< 0.001**	**< 0.001**

PAHSS, Pulmonary Arterial Hypertension Symptom Scale; HADS, Hospital Anxiety & Depression Scale.

Table 5. Effects of participant characteristics, anxiety, depression, and PAHSS scores on EmPHasis-10 scores (n = 58)

Independent variables	B	SEB	t	P	95% CI	
Age	0.205	0.067	3.063	**0.003**	[0.071–0.339]	
PAHSS	0.247	0.029	8.617	**< 0.001**	[0.189–0.304]	**F = 42.892**
HADS-anxiety (ref: non-anxious)	6.417	2.126	3.08	**0.004**	[2.151–10.683]	**P < 0.001**
HADS-depression (ref: non-depressive)	5.214	2.261	2.306	**0.025**	[0.677–9.750]	**R = 0.897**
Vomiting (ref: not vomiting)	7.559	1.935	3.905	**< 0.001**	[3.675–11.443]	**R^2 = 0.805**

Linear regression analysis using the backward model. PAHSS, Pulmonary Arterial Hypertension Symptom Scale; HADS, Hospital Anxiety & Depression Scale; CI: Confidence interval.

Pulmonary hypertension symptoms are primarily associated with right ventricular dysfunction, with shortness of breath being the most prominent symptom, even during mild exertion.[5] Limitations in physical activity, shortness of breath, and fatigue may impair patients' ability to perform daily activities and meet basic self-care needs, thereby contributing to reduced QoL. Low energy levels and sleep disturbances may further exacerbate these limitations, highlighting the importance of effective symptom-management interventions.[29-31]

Although PH treatments improve symptoms and slow disease progression, treatment-related adverse effects and the complexity of treatment regimens may lead to poor adherence or treatment discontinuation, negatively affecting both QoL and clinical outcomes.[32] Therapies targeting the prostacyclin pathway provide substantial clinical and survival benefits in PH; however, they are also associated with a challenging adverse-effect profile.[11] During prostacyclin therapy, patients are closely monitored by nurses and physicians for treatment-related adverse effects.

The most commonly reported adverse effects in the present study were headache, flushing, nausea, vomiting, and diarrhea, most of which were mild to moderate in severity. Depending on the type and severity of these adverse effects, both pharmacological and non-pharmacological interventions are recommended to

support symptom management. Patients may experience more pronounced adverse effects during the dose-titration phase of prostacyclin therapy; however, these effects can largely be managed through close monitoring by physicians and nurses.[33,34] Patients with low socioeconomic status may initiate treatment later and experience poorer health outcomes, possibly because the disease progresses to more advanced stages before treatment begins.[35,36] Additionally, the financial burden associated with PH treatment may indirectly contribute to higher mortality by limiting treatment access and adherence.[37,38] Previous studies have shown that low socioeconomic status negatively affects survival in patients with PAH.[39]

Chronic comorbidities frequently observed in patients with PH may significantly influence disease prognosis and treatment response. Cardiovascular and pulmonary comorbidities are associated with increased symptom burden and mortality, and the prognostic significance of comorbidity burden on clinical outcomes has been emphasized.[40,41] Regarding functional capacity, significant associations have been reported between 6MWT distance, oxygen saturation, and QoL. In a multicenter study conducted at centers treating the majority of PAH patients in the United Kingdom, EmPHasis-10 scores demonstrated a moderate correlation with 6MWT distance, consistent with the findings of the present study.[42] Furthermore, reduced 6MWT distance in patients with PH has been associated with poorer functional status and adverse clinical outcomes, both of which are strongly related to increased symptom burden and impaired health-related QoL.[6,43,44]

The challenges associated with both the disease and treatment processes have a substantial impact on the mental health of patients with PH.[16,17] A meta-analysis of 24 studies reported a pooled prevalence of 37.1% for anxiety and 28% for depression among patients with PH.[21] Numerous studies have demonstrated that anxiety and depression are common in PH and negatively affect health-related QoL.[10,21,45,46,47] Anxiety and depression levels were found to be higher in patients with comorbidities, those requiring continuous oxygen therapy, and those with advanced functional class. Increasing levels of anxiety and depression were also associated with greater symptom burden and poorer QoL.[45] A study evaluating EmPHasis-10 scores in[1,745] patients with PAH over a three-year period demonstrated that these scores are independently associated with QoL and provide important prognostic information regarding patients' future health status and risk profile. This strong association may reflect the close relationship between symptom burden and PH severity. Accordingly, the EmPHasis-10 questionnaire may serve not only as a measure of QoL in patients with PH but also as a valid clinical outcome and prognostic indicator in routine practice.[40,48]

Prostacyclin therapy is frequently associated with vomiting and other gastrointestinal adverse effects, which may negatively affect nutritional status and health-related QoL.[12,33] These symptoms were also among the most commonly reported adverse effects in the present study.

The cross-sectional design of the study, the lack of baseline (pre-prostacyclin) symptom and QoL data, and the relatively small sample size from a single center may limit causal interpretation and generalizability of the findings.

Limitations

This study did not include baseline data on symptom frequency, symptom severity, or quality of life prior to prostacyclin therapy; therefore, pre- and post-treatment comparisons could not be performed. Although treatment-related adverse effects were recorded, their frequency and severity were not systematically assessed, which may have limited a more comprehensive evaluation of their impact on QoL. In addition, the absence of detailed hemodynamic parameters, such as mean pulmonary artery pressure (mPAP) and pulmonary vascular resistance (PVR) obtained by right heart catheterization, limits the clinical applicability of the findings. The cross-sectional design prevented determination of causal relationships among symptom burden, psychological status, and QoL, and the findings may not be generalizable to the broader PH population because of the sample-specific nature of the study. Furthermore, differences in QoL according to the route of prostacyclin administration (oral, inhaled, or parenteral), as well as associations with hemodynamic and echocardiographic parameters, were not evaluated. These limitations should be considered when interpreting the findings and applying them to broader clinical practice.

Conclusion

Patients with pulmonary hypertension receiving prostacyclin therapy experience impaired QoL, which is influenced by factors such as age, symptom severity, anxiety, depression, and vomiting. Vomiting, a common adverse effect of prostacyclin therapy, may substantially impair daily functioning and overall QoL. Routine assessment and effective management of treatment-related adverse effects, particularly gastrointestinal symptoms, may improve treatment adherence and enhance patient QoL.

Ethics Committee Approval: Ethics committee approval was obtained from Acıbadem Mehmet Ali Aydınlar University Medical Research Evaluation Ethics Committee (Approval Number: 2023/10, Date: 16.06.2023).

Informed Consent: Written and verbal informed consent was obtained from all participants included in the study.

Conflict of Interest: The authors have no conflicts of interest to declare.

Funding: The authors declared that this study received no financial support.

Use of AI for Writing Assistance: OpenAI's ChatGPT was used solely to improve the clarity and language of the manuscript. The tool was not used to generate substantive content, develop interpretations, or modify research data or results.

Author Contributions: Concept – F.Y., E.O., V.Ü., D.S., H.A.; Design – F.Y., E.O., V.Ü., D.S.; Supervision – F.Y., E.O., V.Ü., D.S.; Resource – H.A., B.Ş.S.; Materials – F.Y., E.O., V.Ü., D.S.; Data Collection and/or Processing – F.Y., H.A., B.Ş.S.; Analysis and/or Interpretation – F.Y., E.O., V.Ü., D.S.; Literature Review – F.Y., E.O., V.Ü., D.S.; Writing – F.Y., E.O., V.Ü., D.S., H.A.; Critical Review – F.Y., E.O., V.Ü., D.S., H.A.

Peer-review: Externally peer-reviewed.

References

1. Ntiloudi D, Kasinos N, Kalesi A, Vagenakis G, Theodosis-Georgilas A, Rammos S. Diagnosis and Management of Pulmonary Hypertension: New Insights. *Diagnostics (Basel)*. 2024;14(18):2052. [CrossRef]
2. Fukumoto Y. Pathophysiology and Treatment of Pulmonary Arterial Hypertension. *Int J Mol Sci*. 2024;25(2):1166. [CrossRef]

3. Bousseau S, Sobrano Fais R, Gu S, Frump A, Lahm T. Pathophysiology and new advances in pulmonary hypertension. *BMJ Med*. 2023;2(1):e000137. [CrossRef]
4. Arabacı HO, Taşdelen AG, Buğday İ, et al. A Breathtaking Case of Pulmonary Hypertension with Frightening Complications and Intertwining Different Etiologies. *Turk Kardiyol Dern Ars*. 2023;51(7):488–492. [CrossRef]
5. Humbert M, Kovacs G, Hoeper MM, et al.; ESC/ERS Scientific Document Group. 2022 ESC/ERS Guidelines for the diagnosis and treatment of pulmonary hypertension. *Eur Respir J*. 2023;61(1):2200879. [CrossRef]
6. Balasubramanian A, Larive AB, Horn EM, et al.; PVDOMICS Study Group. Health-Related Quality of Life Across the Spectrum of Pulmonary Hypertension. *Chest*. 2024;165(6):1493–1504. [CrossRef]
7. Reeves GEM, Shepherd J, Collins NJ, Twaddell S, Harjit Singh R. Assessing quality of life in pulmonary arterial hypertension: An independent prognostic marker. *Pulm Circ*. 2024;14(2):e12380. [CrossRef]
8. Heresi G, Dean B, Wu B, et al. Burden of illness in patients with pulmonary hypertension due to interstitial lung disease: a real-world analysis. *BMC Pulm Med*. 2024;24(1):335. [CrossRef]
9. Maini A, Cousins S, Holliday T, Memoli JW, Vasu TS, Khaitan PG. Hemoptysis: unilateral pulmonary artery atresia? A case report. *J Cardiothorac Surg*. 2023;18(1):199. [CrossRef]
10. Swisher JW, Weaver E. The Evolving Management and Treatment Options for Patients with Pulmonary Hypertension: Current Evidence and Challenges. *Vasc Health Risk Manag*. 2023;19:103–126. [CrossRef]
11. Zeng C, Liu J, Zheng X, Hu X, He Y. Prostaglandin and prostaglandin receptors: present and future promising therapeutic targets for pulmonary arterial hypertension. *Respir Res*. 2023;24(1):263. [CrossRef]
12. Saleh KM, Mallat J, Mohammed S, et al. Comparative efficacy and safety of prostacyclin therapies for pulmonary arterial hypertension: a systematic review and network meta-analysis. *Front Med (Lausanne)*. 2025;12:1643220. [CrossRef]
13. Wang P, Deng J, Zhang Q, et al. Additional Use of Prostacyclin Analogs in Patients With Pulmonary Arterial Hypertension: A Meta-Analysis. *Front Pharmacol*. 2022;13:817119. [CrossRef]
14. Guillevin L, Armstrong I, Aldrighetti R, et al. Understanding the impact of pulmonary arterial hypertension on patients' and carers' lives. *Eur Respir Rev*. 2013;22(130):535–542. [CrossRef]
15. Rawlings GH, Stark A, Armstrong I, Costin V, Thompson AR. The Role of Psychological Distress on Health-Related Quality of Life, Fatigue, and Pain in Adults With Pulmonary Hypertension. *Pulm Circ*. 2025;15(2):e70101. [CrossRef]
16. Dering MR, Lepsy N, Fuge J, et al. Prevalence of Mental Disorders in Patients With Chronic Thromboembolic Pulmonary Hypertension. *Front Psychiatry*. 2022;13:821466. [CrossRef]
17. Zhang J, Yin Y, Wen Y, Shi F, Wang J. Anxiety and Depression in Patients With Pulmonary Arterial Hypertension in Northwest China: A Cross-Sectional Study. *Front Psychiatry*. 2022;12:758120. [CrossRef]
18. Deshwal H, Weinstein T, Sulica R. Advances in the management of pulmonary arterial hypertension. *J Investig Med*. 2021;69(7):1270–1280. [CrossRef]
19. Christopher Malaisrie S, Chiu S, et al. Outcomes of Multidisciplinary Care at a Chronic Thromboembolic Pulmonary Hypertension Center. *Pulm Circ*. 2025;15(2):e70085. [CrossRef]
20. Guo J, He J, Wang J, et al. A novel nurse-led, multidisciplinary, and guideline-directed disease intensive management program improves long-term survival of pulmonary hypertension patients. *Heart Lung*. 2025;73:190–196. [CrossRef]
21. Mai AS, Lim OZH, Ho YJ, et al. Prevalence, Risk Factors and Intervention for Depression and Anxiety in Pulmonary Hypertension: A Systematic Review and Meta-analysis. *Front Med (Lausanne)*. 2022;9:765461. [CrossRef]
22. Matura LA, McDonough A, Hanlon AL, Carroll DL. Development and initial psychometric properties of the Pulmonary Arterial Hypertension Symptom Scale (PAHSS). *Appl Nurs Res*. 2015;28(1):42–47. [CrossRef]
23. Yılmaz C, Sezgin D. *Turkish validity and reliability of the pulmonary arterial hypertension symptom scale*. Master's Thesis. Dokuz Eylul University; 2018. Turkish.
24. Zigmond AS, Snaith RP. The hospital anxiety and depression scale. *Acta Psychiatr Scand*. 1983;67(6):361–370. [CrossRef]
25. Aydemir Ö, Güvenir T, Küey L, Kültür S. Hastane anksiyete ve depresyon ölçeği Türkçe formunun geçerlilik ve güvenilirlik çalışması. *Turk Psikiyatri Derg*. 1997;8(4):280–287. Turkish.
26. Yorke J, Corris P, Gaine S, et al. emPHasis-10: development of a health-related quality of life measure in pulmonary hypertension. *Eur Respir J*. 2014;43(4):1106–1113. [CrossRef]
27. Odevoglu P, Demir R, Okumus G, Kucukoglu MS, Kuran Aslan G. Validity and reliability of the Turkish version of the EmPHasis-10 questionnaire in patients with pulmonary hypertension. *J Eval Clin Pract*. 2019;25(5):896–902. [CrossRef]
28. Tabachnick BG, Fidell LS, Ullman JB. *Using multivariate statistics*. 6th ed. Boston (MA): Pearson; 2013.
29. Kendrew R, Ajraoui S, Beaudet A, et al. Relevance of patient-centered actigraphy measures in pulmonary arterial hypertension and chronic thromboembolic pulmonary hypertension: a qualitative interview study. *BMC Pulm Med*. 2024;24(1):608. [CrossRef]
30. Lima LNG, Veronez V, Mendes PRA, Kiyota TA, Moreira MM, Pereira MC. Relationships that perceived barriers to physical activity have with functional capacity and quality of life in patients with pulmonary hypertension. *J Bras Pneumol*. 2025;51(1):e20240195. [CrossRef]
31. Ceylan R, Demir R, Zeren M, Sinan UY, Kucukoglu MS. Sleep Quality and Its Predictors among Dyspnea, Fatigue and Exercise Capacity in Pulmonary Arterial Hypertension. *Acta Cardiol Sin*. 2024;40(5):618–626.
32. Qadus S, Naser AY, Ofori-Asenso R, Ademi Z, Al Awawdeh S, Liew D. Adherence and Discontinuation of Disease-Specific Therapies for Pulmonary Arterial Hypertension: A Systematic Review and Meta-Analysis. *Am J Cardiovasc Drugs*. 2023;23(1):19–33. [CrossRef]
33. Kingman M, Archer-Chicko C, Bartlett M, Beckmann J, Hohsfield R, Lombardi S. Management of prostacyclin side effects in adult patients with pulmonary arterial hypertension. *Pulm Circ*. 2017;7(3):598–608. [CrossRef]
34. Sezgin D. Pulmoner hipertansiyon ve bakım yönetimi. In: Özer S, ed. *Olgu Senaryolarıyla İç Hastalıkları Hemşireliği*. 1st ed. İstanbul: İstanbul Tıp Kitabevleri; 2019:141–158.
35. Reinders S, Didden EM, Ong R. Survival, morbidity, and quality of life in pulmonary arterial hypertension patients: a systematic review of outcomes reported by population-based observational studies. *Respir Res*. 2024;25(1):373. [CrossRef]
36. Talwar A, Sahni S, Talwar A, Khon N, Klinger JR. Socioeconomic status affects pulmonary hypertension disease severity at time of first evaluation. *Pulm Circ*. 2016;6(2):191–195. [CrossRef]
37. Ong MS. Socioeconomic status and survival in patients with pulmonary hypertension. *ERJ Open Res*. 2020;6(4):00638-2020. [CrossRef]
38. Ramani G, Bali V, Black H, et al. Exploring the Economic Burden of Pulmonary Arterial Hypertension and Its Relation to Disease Severity and Treatment Escalation: A Systematic Literature Review. *Pharmacoeconomics*. 2025;43(7):741–760. Erratum in: *Pharmacoeconomics*. 2025;43(9):1163. [CrossRef]
39. Wu WH, Yang L, Peng FH, et al. Lower socioeconomic status is associated with worse outcomes in pulmonary arterial hypertension. *Am J Respir Crit Care Med*. 2013;187(3):303–310. [CrossRef]
40. Gialamas I, Arvanitaki A, Rosenkranz S, et al. The impact of cardiovascular and lung comorbidities in patients with pulmonary arterial hypertension: A systematic review and meta-analysis. *J Heart Lung Transplant*. 2024;43(9):1383–1394. [CrossRef]

41. Rosenkranz S, Pausch C, Coghlan JG, et al. Risk stratification and response to therapy in patients with pulmonary arterial hypertension and comorbidities: A COMPERA analysis. *J Heart Lung Transplant*. 2023;42(1):102–114. [CrossRef]
42. Lewis RA, Armstrong I, Bergbaum C, et al. EmPHasis-10 health-related quality of life score predicts outcomes in patients with idiopathic and connective tissue disease-associated pulmonary arterial hypertension: results from a UK multicentre study. *Eur Respir J*. 2021;57(2):2000124. [CrossRef]
43. Choi JH, Shin MJ, Lee BJ, Park JH. Exercise-induced desaturation during a six-minute walk test is associated with poor clinical outcomes in patients with pulmonary arterial hypertension. *Clin Hypertens*. 2023;29(1):33. [CrossRef]
44. Moutchia J, McClelland RL, Al-Naamani N, et al. Minimal Clinically Important Difference in the 6-minute-walk Distance for Patients with Pulmonary Arterial Hypertension. *Am J Respir Crit Care Med*. 2023;207(8):1070–1079. [CrossRef]
45. Pfeuffer-Jovic E, Joa F, Halank M, Krannich JH, Held M. Anxiety, depression and quality of life in pulmonary hypertension: a comparison of incident and prevalent cases. *Respiration*. 2022;101(8):784–792. [CrossRef]
46. Olsson KM, Meltendorf T, Fuge J, et al. Prevalence of Mental Disorders and Impact on Quality of Life in Patients With Pulmonary Arterial Hypertension. *Front Psychiatry*. 2021;12:667602. [CrossRef]
47. Sarzyńska K, Świątoniowska-Lonc N, Dudek K, et al. Quality of life of patients with pulmonary arterial hypertension: a meta-analysis. *Eur Rev Med Pharmacol Sci*. 2021;25(15):4983–4998.
48. Favoccia C, Kempny A, Yorke J, et al. EmPHasis-10 score for the assessment of quality of life in various types of pulmonary hypertension and its relation to outcome. *Eur J Prev Cardiol*. 2019;26(12):1338–1340. [CrossRef]

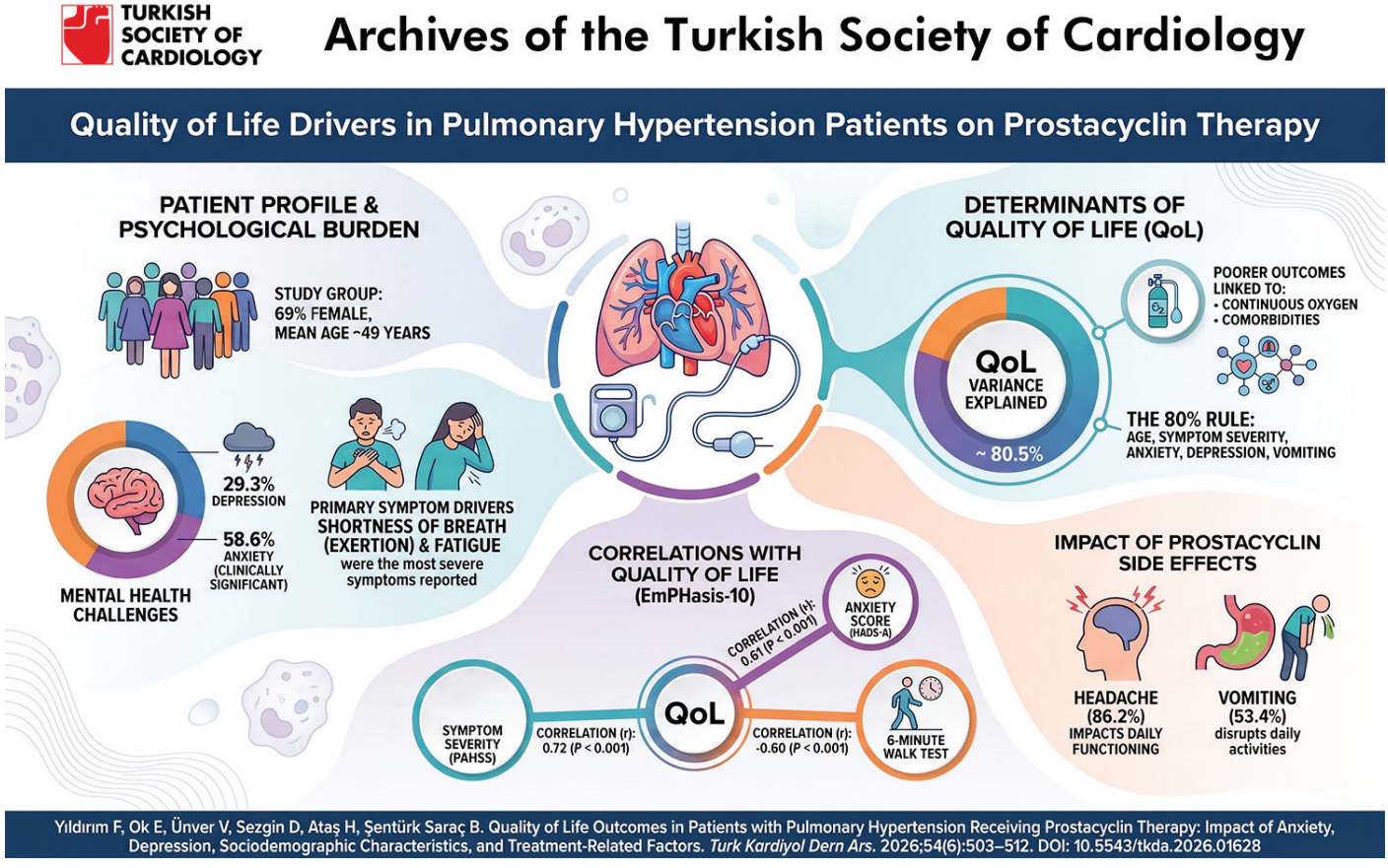

ARCHIVES OF THE TURKISH SOCIETY OF CARDIOLOGY

Official journal of the TURKISH SOCIETY OF CARDIOLOGY

Endothelin-Dependent Myocardial Dysfunction in an Experimental Endotoxic Shock Model

Deneysel Endotoksik Şok Modelinde Endotelin Bağımlı Miyokard Disfonksiyonu

ABSTRACT

Objective: Impaired myocardial contractility is a major contributor to cardiovascular failure during septic shock; however, the underlying mechanisms remain incompletely understood. This study investigated the roles of endothelin and nitric oxide (NO) in cardiac dysfunction using the endothelin receptor antagonist tezosentan and nitric oxide synthase (NOS) inhibitors in an experimental model of endotoxic shock.

Method: Endotoxic shock was induced in rats via intraperitoneal injection of lipopolysaccharide (LPS, 1 mg/kg). Hearts were isolated four hours after LPS or saline administration and perfused using a Langendorff apparatus. Myocardial contractility, coronary perfusion pressure, and heart rate were recorded. The effects of tezosentan and NOS inhibitors (Nω-nitro-L-arginine methyl ester [L-NAME], aminoguanidine, and S-methylisothiourea sulfate [AETU]) were assessed by adding these agents to the perfusate. In parallel, atrial and papillary muscle contractility and spontaneous beating rates were evaluated using isolated tissue preparations in *in vitro* organ bath studies.

Results: Baseline myocardial contractility was significantly reduced in LPS-treated perfused hearts compared with controls (3.03 ± 0.25 vs. 4.94 ± 0.39 g, $P < 0.05$), whereas no significant differences were observed in isolated atrial or papillary muscle preparations. Coronary perfusion pressure was significantly increased in the LPS group (101 ± 6 vs. 79 ± 6 mmHg, $P < 0.05$). Tezosentan significantly attenuated the LPS-induced reduction in myocardial contractility but did not affect the increase in perfusion pressure. None of the NOS inhibitors altered myocardial contractility or perfusion pressure in LPS-treated hearts.

Conclusion: Myocardial contractility impairment in experimental endotoxic shock occurs only in the presence of an intact coronary vasculature and is prevented by endothelin receptor blockade. These findings suggest that vascular endothelium-derived endothelin plays a key role in myocardial depression during endotoxic shock, whereas nitric oxide appears to have a limited contribution in this model.

Keywords: Endothelin, endotoxic shock, myocardial dysfunction, nitric oxide, Nω-nitro-L-arginine methyl ester, tezosentan

ÖZET

Amaç: Septik şok sırasında kardiyovasküler yetmezliğin önemli bir nedeni, patolojik oluşum mekanizması tam olarak bilinmeyen miyokard kasılma bozukluğudur. Bu çalışmada, endotelin reseptör antagonisti tezosentan ve nitrik oksit sentaz (NOS) inhibitörleri kullanılarak, endotelin ve nitrik oksitin (NO) deneysel endotoksik şok modelinde gelişen kardiyak disfonksiyondaki rolleri incelenmiştir.

Yöntem: Sıçanlarda lipopolisakkarit (LPS, 1 mg/kg) intraperitoneal enjeksiyonu ile endotoksik şok indüklenmiştir. Kalpler, LPS veya salin uygulamasından 4 saat sonra izole edilmiş ve Langendorff düzeneği kullanılarak perfüze edilmiştir. Miyokard kasılma gücü, koroner perfüzyon basıncı ve kalp hızı kaydedilmiştir. Tezosentan ve NOS inhibitörleri L-NAME, aminoguanidin ve AETU'nun etkileri, bu ajanların perfüzyon sıvısına eklenmesiyle değerlendirilmiştir. Paralel olarak, izole doku preparatlarında *in vitro* organ banyosu çalışmaları kullanılarak atriyal ve papiller kas kasılma gücü ile spontan atım hızları değerlendirilmiştir.

Bulgular: LPS uygulanan perfüze kalplerde bazal miyokardiyal kasılma kontrollere göre anlamlı olarak azalmıştır (3,03 ± 0,25'e karşı 4,94 ± 0,39 g, $P < 0,05$); buna karşın izole atriyal veya papiller kas preparatlarında anlamlı bir fark gözlenmemiştir. Koroner perfüzyon basıncı LPS grubunda anlamlı olarak artmıştır (101 ± 6'ya karşı 79±6 mmHg, $P < 0,05$). Tezosentan, LPS'ye bağlı miyokardiyal kasılma azalmasını anlamlı olarak azaltmış, ancak perfüzyon basıncındaki artışı etkilememiştir. NOS inhibitörlerinin hiçbiri, LPS uygulanan kalplerde miyokardiyal kasılmayı veya perfüzyon basıncını değiştirmemiştir.

ORIGINAL ARTICLE
ARAŞTIRMA MAKALESİ

Mustafa Boz

Alper Bektaş İskit

Department of Medical Pharmacology, Hacettepe University, Faculty of Medicine, Ankara, Türkiye

Corresponding author:
Alper Bektaş İskit
✉ alperi@hacettepe.edu.tr

Received: April 01, 2026
Accepted: April 28, 2026

Cite this article as: Boz M, İskit AB. Endothelin-Dependent Myocardial Dysfunction in an Experimental Endotoxic Shock Model. *Turk Kardiyol Dern Ars.* 2026;54(6):513-518.

DOI: 10.5543/tkda.2026.27303

Sonuç: Deneysel endotoksik şokta miyokardiyal kasılma bozukluğu yalnızca sağlam bir koroner damar yapısının varlığında gözlenir ve endotelin reseptör blokajı ile önlenir. Bu bulgular, vasküler endotel kaynaklı endotelinin endotoksik şok sırasında miyokardiyal depresyonda önemli bir rol oynadığını, nitrik oksidin ise bu modelde sınırlı katkıya sahip olduğunu göstermektedir.

Anahtar Kelimeler: Endotelin, endotoksik şok, miyokardiyal disfonksiyon, nitrik oksit, Nω-nitro-L-arginin metil ester, tezosentan

Septic shock caused by gram-negative bacterial infections is characterized by profound cardiovascular dysfunction and remains a leading cause of mortality in intensive care units. Lipopolysaccharides (LPS), components of the outer membrane of gram-negative bacteria, initiate a cascade of inflammatory and hemodynamic responses, including hypotension, microvascular injury, impaired tissue perfusion, and disseminated intravascular coagulation. Among these alterations, reduced myocardial contractility plays a pivotal role in the progression of septic shock and multiple organ failure.[1]

Experimental administration of LPS (endotoxic shock) reproduces many features of septic shock and has been widely used to study sepsis-induced myocardial dysfunction. Although myocardial depression has been consistently demonstrated in both clinical and experimental settings, the precise mechanisms responsible for impaired cardiac function remain incompletely defined. Proposed mechanisms include downregulation of β-adrenergic receptors, impaired post-receptor signaling pathways, reduced calcium release from the sarcoplasmic reticulum, and altered electromechanical coupling at the myofibrillar level. Cytokines and nitric oxide (NO) regulate most, if not all, of these changes.[1]

Nitric oxide plays a complex role in cardiac function, exerting both protective and deleterious effects. In vascular and cardiac tissues, nitric oxide is constitutively synthesized from L-arginine by endothelial (eNOS) or neuronal (nNOS) nitric oxide synthases. In response to some cytokines and bacterial products, an inducible form of NOS (iNOS) is expressed in these tissues. In the heart, increased iNOS expression has been observed in various forms of cardiac failure, including dilated cardiomyopathy, inflammatory cardiomyopathy, and ischemic heart disease, suggesting a pathophysiological role.[2] However, some experimental evidence indicates that iNOS may also contribute to cardioprotection.[3,4]

In septic or endotoxic shock, excessive NO production by cardiac myocytes, vascular endothelium, and smooth muscle cells may contribute to vascular dysfunction and myocardial depression. NOS inhibitors have been shown to significantly improve blood pressure and vascular reactivity in both human and animal models of sepsis when administered *in vivo* and *in vitro*. Consistent with strong evidence for activation of the endothelin system in experimental endotoxemia, NO interacts with endothelin in the regulation of vascular tone.[5] In addition to its vascular effects, endothelin plays a significant role in the pathophysiology of endotoxic and septic shock. It induces vasodilatation via endothelin type B (ET_B) receptors and vasoconstriction primarily via endothelin type A (ET_A) receptors, but also through a subtype of ET_B receptors.[6]

ABBREVIATIONS

CPP	Coronary perfusion pressure
ECG	Electrocardiography
eNOS	Endothelial nitric oxide
ET-1	Endothelin-1
IL-1β	Interleukin-1 beta
iNOS	Inducible form of nitric oxide
L-NAME	Nω-nitro-L-arginine methyl ester
LPS	Lipopolysaccharides
nNOS	Neuronal nitric oxide
NO	Nitric oxide
SEM	Standard error of the mean
TNF-a	Tumor necrosis factor-alpha

Given the complex interaction between NO and endothelin in cardiovascular regulation, the present study aimed to investigate their respective contributions to myocardial dysfunction in an experimental model of endotoxic shock. Using isolated perfused hearts and isolated cardiac muscle preparations, we evaluated the effects of nitric oxide synthase (NOS) inhibitors (Nω-nitro-L-arginine methyl ester [L-NAME], aminoguanidine, and S-methylisothiourea sulfate [AETU]) and the dual endothelin receptor antagonist tezosentan on myocardial contractility and coronary perfusion.

Materials and Methods

Animals

Fifty-four adult male Wistar rats (170–200 g) were obtained from the Laboratory Animals Breeding Unit of Hacettepe University. The animals were housed in the Laboratory Animal Facility of the Department of Medical Pharmacology, Hacettepe University Faculty of Medicine, under controlled environmental conditions (temperature 21 ± 2 °C; relative humidity 30–70%). Rats had free access to tap water and standard pellet diet (Murat Yem Sanayi, Ankara, Türkiye).

All procedures were conducted in accordance with the Declaration of Helsinki and the Guiding Principles for the Care and Use of Laboratory Animals. The study protocol was approved by Hacettepe University Local Ethics Committee for Animal Experiments (Approval Number: 2017/74-02 Date: 28.11.2017).

Drug Administration

Endotoxic shock was induced by intraperitoneal (i.p.) injection of LPS (1 mg/kg) derived from Escherichia coli (O55:B5), administered four hours prior to the experiment. Control animals received an equivalent volume (1 mL/kg) of sterile, non-pyrogenic saline (0.9% NaCl, w/v, prepared in pyrogen-free distilled water). Although LPS administration is widely used to

model sepsis-related inflammation, it produces a reproducible state of endotoxemia rather than true polymicrobial sepsis. For the isolated perfused heart experiments described below, hearts were harvested from both control and endotoxemic animals four hours after injection. This time point was selected based on previous studies showing that inducible nitric oxide synthase activity peaks 2–6 hours following endotoxin administration.[7] The control group and LPS-treated group were further subdivided into five groups according to the drugs used, which were added to the perfusate for a 20-minute period following a 20-minute equilibration phase.

Surgical Procedure

Dissection and Preparation of Isolated Atrium and Papillary Muscle

Rats were anesthetized, and the thorax was opened by incising the skin and underlying musculature. Following thoracotomy, the heart was rapidly excised and placed in ice-cold Feigen solution (in mM: NaCl 153.8, $NaHCO_3$ 23.8, KCl 5.6, $CaCl_2$ 5.5, glucose 11.1), continuously bubbled with 95% O2 and 5% CO_2 (pH 7.4). The right ventricular papillary muscle and both atria were dissected from separate hearts, secured with silk threads, and suspended in a tissue chamber containing 20 mL of continuously aerated Feigen solution maintained at 34 °C.

Assessment of Cardiac Muscle Contractility

Contractile force was measured isometrically using a force-displacement system (Biopac MP150) and recorded digitally. The rate of spontaneous contractions was monitored simultaneously. Tissues were allowed to equilibrate for 30 minutes under a resting tension of 0.5 g, which produced maximal contractile force in rat atrial and papillary muscles. During this period, the bath solution was replaced every 15 minutes. Drugs were added directly to the tissue chamber, and cumulative concentration–response data were obtained.

Dissection and Preparation of Isolated Heart

The isolated heart preparation was performed as previously described by Suveren et al.[8] Rats were anaesthetized, and the thorax was opened via a bilateral incision along the rib cage. Hearts were excised and arrested in ice-cold Krebs–Henseleit solution (NaCl: 118, $NaCO_3$: 25, KCl: 4.7, $CaCl_2$: 2.5, KH_2PO_4: 1.2, $MgSO_4$: 1.2, glucose: 10). The solution was filtered (5.0 µm) and gassed with 95% O_2 and 5% CO_2. The aorta was dissected free of surrounding tissue, and the ascending aorta was cannulated. Retrograde perfusion with heparinized Krebs solution was initially performed using a syringe to remove residual blood from the hearts. The hearts were then mounted on a Langendorff apparatus and perfused with oxygenated, warmed (37 °C) Krebs solution using a peristaltic pump (MAY PRS 9508) at a constant flow rate of 5 mL/min throughout the experiment. The apex of the heart was secured with a silk ligature, which was passed over a pulley and connected to an isometric force transducer (Grass force-displacement transducer FT03C) to measure myocardial contractile force.

Coronary perfusion pressure was continuously monitored using a Biopac pressure transducer. Electrocardiographic (ECG) recordings were obtained using stainless-steel needle electrodes placed on the left ventricular apex and right atrial appendage. Signals were recorded using a Biopac MP150 data acquisition system. After a 20-minute stabilization period, myocardial contractility, heart rate, and perfusion pressure were measured at 0, 1, 5, 10, and 20 minutes.

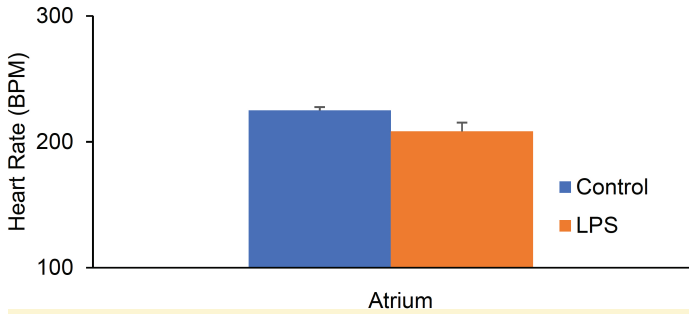

Figure 1. Heart rate, expressed as beats per minute (BPM), in saline- and lipopolysaccharide (LPS; *Escherichia coli* endotoxin, serotype 055:B5, 1 mg/kg^{-1})-treated rat atria. Vertical bars represent the standard error of the mean of the data points included in each observation. n = 6 per group. P > 0.05 for saline vs. LPS groups (Mann–Whitney U test).

Drugs

The following agents were used: sodium thiopental (I.E. Ulagay, Türkiye), sodium chloride (Merck, USA), heparin sodium (Roche, Switzerland), lipopolysaccharide (Escherichia coli 055:B5; Sigma, USA; 1 mL/kg^{-1}), L-NAME (Sigma, USA; 10-5M), tezosentan (provided by Dr. Marc Iglarz and Dr. Martine Clozel, Actelion Pharmaceuticals Ltd., Allschwil, Switzerland; 10-5M), AETU (Sigma, USA; 10-5 M), and aminoguanidine (Sigma, USA; 10-4 M).

All drugs were prepared fresh daily, dissolved in sterile, non-pyrogenic saline, and warmed to 37 °C prior to use. Solutions were protected from light until administration to prevent degradation.

Statistics

Statistical analyses were performed using GraphPad Prism (GraphPad Software Inc., CA, USA). Normality was assessed using the Shapiro–Wilk test. Data are presented as mean ± standard error of the mean (SEM) for normally distributed variables or as median and interquartile range (IQR, 25–75%) for non-normally distributed variables. Changes in perfusion pressure and myocardial contractility over time were analyzed using two-way repeated-measures analysis of variance (ANOVA). Comparisons at individual time points were performed using the unpaired Student's t test. The Mann–Whitney U test or the Kruskal–Wallis test was used to assess differences between groups, followed by Dunn's post hoc test where appropriate. Differences were considered statistically significant at $P < 0.05$.

Results

Effects of LPS on Isolated Atrium and Papillary Muscle

Effects of LPS on Heart Rate

In vitro organ bath studies showed that LPS had no significant effect on heart rate (approximately 225 ± 5 vs. 210 ± 8 beats per minute, P > 0.05, n = 6) (Figure 1).

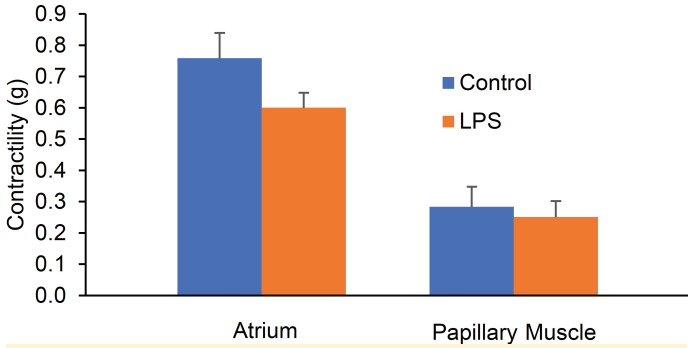

Figure 2. Contractility, expressed in grams (g), in saline- and lipopolysaccharide (LPS; *Escherichia coli* endotoxin, serotype 055:B5, 1 mg/kg^{-1})-treated rat atria and papillary muscle in *in vitro* organ bath studies. Vertical bars represent the standard error of the mean. n = 6 per group. P > 0.05 for saline vs. LPS groups for either tissue (Mann–Whitney U test; adjacent columns compared).

Effects of LPS on Atrial and Papillary Muscle Contractility

No significant differences in atrial or papillary muscle contractility were observed between the control and LPS groups in *in vitro* organ bath experiments (Figure 2).

Effects of LPS on Perfused Heart

Initial Perfusion Pressure and Contractility

Perfusion pressure was increased in the LPS group (*P < 0.05, n = 6) (Figure 3), whereas myocardial contractility was decreased (*P < 0.05, n = 6) (Figure 4). In contrast to the *in vitro* organ bath experiments, these effects were observed only in the isolated perfused heart model.

Effects of Pharmacological Interventions on LPS-Induced Dysfunction

Figure 5 shows the percentage change in perfusion pressure over 20 minutes. Neither NOS inhibitors nor tezosentan significantly affected the LPS-induced increase in perfusion pressure (P > 0.05, n = 6) (Figure 5b). Similarly, no significant effects were observed in the saline-treated group (P > 0.05, n = 6) (Figure 5a).

Figure 6 summarizes the percentage change in contractility over 20 minutes. No drugs affected contractility in the saline group (P > 0.05, n = 6) (Figure 6a). In contrast, the endothelin receptor antagonist tezosentan significantly attenuated the LPS-induced decrease in myocardial contractility (P < 0.05, n = 6) (Figure 6b), whereas NOS inhibitors had no significant effect (P > 0.05, n = 6) (Figure 6b).

Discussion

In this experimental model of endotoxic shock induced by LPS, myocardial contractility was reduced in isolated perfused hearts, but not in isolated atrial or papillary muscles. This finding suggests that mediator(s) released from the intact coronary vasculature may contribute to the observed decrease in myocardial contractility. The prevention of contractile impairment by tezosentan further indicates that endothelium-derived endothelin peptides play a key role in LPS-induced myocardial depression.

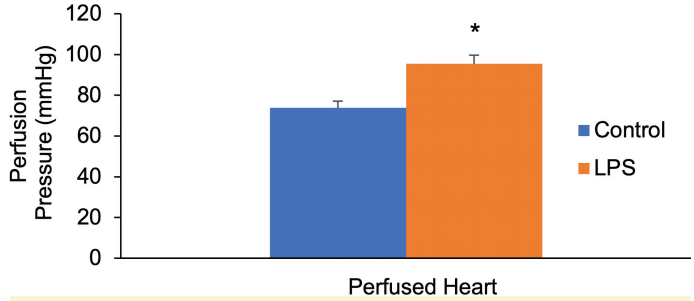

Figure 3. The initial perfusion pressure values as mmHg in saline and LPS (*Escherichia coli* endotoxin, serotype 055:B5, 1 mg kg^{-1})-treated rats on perfused heart. Vertical bars indicate the standard error of the mean of the number of data points included in that observation. n = 6 for each column. *P<0.05 for saline vs LPS (Mann-Whitney U-test).

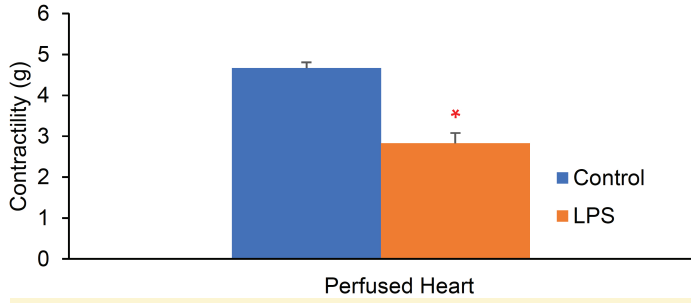

Figure 4. Initial contractility, expressed in grams (g), in saline- and lipopolysaccharide (LPS; *Escherichia coli* endotoxin, serotype 055:B5, 1 mg/kg^{-1})-treated rat perfused hearts. Vertical bars represent the standard error of the mean. n = 6 per group. *P < 0.05 for saline vs. LPS (Mann–Whitney U test).

Although reduced cardiac function in septic shock has long been recognized in both experimental models and clinical settings, the underlying mechanisms are incompletely understood. Serum obtained from patients in the acute phase of septic shock has been shown to depress contractility in isolated ventricular myocytes *in vitro*, suggesting the presence of circulating myocardial depressant factors during sepsis. One contributing factor to myocardial depression may be reduced coronary perfusion.[9]

In recent years, cytokines have attracted considerable attention as mediators of sepsis-related cardiac dysfunction. These proteins are produced and released by various nucleated cells in response to ischemia, trauma, surgery, and infection.[10-12] Studies in mouse models of sepsis have shown that cardiomyocytes exposed *in vitro* to tumor necrosis factor-alpha (TNF-a), interleukin-1 beta (IL-1β), and IL-6 exhibit significantly reduced contractility.[8,11] These findings suggest that cytokines may play a central role in the cardiac depression associated with sepsis.

In septic shock, endothelin-1 (ET-1) levels are elevated concurrently with NO upregulation. Perfused hearts isolated from LPS-treated rats demonstrate a persistent increase in coronary perfusion pressure (CPP) under constant flow conditions, indicating increased coronary resistance. Pretreatment with the ETA receptor-selective antagonist BQ-123 completely abolishes this vasoconstrictor response. As reported by Hohlfeld et al.,[13]

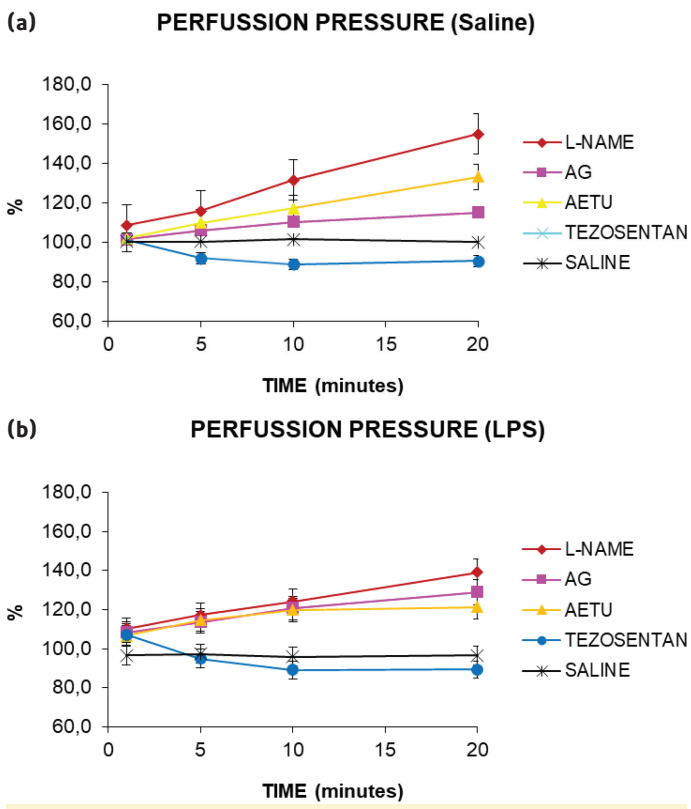

Figure 5. Effects of pharmacological agents on perfusion pressure, expressed in mmHg, in saline-treated (a) and lipopolysaccharide (LPS; *Escherichia coli* endotoxin, serotype 055:B5, 1 mg/kg^{-1})-treated (b) rat perfused hearts. Vertical bars represent the standard error of the mean. n = 6 per curve. P > 0.05 for saline vs. LPS curves (repeated-measures analysis of variance [ANOVA]).

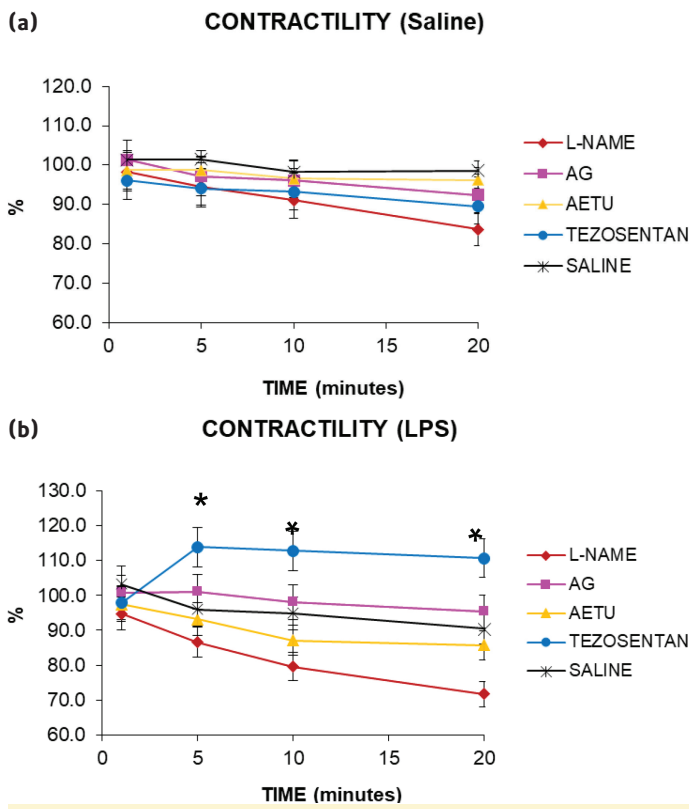

Figure 6. Effects of pharmacological agents on contractility, expressed as percentage change (%), in saline-treated (Figure 6a) and lipopolysaccharide (LPS; *Escherichia coli* endotoxin, serotype 055:B5, 1 mg/kg^{-1})-treated (Figure 6b) rat perfused hearts. Vertical bars represent the standard error of the mean. N = 6 per curve. *P < 0.05 for saline vs. LPS curves (repeated-measures analysis of variance [ANOVA]).

ET-1 plays a dominant role in regulating coronary tone in septic shock, mediating LPS-induced coronary vasoconstriction via ETA receptors. However, although normalization of CPP with BQ-123 restores coronary perfusion, contractile function is only partially recovered.[14] This suggests that endothelin-1–mediated coronary vasoconstriction and flow maldistribution contribute significantly, but not exclusively, to LPS-induced cardiodepression. Furthermore, circulating ET-1 levels may not accurately reflect its role in myocardial dysfunction, as ET-1 release occurs predominantly on the abluminal side.[15]

The limited effectiveness of NOS inhibitors in reversing myocardial dysfunction during septic shock may be explained by excessive coronary vasoconstriction, which is exacerbated by NOS inhibition. This reduction in myocardial blood flow contributes to impaired ventricular function. Tu et al.[16] demonstrated that pretreatment with the iNOS inhibitor aminoguanidine partially improved, but did not fully reverse, LPS-induced myocardial dysfunction. These findings indicate that while NO contributes to myocardial depression in septic shock, it is not the sole mediator. Although aminoguanidine is considered a relatively selective inhibitor of iNOS expression and activity,[17] its additional pharmacological effects, including inhibition of histamine pathways, polyamine catabolism, blockade of enzymes containing iron or copper, and inhibition of advanced glycosylation end-product formation,[18] may also account for its observed benefits. Similarly, non-selective NOS inhibitors such as L-NAME and AETU failed to counteract LPS-induced myocardial dysfunction.

Conclusion

Although cardiac dysfunction in septic shock is associated with increased mortality, the role of endothelium-derived factors remains incompletely understood. In this experimental model of endotoxic shock, impaired myocardial contractility occurs only in the presence of an intact coronary vasculature and is prevented by endothelin receptor blockade. These findings underscore the critical role of vascular endothelium-derived endothelin in sepsis-induced myocardial dysfunction while suggesting a more limited contribution of nitric oxide.

Ethics Committee Approval: Ethics committee approval was obtained from Hacettepe University Local Ethics Committee for Animal Experiments (Approval Number: 2017/74-02 Date: 28.11.2017).

Informed Consent: Written informed consent was not required as the study do not include humans.

Conflict of Interest: The authors have no conflicts of interest to declare.

Funding: The authors declared that this study received no financial support.

Use of AI for Writing Assistance: No use of AI-assisted technologies was declared by the authors.

Author Contributions: Concept – A.B.İ.; Design – M.B., A.B.İ.; Supervision – A.B.İ.; Resource – M.B.; Materials – M.B., A.B.İ.; Data Collection and/or Processing - M.B.; Analysis and/or Interpretation - M.B.; Literature Review – M.B.; Writing – M.B., A.B.İ.; Critical Review – A.B.İ.

Peer-review: Externally peer-reviewed.

References

1. Martin L, Derwall M, Al Zoubi S, et al. The Septic Heart: Current Understanding of Molecular Mechanisms and Clinical Implications. *Chest*. 2019;155(2):427-437. [CrossRef]
2. Hobai IA. Mechanisms of Cardiac Dysfunction in Sepsis. *Shock*. 2023;59(4):515-539. [CrossRef]
3. Iskit AB, Guc MO, Ilhan M. L-canavanine and dexamethasone attenuate endotoxin- induced suppression of ischaemia-reperfusion arrhythmias. *Eur J Pharmacol*. 1997;326(2-3):183-190. [CrossRef]
4. Yilmaz G, Boz M, Iskit AB. The Effects of Lipopolysaccharide Derivatives in Rodent Models of Cardiac Arrhythmia. *Anatol J Cardiol*. 2022;26(12):886-892. [CrossRef]
5. Ozer EK, Iskit AB. Effects of endothelin and nitric oxide on cardiac muscle functions in experimental septic shock model. *Hum Exp Toxicol*. 2016;35(3):267-275. [CrossRef]
6. Ucar BI, Erikci A, Kosemehmetoglu K, et al. Effects of endothelin receptor blockade and COX inhibition on intestinal I/R injury in a rat model: Experimental research. *Int J Surg*. 2020;83:89-97. [CrossRef]
7. Iskit AB, Erkent U, Ertunc M, Guc MO, Ilhan M, Onur R. Glibenclamide attenuates the antiarrhythmic effect of endotoxin with a mechanism not involving K(ATP) channels. *Vascul Pharmacol*. 2007;46(2):129-136. [CrossRef]
8. Suveren E, Baxter GF, Iskit AB, Turker AU. Cardioprotective effects of Viscum album L. subsp. album (European misletoe) leaf extracts in myocardial ischemia and reperfusion. *J Ethnopharmacol*. 2017;209:203-209. [CrossRef]
9. Fan D, Wu R. Mechanisms of the septic heart: From inflammatory response to myocardial edema. *J Mol Cell Cardiol*. 2024;195:73-82. [CrossRef]
10. Dao L, Liu H, Xiu R, Yao T, Tong R, Xu L. Gramine improves sepsis-induced myocardial dysfunction by binding to NF-κB p105 and inhibiting its ubiquitination. *Phytomedicine*. 2024;125:155325. [CrossRef]
11. Hobai IA, Morse JC, Siwik DA, Colucci WS. Lipopolysaccharide and cytokines inhibit rat cardiomyocyte contractility *in vitro*. *J Surg Res*. 2015;193(2):888-901. [CrossRef]
12. Tang F, Zhao XL, Xu LY, Zhang JN, Ao H, Peng C. Endothelial dysfunction: Pathophysiology and therapeutic targets for sepsis-induced multiple organ dysfunction syndrome. *Biomed Pharmacother*. 2024;178:117180. [CrossRef]
13. Hohlfeld T, Klemm P, Thiemermann C, Warner TD, Schrör K, Vane JR. The contribution of tumour necrosis factor-alpha and endothelin-1 to the increase of coronary resistance in hearts from rats treated with endotoxin. *Br J Pharmacol*. 1995;116(8):3309-3315. [CrossRef]
14. Al-Kadi A, Anter AF, Rofaeil RR, Sayed-Ahmed MM, Hafez SMNA, Ahmed AF. Endothelin System Blockade Extenuates Sepsis-Induced Acute Heart and Kidney Injuries via Modulating ET-1/Klotho/p38-MAPK. *Clin Exp Pharmacol Physiol*. 2025;52(6):e70042. [CrossRef]
15. Sventek P, Turgeon A, Schiffrin EL. Vascular endothelin-1 gene expression and effect on blood pressure of chronic ETA endothelin receptor antagonism after nitric oxide synthase inhibition with L-NAME in normal rats. *Circulation*. 1997;95(1):240-244. [CrossRef]
16. Tu J, Shan Q, Jin H, Bourreau JP, Xia Q. Endothelin-1-mediated coronary vasoconstriction deteriorates myocardial depression in hearts isolated from lipopolysaccharide-treated rats: interaction with nitric oxide. *Clin Exp Pharmacol Physiol*. 2004;31(9):571-574. [CrossRef]
17. Wu CC, Chen SJ, Szabó C, Thiemermann C, Vane JR. Aminoguanidine attenuates the delayed circulatory failure and improves survival in rodent models of endotoxic shock. *Br J Pharmacol*. 1995;114(8):1666-1672. [CrossRef]
18. Kavuklu B, Iskit AB, Guc MO, Ilhan M, Sayek I. Aminoguanidine attenuates endotoxin-induced mesenteric vascular hyporeactivity. *Br J Surg*. 2000;87(4):448-453. [CrossRef]

ARCHIVES OF THE TURKISH SOCIETY OF CARDIOLOGY

Official journal of the TURKISH SOCIETY OF CARDIOLOGY

The Efficacy of Sacubitril/Valsartan in the Treatment of Peripartum Cardiomyopathy: A Retrospective Analysis of Four Cases

Peripartum Kardiyomiyopati Tedavisinde Sacubitril/Valsartan'ın Etkinliği: Dört Olgunun Retrospektif Analizi

ABSTRACT

Peripartum cardiomyopathy (PPCM) is a rare form of cardiomyopathy that develops in the last months of pregnancy or during the postpartum period and is characterized by a decrease in left ventricular ejection fraction below 45%. The diagnosis and management of PPCM can be difficult because the symptoms of the disease may be confused with normal pregnancy symptoms. This requires physicians to maintain a high level of clinical suspicion. PPCM can be fatal if not correctly diagnosed and treated. In this case series, we describe the clinical course of four PPCM patients treated with sacubitril/valsartan (S/V) in addition to standard therapy. In these patients, S/V therapy was associated with improvements in left ventricular function. By the end of the first month, all patients demonstrated recovery of ejection fraction above 50% and were classified as New York Heart Association (NYHA) class I. These preliminary observations suggest that S/V may represent a potential treatment option for PPCM, although confirmation in larger studies is required. Although data on the use of S/V in PPCM remain limited, our case series provides preliminary insights that warrant further investigation. The management of PPCM requires a multidisciplinary approach, emphasizing the importance of timely intervention. Our observations indicate that S/V could be considered a possible therapeutic option, but confirmation in larger cohorts is needed.

Keywords: Ejection fraction recovery, peripartum cardiomyopathy, sacubitril/valsartan

ÖZET

Peripartum kardiyomiyopati (PPKM), hamileliğin son aylarında veya doğum sonrası dönemde ortaya çıkan, sol ventrikül ejeksiyon fraksiyonunun %45'in altına düşmesiyle karakterize nadir bir kardiyomiyopati türüdür. PPKM'nin tanısı ve yönetimi, hastalığın belirtilerinin normal gebelik semptomlarıyla karışabilmesi nedeniyle zor olabilir. Bu durum, doktorların yüksek bir klinik şüphe düzeyiyle hareket etmesini gerektirir. PPKM, doğru tanı konmadığında ve tedavi edilmediğinde ölümcül olabilir. Bu olgu serisinde, sacubitril/valsartan (S/V) tedavisi uygulanan dört PPKM hastası retrospektif olarak değerlendirilmiştir. Dört hastanın tamamında takip sürecinde sol ventrikül fonksiyonlarında düzelme izlenmiştir. Birinci ayın sonunda, tüm hastalarda ejeksiyon fraksiyonunun %50'nin üzerine çıktığı ve fonksiyonel kapasitenin NYHA sınıf I düzeyine geldiği kaydedilmiştir. Bu gözlemler, S/V'nin PPKM tedavisinde potansiyel bir seçenek olabileceğini düşündürmektedir. PPKM tedavisinde S/V'nin kullanımıyla ilgili literatürde sınırlı sayıda çalışma olmasına rağmen, bu gözlemler ön veriler olarak değerlendirilmeli ve daha geniş serilerde doğrulanmalıdır. PPKM'nin yönetimi, multidisipliner bir yaklaşım gerektirir, vaka serimiz zamanında müdahalenin önemini vurgularken, S/V'nin potansiyel bir tedavi seçeneği olabileceğini ortaya koymaktadır.

Anahtar Kelimeler: Ejeksiyon fraksiyonunun düzelmesi, peripartum kardiyomiyopati, sacubitril/valsartan

CASE REPORT
OLGU SUNUMU

Seçkin Dereli
Osman Eren Kır
Fatma Demirci

Department of Cardiology, Ordu University Faculty of Medicine, Ordu, Türkiye

Corresponding author:
Seçkin Dereli
✉ drseckindereli@gmail.com

Received: September 14, 2024
Accepted: October 21, 2025

Cite this article as: Dereli S, Kır OE, Demirci F. The Efficacy of Sacubitril/Valsartan in the Treatment of Peripartum Cardiomyopathy: A Retrospective Analysis of Four Cases. *Turk Kardiyol Dern Ars.* 2026;54(6):519–523.

DOI: 10.5543/tkda.2025.33506

Peripartum cardiomyopathy (PPCM) is an idiopathic cardiomyopathy characterized by left ventricular ejection fraction (LVEF) < 45%, occurring in late pregnancy or early postpartum in women without prior heart disease.[1-3] Despite its rarity, PPCM can cause significant morbidity and mortality, with Turkish cohorts reporting 15–30% mortality during follow-up.[4] The etiology is multifactorial, including genetic predisposition, myocarditis, oxidative stress, and abnormal prolactin cleavage.[5,6]

Risk factors include advanced maternal age, multiparity, pre-eclampsia, multiple pregnancy, and hypertension.[6] Early diagnosis using echocardiography and natriuretic peptides is crucial, as outcomes are strongly influenced by baseline left ventricular (LV) size and function.[7,8] Bromocriptine has been discussed as a potential adjunct but is not routinely recommended.[9] Sacubitril/valsartan (S/V) improves survival in patients with heart failure with reduced ejection fraction (HFrEF), but evidence in PPCM is limited to small reports.[10]

The objective of this case series is to describe the early clinical course of four PPCM patients treated with sacubitril/valsartan in addition to guideline-directed therapy and to provide hypothesis-generating observations on recovery trajectories.

Case Report

Baseline Characteristics and Clinical Presentation

This case series included four women aged 25 to 33 years, diagnosed with PPCM in the postpartum period between 2017 and 2023. Two patients were primigravidae, and two were multiparous (Table 1). Two patients had a history of pre-eclampsia, and one had pre-existing hypertension (Table 2). All patients presented with symptoms of severe heart failure, including orthopnea and findings consistent with hypervolemia. At admission, three patients were classified as New York Heart Association (NYHA) Functional Class III, while one patient presented in cardiogenic shock and was classified as NYHA Class IV (Table 3).

Diagnostic Evaluation

The diagnosis of PPCM was established according to European Society of Cardiology (ESC) criteria, with echocardiography confirming an LVEF below 45% and elevated N-terminal pro–B-type natriuretic peptide (NT-proBNP) levels in all patients (Table 4). A comprehensive differential diagnosis was performed to exclude other causes of cardiomyopathy. Myocarditis was ruled out based on clinical presentation and cardiac magnetic resonance imaging (MRI) findings. Cardiac MRI was performed after improvement in LVEF because of scheduling constraints and limited early MRI availability at our center. As acknowledged in the Limitations section, the delayed timing of MRI represents a limitation of our retrospective case series. Other conditions, such as idiopathic or familial dilated cardiomyopathy, Takotsubo syndrome, pregnancy-associated myocardial infarction, pulmonary embolism, and Human Immunodeficiency Virus-associated cardiomyopathy, were excluded through detailed medical histories, clinical assessment, and imaging (Table 3). Genetic testing was not performed.

Treatment and In-Hospital Course

Following hemodynamic stabilization (systolic blood pressure [SBP] ≥ 100 mmHg or mean arterial pressure [MAP] ≥ 65 mmHg without intravenous vasoactive agents, heart rate [HR] < 100 bpm, peripheral capillary oxygen saturation [SpO_2] ≥ 94% on room air), all patients were initiated on S/V. Standard heart failure therapies, including beta-blockers and mineralocorticoid receptor antagonists (MRAs), were administered to all patients (Table 1). In accordance with updated guidelines (2021 European Society of Cardiology Heart Failure [ESC HF] and 2022 American Heart Association/American College of Cardiology/Heart Failure Society of America Heart Failure [AHA/ACC/HFSA HF]),[11,12] a sodium–glucose co-transporter-2 inhibitor (SGLT2i) was added to the treatment regimen of the fourth case, who was diagnosed in 2023. The patient presenting with cardiogenic shock required positive inotropic therapy and non-invasive respiratory support. This patient also developed atrial fibrillation on the third day of hospitalization, which was successfully converted to sinus rhythm with medical therapy. The duration of hospitalization ranged from four to seven days (Table 5).

Follow-up and Outcomes

Patients demonstrated rapid clinical and functional improvement. NT-proBNP levels decreased significantly

ABBREVIATIONS

ACC	American College of Cardiology
AHA	American Heart Association
ESC	European Society of Cardiology
HF	Heart Failure
HFrEF	Heart failure with reduced ejection fraction
HFSA	Heart Failure Society of America
LVEF	Left ventricular ejection fraction
MRA	Mineralocorticoid receptor antagonist
MRI	Magnetic resonance imaging
NT-proBNP	N-terminal pro–B-type natriuretic peptide
NYHA	New York Heart Association
PPCM	Peripartum cardiomyopathy
S/V	Sacubitril/valsartan
SGLT2i	Sodium–glucose co-transporter-2 inhibitor

Table 1. Demographic characteristics and medication usage of patients

	Case 1	Case 2	Case 3	Case 4
Age (years)	25	29	26	33
Number of pregnancies	2	1	2	1
Primigravida	–	+	–	+
Multiple pregnancy	–	–	–	+
Cesarean birth	–	–	+	+
Sacubitril/valsartan (S/V)	+	+	+	+
Beta-blocker	+	+	+	+
MRA	+	+	+	+
SGLT2i	–	–	–	+
Ivabradine	–	–	–	+

MRA, Mineralocorticoid receptor antagonist; SGLT2i, Sodium-glucose cotransporter-2 inhibitor.

Table 2. Maternal and pregnancy characteristics

	Case 1	Case 2	Case 3	Case 4
Admission time (postpartum)	20	5	10	5
Gestation period (weeks)	36	38	38	39
Preeclampsia	–	–	+	+
HT	–	+	–	–

HT, Hypertension.

Table 3. Hemodynamic and echocardiographic parameters

	Case 1	Case 2	Case 3	Case 4
Saturation, %	95%	93%	92%	78%
Systolic blood pressure, mmHg	110	100	120	80
Diastolic blood pressure, mmHg	65	70	75	55
Heart rate, bpm	105	110	120	110
NYHA class	3	3	3	4
Inotropic support required	–	–	–	+
Respiratory support required	–	–	–	+
LVEF, %	30	25	25	20
LVEDD, mm	58	55	54	60
LVESD, mm	44	42	41	46

LVEDD, Left ventricular end-diastolic diameter; LVEF, Left ventricular ejection fraction; LVESD, Left ventricular end-systolic diameter; NYHA, New York Heart Association.

Table 4. Laboratory parameters

	Case 1	Case 2	Case 3	Case 4
Creatinine, mg/dL	0.65	0.58	0.78	0.80
Sodium, mmol/L	141	138	140	135
Potassium, mmol/L	4.1	4.8	4.4	3.9
NT-proBNP, pg/mL	10,000	7,000	5,500	12,000
hs-cTnI, ng/L	5	7	10	70
Hemoglobin, g/dL	11	11.4	11.0	10.5
Platelet count, ×10³/μL	132,000	111,000	180,500	162,300
CRP, mg/L	0.3	0.6	0.4	1.4

CRP, C-reactive protein; NT-proBNP, N-terminal pro-B-type natriuretic peptide.

Table 5. Comparison of prognostic parameters over time

	Case 1	Case 2	Case 3	Case 4
NT-proBNP, pg/mL				
1st week	3,000	7,000	5,500	12,000
2nd week	800	650	900	1,200
1st month	100	80	100	90
hs-cTnI, ng/L				
1st week	5	7	10	25
2nd week	10	5	7	15
1st month	10	8	12	12
NYHA class				
1st week	2	2	3	3
2nd week	2	2	2	2
1st month	1	1	1	1
LVEDD, mm				
1st week	58	55	54	60
2nd week	50	52	48	52
1st month	44	45	42	46
LVEF, %				
1st week	35	25	35	25
2nd week	45	40	55	40
1st month	55	50	60	50
Number of hospitalization days	4	4	5	7

LVEDD, Left ventricular end-diastolic diameter; LVEF, Left ventricular ejection fraction; NT-proBNP, N-terminal pro-B-type natriuretic peptide; NYHA, New York Heart Association.

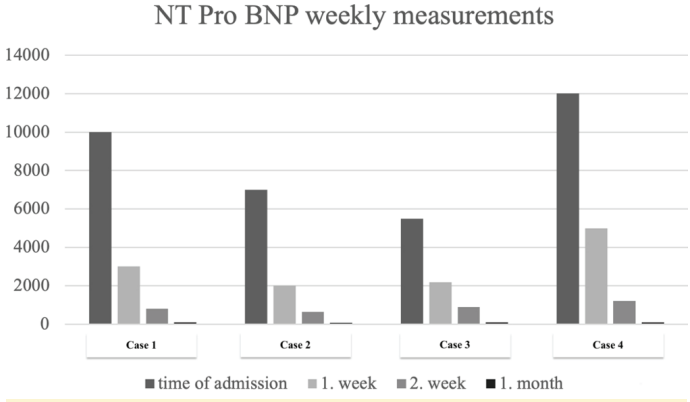

Figure 1. Trajectory of N-terminal pro-B-type natriuretic peptide (NT-proBNP) levels from admission to the first month.

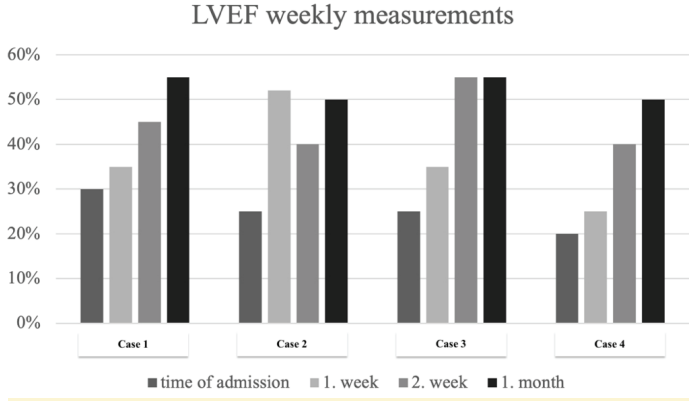

Figure 2. Functional improvement from admission to the first month.

from the first week and normalized in all patients by the first month (Table 5, Figure 1). Descriptively, median LVEF increased from 25.0% at baseline to 52.5% at one month (+27.5 percentage points), median left ventricular end-diastolic diameter decreased from 56.5 mm to 44.5 mm (–12.0 mm), and median NT-proBNP fell from 8,500 pg/mL (interquartile range [IQR]: 6,625–10,500) to 95 pg/mL (IQR: 87.5–100), representing an approximate 99% reduction (Table 5). Concurrently, all patients reported symptomatic improvement and were classified as NYHA class I within the first month (Table 5, Figure 2). During follow-up, no malignant ventricular arrhythmias were observed. One patient had ventricular extrasystoles, but the burden was less than 1% on 24-hour Holter monitoring. All patients tolerated S/V well and completed a 12-month treatment course without any significant adverse events.

Discussion

Peripartum cardiomyopathy is a rare but serious cardiomyopathy with heterogeneous trajectories despite guideline-directed therapy. Our case series describes four women who, in addition to standard heart failure management, received S/V and experienced rapid functional and echocardiographic recovery. Although conclusions are limited by the small sample size and the potential for spontaneous recovery, these observations are noteworthy and hypothesis-generating.[13]

Although bromocriptine has been proposed as an adjunct therapy in PPCM based on mechanistic and limited clinical data, it was not used in our patients due to the absence of robust randomized evidence and safety considerations. Current guidelines emphasize optimization of conventional therapy.[14] Bromocriptine may be considered selectively in patients with severe disease or poor recovery, but larger trials are needed to clarify its role.

Breastfeeding, despite its benefits, poses challenges in PPCM management. The World Health Organization strongly recommends breastfeeding; however, in PPCM patients with NYHA Class III or IV, it is discouraged due to the increased metabolic demands.[15] After being informed about their condition and breastfeeding recommendations, our patients chose to forgo breastfeeding to prioritize optimal medical treatment. For women with severe heart failure, preventing lactation can enhance the efficacy of heart failure medications without posing risks to the infant.

Recovery trajectories in our series appeared faster than those typically reported. Contemporary cohorts and registries—including the ESC EORP registry (European Society of Cardiology EURObservational Research Programme),[8] the 20-year Scottish population study,[16] the Ugandan prospective case–control study,[17] and the multicenter Nigerian cohort[18]—generally report substantial improvements in LVEF and functional status over 3–6 months, with some patients continuing to recover up to 12 months.[19] In contrast, all four of our patients reached an LVEF > 50% and NYHA Class I within one month, and NT-proBNP levels normalized during the same period.

Although such rapid improvement may partially reflect the natural course of PPCM, it is biologically plausible that S/V could contribute to accelerated recovery.[20] Beyond its established benefits in HFrEF, neprilysin inhibition augments natriuretic peptides, leading to improved diuresis, afterload reduction, and reverse remodeling. In PPCM, where maladaptive hemodynamics, neurohormonal activation, and oxidative stress are implicated, early S/V initiation might potentiate rapid unloading and myocardial recovery.[21] Animal models also suggest favorable effects on myocardial fibrosis and remodeling, which could translate to clinical benefit. Nevertheless, causality cannot be inferred from our small, uncontrolled series.

This report is limited by the absence of a control group, the small sample size, delayed MRI timing, and the lack of genetic testing. Accordingly, our findings should be interpreted with caution. However, these cases highlight the need for larger prospective studies and registries evaluating the role of S/V in PPCM. If confirmed, early initiation of S/V may represent a promising adjunct to standard therapy in this high-risk population.

All four cases tolerated S/V well, with no unexpected adverse events. ESC recommends continuing treatment for 12 months post-recovery. We completed the 12-month treatment course, underscoring S/V therapy as a promising approach for managing heart failure in PPCM patients. While S/V may be a potentially life-saving treatment, more data on its safety and efficacy in larger populations are necessary. The broader application of S/V in PPCM treatment hinges on the outcomes of future large-scale clinical trials.

Ethics Committee Approval: Ethics committee approval was obtained from Ordu University Clinical Research Ethics Board (Approval Number: 33, Date: 19.07.2024).

Informed Consent: Patients were informed about the treatment recommended by the guideline and their consent was obtained.

Conflict of Interest: The authors have no conflicts of interest to declare.

Funding: The authors declared that this study received no financial support.

Use of AI for Writing Assistance: We did not use artificial intelligence (AI) or any assistive technology in the production of this case series.

Author Contributions: Concept – S.D.; Design – S.D.; Supervision – S.D.; Resource – S.D., F.D.; Materials – S.D.; Data Collection and/or Processing – S.D., F.D.; Analysis and/or Interpretation – S.D., O.E.K.; Literature Review – S.D., O.E.K.; Writing – S.D., O.E.K.; Critical Review – S.D.

Peer-review: Externally peer-reviewed.

References

1. Gleicher N. Peripartum Cardiomyopathy. *N Engl J Med*. 2024;390(15):1443. [CrossRef]
2. Ejim EC, Karaye KM, Antia S, Isiguzo GC, Njoku PO. Peripartum cardiomyopathy in low- and middle-income countries. *Best Pract Res Clin Obstet Gynaecol*. 2024;93:102476. [CrossRef]
3. Mbakwem AC, Bauersachs J, Viljoen C, et al.; Peripartum Cardiomyopathy Investigators Group. Electrocardiographic features and their echocardiographic correlates in peripartum cardiomyopathy: results from the ESC EORP PPCM registry. *ESC Heart Fail*. 2021;8(2):879-889. [CrossRef]
4. Akil MA, Bilik MZ, Yildiz A, et al. Peripartum cardiomyopathy in Turkey: Experience of three tertiary centres. *J Obstet Gynaecol*. 2016;36(5):574-580. [CrossRef]
5. Koziol KJ, Aronow WS. Peripartum Cardiomyopathy: Current Understanding of Pathophysiology, Diagnostic Workup, Management, and Outcomes. *Curr Probl Cardiol*. 2023;48(8):101716. [CrossRef]
6. Ganiyu S, Lawal TA, Petrie S. Peripartum Cardiomyopathy; Understanding and Improving Outcomes-A Systematic Review. *J Cardiovasc Dis Res*. 2024;15(6):1106.
7. Carlson S, Schultz J, Ramu B, Davis MB. Peripartum Cardiomyopathy: Risks Diagnosis and Management. *J Multidiscip Healthc*. 2023;16:1249-1258. [CrossRef]
8. Rakisheva A, Sliwa K, Bauersachs J, et al. Multidisciplinary care of peripartum heart failure: A scientific statement of the Heart Failure Association of the ESC. *Eur J Heart Fail*. 2024;26(4):742-753. [CrossRef]
9. Pfeffer TJ, Mueller JH, Haebel L, et al. Cabergoline treatment promotes myocardial recovery in peripartum cardiomyopathy. *ESC Heart Fail*. 2023;10(1):465-477. [CrossRef]
10. Elendu C, Okoye OK. Peripartum cardiomyopathy: A case report of decompensated heart failure in a hypertensive patient. *Medicine (Baltimore)*. 2024;103(13):e37600. [CrossRef]
11. McDonagh TA, Metra M, Adamo M, et al.; ESC Scientific Document Group. 2023 Focused Update of the 2021 ESC Guidelines for the diagnosis and treatment of acute and chronic heart failure. *Eur Heart*

J. 2023;44(37):3627–3639. Erratum in: *Eur Heart J*. 2024;45(1):53. [CrossRef]
12. Heidenreich PA, Bozkurt B, Aguilar D, et al.; ACC/AHA Joint Committee Members. 2022 AHA/ACC/HFSA Guideline for the Management of Heart Failure: A Report of the American College of Cardiology/American Heart Association Joint Committee on Clinical Practice Guidelines. *Circulation*. 2022;145(18):e895–e1032. Erratum in: *Circulation*. 2022;145(18):e1033. Erratum in: *Circulation*. 2022;146(13):e185. Erratum in: *Circulation*. 2023;147(14):e674. [CrossRef]
13. Bala R, Mehta S, Roy VC, Kaur G, de Marvao A. Peripartum cardiomyopathy: A review. *Rev Port Cardiol*. 2023;42(11):917–924. English, Portuguese. [CrossRef]
14. Attachaipanich T, Attachaipanich S, Kaewboot K. Efficacy and safety of bromocriptine in peripartum cardiomyopathy: A systematic review and meta-analysis. *Int J Cardiol*. 2025;427:133105. [CrossRef]
15. Maulaadianovi DI, Almashur FZ. Breastfeeding in peripartum cardiomyopathy mothers: A systematic review. *WJARAI*. 2023;18(3):591–603. [CrossRef]
16. Jackson AM, Macartney M, Brooksbank K, et al. A 20-year population study of peripartum cardiomyopathy. *Eur Heart J*. 2023;44(48):5128–5141. [CrossRef]
17. Nabbaale J, Karen K, Emmy E, Annettee A, Graham G. Clinical presentation, risk factors and six-month outcomes in Ugandan women with peripartum cardiomyopathy: prospective case-control study. *Eur Heart J*. 2024;45(Supplement_1):ehae666.3067. [CrossRef]
18. Karaye KM, Sa'idu H, Balarabe SA, et al.; PEACE Registry Investigators. Clinical Features and Outcomes of Peripartum Cardiomyopathy in Nigeria. *J Am Coll Cardiol*. 2020;76(20):2352–2364. [CrossRef]
19. İnan D, Demirtola Mammadli Aİ. Predictors of ejection fraction recovery and baseline differences in patients with peripartum cardiomyopathy and dilated cardiomyopathy. *Anatolian Curr Med J*. 2024;6(4):286–291. [CrossRef]
20. Basic C, Schaufelberger M. Peripartum cardiomyopathy: the challenge of predicting cardiac function recovery. *Eur Heart J*. 2024;45(16):1440–1442. [CrossRef]
21. McMurray JJ, Packer M, Desai AS, et al.; PARADIGM-HF Committees and Investigators. Dual angiotensin receptor and neprilysin inhibition as an alternative to angiotensin-converting enzyme inhibition in patients with chronic systolic heart failure: rationale for and design of the Prospective comparison of ARNI with ACEI to Determine Impact on Global Mortality and morbidity in Heart Failure trial (PARADIGM-HF). *Eur J Heart Fail*. 2013;15(9):1062–1073. [CrossRef]

ARCHIVES OF THE TURKISH SOCIETY OF CARDIOLOGY

Official journal of the TURKISH SOCIETY OF CARDIOLOGY

Management of a Fully Deployed Coronary Stent Migrated to the Left Main Artery

Sol Ana Koroner Artere Göç Eden Tam Açılmış Koroner Stentin Yönetimi

ABSTRACT

Migration of a coronary stent is an uncommon but potentially dangerous event during percutaneous coronary intervention (PCI), and it is even rarer once the stent has been fully deployed. We describe a 39-year-old man presenting with non-ST elevation myocardial infarction (NSTEMI) who underwent PCI of the left circumflex artery (LCx). After implantation, a drug-eluting stent unexpectedly migrated backward into the left main coronary artery (LMCA). An attempt to capture it with a snare via the femoral approach was unsuccessful. Using a balloon anchoring maneuver, the stent was carefully advanced to the radial artery and fixed in position with an additional stent, preserving arterial flow. PCI of the LCx was then completed with a good angiographic outcome. This case underlines the importance of choosing an appropriate stent size, recognizing predisposing factors such as vessel spasm, and being familiar with different retrieval or management techniques to deal with such rare complications.

Keywords: Coronary stent migration, left main coronary artery, percutaneous coronary intervention, radial artery

ÖZET

Koroner stent göçü, perkütan koroner girişim (PCI) sırasında nadiren görülen ancak potansiyel olarak tehlikeli bir durumdur ve stentin tamamen yerleştirilmesinden (implante edilmesinden) sonra ortaya çıkması ise çok daha enderdir. Bu yazıda, sol sirkumfleks arter (LCx) PCI uygulanan 39 yaşında, ST yükselmesiz miyokard enfarktüsü (NSTEMI) tanılı bir erkek olgu sunulmaktadır. İmplantasyon sonrasında, ilaç salınımlı stentlerden biri beklenmedik şekilde geri kayarak sol ana koroner arter (LMCA) içine göç etmiştir. Femoral yoldan yapılan snare ile yakalama girişimi başarısız olmuştur. Balon ankraj manevrası kullanılarak stent dikkatlice radyal artere ilerletilmiş ve ek bir stent ile bu konumda sabitlenerek damar akımı korunmuştur. Ardından LCx'ye yönelik PCI başarıyla tamamlanmış ve iyi bir anjiyografik sonuç elde edilmiştir. Bu olgu, uygun stent boyutunun seçiminin, damar spazmı gibi predispozan faktörlerin farkında olmanın ve bu tür nadir komplikasyonlarla başa çıkmak için farklı geri alma veya yönetim tekniklerine hâkim olmanın önemini vurgulamaktadır.

Anahtar Kelimeler: Koroner stent göçü, sol ana koroner arter, perkütan koroner girişim, radyal arter

CASE REPORT
OLGU SUNUMU

Enes Çelik[1]
Neryan Özgül Özden[2]
Gürkan İmre[1]
Çağatay Ertan[1]

[1]*Department of Cardiology, Bilecik Şeyh Edebali University, Faculty of Medicine, Bilecik, Türkiye*
[2]*Department of Cardiology, Bilecik Training and Research Hospital, Bilecik, Türkiye*

Corresponding author:
Enes Çelik
✉ enescelikmd@gmail.com

Received: November 07, 2025
Accepted: December 12, 2025

Cite this article as: Çelik E, Özden NÖ, İmre G, Ertan Ç. Management of a Fully Deployed Coronary Stent Migrated to the Left Main Artery. *Turk Kardiyol Dern Ars.* 2026;54(6):524–527.

DOI: 10.5543/tkda.2025.68496

Displacement of a stent implanted in a coronary artery is a rare complication of percutaneous coronary intervention.[1]

Complications related to stent migration in patients presenting with acute coronary syndrome (ACS) can result in serious, potentially life-threatening complications.[2]

A migrated stent can be retrieved using various surgical or percutaneous techniques.[3] In this case report, we describe a patient with ACS in whom a fully deployed coronary stent became dislodged and migrated into the left main coronary artery. By anchoring a balloon distal to the dislodged stent, we were able to guide it along the vasculature to the radial artery, where it was ultimately secured.

Case Report

We evaluated a 39-year-old male patient, an active smoker with no prior comorbidities, who presented to the emergency department with chest pain and was admitted to the catheterization laboratory with a diagnosis of non-ST elevation

myocardial infarction (NSTEMI). Due to persistent chest pain, he was scheduled for early percutaneous intervention and taken to the catheterization laboratory. Diagnostic coronary angiography performed via the right radial route revealed an ulcerated atherosclerotic plaque occluding 70% of the lumen of the left circumflex artery (LCx). The second obtuse marginal (OM2) branch was completely occluded, with no significant stenosis in other vessels. The LCx was considered the culprit lesion, and PCI was planned accordingly.

The diagnostic catheter was exchanged for a 6 Fr left Judkins 4.0 guiding catheter. The LCx was crossed with a floppy guidewire, and the OM2 was then wired with a floppy guidewire. However, the vessel diameter was less than 2 mm, and flow was restored with the wire. After predilatation with a 2.5 × 10 mm non-compliant balloon, a 3.0 × 16 mm drug-eluting stent (DES) (Promus Premier, Boston Scientific, MN, USA) was implanted into the LCx lesion at 14 atm pressure (Figure 1A). Upon withdrawal of the stent balloon, the proximal stent unexpectedly migrated toward the LCx ostium. To address this, a 3.0 × 12 mm drug-eluting stent (DES) (Promus Premier) was implanted distally, overlapping the proximal stent (Figure 1B). Despite this intervention, the proximal stent migrated into the left main coronary artery (LMCA), while the distal stent shifted beneath the lesion (Figure 1C). Initially, removal of the LMCA stent via the femoral approach was attempted. The LMCA was intubated with a second catheter using a 7 Fr left Judkins catheter, but the stent could not be grasped with the snare. To avoid systemic embolism and complications within the LMCA, it was decided to remove the stent via the radial route. A 2.75 × 20 mm semi-compliant balloon (Shunmei Medical, Guangdong, China) was advanced distal to the stent and inflated to 8 atm, compressing the stent between the balloon and the catheter and guiding it to the radial artery (Figure 1D).

ABBREVIATIONS

ACS	Acute coronary syndrome
DES	Drug-eluting stent
LCx	Left circumflex artery
LMCA	Left main coronary artery
NSTEMI	Non-ST elevation myocardial infarction
OM2	Second obtuse marginal
PCI	Percutaneous coronary intervention
TIMI	Thrombolysis in myocardial infarction

However, the deformed stent caused severe radial spasm. Right upper extremity angiography revealed good ulnar artery calibration, and the stent was located at the level of the mid-radial artery (Figure 1E). A 3.0 × 12 mm DES (Promus Premier, Boston Scientific, MN, USA) was introduced adjacent to the existing stent and implanted into the radial artery at 12 atm. Radial artery flow was observed to be preserved (Figure 1F). The LCx procedure was then resumed. A 4.0 × 15 mm DES (Xience Xpedition, Abbott Vascular, Santa Clara, CA, USA) was implanted into the LCx at 14 atm, overlapping the distal stent (Figure 1G). Thrombolysis in myocardial infarction (TIMI) grade 3 flow was achieved in the LCx and OM2 vessels, and the procedure was concluded (Figure 1H, Video 1).

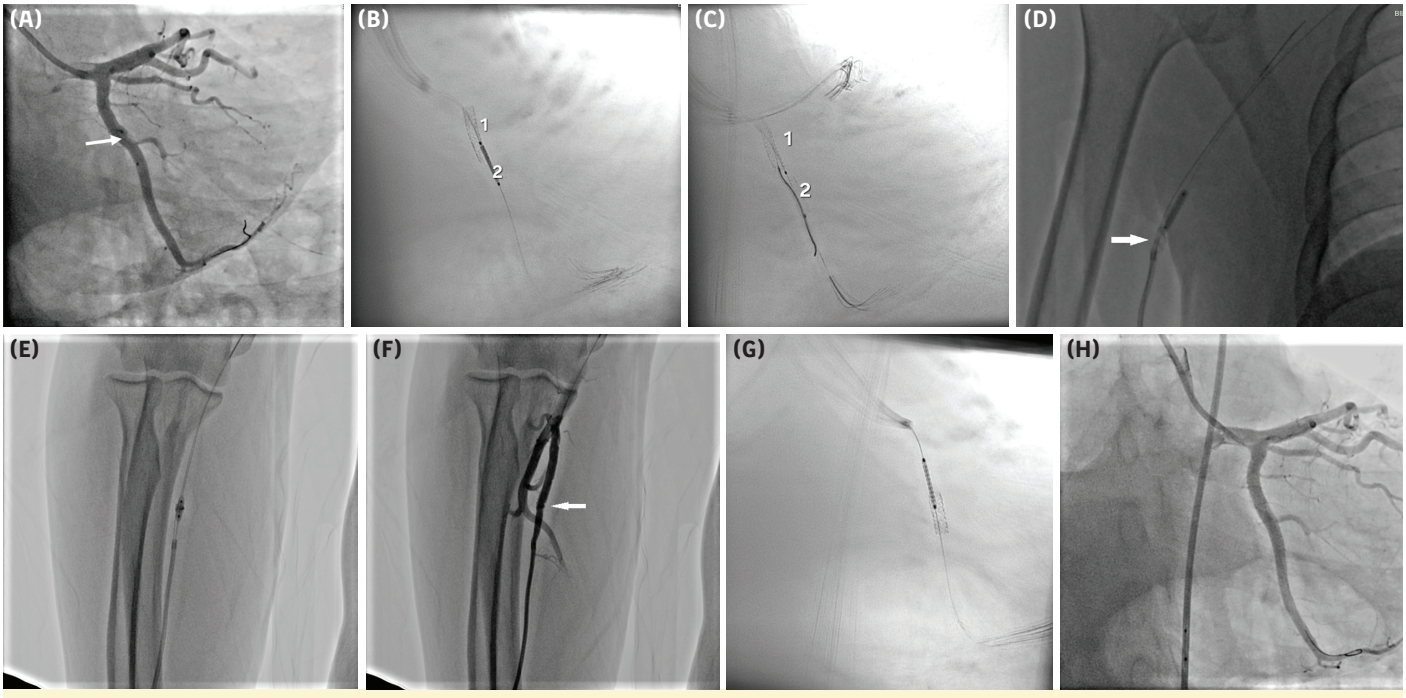

Figure 1. (A) Coronary angiogram showing the left circumflex artery (LCx) lesion. (B) Deployment of a second stent (2) distally to stabilize the first stent (1) using the overlap technique. (C) Proximal migration of the first stent (1) into the left main coronary artery and distal displacement of the second stent (2) below the lesion. (D) Balloon anchoring maneuver for stent retrieval. (E) Localization of the migrated stent in the radial artery. (F) Fixation of the migrated stent in the radial artery. (G) Final stent deployment in the left circumflex artery. (H) Final angiographic result after percutaneous coronary intervention (PCI) completion.

Discussion

Coronary stent migration is a rare complication of percutaneous coronary intervention (PCI), and migration of already deployed stents is even less common.[1,4] Depending on the stent's location, migration can result in serious morbidities, including obstruction, perforation, or dissection of coronary or peripheral arteries, and even death.[2] Stent dislodgement is typically observed in undeployed stents, often occurring during attempts to retrieve the stent within the guide catheter or due to slippage of the delivery system through calcified or tortuous lesions.[5]

There is no standardized approach for managing stent migration, embolization, or separation from delivery balloon systems during PCI; strategies generally depend on operator experience and the equipment available in the laboratory. Common causes of dislodgement include entanglement in side-branch wires, compression of a newly placed stent while passing through a previously deployed stent, and deformation or displacement of the stent during wire manipulation beneath the stent to facilitate lesion passage.[5,6]

In our case, the stent was likely undersized due to initial coronary spasm, which contributed to proximal migration toward the left main coronary artery. A similar scenario was reported by Celik et al.,[7] in which a stent placed in the right coronary artery embolized distally after intracoronary glyceryl trinitrate administration and was subsequently implanted in the branch it migrated into. In our patient, the stent was deployed at nominal pressure, but proximal migration was still observed. Migration can sometimes occur during stent implantation due to deep inspiration or extrasystolic beats.

To manage this, a 3.0 × 12 mm DES was deployed distal to the lesion, overlapping the proximal stent at 16 atm. The balloon was slightly withdrawn and re-inflated at the stent junction. Follow-up imaging revealed that the proximal stent had reached the mid-LMCA, while the distal stent had migrated even further distal to the lesion.

There is no definitive approach for stents that migrate in this manner or slip from the balloon system during lesion advancement. If the stents do not compromise flow, they may be left in place, dilated with a balloon, or, if deformed, crushed and secured with a new stent.[8] In our patient, considering his young age and the relatively small stent size compared to the LMCA diameter, leaving the stent in place was deemed unsafe. Initial attempts to advance the stent from the LMCA to the LCx using a 2.75 × 20 mm semi-compliant balloon were unsuccessful.

Because maneuvers performed in the main coronary artery could cause complications, a 7 Fr catheter was advanced via the femoral route to approach the left main coronary artery. The plan was to cross the stent struts and capture the stent with a microsnare over the wire. However, as the stent had already been fully deployed, it could not be grasped with the snare, and the retrieval attempt via the femoral approach was unsuccessful. To avoid systemic embolization, the stent was withdrawn toward the radial artery using a balloon anchoring technique. Alternative methods, such as twisting wires through the stent or using forceps, may also be considered, though they carry a risk of peripheral embolization.[9,10] Barçın et al.[10] successfully retrieved a stent using a larger sheath from the contralateral femoral artery. Some authors suggest that leaving a stent embolized in a peripheral artery may be acceptable.

In our patient, the deformed stent was ultimately anchored to the radial artery wall with an additional stent. A similar approach was reported by Greathouse et al.,[5] who transferred an extruded LCx stent to the femoral artery using a small-balloon anchoring technique and left it embolized in the right superior gluteal artery. If percutaneous retrieval is unsuccessful, surgical removal remains an option. Cha et al.[11] described two cases in which uninflated, deformed stents that could not be mounted on the guide catheter were surgically removed from the radial artery.

Conclusion

Stent migration is a rare but potentially serious complication of percutaneous coronary intervention. Failure to retrieve a migrated stent lodged in a coronary artery can pose life-threatening risks. This case is notable due to retrograde migration of the stent, likely resulting from undersizing during implantation in the LCx, possibly related to coronary spasm. When the patient's hemodynamic condition allows, stent sizing should ideally be performed after intracoronary glyceryl trinitrate administration. Furthermore, it is essential for interventional cardiologists to be familiar with techniques for managing stent dislocation and for catheterization laboratories to be equipped with the appropriate devices to effectively address such complications.

Ethics Committee Approval: This is a single case report; therefore, ethics committee approval was not required in accordance with institutional policies.

Informed Consent: The patient provided written informed consent for publication of this case.

Conflict of Interest: The authors have no conflicts of interest to declare.

Funding: The authors declare that this study received no financial support.

Use of AI for Writing Assistance: The authors confirm that no artificial intelligence (AI)-based tools were used.

Author Contributions: Concept – E.Ç.; Design – E.Ç., N.Ö.Ö.; Supervision – E.Ç., N.Ö.Ö.; Resource – G.İ., Ç.E.; Materials – Ç.E.; Data Collection and/or Processing – N.Ö.Ö., G.İ.; Analysis and/or Interpretation – E.Ç., N.Ö.Ö.; Literature Review – Ç.E.; Writing – E.Ç.; Critical Review – E.Ç.

Peer-review: Externally peer-reviewed.

Video 1. Angiographic sequence of stent migration and management.

References

1. Chikkabasavaiah NA, Raju SR, Jadav S, Rao SK, Nanjappa MC. Device embolization during trans-radial percutaneous coronary intervention: various approaches - a case series. *IHJ Cardiovasc Case Rep*. 2021;5:134-141. [CrossRef]
2. Alomar ME, Michael TT, Patel VG, et al. Stent loss and retrieval during percutaneous coronary interventions: a systematic review and meta-analysis. *J Invasive Cardiol*. 2013;25(12):637-641.
3. Malik SA, Brilakis ES, Pompili V, Chatzizisis YS. Lost and found: Coronary stent retrieval and review of literature. *Catheter Cardiovasc Interv*. 2018;92(1):50-53. [CrossRef]
4. Brilakis ES, Best PJ, Elesber AA, et al. Incidence, retrieval methods, and outcomes of stent loss during percutaneous coronary intervention: a large single-center experience. *Catheter Cardiovasc Interv*. 2005;66(3):333-340. [CrossRef]
5. Greathouse F, Desai PV, Humayun W, Darki A. A Challenging Case of Stent Dislodgement During Percutaneous Coronary

Intervention Complicated by Peripheral Embolization. *Cureus*. 2023;15(8):e43212. [CrossRef]
6. Kumar J R, G K, Guleria VS, Abbot AK. Percutaneous Extraction of Deployed Coronary Stent During Retrieval of Jailed Buddy Wire. *JACC Case Rep*. 2023;22:101989. [CrossRef]
7. Celik M, Cagdas Yuksel U, Gokoglan Y. Migration of fully deployed stent after intracoronary glyceryl trinitrate administration: An unusual percutaneous coronary intervention complication. *Pak J Med Sci*. 2013;29(3):863-865. [CrossRef]
8. Çetin Şanlıalp S, Tekin I, Şanlıalp M. Dislodgement of the Fully Expanded Stent and the Management of This Complication by Using Crushing Technique. *J Updates Cardiovasc Med*. 2020;8(3):157-162. [CrossRef]
9. Egglin TK, Dickey KW, Rosenblatt M, Pollak JS. Retrieval of intravascular foreign bodies: experience in 32 cases. *AJR Am J Roentgenol*. 1995;164(5):1259-1264. [CrossRef]
10. Barçın C, Yüksel UC, Kabul HK, Yalçınkaya E. Retrieval of embolized coronary stent: combination of various approaches. *Turk Kardiyol Dern Ars*. 2013;41(5):440-444. Turkish. [CrossRef]
11. Cha KS. Surgical retrieval of dislodged stent during transradial coronary intervention. *J Invasive Cardio*l. 2012;24(8):E179-E181.

ARCHIVES OF THE TURKISH SOCIETY OF CARDIOLOGY

Official journal of the TURKISH SOCIETY OF CARDIOLOGY

A Tortuous "Corkscrew" Aortic Arch Mimicking Coarctation: A Diagnostic Pitfall in Multimodality Imaging

Koarktasyonu Taklit Eden Tortiyöz "Tirbuşon" Aort Arkı: Multimodal Görüntülemede Tanısal Bir Tuzak

CASE IMAGE
OLGU GÖRÜNTÜSÜ

A 13-year-old boy was referred with a preliminary diagnosis of aortic coarctation because of intermittent chest pain and exertional fatigue that had persisted for 1 year. Physical examination revealed no significant upper–lower extremity blood pressure gradient, and no continuous murmur was detected. Transthoracic echocardiography demonstrated a left-sided aortic arch with elongation and a pseudocoarctation appearance. Continuous-wave Doppler revealed a peak gradient of 35–40 mmHg without evidence of significant turbulence. However, the suprasternal view was suboptimal, raising uncertainty regarding the arch anatomy.

To further delineate the anatomy, contrast-enhanced computed tomography angiography was performed. It demonstrated a markedly elongated and tortuous aortic arch extending to the cervical level (Figure 1). The arch followed a superior–inferior–superior course, forming a characteristic "corkscrew" configuration (Video 1). No evidence of true coarctation or isthmic hypoplasia was identified.

No dysmorphic features, syndromic characteristics, or additional congenital cardiovascular abnormalities were identified during clinical evaluation. Genetic testing was not performed because there were no clinical findings suggestive of an underlying genetic disorder. Because no hemodynamically significant obstruction was present, no intervention was indicated, and clinical follow-up was planned. Most reported patients without true coarctation are managed conservatively; however, associated vascular abnormalities and aneurysmal dilatation have occasionally been described in the literature. Recognition of this anatomy remains important during long-term follow-up because marked aortic arch tortuosity may create technical challenges during future catheter-based procedures, including coronary angiography and endovascular interventions. Echocardiographic evaluation (Videos 2 and 3) demonstrated an elongated aortic arch without significant flow acceleration or turbulence on color Doppler imaging.

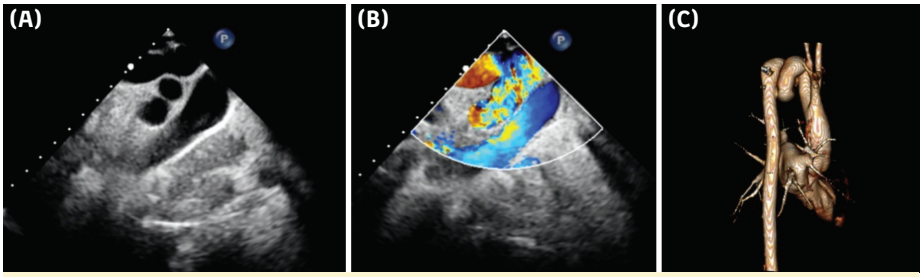

Figure 1. Multimodality imaging of a tortuous "corkscrew" aortic arch mimicking coarctation. (A) Suprasternal transthoracic echocardiographic view demonstrating elongation and tortuosity of the aortic arch. (B) Color Doppler image showing the absence of significant flow acceleration or turbulent flow across the elongated arch. (C) Three-dimensional computed tomography angiography image revealing a markedly elongated and tortuous aortic arch extending to the cervical level, with a characteristic "corkscrew" configuration.

Aslıhan Karaman
Selman Gökalp
Alper Güzeltaş

Department of Pediatric Cardiology, University of Health Sciences, Mehmet Akif Ersoy Thoracic and Cardiovascular Surgery Training and Research Hospital, Istanbul, Türkiye

Corresponding author:
Aslıhan Karaman
✉ aslihankaraman34@gmail.com

Received: June 03, 2026
Accepted: June 09, 2026

Cite this article as: Karaman A, Gökalp S, Güzeltaş A. A Tortuous "Corkscrew" Aortic Arch Mimicking Coarctation: A Diagnostic Pitfall in Multimodality Imaging. *Turk Kardiyol Dern Ars.* 2026;54(6):528–529.

DOI: 10.5543/tkda.2026.29562

Ethics Committee Approval: This is a single case image, and therefore ethics committee approval was not required in accordance with institutional policies.

Informed Consent: Written informed consent for publication of the clinical information and imaging materials was obtained from the patient's legal guardians.

Conflict of Interest: The authors have no conflicts of interest to declare.

Funding: The authors declared that this study received no financial support.

Use of AI for Writing Assistance: Artificial intelligence-assisted language editing tools were used for language improvement and manuscript preparation. All scientific content, interpretation, and final approval of the manuscript were performed by the authors.

Author Contributions: Concept – A.K., A.G.; Design – A.K.; Supervision – A.G.; Resource – A.K., S.G., A.G.; Materials – A.K.; Data Collection and/or Processing – A.K., S.G.; Analysis and/or Interpretation – A.K., S.G.; Literature Review – A.K.; Writing – A.K.; Critical Review – A.G.

Peer-review: Internally peer-reviewed.

Video 1. Three-dimensional computed tomography angiography demonstrating a markedly elongated and tortuous aortic arch with a characteristic "corkscrew" configuration extending to the cervical level.

Video 2. Two-dimensional transthoracic echocardiographic suprasternal view demonstrating elongation of the aortic arch.

Video 3. Color Doppler echocardiographic image showing no significant flow acceleration or turbulence across the aortic arch.

ARCHIVES OF THE
TURKISH SOCIETY
OF CARDIOLOGY

Official journal of the
TURKISH
SOCIETY OF
CARDIOLOGY

Pacemaker Pocket Infection with Generator Migration and Extrusion from the Left Mammary Areola

Bataryanın Kayması ve Sol Meme Areolasından Dışarı Çıkması ile Seyreden Kalp Pili Cebi Enfeksiyonu

CASE IMAGE
OLGU GÖRÜNTÜSÜ

A 70-year-old woman had undergone implantation of a cardiac resynchronization therapy–defibrillator in 2017 for non-ischemic dilated cardiomyopathy (left ventricular ejection fraction 25% and left bundle branch block) and generator replacement in 2023. She presented with progressive pain and drainage at the left mammary areolar region for one month, followed by skin breakdown and extrusion of the device from the areolar region. She had been hospitalized for antibiotic therapy at a private hospital two weeks earlier. Device interrogation revealed normal sensing and pacing parameters, with normal pacing impedances, and device therapies had been set to OFF during the previous hospitalization. Chest X-ray on admission demonstrated a stretched and dislocated atrial lead, while other leads were in place; the generator was located at the level of the left mammary region (Figure 1). Panels B and C show extrusion of the generator through the left mammary areolar region with adherent debris and inflammation. Blood cultures grew Pseudomonas aeruginosa (there were no risk factors other than recent hospitalization). The findings were consistent with cardiac implantable electronic device (CIED) infection complicated by pocket erosion and extrusion of the generator from an unexpected location. The device system was successfully removed using a locking stylet (Lead Locking Device® EZ, Spectranetics Corp, Colorado, USA) and a 13-French mechanical dilator sheath (Tight Rail, Spectranetics Corp, Colorado, USA) without periprocedural complication, and targeted intravenous antibiotic therapy was initiated. The areolar region was primarily sutured (Figure 1). The patient was consulted for reconstruction of the areolar region; however, she refused reconstructive surgery. Breast ultrasonography revealed no damage to the breast tissue or glandular structures. The CIED battery should be carefully secured and fixed to the pectoral muscular tissue, particularly in women with a large amount of subcutaneous fatty tissue. During the replacement procedure, the new CIED battery should be implanted within the previous capsule, and the capsule should be securely closed without disruption of its integrity. If capsule formation has not occurred despite an adequate time interval at the time of battery replacement, operators should create a new, deeper subfascial or submuscular pocket to ensure safe placement of the new battery. Written informed consent was obtained from the patient for publication of this article and the accompanying images.

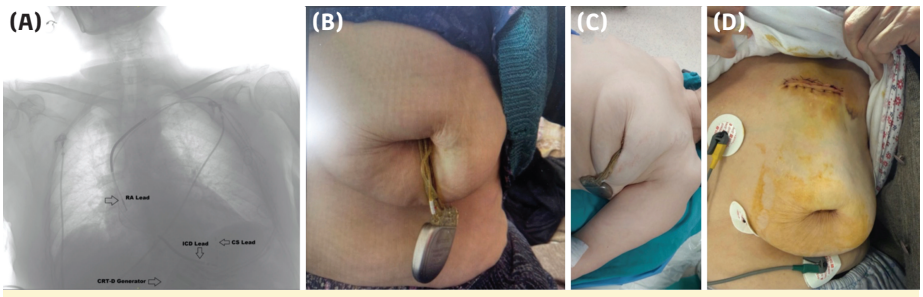

Figure 1. Chest X-ray on admission demonstrated a stretched and dislocated atrial lead; the other leads were in place, and the generator was located at the level of the left mammary (A). Extrusion of the generator through the left mammary areolar region with adherent debris and inflammation (B and C). The left mammary areolar region was primarily sutured (D).

Uğur Canpolat
Ahmet Hakan Ateş

Department of Cardiology, Hacettepe University Faculty of Medicine, Ankara, Türkiye

Corresponding author:
Uğur Canpolat
✉ dru_canpolat@yahoo.com

Received: February 02, 2026
Accepted: March 16, 2026

Cite this article as: Canpolat U, Ateş AH. Pacemaker Pocket Infection with Generator Migration and Extrusion from the Left Mammary Areola. *Turk Kardiyol Dern Ars.* 2026;54(6):530–531.

DOI: 10.5543/tkda.2026.69037

Ethics Committee Approval: This is a single case image, and therefore ethics committee approval was not required in accordance with institutional policies.

Informed Consent: Written informed consent was obtained from the patient for publication of this article and the accompanying images.

Conflict of Interest: The authors have no conflicts of interest to declare.

Funding: The authors declared that this study received no financial support.

Use of AI for Writing Assistance: No use of AI-assisted technologies was declared by the authors.

Author Contributions: Concept – U.C., A.H.A.; Design – U.C., A.H.A.; Supervision – U.C., A.H.A.; Resource – U.C., A.H.A.; Data Collection and/or Processing – U.C., A.H.A.; Analysis and/or Interpretation – U.C., A.H.A.; Literature Review – U.C., A.H.A.; Writing – U.C., A.H.A.; Critical Review – U.C., A.H.A.

Peer-review: Externally peer-reviewed.

ARCHIVES OF THE TURKISH SOCIETY OF CARDIOLOGY

Official journal of the TURKISH SOCIETY OF CARDIOLOGY

Mini-Crush Technique for Iliac Bifurcation Disease

İliak Arter Bifurkasyon Hastalığında Mini-crush Tekniği

CASE IMAGE
OLGU GÖRÜNTÜSÜ

A 63-year-old man with a history of peripheral artery disease underwent peripheral angiography because of bilateral claudication. Peripheral angiography revealed severe bilateral external iliac artery (EIA) disease, total occlusion of the left internal iliac artery (IIA), and critical stenosis of the right IIA (Figure 1A). Initially, the patient underwent stent implantation extending from the left common iliac artery (CIA) to the left EIA. Because of total occlusion of the left IIA, a planned two-stent strategy using the mini-crush technique was selected to preserve perfusion through the right IIA. This approach was considered essential to minimize the risk of pelvic ischemic complications, including buttock claudication, gluteal ischemia, erectile dysfunction, and, in rare cases, colonic or spinal cord ischemia in the event of right IIA loss. Antegrade wiring of the right IIA was successfully performed using a 0.014-inch, 300-cm V-14 ControlWire (Boston Scientific, Massachusetts, USA) (Figure 1B). Retrograde crossing from the right EIA to the aorta was achieved using a 0.035-inch, 260-cm guidewire, which was then advanced into the aorta. A 6 × 19 mm balloon-expandable stent was positioned at the orifice of the right IIA with 1–2 mm protrusion into the CIA (Figure 1C–D). Subsequently, an 8 × 57 mm balloon-expandable stent was implanted in the right EIA. A 9 × 57 mm balloon-expandable stent was then deployed proximally, overlapping with the first stent and extending into the CIA, thereby crushing the protruding IIA stent segment within the CIA (Figure 1E). Proximal optimization technique (POT) was subsequently performed using a 10 × 27 mm balloon inflated to 12–14 atm (Figure 1F). The previously used 6 × 19 mm stent balloon and the 9 × 57 mm stent balloon were repositioned at the IIA ostium. Sequential balloon inflations were performed, followed by simultaneous kissing balloon inflation to achieve optimal configuration (Figure 1G). A final POT procedure was then performed using a 10 × 27 mm balloon. The procedure was completed successfully without complications. Reports describing a systematic two-stent approach for iliac artery bifurcation disease remain limited in the literature. In these complex cases, antegrade access to the side branch (right IIA) and retrograde access to the main vessel should be considered the standard technical approach. This strategy facilitates optimal side-branch stent expansion while reducing the risk of geographic miss at the side-branch ostium. Potential procedural complications include arterial rupture, dissection, abrupt occlusion, thrombus formation, stent migration, and impingement.

Ethics Committee Approval: This is a single case image, and therefore ethics committee approval was not required in accordance with institutional policies.

Informed Consent: Written informed consent was obtained from the patient for publication of this case and the accompanying images.

Conflict of Interest: The authors have no conflicts of interest to declare.

Funding: The authors declared that this study received no financial support.

Use of AI for Writing Assistance: No use of AI-assisted technologies was declared by the authors.

Author Contributions: Concept – A.G., A.Y.Ç., E.A.; Design – A.G., A.Y.Ç., E.A.; Supervision – F.U.; Materials – B.S.; Literature Review – B.S.; Writing – A.G.; Critical Review – F.U.

Peer-review: Internally peer-reviewed.

Ahmet Güner
Ahmet Yaşar Çizgici
Enes Arı
Berkay Serter
Fatih Uzun

Department of Cardiology, İstanbul Mehmet Akif Ersoy Thoracic and Cardiovascular Surgery Training and Research Hospital, İstanbul, Türkiye

Corresponding author:
Berkay Serter
✉ serter34@gmail.com

Received: April 11, 2026
Accepted: May 20, 2026

Cite this article as: Güner A, Çizgici AY, Arı E, Serter B, Uzun F. Mini-Crush Technique for Iliac Bifurcation Disease. *Turk Kardiyol Dern Ars.* 2026;54(6):532-533.

DOI: 10.5543/tkda.2026.26793

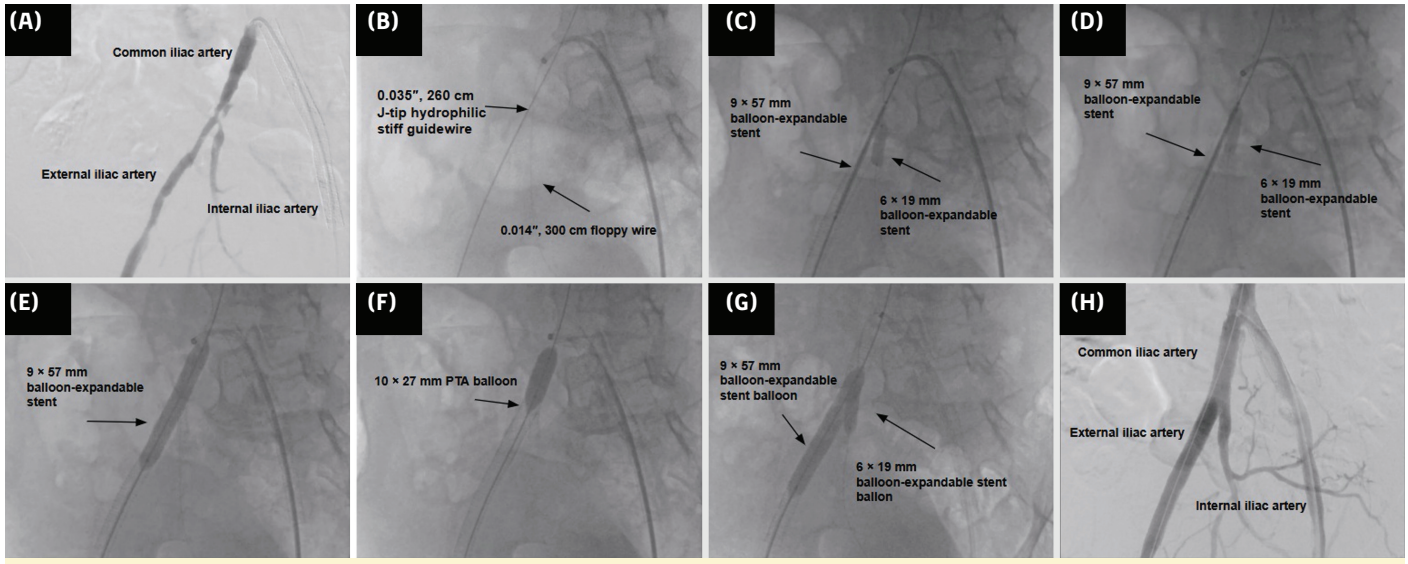

Figure 1. (A) Critical stenosis at the iliac bifurcation segment and internal iliac artery. (B) Wiring of the side branch (internal iliac artery) and main vessel using antegrade and retrograde approaches, respectively. (C) Stent implantation into the internal iliac artery with 1–2 mm protrusion into the common iliac artery. (D) Proximal side-branch optimization. (E) Main vessel (common iliac artery) stent implantation with crushing of the side-branch (internal iliac artery) stent. (F) First proximal optimization technique. (G) Kissing balloon inflation. (H) Final angiographic result after the final proximal optimization technique.

ARCHIVES OF THE
TURKISH SOCIETY
OF CARDIOLOGY

Official journal of the
TURKISH
SOCIETY OF
CARDIOLOGY

Letter to the Editor: Stress Hyperglycemia Ratio is Associated with Intracardiac Thrombus in Acute Ischemic Stroke

Editöre Mektup: Akut İskemik İnmede Stres Hiperglisemi Oranı ile İntrakardiyak Trombüs Arasındaki İlişki

LETTER TO THE EDITOR
EDİTÖRE MEKTUP

To the Editor,

I read with great interest the article by Cicek et al.[1] entitled "Stress Hyperglycemia Ratio Is Associated with Intracardiac Thrombus in Acute Ischemic Stroke." The authors are to be commended for addressing a clinically important challenge in acute ischemic stroke: identifying occult intracardiac thrombus in patients with otherwise unremarkable transthoracic echocardiographic findings. In a cohort of patients with acute ischemic stroke and negative transthoracic echocardiographic (TTE) findings, they demonstrated that the stress hyperglycemia ratio (SHR) was independently associated with intracardiac thrombus detected by transesophageal echocardiography (TEE). Their findings suggest that SHR may serve as a practical and readily available biomarker for identifying patients who may benefit from further cardioembolic evaluation.

The study is particularly valuable because it addresses a common clinical dilemma: selecting patients for TEE despite unremarkable transthoracic imaging findings. Because TEE is semi-invasive and not routinely performed in every patient with ischemic stroke, identifying simple biomarkers that may improve patient selection is of considerable clinical importance. However, I would like to offer an additional perspective on the interpretation of the association between SHR and intracardiac thrombus. Stress hyperglycemia is increasingly recognized as a marker of systemic inflammatory activation, sympathetic overactivity, and acute physiological stress.[2] Therefore, elevated SHR may not solely reflect a prothrombotic state but may also represent the magnitude of the inflammatory and neuroendocrine response.[3] In the present study, C-reactive protein levels were also independently associated with intracardiac thrombus, supporting the possibility that inflammation may play a central role in the observed relationship.

Another noteworthy observation is the remarkably high prevalence of paroxysmal atrial fibrillation among patients with intracardiac thrombus. Contemporary evidence suggests that thromboembolic risk is influenced not only by the presence of atrial fibrillation but also by atrial remodeling, atrial cardiomyopathy, and overall atrial fibrillation burden.[4,5] Consequently, the association between SHR and intracardiac thrombus may partially reflect a more advanced atrial disease substrate rather than a direct effect of stress hyperglycemia itself. Future studies incorporating prolonged rhythm monitoring, left atrial functional assessment, and markers of atrial cardiopathy may provide additional mechanistic insights.

Furthermore, because both inflammatory and metabolic pathways appear to contribute to thrombus formation, it would be interesting to investigate whether combining SHR with inflammatory markers could improve risk stratification beyond either parameter alone. Such an integrated approach may better identify patients who are most likely to harbor occult cardioembolic sources and, therefore, derive greater benefit from TEE evaluation.

I congratulate the authors for their valuable contribution to the literature. Their findings provide an important foundation for future investigations exploring the complex interplay among metabolic stress, inflammation, atrial remodeling, and thromboembolic risk in patients with acute ischemic stroke.

Tuğba Çetin

Department of Cardiology, Tekirdağ Çorlu State Hospital, Tekirdağ, Türkiye

Corresponding author:
Tuğba Çetin
✉ drtugbacetin@gmail.com

Received: July 05, 2026
Accepted: July 06, 2026

Cite this article as: Çetin T. Letter to the Editor: Stress Hyperglycemia Ratio is Associated with Intracardiac Thrombus in Acute Ischemic Stroke. *Turk Kardiyol Dern Ars.* 2026;54(6):534-535.

DOI: 10.5543/tkda.2026.79395

Conflict of Interest: The author have no conflicts of interest to declare.

Funding: The author declared that this study received no financial support.

References

1. Cicek V, Erdem A, Kozan Çıkırıkçı EH, et al. Stress Hyperglycemia Ratio Is Associated with Intracardiac Thrombus in Acute Ischemic Stroke. *Turk Kardiyol Dern Ars*. 2026;54(5):395–402. [CrossRef]
2. Ömür SE, Zorlu Ç, Yılmaz M. Comparison of the Relationship Between Inflammatory Markers and Atrial Fibrillation Burden. *Anatol J Cardiol*. 2023;27(8):486–493. [CrossRef]
3. Roberts GW, Quinn SJ, Valentine N, et al. Relative Hyperglycemia, a Marker of Critical Illness: Introducing the Stress Hyperglycemia Ratio. *J Clin Endocrinol Metab*. 2015;100(12):4490–4497. [CrossRef]
4. Martignani C, Spadotto A, Carelli M, et al. Atrial Cardiomyopathy: A "Distinct Clinical Entity" for a Deeper Understanding of Atrial Fibrillation and Cardioembolic Stroke. *J Clin Med*. 2025;14(23):8363. [CrossRef]
5. Goette A, Lendeckel U. Atrial Cardiomyopathy: Pathophysiology and Clinical Consequences. *Cells*. 2021;10(10):2605. [CrossRef]

ARCHIVES OF THE TURKISH SOCIETY OF CARDIOLOGY

Official journal of the TURKISH SOCIETY OF CARDIOLOGY

Reply to the Letter to the Editor: "Stress Hyperglycemia Ratio is Associated with Intracardiac Thrombus in Acute Ischemic Stroke"

Editöre Mektup Yanıtı: Akut İskemik İnmede Stres Hiperglisemi Oranı ile İntrakardiyak Trombüs Arasındaki İlişki

LETTER TO THE EDITOR REPLY
EDİTÖRE MEKTUP YANITI

Vedat Çiçek[1,2]
Almina Erdem[3]
Ezgi Hasret Kozan Çıkırıkçı[4]
İrem Yılmaz[3]
Elif Günhan[3]
Emrecan Uygun[3]
Salih Karaismail[5]
Mehmet Uzun[3]
Mert İlker Hayıroğlu[6]
Ahmet Lütfullah Orhan[3]
Tufan Çınar[7]

[1]Department of Radiology, Machine & Hybrid Intelligence Lab, Northwestern University, Chicago, IL, United States
[2]Tatvan State Hospital, Bitlis, Türkiye
[3]Department of Cardiology, Sultan II. Abdulhamid Han Training and Research Hospital, Health Sciences University, İstanbul, Türkiye
[4]Department of Public Health Nursing, Koç University School of Nursing, İstanbul, Türkiye
[5]Department of Neurology, Sultan II. Abdulhamid Han Training and Research Hospital, Health Sciences University, İstanbul, Türkiye
[6]Department of Cardiology, Dr. Siyami Ersek Cardiovascular and Thoracic Surgery Research and Training Hospital, İstanbul, Türkiye
[7]School of Medicine, University of Maryland, Baltimore, USA

Corresponding author:
Vedat Çiçek
✉ vedatacicek@gmail.com

Cite this article as: Çiçek V, Erdem A, Kozan Çıkırıkçı EH, et al. Reply to the Letter to the Editor: "Stress Hyperglycemia Ratio is Associated with Intracardiac Thrombus in Acute Ischemic Stroke". *Turk Kardiyol Dern Ars.* 2026;54(6):536–537.

DOI: 10.5543/tkda.2026.67374

To the Editor,

The correspondence raises three important points regarding the biological mechanisms and methodology underlying intracardiac thrombus formation in acute ischemic stroke (AIS). We address each point in turn.[1]

Stress Hyperglycemia as an Integrated Metabolic–Inflammatory Signal

The stress hyperglycemia ratio (SHR) is not solely a prothrombotic index. Relative hyperglycemia during acute illness reflects a broader neuroendocrine and inflammatory response, including catecholamine and cortisol surges, insulin resistance, and cytokine activation.[2,3] This is one reason why SHR may serve as a useful biomarker: it integrates multiple converging pathways rather than isolating a single mechanism. However, the data indicate that this integrative signal is not fully captured by systemic inflammation alone. In the same multivariable model, C-reactive protein (CRP) and SHR each retained an independent association with intracardiac thrombus.[4] (Adjusted odds ratio [OR] for SHR, 2.39; 95% CI, 1.11–5.17; P = 0.027; adjusted OR for CRP, 1.015; 95% CI, 1.009–1.021; P < 0.001.) Their retention after mutual adjustment indicates that metabolic stress and inflammation act as partially independent, complementary contributors to thrombogenesis rather than one serving as a proxy for the other. This finding is mechanistically coherent: acute dysglycemia promotes endothelial dysfunction through oxidative stress and reduced nitric oxide bioavailability, enhances platelet activation and tissue factor–mediated coagulation, and impairs fibrinolysis by increasing plasminogen activator inhibitor-1 levels.[5]

The Atrial Substrate and Atrial Cardiomyopathy

The high prevalence of paroxysmal atrial fibrillation (PAF) among patients with intracardiac thrombus suggests the presence of an advanced atrial substrate.[4] Contemporary evidence increasingly conceptualizes thromboembolic risk as a property of the atrial myocardium itself—the concept of atrial cardiomyopathy—rather than as a binary consequence of atrial fibrillation. A thrombogenic atrial substrate, characterized by structural, architectural, contractile, and electrophysiological remodeling, can give rise to atrial thromboembolism even in the absence of documented arrhythmia and confers risk in proportion to the degree of remodeling, fibrosis, and arrhythmia burden.[6–8] Part of the observed association between SHR and intracardiac thrombus may therefore reflect more advanced atrial disease. Two aspects of the analysis support this interpretation. First, all patients were in sinus rhythm at admission and underwent 24–72-hour Holter monitoring, and PAF was included in the multivariable model; SHR remained independently associated with intracardiac thrombus after adjustment for PAF.[4] Second, patients with intracardiac thrombus had a larger left atrial anteroposterior diameter than those without thrombus (44.1 vs. 42.6 mm, P = 0.009), a crude marker of atrial remodeling.[9] However, dedicated measures of atrial cardiomyopathy, such as left atrial strain, atrial fibrosis imaging, P-wave indices, natriuretic peptide levels, and quantified atrial fibrillation burden obtained through prolonged rhythm monitoring, were not available. Therefore, residual

confounding related to the atrial substrate cannot be excluded. Prospective studies incorporating these markers will be required to disentangle the respective contributions of metabolic stress and structural atrial remodeling.

Toward an Integrated, Multi-Marker Risk Model

Combining SHR with inflammatory markers may improve risk stratification beyond that achieved with any single parameter. A model integrating a metabolic stress axis (SHR), an inflammatory axis (CRP), and an atrial cardiomyopathy axis (left atrial strain, natriuretic peptide levels, and P-wave abnormalities) is biologically plausible and may more accurately identify patients with occult cardioembolic sources who are most likely to benefit from transesophageal echocardiography. The development of such a model in the present study was limited by its single-center, retrospective design, the modest number of outcome events (64 thrombi), and the fact that the SHR cutoff value was derived from the study cohort without external validation.[4] Adequately powered, prospective, multicenter studies with external validation are needed to determine whether an integrated biomarker panel provides superior predictive performance compared with SHR alone.

In summary, metabolic stress, systemic inflammation, and atrial remodeling represent interrelated yet partially independent contributors to cardioembolic risk. These considerations do not diminish the value of SHR as a simple, inexpensive, and widely available biomarker. Rather, they provide a rationale for prospective, mechanistically informed validation and the eventual integration of SHR into a broader risk-stratification strategy for acute ischemic stroke.

References

1. Çetin T. Letter to the Editor: Stress Hyperglycemia Ratio is Associated with Intracardiac Thrombus in Acute Ischemic Stroke. *Turk Kardiyol Dern Ars*. 2026;54(6):534–535.
2. Roberts GW, Quinn SJ, Valentine N, et al. Relative Hyperglycemia, a Marker of Critical Illness: Introducing the Stress Hyperglycemia Ratio. *J Clin Endocrinol Metab*. 2015;100(12):4490–4497. [CrossRef]
3. Capes SE, Hunt D, Malmberg K, Gerstein HC. Stress hyperglycaemia and increased risk of death after myocardial infarction in patients with and without diabetes: a systematic overview. *Lancet*. 2000;355(9206):773–778. [CrossRef]
4. Cicek V, Erdem A, Kozan Çıkırıkçı EH, et al. Stress Hyperglycemia Ratio Is Associated with Intracardiac Thrombus in Acute Ischemic Stroke. *Turk Kardiyol Dern Ars*. 2026;54(5):395–402. [CrossRef]
5. Huang Y, Yue L, Qiu J, Gao M, Liu S, Wang J. Endothelial Dysfunction and Platelet Hyperactivation in Diabetic Complications Induced by Glycemic Variability. *Horm Metab Res*. 2022;54(7):419–428. [CrossRef]
6. Kamel H, Healey JS. Cardioembolic Stroke. *Circ Res*. 2017;120(3):514–526. [CrossRef]
7. Goette A, Kalman JM, Aguinaga L, et al.; Document Reviewers: EHRA/HRS/APHRS/SOLAECE expert consensus on atrial cardiomyopathies: definition, characterization, and clinical implication. *Europace*. 2016;18(10):1455–1490. [CrossRef]
8. Goette A, Corradi D, Dobrev D, et al. Atrial cardiomyopathy revisited–evolution of a concept: a clinical consensus statement of the European Heart Rhythm Association (EHRA) of the ESC, the Heart Rhythm Society (HRS), the Asian Pacific Heart Rhythm Society (APHRS), and the Latin American Heart Rhythm Society (LAHRS). *Europace*. 2024;26(9):euae204. Erratum in: *Europace*. 2025;27(10):euaf248. [CrossRef]
9. Tang R, Dong J, Shang M, et al. Impact of left atrium size on left atrial thrombus in patients with non-valvular persistent atrial fibrillation. *Zhonghua Yi Xue Za Zhi*. 2015;95(14):1083–1087.

ARCHIVES OF THE TURKISH SOCIETY OF CARDIOLOGY

Official journal of the TURKISH SOCIETY OF CARDIOLOGY

NOS3 T-786C: Methodological Considerations

NOS3 T-786C: Metodolojik Hususlar

LETTER TO THE EDITOR
EDİTÖRE MEKTUP

To the Editor,

We read with great interest the article by Zakirova et al.,[1] which reports an association between the NOS3 T-786C polymorphism and renal dysfunction in patients with CHF from Uzbekistan. It is a valuable contribution to the literature on an understudied population. However, we believe that three issues merit attention.

First, the 35.8% decrease in NO concentration among patients with an eGFR < 60 mL/min/1.73 m^2 was attributed to reduced NOS3 activity, despite the absence of statistically significant genotype differences between the groups (P = 0.1–0.4). Levels of ADMA and SDMA—the former being a well-established endogenous eNOS inhibitor that is elevated in uremia—were not evaluated.[2] Controlling for these potential confounders would have strengthened the credibility of the proposed association between genotype and NO levels.

Second, 200 patients with CHF (90 with an eGFR < 60 mL/min/1.73 m^2) and 120 controls were enrolled without any reported sample size calculation. The required sample size should depend on the allele frequency and the expected effect size.[3] The absence of these considerations makes the adequacy of the sample size questionable.

Finally, throughout the manuscript, non-significant results (P = 0.1–0.4) are repeatedly described as indicative of a "trend" or a "possible role" of the C allele. The inability to reject the null hypothesis does not demonstrate an association.[4] Moreover, the 95% confidence interval for the odds ratio (0.98–1.97) includes 1, indicating that the data are also compatible with the absence of a true effect.[5]

None of these points diminishes the value of the study. Addressing them in future work would strengthen confidence in the role of the NOS3 T-786C polymorphism in cardiorenal dysfunction.

Conflict of Interest: The authors have no conflicts of interest to declare.

Funding: The authors declared that this study received no financial support.

References

1. Zakirova G, Masharipova D, Boboev Q, Tagaeva D. T-786C Polymorphism of the NOS3 Gene and Its Role in the Development of Renal Dysfunction in Patients of the Uzbek Population with Chronic Heart Failure. *Turk Kardiyol Dern Ars*. 2026;54(4):310-315. [CrossRef]
2. Liu X, Xu X, Shang R, Chen Y. Asymmetric dimethylarginine (ADMA) as an important risk factor for the increased cardiovascular diseases and heart failure in chronic kidney disease. *Nitric Oxide*. 2018;78:113-120. [CrossRef]
3. Politi C, Roumeliotis S, Tripepi G, Spoto B. Sample Size Calculation in Genetic Association Studies: A Practical Approach. *Life (Basel)*. 2023;13(1):235. [CrossRef]
4. Laven R, Yang DA. Common misinterpretations of statistical significance and P-values in dairy research. *JDS Commun*. 2025;6(6):721-726. [CrossRef]
5. Sterne JA, Davey Smith G. Sifting the evidence-what's wrong with significance tests? *BMJ*. 2001;322(7280):226-231. [CrossRef]

Alishba Jabbar
Minahil Fatima
Saleha Gul
Kashaf Noor

King Edward Medical University, Lahore, Punjab, Pakistan

Corresponding author:
Alishba Jabbar
✉ alishbaj008@gmail.com

Received: July 10, 2026
Accepted: July 19, 2026

Cite this article as: Jabbar A, Fatima M, Gul S, Noor K. NOS3 T-786C: Methodological Considerations. *Turk Kardiyol Dern Ars.* 2026;54(6):538.

DOI: 10.5543/tkda.2026.48757

ARCHIVES OF THE TURKISH SOCIETY OF CARDIOLOGY

Official journal of the TURKISH SOCIETY OF CARDIOLOGY

Reply to the Letter to the Editor: NOS3 T-786C: Methodological Considerations

Editöre Mektup Yanıtı: NOS3 T-786C: Metodolojik Hususlar

LETTER TO THE EDITOR REPLY
EDİTÖRE MEKTUP YANITI

To the Editor,

We sincerely appreciate the authors' interest in our article, "T-786C Polymorphism of the NOS3 Gene and Its Role in the Development of Renal Dysfunction in Patients of the Uzbek Population with Chronic Heart Failure,"[1] as well as their thoughtful comments.[2] We value the opportunity to clarify several aspects of our study. Our detailed responses are provided below.

We appreciate the authors' insightful observation. We agree that symmetric dimethylarginine (SDMA) and asymmetric dimethylarginine (ADMA) are important modulators of endothelial dysfunction and nitric oxide metabolism, particularly in patients with chronic kidney disease. Unfortunately, because of financial and technical limitations at the time of the study, these biomarkers were not evaluated.[3]

Our intention was not to imply that the lower NO concentration was solely attributable to the NOS3 T-786C polymorphism. Rather, we proposed that, in patients with chronic heart failure and renal impairment, this polymorphism may represent one of several factors contributing to endothelial dysfunction. We agree that NO production may be influenced by multiple biological mechanisms, including oxidative stress, inflammation, the accumulation of endogenous NOS inhibitors such as ADMA, renal dysfunction itself, and other genetic and environmental factors.

We also agree that future studies incorporating oxidative stress markers, ADMA, SDMA, and functional assessments of endothelial function would provide a more comprehensive understanding of these mechanisms.

We appreciate the authors for raising this important methodological issue. Our study was designed as an exploratory genetic association analysis involving patients from the Uzbek population, for whom published data on NOS3 T-786C allele frequencies and expected effect sizes were unavailable at the time of the study design. Consequently, it was not possible to perform a reliable a priori sample size calculation.

The final study cohort consisted of 200 patients with chronic heart failure and 120 healthy controls. These participants represented all eligible individuals recruited during the study period according to the predefined inclusion and exclusion criteria. Although we acknowledge that formal power calculations strengthen genetic association studies, our sample size is comparable to those of several previous candidate-gene studies investigating cardiovascular diseases.[4]

We agree that larger cohorts and formal statistical power calculations in future multicenter studies are necessary to validate our findings.

We appreciate this important statistical observation. We fully agree that statistically non-significant results should not be interpreted as evidence of a true association and should instead be interpreted with caution.

Our objective was to explore a plausible biological hypothesis regarding the role of endothelial nitric oxide synthase in cardiovascular disease, supported by previous experimental and clinical evidence, rather than to claim a definitive association between the C allele and renal dysfunction. Accordingly, the terms "possible role" and "trend" were used to emphasize the exploratory nature of our findings rather than to imply statistical evidence.[5]

Gulnoza Zakirova[1*]
Dilyafruz Masharipova[1]
Qodirjon Boboev[2]
Dilnoza Tagaeva[1]

[1]*Republican Specialized Scientific and Practical Medical Center of Therapy and Medical Rehabilitation, Tashkent, Uzbekistan*
[2]*Republican Specialized Scientific and Practical Medical Center of Hematology, Tashkent, Uzbekistan*

**The current affiliation of the author: Tashkent State Medical University, Tashkent, Uzbekistan*

Corresponding author:
Dilnoza Tagaeva
✉ dilnoza_tagaeva@mail.ru

Cite this article as: Zakirova G, Masharipova D, Boboev Q, Tagaeva D. Reply to the Letter to the Editor: T-786C Polymorphism of the NOS3 Gene. *Turk Kardiyol Dern Ars.* 2026;54(6):539-540.

DOI: 10.5543/tkda.2026.81052

We acknowledge that this wording may have been interpreted too literally, and we appreciate the opportunity to clarify our intent. We agree that larger prospective studies are needed before definitive conclusions can be drawn regarding the clinical significance of the NOS3 T-786C polymorphism.

We are sincerely grateful to the authors for their valuable comments. We believe their observations will contribute to improving future research in this important field. Although we recognize the limitations of our study, we believe our findings provide preliminary evidence supporting a potential role of the NOS3 T-786C polymorphism in cardiorenal dysfunction among Uzbek patients with chronic heart failure and may serve as a foundation for larger multicenter investigations.

References

1. Zakirova G, Masharipova D, Boboev Q, Tagaeva D. T-786C Polymorphism of the NOS3 Gene and Its Role in the Development of Renal Dysfunction in Patients of the Uzbek Population with Chronic Heart Failure. *Turk Kardiyol Dern Ars*. 2026;54(4):310-315. [CrossRef]
2. Jabbar A, Fatima M, Gul S, Noor K. NOS3 T-786C: Methodological Considerations. *Turk Kardiyol Dern Ars*. 2026;54(6):538.
3. Schlesinger S, Sonntag SR, Lieb W, Maas R. Asymmetric and Symmetric Dimethylarginine as Risk Markers for Total Mortality and Cardiovascular Outcomes: A Systematic Review and Meta-Analysis of Prospective Studies. *PLoS One*. 2016;11(11):e0165811. [CrossRef]
4. Sham PC, Purcell SM. Statistical power and significance testing in large-scale genetic studies. *Nat Rev Genet*. 2014;15(5):335-346. [CrossRef]
5. Ioannidis JP, Thomas G, Daly MJ. Validating, augmenting and refining genome-wide association signals. *Nat Rev Genet*. 2009;10(5):318-329. [CrossRef]

ARCHIVES OF THE TURKISH SOCIETY OF CARDIOLOGY

Official journal of the TURKISH SOCIETY OF CARDIOLOGY

Comment on the Clinical Course of Methemoglobinemia After Cardiac Device Implantation

Kalp Cihazı İmplantasyonu Sonrası Methemoglobineminin Klinik Seyrine İlişkin Yorum

LETTER TO THE EDITOR
EDİTÖRE MEKTUP

To the Editor,

We read with great interest the recent article by Sertdemir et al.,[1] "Prevalence and Clinical Course of Methemoglobinemia After Cardiac Device Implantation: An Observational Study at Necmettin Erbakan University Hospital in Konya, Türkiye," published in the Archives of the Turkish Society of Cardiology. The authors addressed an important issue by designing a well-structured observational study to better understand the complications associated with local anesthesia during cardiology procedures. This study fills an important knowledge gap and provides a solid scientific basis for improving patient safety in electrophysiology laboratories. However, several areas require further consideration because they may affect the reliability of the study. First, the authors reported a clear relationship between the administered dose and methemoglobin levels, indicating that methemoglobin levels increased with the dose. However, according to Table 3 of the same study, the group with methemoglobin levels of 1.5–3% received a lower mean dose (22.33 mg) than the group with normal levels of ≤ 1.5%, which received a higher mean dose (24.35 mg) (Table 1).[1] This contradictory finding is consistent with the study by Gutenberg et al.,[2] which suggested that the dose is not the only factor affecting methemoglobin levels. Instead, other factors, such as drug metabolism, blood flow to the injection site, and genetic differences, may play a greater role in determining methemoglobin levels. Although the authors remeasured methemoglobin levels at 60 and 120 minutes, providing preliminary kinetic data, the study by Hjelm and Holmdahl[3] suggested that methemoglobin levels peak approximately 6 hours after prilocaine administration and return to normal within 24 hours in most patients. Therefore, the preliminary pharmacokinetic data in the present study may have been insufficient to accurately estimate the prevalence and incidence of the condition.

Nonetheless, this research provides valuable information about the clinical effects and safety of local anesthesia. In summary, we advocate the implementation of extended monitoring protocols and multivariable modeling incorporating host-specific factors, as these practices will likely improve anesthesia safety.

Table 1. Mean drug dose according to FMetHb level

FMetHb group	Mean drug dose (mg)
≤ 1.5% (normal)	24.35
1.5–3% (mild elevation)	22.33
> 3% (significant elevation)	28.04

FMetHb, Fractional methemoglobin.

Conflict of Interest: The authors have no conflicts of interest to declare.

Funding: The authors declared that this study received no financial support.

References

1. Sertdemir AL, Şahin AT, Kan H, et al. Prevalence and Clinical Course of Methemoglobinemia After Cardiac Device Implantation. *Turk Kardiyol Dern Ars*. 2026;54(5):421-426. [CrossRef]
2. Gutenberg LL, Chen JW, Trapp L. Methemoglobin levels in generally anesthetized pediatric dental patients receiving prilocaine versus lidocaine. *Anesth Prog*. 2013;60(3):99-108. [CrossRef]
3. Hjelm M, Holmdahl MH. Biochemical Effects Of Aromatic Amines. Ii. Cyanosis, Methaemoglobinaemia And Heinz-Body Formation Induced By A Local Anaesthetic Agent (Prilocaine). *Acta Anaesthesiol Scand*. 1965;9:99-120. [CrossRef]

Maryam Arain
Inshira Noor

Liaquat University of Medical and Health Sciences, Jamshoro, Pakistan

Corresponding author:
Maryam Arain
✉ maryammaharali@gmail.com

Received: July 17, 2026
Accepted: August 03, 2026

Cite this article as: Arain M, Noor I. Comment on the Clinical Course of Methemoglobinemia After Cardiac Device Implantation. *Turk Kardiyol Dern Ars.* 2026;54(6):541.

DOI: 10.5543/tkda.2026.74389

ARCHIVES OF THE TURKISH SOCIETY OF CARDIOLOGY

Official journal of the TURKISH SOCIETY OF CARDIOLOGY

Reply to the Letter to the Editor: "Comment on the Clinical Course of Methemoglobinemia After Cardiac Device Implantation"

Editöre Mektup Yanıtı: "Kalp Cihazı İmplantasyonu Sonrası Methemoglobineminin Klinik Seyrine İlişkin Yorum"

LETTER TO THE EDITOR REPLY
EDİTÖRE MEKTUP YANITI

To the Editor,

We are grateful to the authors[1] for their thoughtful comments regarding our study, "Prevalence and Clinical Course of Methemoglobinemia After Cardiac Device Implantation."[2] The authors appropriately highlight that the relationship between prilocaine dose and fractional methemoglobin (FMetHb) level should not be interpreted as a strictly linear or monotonic dose–response relationship. Although patients with FMetHb > 3% received the highest mean prilocaine dose, the mean dose in the 1.5–3% group was slightly lower than that observed in the ≤ 1.5% group. Our intention was therefore not to suggest that prilocaine dose alone determines the magnitude of methemoglobin formation. Rather, our findings demonstrated that higher prilocaine exposure was associated with the group showing the greatest biochemical elevation, while ROC analysis identified a dose of ≥ 24.50 mg as being associated with FMetHb > 3%, albeit with only moderate discriminatory performance.

The authors also raise an important point regarding the timing of methemoglobin measurements. Our study evaluated methemoglobin concentrations during the early periprocedural period, with measurements obtained at baseline and at 60 and 120 minutes. The 120-minute observation period also reflects our institution's established postprocedural care protocol for CIED implantation. At our center, patients undergoing uncomplicated device implantation are routinely considered for same-day discharge approximately 2 hours after the procedure, provided that the postprocedural chest radiograph is satisfactory and no other clinical concerns are present. We acknowledge that later measurements, including assessments at approximately 4–6 hours and potentially up to 24 hours, could provide a more complete pharmacokinetic profile and may identify delayed peaks in some patients. Accordingly, our findings should primarily be interpreted as describing the early biochemical course of methemoglobinemia following prilocaine administration during CIED implantation rather than its complete pharmacokinetic evolution.

Nevertheless, the principal objective of our study was to increase awareness of early methemoglobin elevation in the CIED implantation setting, where routine measurement is uncommon and most biochemical elevations may remain clinically silent. We therefore agree that future prospective studies incorporating extended serial measurements, weight-adjusted anesthetic exposure, and host-specific variables would provide important additional information. Such studies may help better define individual susceptibility, the temporal profile of methemoglobin formation, and clinically meaningful predictors of symptomatic toxicity.

References

1. Arain M, Noor I. Comment on the Clinical Course of Methemoglobinemia After Cardiac Device Implantation. *Turk Kardiyol Dern Ars*. 2026;54(6):541.
2. Sertdemir AL, Şahin AT, Kan H, et al. Prevalence and Clinical Course of Methemoglobinemia After Cardiac Device Implantation. *Turk Kardiyol Dern Ars*. 2026;54(5):421-426. [CrossRef]

Ahmet Lütfü Sertdemir
Ahmet Taha Şahin
Hasan Kan
Büşra Özyeşil
Muhammet Fatih Kaleli
Öznur Keskin
Yakup Alsancak
Ahmet Seyfeddin Gürbüz
Mustafa Çelik
Hakan Akıllı
Abdullah İçli
Enes Elvin Gül

Department of Cardiology, Necmettin Erbakan University Hospital, Konya, Türkiye

Corresponding author:
Ahmet Taha Şahin
✉ tahasahin94@gmail.com

Cite this article as: Sertdemir AL, Şahin AT, Kan H, et al. Reply to the Letter to the Editor: "Comment on the Clinical Course of Methemoglobinemia After Cardiac Device Implantation". *Turk Kardiyol Dern Ars.* 2026;54(6):542.

DOI: 10.5543/tkda.2026.90256

ARCHIVES OF THE TURKISH SOCIETY OF CARDIOLOGY

Official journal of the TURKISH SOCIETY OF CARDIOLOGY

From Measuring Treatment Burden to Acting on Patient-Reported Outcomes

Tedavi Yükünün Ölçülmesinden Hasta Tarafından Bildirilen Sonuçlara Göre Harekete Geçmeye

LETTER TO THE EDITOR
EDİTÖRE MEKTUP

To the Editor,

Yıldırım et al.[1] provide an important patient-centered assessment of quality of life, symptom burden, anxiety, and depression among patients with pulmonary hypertension receiving therapies targeting the prostacyclin pathway. Their findings are clinically relevant: health-related quality of life was markedly impaired, anxiety and depression were common, and vomiting was independently associated with a 7.6-point increase in the emPHasis-10 score.

The challenge is determining how these patient-reported findings should influence care. Screening for symptoms, psychological distress, and impaired quality of life is valuable, but measurement alone does not ensure a clinically meaningful response. The study identifies several potentially actionable problems, including vomiting, anxiety, depression, and a high symptom burden, yet the corresponding clinical pathways remain undefined.

For example, what degree of deterioration in the emPHasis-10 score should trigger reassessment of treatment tolerability? When should vomiting prompt intensified supportive management, a review of dose titration, dose adjustment, or reconsideration of the route of treatment administration?[2] Similarly, positive screening results for anxiety or depression may require different responses depending on symptom severity, functional impact, patient preferences, and the availability of psychological or psychiatric support. Without predefined response pathways, patient-reported outcome measures risk documenting burden without alleviating it.

This issue is particularly important in pulmonary hypertension care, in which symptoms may reflect the disease itself, treatment-related adverse effects, psychological distress, comorbidities, or several of these factors simultaneously. A high score should therefore not automatically lead to a single intervention. Instead, it could initiate a structured assessment to distinguish disease progression from treatment intolerance and identify the healthcare professional best positioned to respond.

Patient-reported outcomes are increasingly incorporated into contemporary PAH research.[3] The emPHasis-10 questionnaire is among the most frequently used disease-specific instruments because of its established association with clinical outcomes and prognosis.[4,5] One unresolved question is whether the observed relationship between quality of life and clinical severity would also persist if quality of life were compared with categorical risk-stratification tools rather than continuous functional or biochemical markers—a comparison that, to our knowledge, remains underexplored in real-world PAH cohorts.

However, broader measurement does not, by itself, ensure better care. Future studies should move beyond cross-sectional associations and evaluate longitudinal care models in which patient-reported outcomes are linked to prespecified clinical actions. Relevant outcomes could include improvements in emPHasis-10 scores, reductions in gastrointestinal symptoms, treatment persistence, adherence, psychological well-being, and the avoidance of unnecessary treatment discontinuation. Such studies could also determine whether repeated assessments during titration and routine follow-up identify deterioration earlier than conventional clinical evaluations.

Ilma Nascimento

Caio Júlio Cesar dos Santos Fernandes

Pulmonary Circulation Unit, Heart Institute (InCor), Hospital das Clínicas, Faculty of Medicine, University of São Paulo, São Paulo, Brazil

Corresponding author:
Ilma Nascimento
✉ ilma.nascimento@usp.br

Received: July 18, 2026
Accepted: July 30, 2026

Cite this article as: Nascimento I, dos Santos Fernandes CJC. From Measuring Treatment Burden to Acting on Patient-Reported Outcomes. *Turk Kardiyol Dern Ars.* 2026;54(6):543-544.

DOI: 10.5543/tkda.2026.73624

The value of patient-reported outcomes lies not only in revealing what patients experience but also in ensuring that this information leads to timely and appropriate care. The findings of Yıldırım et al.[1] provide a strong rationale for developing response pathways that translate measured treatment burden into individualized clinical action and for examining how quality-of-life assessments may complement, rather than simply reproduce, conventional risk stratification.

Conflict of Interest: The authors have no conflicts of interest to declare.

Funding: The authors declared that this study received no financial support.

References

1. Yıldırım F, Ok E, Ünver V, Sezgin D, Ataş H, Şentürk Saraç B. Quality of Life Outcomes in Patients with Pulmonary Hypertension Receiving Prostacyclin Therapy: Impact of Anxiety, Depression, Sociodemographic Characteristics, and Treatment-Related Factors. *Turk Kardiyol Dern Ars*. Jul 10, 2026. doi: 10.5543/tkda.2026.01628. [Epub ahead of print]. [CrossRef]
2. Kingman M, Archer-Chicko C, Bartlett M, Beckmann J, Hohsfield R, Lombardi S. Management of prostacyclin side effects in adult patients with pulmonary arterial hypertension. *Pulm Circ*. 2017;7(3):598-608. [CrossRef]
3. Nascimento IAO, Souza R, Fernandes CJCS. 2025 annual review of pulmonary arterial hypertension clinical research. *Pulm Ther*. 2026;12:463-483. [CrossRef]
4. Yorke J, Corris P, Gaine S, et al. emPHasis-10: development of a health-related quality of life measure in pulmonary hypertension. *Eur Respir J*. 2014;43(4):1106-1113. [CrossRef]
5. Lewis RA, Armstrong I, Bergbaum C, et al. EmPHasis-10 health-related quality of life score predicts outcomes in patients with idiopathic and connective tissue disease-associated pulmonary arterial hypertension: results from a UK multicentre study. *Eur Respir J*. 2021;57(2):2000124. [CrossRef]

ARCHIVES OF THE TURKISH SOCIETY OF CARDIOLOGY

Official journal of the TURKISH SOCIETY OF CARDIOLOGY

Reply to the Letter to the Editor: "From Measuring Treatment Burden to Acting on Patient-Reported Outcomes"

Editöre Mektup Yanıtı: "Tedavi Yükünün Ölçülmesinden Hasta Tarafından Bildirilen Sonuçlara Göre Harekete Geçmeye"

LETTER TO THE EDITOR REPLY
EDİTÖRE MEKTUP YANITI

To the Editor,

We thank the authors for their thoughtful and constructive comments on our article entitled "Quality of Life Outcomes in Patients with Pulmonary Hypertension Receiving Prostacyclin Therapy: Impact of Anxiety, Depression, Sociodemographic Characteristics, and Treatment-Related Factors" and for the opportunity to respond to the points raised in the Letter to the Editor.[1]

A high EmPHasis-10 score reflects poor quality of life, whereas a low score reflects good quality of life. However, no specific EmPHasis-10 threshold has been defined for reassessing a patient's ability to tolerate treatment. Given the cross-sectional design of our study and the absence of quality-of-life data before prostacyclin therapy, the magnitude of change in the EmPHasis-10 score that would warrant such reassessment cannot be determined from our current data. Therefore, we believe that the EmPHasis-10 score, or any change in it, should not be considered a standalone threshold and that the results should be evaluated alongside the patient's symptom burden, clinical status, psychological status, and treatment-related adverse effects.

In our study, prostacyclin-related vomiting was independently associated with higher EmPHasis-10 scores (B=7.559; 95% CI: 3.675–11.443; P<0.001).[2] However, because the frequency and severity of treatment-related adverse effects were not systematically assessed in our study, this finding alone is insufficient to conclude that vomiting should prompt intensified supportive management, dose adjustment, modification of titration, or reconsideration of the treatment route. Our findings support the importance of routinely assessing gastrointestinal adverse effects, such as vomiting, and individualizing their management according to the type and severity of symptoms and the patient's overall clinical status.

In our study, symptoms of anxiety were identified in 58.6% of patients and symptoms of depression in 29.3%; both anxiety and depression were significantly associated with higher EmPHasis-10 scores.[2] These findings support the importance of considering psychological status as part of the assessment of patients with PH. However, psychological or psychiatric interventions that could be implemented following the assessment of anxiety and depression symptoms were not evaluated in this study. In this context, taking into account patients' individual needs and symptom severity, psychosocial support approaches, such as peer-support sessions, may also be considered alongside professional psychological or psychiatric support.

This assessment is also important in the context of the findings of our study. In our multivariate analysis, age, symptom burden, anxiety, depression, and prostacyclin therapy-related vomiting were independently associated with higher EmPHasis-10 scores, and together, these variables explained 80.5% of the variance in EmPHasis-10 scores.[2] These findings suggest that high EmPHasis-10 scores should not be attributed to a single cause and that multiple factors, such as symptom burden, psychological status, and treatment-related adverse effects, should be considered together when assessing quality of life.

Fatma Yıldırım[1]
Elif Ok[2]
Vesile Ünver[3]
Dilek Sezgin[4]
Halil Ataş[5]
Betül Şentürk Saraç[6]

[1]*Acıbadem Mehmet Ali Aydınlar University, Institute of Health Sciences, Nursing Doctorate Program, İstanbul, Türkiye*
[2]*Department of Nursing, Health Science Faculty, Izmir Democracy University, İzmir, Türkiye*
[3]*Department of Nursing, Institute of Health Sciences, Açibadem Mehmet Ali Aydınlar University, Istanbul, Türkiye*
[4]*Department of Internal Medical Nursing, Nursing Faculty, Dokuz Eylül University, İzmir, Türkiye*
[5]*Department of Cardiology, Faculty of Medicine, Marmara University, İstanbul, Türkiye*
[6]*Marmara University Pendik Training and Research Hospital, İstanbul, Türkiye*

Corresponding author:
Fatma Yıldırım
✉ fkahve6@gmail.com

Cite this article as: Yıldırım F, Ok E, Ünver V, Sezgin D, Ataş H, Şentürk Saraç B. Reply to the Letter to the Editor: "From Measuring Treatment Burden to Acting on Patient-Reported Outcomes". *Turk Kardiyol Dern Ars.* 2026;54(6):545–546.

DOI: 10.5543/tkda.2026.26287

In our study, EmPHasis-10 scores were significantly associated with symptom burden, anxiety, depression, oxygen saturation, and six-minute walk distance.[2] However, no direct comparison was made between EmPHasis-10 and categorical risk-stratification tools. Therefore, we believe that future prospective studies should evaluate whether these observed associations persist when categorical risk-stratification approaches are used.

This consideration is important in terms of the potential role of patient-reported outcomes in clinical follow-up. As our study was cross-sectional, changes in EmPHasis-10 scores over time and whether repeated assessments could identify clinical deterioration earlier could not be evaluated. We believe that future longitudinal studies would be valuable for determining the relationship between changes in patient-reported outcomes and clinical status, treatment tolerability, and treatment persistence. In this process, regular monitoring of patients' symptoms and treatment-related adverse effects by healthcare professionals may contribute to the integration of patient-reported outcomes with clinical assessment.

References

1. Nascimento I, dos Santos Fernandes CJC. From Measuring Treatment Burden to Acting on Patient-Reported Outcomes. *Turk Kardiyol Dern Ars*. 2026;54(6):543–544.
2. Yıldırım F, Ok E, Ünver V, Sezgin D, Ataş H, Şentürk Saraç B. Quality of Life Outcomes in Patients with Pulmonary Hypertension Receiving Prostacyclin Therapy: Impact of Anxiety, Depression, Sociodemographic Characteristics, and Treatment-Related Factors. *Turk Kardiyol Dern Ars*. Jul 10, 2026. doi: 10.5543/tkda.2026.01628. [Epub ahead of print]. [CrossRef]